

Surface Activity of Pulmonary Surfactant Protein B

From Biophysical Properties to Clinical Application

Rob Diemel

Surface activity of pulmonary surfactant protein B
From biophysical properties to clinical application
Robert V. Diemel
Ph.D. thesis, with summary in Dutch
Utrecht University, the Netherlands
January 2002

The studies described in this thesis were performed at the Department of Anaesthesiology and Critical Care Medicine, The Leopold-Franzens-University of Innsbruck, Austria, *and* at the Department of Biochemistry and Cell Biology, Faculty of Veterinary Medicine, Utrecht University, the Netherlands.

Copyright © 2002 by R.V. Diemel. All rights reserved. No part of this thesis may be reproduced or transmitted in any form or by any means, without written permission from the author.

Surface Activity of Pulmonary Surfactant Protein B

From Biophysical Properties to Clinical Application

**Oppervlakte-Activiteit van Long Surfactant Eiwit B
Van Biofysische Eigenschappen tot Klinische Toepassing**

(met een samenvatting in het Nederlands)

Proefschrift

ter verkrijging van de graad van doctor aan de Universiteit Utrecht
op gezag van de Rector Magnificus, Prof. Dr. W.H. Gispen,
ingevolge het besluit van het College voor Promoties
in het openbaar te verdedigen

op 10 januari 2002 des middags te 14.30 uur

door

Robert Victor Diemel

geboren op 29 augustus 1972, te Driebergen-Rijsenburg

Promotores: Prof. Dr. L.M.G. van Golde
Hoofdafdeling Biochemie & Celbiologie
Faculteit der Diergeneeskunde, Universiteit Utrecht

Prof. Dr. H.P. Haagsman
Hoofdafdeling Voedingsmiddelen van Dierlijke Oorsprong
Faculteit der Diergeneeskunde, Universiteit Utrecht

Co-promotores: Dr. J.J. Batenburg
Hoofdafdeling Biochemie & Celbiologie
Faculteit der Diergeneeskunde, Universiteit Utrecht

Prof. Dr. G. Putz
Universitätsklinik für Anästhesie und allgemeine Intensivmedizin
Leopold-Franzens Universität Innsbruck, Österreich

The work described in this thesis was financially supported by the Fonds zur Förderung der Wissenschaftlichen Forschung (FWF) (P11527-MED), Austria.

The printing of this thesis was financially supported by the Department of Biochemistry and Cell Biology, the Graduate School of Animal Health, Boehringer-Ingelheim (manufacturer of Alveofact®).

Printed by Drukkerij Labor, Utrecht, December 2001.

CIP-GEGEVENS KONINKLIJKE BIBLIOTHEEK, DEN HAAG

Surface activity of pulmonary surfactant protein B. From biophysical properties to clinical application / Robert Victor Diemel.- Utrecht: Utrecht University, Faculteit Diergeneeskunde. Proefschrift Universiteit Utrecht.- With ref.- With summary in Dutch.
ISBN 90-393-2958-3

CONTENTS

	Preface	6
Chapter 1	Surfactant-associated proteins: functions and structural variation	9
Chapter 2	Effect of the hydrophobic surfactant proteins on the surface activity of spread films in the captive bubble surfactometer	27
Chapter 3	Effects of cholesterol on surface activity and surface topography of spread surfactant films	37
Chapter 4	Multilayer formation upon compression of surfactant monolayers depends on protein concentration as well as lipid composition: an atomic force microscopy study	59
Chapter 5	Functional tests for the characterization of surfactant protein B (SP-B) and a fluorescent SP-B analog	79
Chapter 6	<i>In vitro</i> and <i>in vivo</i> -intrapulmonary distribution of fluorescently labeled surfactant	97
Chapter 7	Summarizing discussion	115
	Reference list	130
	List of abbreviations	148
	Samenvatting	149
	Dankwoord	156
	List of publications	158
	Curriculum Vitae	159

Preface

The first connection between lungs and surface tension was made in 1929 when it was observed that it takes more pressure to fill up lungs with air than with an aqueous buffer [1]. This demonstrated that the addition of buffer resulted in the elimination of a pulmonary surface tension. From this it was hypothesized that the surface tension in the alveoli can be altered by a surface-active substance, which was later called 'surfactant'. The properties, function and origin of a surface-active alveolar lining layer were described several decades later [2,3,4]. Shortly thereafter, it was observed that neonatal respiratory distress syndrome, from which prematurely born infants suffer, was related to a deficiency of surface-active material [5]. The important role of dipalmitoyl phosphatidylcholine (DPPC) in surface tension lowering was recognized in the 1960's [6,7]. In the 1970's the presence of proteins in surfactant was shown, leading to a growth in surfactant research [8]. The interest for surfactant leaped in 1980 when surfactant was used successfully in the treatment of prematurely born infants suffering from respiratory distress syndrome [9]. From then on clinicians and scientist made great efforts investigating whether surfactant can be used to treat adult patients suffering from acute respiratory distress syndrome (ARDS) as well [10,11]. Although the results obtained in several clinical studies look promising, a successful therapeutic strategy for ARDS patients has not yet been developed, due to the complex nature of the syndrome as well as to insufficient knowledge on the mode of action of the surfactant components. Therefore, scientific research is performed on individual surfactant components, which will ultimately lead to the development of synthetic surfactants to be used for the treatment of ARDS patients in the clinic.

Reduction of the surface tension at the alveolar air/liquid interface is achieved by formation of a surface-active film that consists of a lipid monolayer highly enriched in DPPC, and bilayer or multilayer structures ('surface-associated reservoir') closely attached to the monolayer. The presence of a surfactant film prevents the alveoli from collapsing at end-expiration and makes breathing with minimal effort possible. The existence of such a film has been visualized *in vivo* by electron microscopy [12] and *in vitro* by atomic force microscopy (AFM) and fluorescence light microscopy [13]. The two hydrophobic surfactant proteins SP-B and SP-C play key roles in the events leading to the formation of a layered surface film as well as in its stabilization. The activities of SP-B include promotion of adsorption of lipids into the air/liquid interface [14], respreading of films from the collapse phase [15], membrane fusion and lysis [16], formation of tubular myelin [17], and surfactant reuptake by type II cells [18]. The importance of SP-B is further documented by the observation that neonates that had a frame-shift mutation in the SP-B gene died from respiratory failure [19]. Similarly, homozygous SP-B knock-out mice died of respiratory failure immediately after birth [20]. Moreover, blocking of SP-B with monoclonal antibodies in rabbits led to respiratory failure and the loss of surfactant activity [21]. Despite the fact that the structures of SP-B and SP-C are quite different, their activities overlap to a large extent. Therefore it was unexpected to

find that homozygous SP-C knockout mice are viable [22,23]. In addition to its function to reduce the surface tension, lung surfactant plays an important role in the host defense system of the lung, mediated by the hydrophilic surfactant proteins SP-A and SP-D.

The global aim of our studies was to obtain more information about the mechanisms involved in the action of the hydrophobic surfactant components, with a special attention for SP-B. To reach this goal, many different assays and devices were used, including a pressure driven captive bubble surfactometer (CBS), a spreading trough and an atomic force microscope. The thesis starts with a general overview about the function and structural variation of the surfactant proteins (chapter 1). It is described that the activity and structure of the hydrophobic surfactant proteins SP-B and SP-C is very conserved among species throughout evolution, while more variation exists for that of SP-A and SP-D.

Aim *i*) of the thesis research was to obtain knowledge about the effect of SP-B and SP-C on the surface activity of spread films. This study, described in chapter 2, was done using the CBS, an apparatus that allows accurate determination of surface tension under dynamic conditions [24,25,26]. Surfactant components were spread at the air/liquid interface of an air-bubble, which was subsequently repeatedly compressed and expanded, thereby mimicking the breathing cycle. In this way information can be obtained on the role of individual surfactant components. Both SP-B and SP-C activity depended on the concentration of the proteins. Differences in surface dynamics between both proteins were found when lipid vesicles were omitted from the subphase.

Aim *ii*) was to investigate the role of cholesterol in surfactant. The effect of cholesterol on surface tension was examined by CBS, using spread lipid films containing SP-B and/or SP-C (chapter 3). It was shown that a cholesterol content of 10 mol% is optimal for surfactant activity in films containing SP-B, but not in films containing both SP-B and SP-C, or SP-C alone. Furthermore, differences in network structures were seen between films containing and those lacking cholesterol, as visualized by AFM.

Aim *iii*) was to investigate which surfactant components are responsible for the formation of protrusions upon monolayer compression towards low surface tensions (described in chapter 4). The appearance of compressed films containing saturated phospholipids plus native bovine SP-B was visualized by AFM. These films had similar appearance as those containing synthetic peptides based on the 25 N-terminal amino acids of SP-B. Protrusion height of lipid films containing SP-B₁₋₂₅ peptide, however, was lower than that found for films containing native SP-B. It was further shown that the number of protruded layers depends on whether the phospholipids contain an unsaturated fatty acyl chain, and on whether the unsaturated acyl chain is present in phosphatidylcholine or in phosphatidylglycerol.

Aim *iv*) was to label a surfactant component and determine its distribution in a model of ARDS. In chapter 5 a method to label SP-B covalently at specific sites with the fluorophore Bodipy FL CASE is described. Using an array of techniques, fluorescently labeled SP-B was characterized and subsequently compared to the native protein. For

Preface

instance, in a glass spreading trough mimicking dichotomic lung anatomy labeled SP-B spread on top of an aqueous surface and lowered surface tension independent of trough geometry. Since Bodipy-labeled SP-B was shown to have retained its biophysical activity, it was supplemented to bovine lung surfactant extract and this was administered to rats in a model of ARDS (chapter 6). In this way the distribution of exogenous surfactant during surfactant replacement therapy was determined at the alveolar level. It was found that the majority of administered surfactant reached underinflated (dystelectatic) as well as aerated (open) alveoli, but hardly spread into severely damaged and collapsed (atelectatic) alveoli. This thesis is concluded with a summarizing discussion.

Chapter 1

Surfactant-Associated Proteins: Functions and Structural Variation

REVIEW

Henk P. Haagsman ^{a,b} and Robert V. Diemel ^a

^a Department of Biochemistry and Cell Biology, and ^b Department of the Science of Food of Animal Origin, Faculty of Veterinary Medicine, Graduate School of Animal Health, Utrecht University, Utrecht, The Netherlands

Comparative Biochemistry and Physiology
(Part A: Molecular & Integrative Physiology)
2001, **129**: 91-108

Abstract

Pulmonary surfactant is a barrier material of the lung and has a dual role: firstly, as a true surfactant, lowering the surface tension; and secondly, participating in innate immune defence of the lung and possibly other mucosal surfaces. Surfactant is composed of approximately 90% lipids and 10% proteins. There are four surfactant-specific proteins, designated surfactant protein A (SP-A), SP-B, SP-C and SP-D. Although the sequences and post-translational modifications of SP-B and SP-C are quite conserved between mammalian species, variations exist. The hydrophilic surfactant proteins SP-A and SP-D are members of a family of collagenous carbohydrate binding proteins, known as collectins, consisting of oligomers of trimeric subunits. In view of the different roles of surfactant proteins, studies determining the structure-function relationships of surfactant proteins across the animal kingdom will be very interesting. Such studies may reveal structural elements of the proteins required for surface film dynamics as well as those required for innate immune defence. Since SP-A and SP-D are also present in extrapulmonary tissues, the hydrophobic surfactant proteins SP-B and SP-C may be the most appropriate indicators for the evolutionary origin of surfactant. SP-B is essential for air-breathing in mammals and is therefore largely conserved. Yet, because of its unique structure and its localization in the lung but not in extrapulmonary tissues, SP-C may be the most important indicator for the evolutionary origin of surfactant.

1. Introduction

The first time that surface tension was related to lungs was as early as 1929 when von Neergaard found that the pressure needed to fill up lungs with air is higher than the pressure needed to fill them up with water [1]. From this he hypothesized that the alveolar lining had to be stabilized by a surface tension lowering substance. The properties, function and origin of the alveolar lining layer were later described by Pattle in 1955, postulating that air-bubbles surrounded by lung fluid material were stabilized by the quality and quantity of the surface-active lung material [2]. Using a surface balance Clements showed in 1957 that surface films from lung extract reached very low surface tension values upon compression [3]. From this he theorized about the role of surfactant in surface tension lowering and maintaining the structural stability of the lung [4]. Shortly thereafter, the connection between neonatal respiratory distress syndrome (RDS) and a deficiency of surface active material was made [5]. The important role of dipalmitoyl phosphatidylcholine (DPPC) in surface tension lowering [6] and its production and secretion into the alveolar space [7] was described in the 60's. The first indication for the presence of proteins in surfactant came in the 70's from King and co-workers [8], but it was not until the first successful treatment of RDS infants by Fujiwara *et al.* in 1980 using surfactant replacement therapy [9] that it was generally recognized that surfactants containing lipids only were not sufficiently efficient and more attention had to be

focused on the surfactant proteins.

Surfactant comprises two types of specific surfactant proteins: hydrophilic SP-A and SP-D (Fig. 1), and hydrophobic SP-B and SP-C (Fig. 2). SP-A and SP-D are related and belong to a subgroup of mammalian lectins called “collectins”, (or C-type lectins, group III). These proteins consist of oligomers with C-terminal carbohydrate recognition domains in association with N-terminal collagen-like domains. In lung lavage most SP-A is associated with surfactant lipids, whereas most SP-D is not. SP-A and SP-D are believed to be molecules of the innate immune system through their ability to recognize a broad spectrum of pathogens. Several studies have shown that SP-A and SP-D interact with a number of viruses, bacteria and fungi [27-29], and with inhaled glycoconjugate allergens, such as pollen grains [30] and mite allergens [31]. SP-A and SP-D have been shown to bind to alveolar macrophages, which carry receptors for SP-A and SP-D on their surface. Furthermore, SP-A has a role in the structural organization of surfactant. Recent work suggests that SP-D may be involved in surfactant homeostasis.

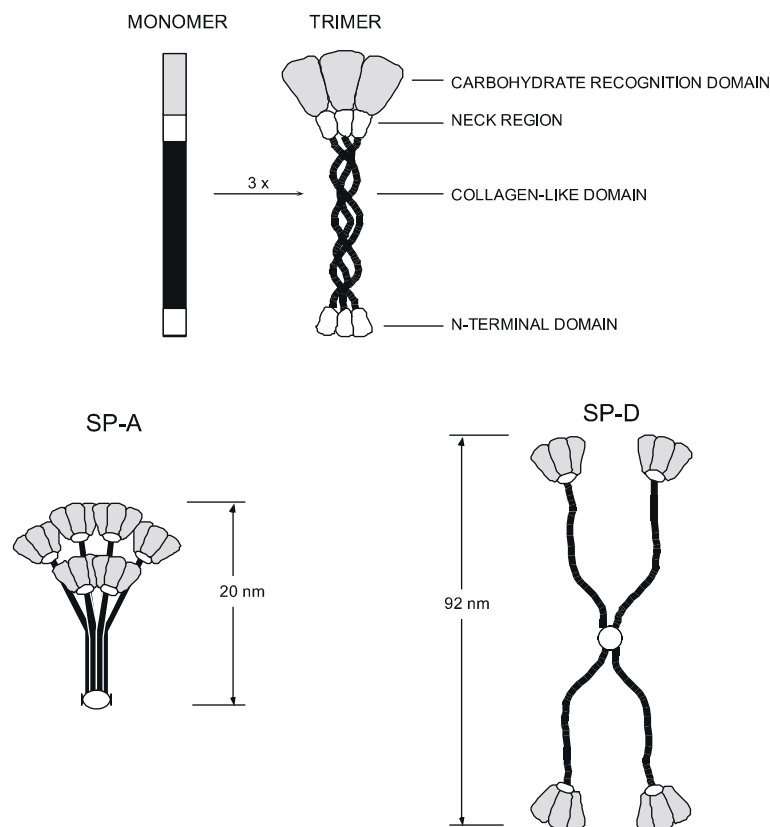


Figure 1. Models of the structure of SP-A and SP-D.

The first description of the presence of hydrophobic surfactant proteins came from Phizackerley and co-workers [32]. Two proteins with molecular mass of approximately 9000

Chapter 1

(reduced form) and 4000 were subsequently identified by a number of groups. According to the current nomenclature for surfactant proteins, proposed by Possmayer [33], these hydrophobic proteins are named SP-B and SP-C, respectively. The amino acid sequence of the N-termini of both proteins was determined by several groups and the use of oligonucleotide probes based on this sequence led to the identification of cDNA clones encoding SP-B and SP-C [34-38]. Both proteins turned out to have an unusually high content of hydrophobic amino acids. Their extreme hydrophobicity is best characterized by the necessity of mixtures of organic solvents like methanol/chloroform, methanol/water or acetonitrile/water to fully dissolve them [39].

First, we will describe the hydrophobic surfactant proteins SP-B and SP-C and focus on the amino acid homology of these proteins in various vertebrates. With respect to SP-B we will focus on the role of disulfide bonding patterns. A possible role for SP-B as an antibacterial protein, in addition to the classic role of surface tension adjustment, will be proposed. For SP-C the role of palmitoyl chains will be discussed. Subsequently, variations in the structure of SP-A and SP-D will be discussed and related to the putative functions of these collectins.

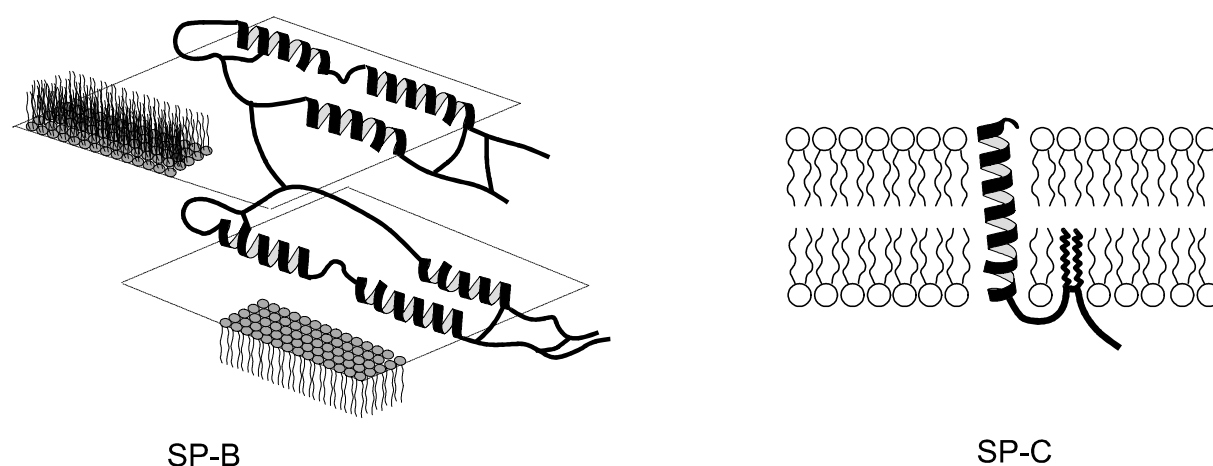


Figure 2. Models of the structure of SP-B and SP-C.

2. Structural variation and functions of the hydrophobic surfactant proteins

2.1. Surfactant Protein B

Human SP-B is encoded on a single gene on the short arm of chromosome 2. The complete human gene has been characterized [40] and was found to contain approximately 9500 base pairs, subdivided in 11 exons. The genes of mice and rabbits are a little smaller,

due to the shorter size of several introns. SP-B is expressed in alveolar type II epithelial cells as well as bronchiolar epithelial (Clara) cells. The primary translation product of human SP-B is a preproprotein of 381 amino acids (a.a.). This preproprotein is translocated into the lumen of the endoplasmic reticulum (ER) with aid of a 23 a.a. N-terminal signal sequence. Cotranslational cleavage of this signal sequence yields a proprotein of 358 a.a. The proprotein consists of the mature protein (a.a. 201 - 279) flanked by an N-terminal proprotein (a.a. 24 - 200) and a C-terminal proprotein (a.a. 280 - 381). To release the mature form of SP-B the N-terminal proprotein is cleaved, followed by the C-terminal flank. While the N-terminal and C-terminal flanking arms have an anionic net charge (-4 and -2, respectively), the charge of mature SP-B is highly cationic (+7). Experiments in which the C-terminal side, containing a glycosylated asparagine, is deleted showed that this deletion does not affect intracellular trafficking of the proprotein. Deletion of the N-terminal side of the proprotein, on the other hand, leads to an accumulation of SP-B in the ER. The N-terminal propeptide was found to be necessary and sufficient for intracellular trafficking of the mature peptide [41]. Because of the hydrophobic nature of SP-B, it has been suggested that the N-terminal propeptide fulfills the role of an intramolecular chaperone for the mature protein. After translocation into the ER both SP-B and SP-C are transported to the Golgi and from here to so-called lamellar bodies, which are granules containing SP-A, SP-B, SP-C and lipids [42]. After secretion, surfactant is transformed into an interesting membrane structure, called tubular myelin, from which it is inserted into the monolayer present at the alveolar air/liquid interface.

Mature SP-B is encoded in exons 6 and 7 of the SP-B gene. Mutations in the SP-B gene can cause severe lung diseases [43]. Furthermore, SP-B polymorphisms could be associated with the development of life-threatening respiratory failure in newborns suffering from RDS and in adults having acute respiratory distress syndrome (ARDS) [44]. From these findings it can be concluded that SP-B is a key-player in the events that adjust the surface tension at the alveolar lining in the lung. SP-B, as well as SP-C, has been demonstrated to enhance lipid insertion into the monolayer at the air/liquid interface. In this way a relatively low surface tension is maintained upon inhalation, that protects the surface film from being contaminated by non-surfactant (serum) proteins [14,35]. In addition, both SP-B and SP-C influence the molecular ordering of the phospholipid monolayer [45,46]. Furthermore, SP-B is required for the formation of tubular myelin [17,47].

SP-B is a member of a sequence-related family of saposins, sphingolipid activator proteins. Saposins activate several lysosomal hydrolases involved in the metabolism of various sphingolipids [48]. Saposins share strictly conserved structural features with SP-B, with implications for helix topology and lipid interaction [49]. An important similarity within the saposin family is the presence of six cysteine residues with the same disulfide bonding pattern. In Fig. 3 all known SP-B amino acid sequences among species, available at the protein sequence database SWISS-PROT (www.expasy.ch), are aligned. Dimerization of the 79 a.a. monomeric SP-B occurs through the intermolecular disulfide bond at Cys48 (= Cys248 in SP-B proprotein) [50]. In type II cells the dimerization probably occurs when the cleavage of the proprotein is complete [51]. Dimerization has been shown to be required

Chapter 1

for optimal activity *in vivo*: although mice expressing a monomeric SP-B mutant in a SP-B -/- background had a normal lung structure, slower adsorption kinetics and higher minimal surface tension during cycling in a captive bubble surfactometer were found [52]. The importance of dimerization for SP-B activity is further stressed by a recent study showing that a dimeric N-terminal segment of human SP-B had enhanced *in vitro* surface properties compared to the monomeric segment [53]. Next to the interchain disulfide bond, three intrachain S-S bridges are formed between Cys8-Cys77, Cys11-Cys71 and Cys35-Cys46.

			I		
Human	201	FPIPLPYCWL	CRALIKRIQAMIPK	GAL ^A	VAVAQVCRV
				R	VPLVAGGICQCLAERYSVILLDTLLGRMLPQLVCR
					LVLRCSM 279
Sheep	189F.....T.....V.....V.....MT.....H.....LV.....V.....G.....S			266
Dog	181	L.....T.....V.....T.G...H.....V.....G...T.L...A.....G.....H			259
Rabbit	185L.....T.L.....V.....M ^{VA}H.....V.....R.....T...EV...HV.....G.....S			263
Mouse	192	L.....F.....T...V.V...V.....S...H.....V.....T.L...A...VV.....G.....T			270
Rat	191	L.....F.....T...V.V...V.....S...H.....V.....T.L...A...VV.....G.....T			269
Guineapig	196R..KT.L.V.....V..M.....H.....T.L...A..SHL.....G.....			274
Pig	F.....T.....VV..V.LK.....H...PV.....I..C.NM..D.T.....G.....S			
Bovine		...I...L.T...K...V...V..MT.....H...LV...I.Q.VIE.....T.....N...G.R...G			
BovineSAP-C		..QV.EFVV.EVAKL.DNNRILH.LDK..SKL.TSLAEQ..EVVDT.GRSI.SI..DEAS.E...SMLHL..		X	
			TEKE		
Human preSAP		..EV.EF.V.EVTKL.DNNKILD.FDKM.SKL.KSLSEE..EVVDT.GSSI.SI..EEVS.E...SMLHL..			
			TEKE		
Pig NKL		GLI.ES..KI.QKLEDMVGPDTVTQ.ASR..DKLKI-LR.V.KKIMRTFLRRISKDI.TGKK..AI.VDIKI.KE			
			QPNE		

Figure 3. Amino acid sequence alignment of SP-B and the related proteins bovine Saposin C (SAP-C), human Saposin precursor (preSAP) and porcine NK-lysin (NKL).

Human SP-B is taken as the primary sequence. The number of the N-terminal and C-terminal residues are mentioned. Human (*Homo sapiens sapiens*), sheep (*Ovis aries*), dog (*Canis familiaris*), rabbit (*Oryctolagus cuniculus*), house mouse (*Mus musculus*), Norway rat (*Rattus norvegicus*), guinea pig (*Cavia porcellus*), pig (*Sus scrofa*) and cattle (*Bos taurus*). X represents an unknown amino acid.

The only exception to the pattern of disulfide bridges is bovine SP-B. In the deduced bovine amino acid sequence Ile46 was found instead of Cys46 and Leu11 was observed instead of Cys11 [54,55]. Furthermore, Gln48 was observed instead of Cys48, that is

Function and structure of the surfactant proteins

responsible for dimerization. These amino acid alterations would implicate a dramatic change of structure: the remaining four cysteines could only form two disulfide bridges. Therefore, dimerization would be impossible unless it would occur by two cysteines per monomer. Although bovine SP-B has occasionally been reported as an oligomer of 28 kDa on SDS-PAGE gel [56], it is the experience of the authors that SP-B isolated from bovine bronchoalveolar lavage is predominantly present as a dimer with a molecular mass of approximately 18 kDa [57]. Only trace amounts of monomeric and oligomeric bovine SP-B were found, probably resulting from the isolation procedure and storage conditions. So, the existence of only four cysteines in bovine SP-B might cause an alternative folding not influencing the electrophoretic separation. Interestingly, in several lysosomal hydrolases mutation analysis showed that the failure of formation of the common disulfide bridges results in alteration of their action [58,59]. Nevertheless, it is the authors' experience that bovine SP-B is surface active, as determined by captive bubble surfactometry [57]. Contrary to SP-B from most of the other species, bovine SP-B has not been deduced from cDNA yet. It will be very interesting to see whether the amino acid sequence derived from bovine cDNA will be different from the known sequence.

Nine positive and two negative charges are present in mature human SP-B. Similar charge density and distribution have been found in other species. Since the tertiary structure of SP-B is still under debate [60,61], it is unknown how the charged amino acids are arrayed in the monolayer containing anionic phospholipids.

A sequence similarity to saposins has been found for the small subunit of acyloxyacyl hydrolase, a phagocytic cell enzyme that cleaves acyl chains from bacterial lipopolysaccharide (LPS) [62]. It is this small subunit that recognizes LPS as a substrate and is essential for the enzyme's catalytic activity towards LPS [63]. Given the structural resemblance of LPS to glycosphingolipids and of SP-B to saposins, it could be hypothesized that SP-B has an extra function in immune defence, in addition to its role in the regulation of surface tension in the lung. SP-B may bind to LPS and catalyze the deacylation of LPS. In this way it could play an important role in the detoxification of LPS in macrophages after delivery of LPS by SP-A [64,65] or SP-D [66]. Support for the theory of SP-B involvement in immune defence comes from recent findings of a synthetic SP-B peptide that was able to inhibit bacterial growth [67]. Interestingly, other proteins in the saposin group are involved in immune defence as well. For instance, the 78 amino acid protein NK-lysin possesses marked antibacterial activity and is capable to lyse tumor cell lines but not red blood cells [68]. Furthermore, amoebapores, which are highly cytotoxic peptides from *Entamoeba histolytica*, are able to form ion channels in cell membranes [69]. The amoebapore peptides, as well as Saposin C and SP-B, bind to lipid bilayers and/or cell membranes with a preference for negatively charged lipids [70-72]. Since the charge distribution in NK-lysin is not conserved in SP-B, amoebapores or saposin C, there might be different interaction modes with membranes.

Chapter 1

2.2 Surfactant Protein C

Human SP-C is encoded by a single gene located on the short arm of chromosome 8 [73]. This 3500 base pair gene contains five introns and six exons. SP-C is expressed as a 179 a.a. proprotein, only in type II cells. Like SP-B, the SP-C proprotein contains N-terminal (a.a. 1 - 23) and C-terminal (a.a. 59 - 179) propeptides. SP-C proprotein is partially translocated through the ER membrane. The observation that a truncated precursor lacking the last 22 amino acids at the C-terminus was restricted to the ER suggests that these amino acids are necessary for intracellular targeting [74].

<i>Human</i>	27	FGIPCCPVHLKRLLIIVVVVVV ^L _S IVVVIVGALLMGL	61
<i>Rabbit</i>	24LV.....	58
<i>Monkey</i>	24LV.....	58
<i>Rat</i>	24	.R.....LV.....	58
<i>Mouse</i>	24	.R.....LV.....	58
<i>Pig</i>		LR.....N.....V.....LV.....	
<i>Sheep</i>	24	LR.....NI.....LV.....	58
<i>Bovine</i>		L.....NI.....LL.....	
<i>Mink</i>	24	.L..F.SS.....I...I.LV.....	58
<i>Dog</i>		L....F.SS.....I...I.LV.....	

Figure 4. Amino acid sequence alignment of SP-C.

Human SP-C is taken as the primary sequence. The number of the N-terminal and C-terminal residues are mentioned. Human (*Homo sapiens sapiens*), rhesus monkey (*Macaca mulatta*), rabbit (*Oryctolagus cuniculus*), Norway rat (*Rattus norvegicus*), house mouse (*Mus musculus*), pig (*Sus scrofa*), sheep (*Ovis aries*), cattle (*Bos taurus*), American mink (*Mustela vison*) and dog (*Canis familiaris*).

Mature SP-C is located on exon 2. The amino acid sequence of mature human SP-C shares a lot of similarity with all known sequences among species, see Fig. 4. Even in the flanking arms of proSP-C the majority of amino acids have been conserved. The amino acids 9-34 of the mature protein (a.a. 32 - 57 of the propeptide) form an α -helix capable of spanning a membrane bilayer [75]. This α -helix is made up of highly hydrophobic a.a., mostly valines and leucines. Although these are not typical α -helix forming amino acids, the SP-C α -helix is still very stable and rigid. The minor part of SP-C that is not spanning a membrane is hydrophobic as well. This is due to the presence of two palmitoyl chains at a.a. 5 and 6 of the mature protein. In a lipid environment the α -helical content is increased and

Function and structure of the surfactant proteins

might extend to these palmitoyl chains [76,77]. The precise function of palmitoylation, which probably occurs during transit from ER to Golgi, is not known. In cytosolic proteins like the G-proteins, palmitoylation might be necessary for their attachment to membranes [78]. For integral membrane proteins palmitoylation is often linked to receptor activation and translocation [79]. Like in SP-C, palmitoylation of these proteins often occurs at cysteines close to a membrane spanning helix and in the proximity of positively charged amino acids. In all species described, the SP-C cysteines have been found to be palmitoylated, no other acylation has been observed. Since the palmitoyl chains do not seem to be necessary for translocation [80], their role could possibly be in maintaining a dense packing during transport in lamellar bodies or in keeping surfactant lipids in very near proximity to the monolayer [12,13,81,82].

In dog and mink the cysteine at position 6 is replaced by a phenylalanine. Since this amino acid contains a bulky hydrophobic group, it might therefore be able to carry out the same functions as a palmitoyl chain. Curiously, canine SP-C has been described to exist in a mono-palmitoylated monomeric form as well as a non-palmitoylated dimeric form [83]. Circular dichroism showed that both canine forms exhibit similar secondary structure. Furthermore, both forms were able to induce the insertion of phospholipids into a monolayer. Contrary to the canine monomeric SP-C, the non-palmitoylated dimeric form did not require calcium ions to insert phospholipids into a neutrally charged phospholipid monolayer. It is not clear whether dimeric canine SP-C is formed by depalmitoylation and subsequent dimerization in secreted surfactant, or that it is formed within the type II cell with or without previous palmitoylation. Moreover, the importance of SP-C dimerization for surface film formation and stability *in vivo* is not known.

In all known species the positive charges at positions 11 and 12, lysine and arginine respectively, have been conserved. These positive charges are thought to be important for SP-C's interaction with the monolayer, especially with negatively charged phospholipids [84]. In rat, mouse, pig and sheep an extra positive charge is present: arginine is found instead of glycine at position 2.

Although the SP-C sequence is the most conserved of all surfactant proteins, there are only a few roles described that are specific for SP-C. The majority of SP-C activities overlap the activities of SP-B. Next to these already described functions, SP-C seems to be important for monolayer film stability [85]. Mutations in the SP-C gene have not yet been identified or shown to cause lung disease. Moreover, SP-C knockout mice have been shown to survive without clear lung dysfunction [22,86]: oxygenation, surfactant pool sizes and phospholipid composition have not changed and respiratory failure was not observed. With these observations in mind one could wonder whether SP-C is really obligatory for the classic role of the surfactant system. However, the SP-C knockout mice have not yet been subjected to stress situations in which a properly working SP-C might be obligatory. Moreover, a combination of scanning force microscopy and fluorescence microscopy showed that compression of saturated lipid films containing SP-C resulted in layered protrusions rich in SP-C [13,81,82]. These protrusions were not found in protein-free films. The protrusions were

Chapter 1

reversibly inserted into the monolayer upon expansion of the surface area. The heights of the protrusions embodied equidistant steps of DPPC bilayers, suggesting an important regulatory role for SP-C in keeping membranes in close proximity to the monolayer at the alveolar air/liquid interface.

3. Structural variation and functions of the hydrophilic surfactant proteins

3.1. Structures of surfactant proteins A and D

The primary structure of SP-A has been determined for the human [87-89], dog [90], rat [91], rabbit [92], mouse [93] and pig [94] protein and is highly conserved in these species. Since the protein is highly conserved across species the discussion on human SP-A also applies, with small variations, to dog, rat, rabbit, mouse, and pig SP-A. SP-A is a large complex molecule assembled from eighteen polypeptide chains [95,96]. The structure of the assembled molecule will be discussed starting with the features deduced from the primary sequence of the polypeptide chain of the human protein.

The primary translation product of human SP-A is 248 amino acids long and has distinct structural domains. The N-terminal part of the primary translation product is a signal peptide of twenty amino acids. This peptide directs the translocation of the protein into the lumen of the rough ER and into the secretory pathway of the cell. The signal peptide is removed during the translocation process. Secreted SP-A has an N-terminal end of seven amino acids that contains a cysteine residue that forms an intermolecular disulfide bond with another polypeptide chain of SP-A. These intermolecular cross-links are important in the alignment of the polypeptide chains during SP-A assembly [97,98]. In the dog, rat and mouse peptide the N-terminal domain contains a consensus NH_2 -linked glycosylation site asparagine-X-threonine (X is any amino acid). The short N-terminal domain is flanked by a domain that is characterized by twenty-four repeating triplets with the sequence glycine-X-Y (X is any amino acid and Y is hydroxyproline) in thirteen of the twenty-four triplets, the collagen domain. The collagen triple helix unfolds when the temperature is raised. Human and canine SP-A have a midpoint transition temperatures of 52.3 ± 1.7 °C and 51.5 ± 1.5 °C, respectively [96]. The sequence of repeating triplets is interrupted between the thirteenth and fourteenth repeat by the sequence proline-cysteine-proline-proline. Rotary shadowing electron microscopy of SP-A suggests that the six collagen triple helices of the molecule form a bundle of about 10 nm in length and about 4.5 nm in diameter along the first thirteen triplets [95]. The break of the collagen-like sequence introduces a flexible kink in the collagen rods in such a way that beyond the thirteenth triplet the six individual triple helices fan out radially from the tightly associated stem (Fig. 1). A similar funnel-shaped structure has been described for complement factor C1q [99] and mannose binding lectin [100]. Both non-covalent and covalent interactions between the helices provide stability to the stem. If the collagen-like domain is modeled as a $7/2$ helical net it becomes apparent that the hydrophobic and charged residues are clustered [96]. This charge distribution may help stabilize the oligomeric

structure of SP-A.

The collagen-like domain is linked to the globular C-terminal carbohydrate recognition domain (CRD) by a stretch of amino acids, the 'neck-region'. The C-terminal domain of SP-A is encoded by a single exon [87] and has structural and functional similarities to domains found in an increasing number of proteins. These proteins bind carbohydrates in a calcium-dependent fashion and are termed C-type lectins [101]. The CRDs of these proteins are characterized by fourteen invariant residues and eighteen that are conserved in character in fixed positions within a 120 - 130 amino acid domain. Four of these residues are cysteines that form two intrachain disulfide bonds that are necessary for carbohydrate binding. The cysteines in SP-A form bonds between residues 135 - 226 and 204 - 218 [96]. The same bonding pattern was observed in lectins from the acorn barnacle [102] and sea urchin [103]. SP-A was the first vertebrate C-type lectin of which the pattern of disulfide pairing was elucidated. Another post-translational modification of this part of SP-A is the N-linked glycosylation of asparagine at position 187. The structure of the predominantly triantennary oligosaccharide has been elucidated [104]. The presence of sialic acid contributes to the charge heterogeneity of SP-A. The oligosaccharide moiety may play a role in the SP-A dependent formation of tubular myelin by 'self-recognition' [105]. The antiviral properties of SP-A may be mediated in part by binding of the oligosaccharide moiety to viral proteins [106]. The oligosaccharide moiety of SP-A isolated from an alveolar proteinosis patient with blood group A is recognized by antibodies directed against A blood group antigens [107]. Antibodies specific for B blood group antigens did not react with SP-A from A or B blood group individuals.

In 1988 Persson and collaborators described the presence of a collagenous glycoprotein in culture medium of freshly isolated rat type II cells [108]. The protein, initially termed CP4 (collagenous protein 4), was also isolated from rat bronchoalveolar lavage and from EDTA extracts of crude rat surfactant [108,109]. CP4 has a molecular mass of 43 kDa under denaturing and reducing conditions, which is higher than that of surfactant protein A (SP-A). Immunologically and with regard to amino acid composition the protein was different from SP-A [108,109]. Isoelectric focusing revealed that both collagenous proteins have different isoelectric points. In contrast to SP-A, CP4, a protein with acidic isoforms, migrates as a charge train of basic isoforms. Basic proteins of 40-45 kDa in surfactant were previously referred to as class D proteins [110]. These observations and the fact that CP4 can be isolated from crude surfactant prompted the renaming of the protein into surfactant protein D (SP-D) in accordance with the accepted nomenclature for proteins associated with surfactant [33]. Post-translational modification of the protein was detected by amino acid analysis. The rat protein contains hydroxyproline, hydroxylysine and acid-labile components co-eluting with hydroxylysine glycosides in line with the collagenous nature of the protein [109]. SP-D contains asparagine-linked oligosaccharides. Endoglycosidase F treatment results in a deglycosylated protein of 40 kDa. The primary *in vitro* translation products of rat and human SP-D have an apparent molecular mass of 39 kDa [111,112]. SP-D consists of four regions: a short N-terminal non-collagen sequence, a collagen domain of fifty-nine Gly-X-Y repeats

SP-D:

Porcine SP-D



Other SP-D's:
Human, Mouse, Rat
and Bovine



Other Collectins:

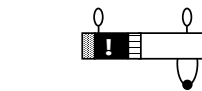
Conglutinin



CL-43



MBL



SP-A



100 Amino
Acids

Figure 5. Graphical comparison of the primary protein sequence of porcine SP-D with other collectins.

Boxes indicate protein domains. From left to right: N-terminal, collagen-like, neck, and carbohydrate recognition domain. The ball and sticks indicate potential N-linked glycosylation sites. The C refers to the presence of a cysteine in the collagen-like region. The exclamation mark indicates a disruption in the collagen region. The loop indicates loop 4 in the X-ray crystal structure of Mannose Binding Lectin. The beads on the loop refer to the number of extra amino acids contained in loop 4 (compared to the smallest loop of only 7 a.a. in SP-A). Open, white symbols for glycosylation sites indicate motifs that are not conserved across all species examined (adapted from [94]).

and a short linking domain ('neck' region) that connects the collagen domain to the fourth region: the C-terminal carbohydrate recognition domain. This latter domain contains all of the invariant residues, including four conserved cysteine residues, characteristic of the family of the Ca^{2+} -dependent C-type lectins. The primary structure of SP-D has been determined for the human [112-114], rat [115], bovine [116] and porcine [94] protein. All studied species thus far have a consensus sequence for asparagine-linked oligosaccharides (Asn-Gly-Ser) within the collagen domain. Porcine SP-D is the only SP-D that also has a consensus sequence for N-linked glycosylation in the carbohydrate recognition domain [94] (Fig. 5). Indeed, recent results showed that porcine SP-D is glycosylated both in the collagen domain

and in the carbohydrate recognition domain (van Eijk *et al.*, unpublished results). Other unique features of porcine SP-D are (1) an extra cysteine residue in the collagen region and (2) an insertion of three amino acids close to the carbohydrate binding region. These features may have important structural and functional implications.

Thus, SP-D is a member of the fast growing family of calcium-dependent C-type lectins. Like SP-A it belongs to the sub-group of collectins, proteins that may play an important role in the first-line defence system [117]. Mannose binding lectin (MBL) is structurally, and maybe also functionally, equivalent to SP-A. SP-D also has its counterpart in the circulation: conglutinin. This protein has been described first in the beginning of the twentieth century. Electron microscopy revealed that conglutinin is an X-shaped tetramer of four lollipop structures emanating from a central hub [118]. SP-D was found to have a similar cruciform structure by rotary shadowing electron microscopy. These SP-D dodecamers can self-associate at their N-termini to form highly ordered multimers [119]. The collagen domain of SP-D is much longer than that of SP-A (59 vs. 24 Gly-X-Y repeats). Furthermore, the collagen domain of SP-D has no kink in the triple helix. This results in a length of the collagen triple helix of about 46 nm (Fig. 1).

3.2. Functions of surfactant proteins A and D

The localization, structure and properties of SP-A have led to speculations on the possible physiological functions of this protein. SP-A was the first protein detected in pulmonary surfactant. Not surprisingly, the initial studies were aimed to find out whether SP-A has a role in surface film formation. After the demonstration that surfactant deficiency can be effectively treated with natural surfactant preparations containing SP-B and SP-C but not SP-A, SP-A was not considered to be important in surface film formation. From the clinical point of view this may have been true but intratracheal surfactant instillation is very different from a physiological situation that requires constant regulation of extracellular surfactant metabolism. A role has been attributed to SP-A in the regulation of surface film formation [120]. These observations are probably in some way related to the role of SP-A in tubular myelin formation. Tubular myelin, a structure formed from secreted lamellar bodies, is thought to be the structure from which the surface film forms *in vivo*. From work on the immunolocalization of SP-A [121] and *in vitro* reconstitution [17,122] it is clear that tubular myelin formation is dependent on the presence of SP-A. In tubular myelin SP-A has a preferential localization suggesting that the protein provides the framework of this lattice [123]. The SP-A - SP-A interactions may be mediated in part by CRD - oligosaccharide interactions [105]. In lungs of infants dying from respiratory distress syndrome, the lack of tubular myelin correlates with SP-A deficiency [124]. A second physiological function of SP-A was thought to be the regulation of surfactant homeostasis. This putative function of SP-A has been suggested because the protein modulates uptake and secretion of phospholipids by isolated alveolar type II cells *in vitro*. SP-A binds with a high affinity to type II cells [125,126]. In the presence of SP-A more lipids from radioactive liposomes are associated with alveolar type II cells in suspension [127]. SP-A has also been shown to inhibit

Chapter 1

secretion of phosphatidylcholines by type II cells that were labeled overnight with labeled choline [128,129]. Taken together these *in vitro* studies suggest that SP-A may play a role in regulating alveolar pool size by balancing surfactant release and clearance. However, Korfhagen *et al.* showed that SP-A knock-out mice show no signs of respiratory problems [130]. Therefore, the main function of SP-A is probably neither its role in surface film formation nor in surfactant homeostasis but its role in innate host defence, as will be discussed below.

Although termed surfactant protein D, it is not immediately clear how this protein would play a role in surfactant homeostasis. SP-D is not a real surfactant protein in the true sense since about 90 % of the protein present in 48,000 g supernatants of lavages from normal rats is not associated with lipids [109]. In 10,000 g supernatants 92 % of total SP-D is present [131]. One of the few indications that SP-D could be involved in surfactant metabolism were the observations that SP-D may be associated with lipids under some conditions [132]. SP-D binds to phosphatidylinositol [133,134] and to glucosylceramide [135]. Therefore, it was a great surprise that SP-D knock-out mice show altered surfactant lipid homeostasis [136,137]. It will be exciting to determine how SP-D modulates surfactant lipid turn-over. It is tempting to speculate that in the absence of SP-D the balance between anti- and pro-inflammatory effector molecules in the lung is disturbed leading to lipid accumulation. The role of SP-D in innate host defence will be discussed below. The reader is referred to the excellent reviews by McCormack and Crouch for more information on structure and properties of SP-A and SP-D [27,138].

3.3. Surfactant proteins A and D and host defence

The lung exhibits a large epithelial surface which is continuously exposed to the environment. The fact that pulmonary infections are uncommon in most animals suggests the existence of efficient defence mechanisms in the lung that are capable of eliminating microorganisms before they cause disease. Several non-specific and specific defence systems have evolved to protect the lung. It has been appreciated for many years that non-specific, innate mechanisms must be important components of this defence system, particularly in the period between maternally acquired immunity and development of the adaptive immune system, in the time interval between first exposure to a pathogen and generation of specific antibodies, and in states of impaired immune function. SP-A and SP-D are believed to be molecules of this innate immune system through their ability to recognize a broad spectrum of pathogens. Several studies have shown that SP-A and SP-D interact with a number of viruses, bacteria and fungi [28,29], and with inhaled glycoconjugate allergens, such as pollen grains [30] and mite allergens [139]. Furthermore, SP-A and SP-D have been shown to bind to alveolar macrophages, which carry receptors for SP-A and SP-D on their surface. In general, interaction of SP-A with pathogens and phagocytes leads to an increased uptake of pathogens. Binding of SP-D with pathogens results in agglutination, but there are contrasting reports on whether this interaction leads to increased or decreased phagocytosis of microorganisms.

Mucosal surfaces of the gastrointestinal, respiratory, and genitourinary tract are the sites where more than 95 % of infections are initiated. Thus, mucosal immunity is an important arm of the immune system because it operates in tissues involved in everyday infectious defence as well as in tolerance against environmental and dietary antigens. SP-A and SP-D may also be important host defence molecules in extrapulmonary mucosal compartments, such as the gastrointestinal tract, where the plasma-based complement system is virtually absent. Surfactant-like materials have now been reported in a wide variety of tissues, including middle ear duct, oesophagus, stomach, and intestine [140]. In view of the presence of surfactant-like materials at various mucosal surfaces, several studies have been performed that describe the presence of surfactant-associated proteins in these extrapulmonary tissues. The interactions of SP-A and SP-D with pathogens and phagocytes have recently been reviewed [27-29,141]. For more information on the role of surfactant proteins in the digestive tract and mesentery the reader is referred to the article by Bourbon [278].

4. A possible role for the surfactant proteins through evolution

Pulmonary surfactants have been documented in the lungs of all air-breathing vertebrate groups [142,143]. Especially surfactant lipids have been extensively researched. In mammals two important functions of surfactant are (1) providing alveolar stability and (2) increasing the compliance of the relatively stiff bronchoalveolar lung. Contrary to mammals of similar body size, the respiratory units (faveoli) in most non-mammals are circa 1000-fold larger and 100-fold more compliant. Moreover, faveoli have an enhanced backbone of elastin and collagen and an inner trabecular network that supports and stabilizes the interconnecting units. Therefore, in non-mammalian vertebrates surfactant is not obligatory for alveolar stability and improvement of compliance. Furthermore, contrary to mammalian surfactants, in amphibians, fish and most reptiles the surface activity of surfactant is generally very low. This correlates with a low body temperature and a low content of disaturated phospholipids. The activity of surfactant in these animals is purely detergent-like: reducing surface tension without the ability to vary surface tension greatly with surface area. Therefore, in non-mammals surfactant is thought to act as an 'anti-glue', preventing adhesion of respiratory surfaces during lung collapse (like during expiration or during diving at depths when external compression forces are elevated). For this function a surfactant displaying only a relatively low surface activity is suitable, like the surfactants found in reptiles and amphibians. This may represent the primitive function of surfactant in vertebrate lungs.

The presence of SP-A protein and mRNA in members of all vertebrate groups has been used as a proof that the surfactant system had a single evolutionary origin in the vertebrates [144]. However, it should be realized that SP-A (and SP-D) are present in extrapulmonary tissues as has been discussed in the preceding section. Since these collectins may have a general role in innate mucosal immunity, their presence in many vertebrates may

Chapter 1

not be a good indicator for the evolutionary origin of surfactant. The C-type lectin domain is a widespread motif in the animal kingdom. On the basis of structural analogies between proteins, different fields converged and a renaissance of (C-type) lectin biology was started in immunology. Although there are still many unanswered questions it may be concluded that many mosaic proteins containing C-type carbohydrate recognition domains have important immunological functions in vertebrates. The presence of hybrid proteins with C-type carbohydrate recognition domains has also been described in invertebrates [145,102,103]. These proteins may fulfill a primitive immune function in lower organisms [146]. Proteins containing CRD are a subfamily of a superfamily of proteins containing C-type lectin-like domains (CTLD). Members of this superfamily do not necessarily recognize saccharides but may recognize certain protein motifs. The evolution of the C-type lectin-like domain fold was recently reviewed by Drickamer [147]. Examination of the genome sequence of *Caenorhabditis elegans* revealed that at least 125 proteins encoded by this organism contain C-type lectin-like domains [148]. In these 125 proteins 19 domains show conservation of the features found in vertebrate C-type carbohydrate-recognition domains. A small subset of 7 domains may have mannose and N-acetyl glucosamine binding properties similar to proteins from vertebrates containing these domains. The role of proteins of the C-type lectin superfamily in the immune system has recently been reviewed [149].

There is a clear relationship between SP-B, surface activity and the complex lungs of mammals. Therefore, if surfactant is poorly surface active, then it is unlikely that SP-B will be present. Intermediate to high surface activity was found for surfactant of certain reptiles and birds [143]. Unfortunately, only scarce information is available about the presence of SP-B in these classes of higher vertebrates. In chicken, SP-B is detected in the epithelial cells of parabronchi [150], and found to be surface active when isolated from the air capillaries, as measured by CBS [279]. SP-B was furthermore seen in respiratory epithelium cells of turtle [151] and salamander [152]. These proteins were detected by antibodies raised against bovine SP-B. It will be interesting to purify and sequence these immunoreactive proteins to determine the resemblance of SP-B of reptiles, amphibians and birds to SP-B of mammals. Furthermore, measurements in a system like a captive bubble surfactometer in which surfactant components can be tested separately would give more insight into the surface activity of the hydrophobic surfactant proteins of these animals compared to that of mammals.

Most animal lungs do not have the folds and sacs present in mammals. When considering the difference in lung structure in these animals, as opposed to mammals, and when applying the idea of surfactant's main function as an anti-glue in these animals, it devalues the function of the hydrophobic proteins as surface activity regulators in non-mammals. Since the main function of SP-B and SP-C in mammalian lungs is to aid in regulating the surface tension, both proteins could be absent in the majority of non-mammals. Alternatively, they could have a different function (a more "static" one, like aiding in the formation of a monolayer from subphase structures, instead of a "dynamic" one, like the formation and maintenance of a surface-associated reservoir), or their secondary function in mammals could be their primary function in non-mammals. Since it has been found that the

Function and structure of the surfactant proteins

saposin-class proteins NK-lysin and the amoebapore proteins are able to form channels in membranes, and since LPS-deacylating enzyme has been found to contain a saposin-like domain, the role of SP-B in primitive lungs could be mainly in lung defence. Considering the possibility to survive in non-stress situations without the presence of SP-C in the lung, this protein might not at all be present in the earliest life-forms containing respiratory structures.

Many factors, including body temperature, habitat and lung structure can alter surfactant lipid composition, suggesting that lipids are not suitable evolutionary indicators. Surfactant proteins may be better evolutionary indicators. However, the presence of particularly SP-A and SP-D in extrapulmonary tissues suggests that these lung collectins are not the most reliable indicators of the evolution of the pulmonary surfactant system. Furthermore, the surfactant proteins which have been most conserved are the hydrophobic ones. Hence, hydrophobic surfactant proteins may be the most appropriate indicators for the evolutionary origin of surfactant. SP-C may be the most important indicator for the evolutionary origin of mammalian surfactant, because it has a unique structure and it is only localized in the mammalian lung, in contrast to other surfactant proteins.

Acknowledgments

Paul Deley and Co Eyndhoven are acknowledged for their art work. This work was financially supported by the Netherlands Foundation for Chemical Research and by the Netherlands Asthma Foundation.

Chapter 2

Effect of the Hydrophobic Surfactant Proteins on the Surface Activity of Spread Films in the Captive Bubble Surfactometer

Edwin J.A. Veldhuizen ^{a,*}, Robert V. Diemel ^{a,b,*}, Günther Putz ^b,
Lambert M.G. van Golde ^a, Joseph J. Batenburg ^a and Henk P. Haagsman ^{a,c}

* Both authors contributed equally to this study

^a Department of Biochemistry and Cell Biology, and ^c Department of the Science of Food of Animal Origin, Faculty of Veterinary Medicine, Institute of Biomembranes and Graduate School of Animal Health, Utrecht University, Utrecht, The Netherlands

^b Department of Anaesthesiology and Critical Care Medicine,
The Leopold-Franzens-University of Innsbruck, Innsbruck, Austria

Chemistry and Physics of Lipids, 2001, **110**: 47-55

Abstract

The main function of pulmonary surfactant, a mixture of lipids and proteins, is to reduce the surface tension at the air/liquid interface of the lung. The hydrophobic surfactant proteins SP-B and SP-C are required for this process. When testing their activity in spread films in a captive bubble surfactometer, both SP-B and SP-C showed concentration dependence for lipid insertion as well as for lipid film refinement. Higher activity in DPPC refinement of the monolayer was observed for SP-B compared to SP-C. Further differences between both proteins were found when subphase phospholipid vesicles, able to create a monolayer-attached lipid reservoir, were omitted. SP-C containing monolayers showed gradually increasing minimum surface tensions upon cycling, indicating that a lipid reservoir is required to prevent loss of material from the monolayer. Despite reversible cycling dynamics, SP-B containing monolayers failed to reach near-zero minimum surface tensions, indicating that the reservoir is required for stable films.

1. Introduction

Pulmonary surfactant is a mixture of lipids and specific proteins which is secreted into the alveolar fluid by the alveolar type II cells. Its main function is to reduce the surface tension at the air/liquid interface in the lung. This is achieved by forming a surface film that consists of a lipid monolayer which is highly enriched in dipalmitoylphosphatidylcholine (DPPC) and bilayer lipid/protein structures closely attached to it (the 'lipid reservoir'). The surface film reduces the work of breathing and prevents alveolar collapse upon end-expiration. The existence of such a film *in vivo* has been visualized by electron microscopy [153,12].

The highly hydrophobic surfactant specific proteins B and C (SP-B and SP-C) are required for several aspects of surface film homeostasis. They induce a rapid insertion of lipids into the air/liquid interface upon inspiration. This lowers the surface tension which, in turn, prevents serum components from entering the interface and interfering with the surfactant system. Besides that, SP-B and SP-C are also involved in the DPPC enrichment of the monolayer (for review, see [154]). An enrichment of the monolayer in DPPC is required to create stable surface films with near-zero surface tensions upon expiration which prevents alveolar collapse during breathing.

SP-B is a homodimer of approximately 17 kDa. Secondary structure analysis and homology with related proteins, especially members of the saposin-like family [49,155] predict an SP-B structure that contains four amphipathic α -helices [61]. These helices are thought to interact with the surfactant lipids with a specific interaction between anionic lipids and the positive charges of SP-B [56,156]. SP-C is a 4.2 kDa protein containing 35 amino acids and is very conserved among species. Its structure in solution has been completely resolved [75]. SP-C contains a valyl-rich α -helix which can exactly span a lipid bilayer. Other

characteristics are two palmitoylated cysteines at positions 5 and 6 and two conserved positively charged amino acids at positions 11 and 12, which are thought to interact with negatively charged lipid head groups.

Several model systems have been developed to test the surface activity of the hydrophobic surfactant proteins by mimicking the situation within the alveoli. In this study we used a pressure driven captive bubble surfactometer (CBS), which has several advantages over other systems used [25]. The proteins can be tested under dynamic conditions and lipid/protein mixtures can be spread at the interface, making the exact composition at the surface known at the start of the experiments [26]. The pressure driven CBS has already been used to test SP-B / SP-C mixtures [157]. These experiments showed a concentration dependent surface activity of the proteins. Here we extend these studies and test SP-B and SP-C separately to increase our insight into the individual roles of the proteins in lipid adsorption, lipid reservoir formation and DPPC enrichment of the surface monolayer.

2. Materials and Methods

2.1. Materials

1,2-dipalmitoyl-*sn*-glycero-3-phosphocholine (DPPC) and 1-palmitoyl-2-oleoyl-*sn*-glycero-3-phospho-*rac*-(1-glycerol) (POPG) were obtained from Avanti Polar Lipids Inc. (Alabaster, AL), HEPES was from Life Technologies (Paisley, Scotland), EDTA, calcium chloride (CaCl₂), chloroform (CHCl₃) and methanol (MeOH) were from Baker Chemicals B.V. (Deventer, the Netherlands). Organic solvents were distilled before use. Bovine SP-B and porcine SP-C were isolated from lung lavage as described previously [158].

2.2. Vesicle preparation

Small unilamellar vesicles (SUV) and multilamellar vesicles (MLV) were prepared as follows. Lipids (DPPC/POPG, 8/2, mol/mol) from stock solutions in CHCl₃/MeOH (1/1, v/v) were dried under a continuous stream of nitrogen at room temperature. The resulting dry lipid film was rehydrated by adding subphase buffer (140 mM NaCl, 10 mM HEPES, 0.5 mM EDTA, 2.5 mM CaCl₂, pH 6.9), incubating at 55 °C for 15 min and extensive vortexing. The multilamellar vesicles thus formed were sonicated two times 1 min at 55 °C with a 10 s interval to prepare SUV. The vesicles (MLV after rehydration or SUV after sonication) were cooled to 37 °C and used immediately.

2.3. Captive Bubble Surfactometry

The surface activity of surfactant proteins B and C was determined using a pressure driven captive bubble surfactometer. A detailed description of this method has been published [25,26]. Briefly, a bubble (0.5 cm²) was formed in the sample chamber containing subphase buffer by injecting air (28.5 μl) into the sample chamber at 1.0 bar and 37 °C. A stock solution of DPPC/POPG (8/2, mol/mol) with or without surfactant proteins was prepared in

Chapter 2

CHCl₃/MeOH (1/1, v/v). From this stock solution 0.05 μ l (0.25 nmol lipids) was spread at the air/liquid interface using a glass syringe (7000.5, blunt tip, Hamilton, Bonaduz, Switzerland). The subphase was stirred for 60 min to enhance desorption of solvent, after which the sample chamber was perfused with 7 ml buffer over a period of 30 min. Subsequently, 30 μ l SUV or MLV (DPPC/POPG, 8/2, mol/mol) or buffer was injected into the subphase (final concentration 1 mg DPPC/ml) and stirring was continued for another 15 min. The bubble area was increased by sudden lowering of the pressure to 0.5 bar for 10 s. Subsequently, the pressure inside the sample chamber was cycled five times between two preset pressure values of 0.5 and 2.8 bar in 1 min, resulting in a dynamic compression and expansion of the air bubble. The shape and surface area of the bubble depended on the surface tension. At maximal bubble expansion (maximal surface tension) the area was 1.0 cm². At maximal bubble compression (minimal surface tension) the area ranged from 0.5 cm² at surface tensions lower than 1 mN/m to 0.25 cm² at 20 mN/m. A video camera continuously monitored the shape of the bubble, from which the surface tension values were calculated.

3. Results

The effect of SP-B and SP-C on surface activity of spread films was tested in a pressure driven CBS. Both proteins showed a concentration dependence which is shown in Fig. 1. The surface tension at maximum bubble size (γ_{\max}) dropped from 67 mN/m for the protein-free sample to approximately 40 mN/m for 0.5 mol% SP-B and 3 mol% SP-C at the fifth cycle. The surface tensions at minimum bubble size (γ_{\min}) were all lower than 2 mN/m, also for the protein-free sample. This implies that enough material, especially DPPC, was spread at the surface to be able to reach these low values upon compression. However, also in the γ_{\min} values a protein concentration dependence is observed which is depicted for SP-C in Fig. 2B. For SP-B this was not clearly observed (Fig. 2A).

In the next set of experiments DPPC/POPG (8/2, mol/mol) surface films were spread containing 0.5 mol% SP-B, 5 mol% SP-C or no proteins. This high percentage of SP-C was chosen to maintain the SP-B:SP-C ratio of 1:10 normally found in pulmonary surfactant [159,57] and to maintain the ratio used in an earlier previous study, in which a mixture of both proteins was used [157]. The contents of the subphase was varied by injecting SUV, MLV or no vesicles into the sample chamber, after which cycling was performed. To test the ability of SP-B and SP-C to respread a phospholipid film after bubble compression, a pressure of 4.0 bar was used to induce a larger overcompression of the bubble. The presence of subphase vesicles, with a more pronounced effect for SUV than for MLV, resulted in lowered γ_{\max} values. When no subphase vesicles were present, a surface tension at the first bubble expansion of 54 mN/m was observed, versus 32 and 23 mN/m for MLV and SUV, respectively. No significant differences were observed between SP-B and SP-C. Interestingly, the γ_{\min} values changed more drastically. When vesicles (MLV or SUV) were present, very low γ_{\min} values were reached, comparable to the results in Fig. 1 and 2, both in the presence

Effect of SP-B and SP-C on spread surface films

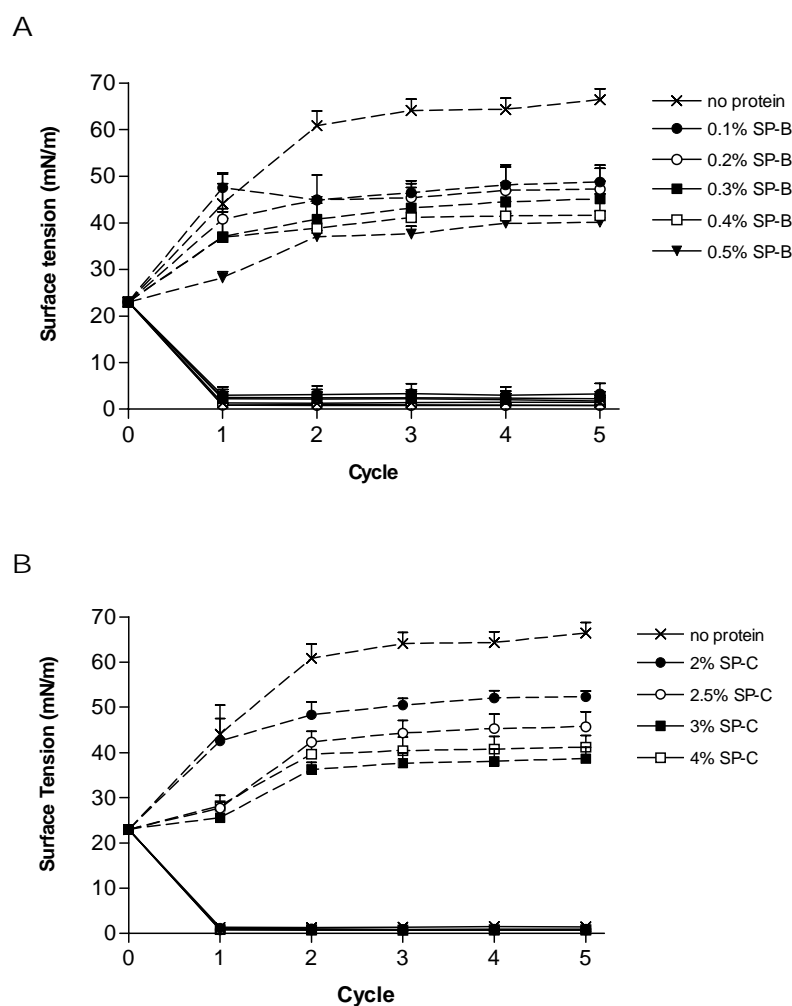


Figure 1. Effect of SP-B and SP-C on the surface tensions of an air bubble during cycling in the presence of SUV.

Concentration curves of SP-B (A) and SP-C (B) are shown. Dashed lines represent γ_{\max} values, solid lines represent γ_{\min} values. Values shown are the average of at least three separate experiments \pm SEM.

or absence of proteins (not shown). However, when no lipid vesicles were present, the SP-B containing film failed to reach near-zero surface tensions and a γ_{\min} of approximately 10 mN/m at each compression was observed (Fig. 3). When SP-C was present in the surface film, very low γ_{\min} was reached upon the first compression, but a step-wise increase towards 17 mN/m at the fifth compression was seen. We interpret this increase as an irreversible loss of material from the surface film upon each compression. When no proteins were incorporated in the film, an average minimum surface tension of approximately 15 mN/m was observed. However, in this set of experiments a strange phenomenon was seen. In two out of six experiments a very low minimum surface tension was achieved throughout the whole cycling procedure, while the other four experiments resulted in high γ_{\min} values of approximately 20 mN/m. No γ_{\min} values in between these two extreme values were observed.

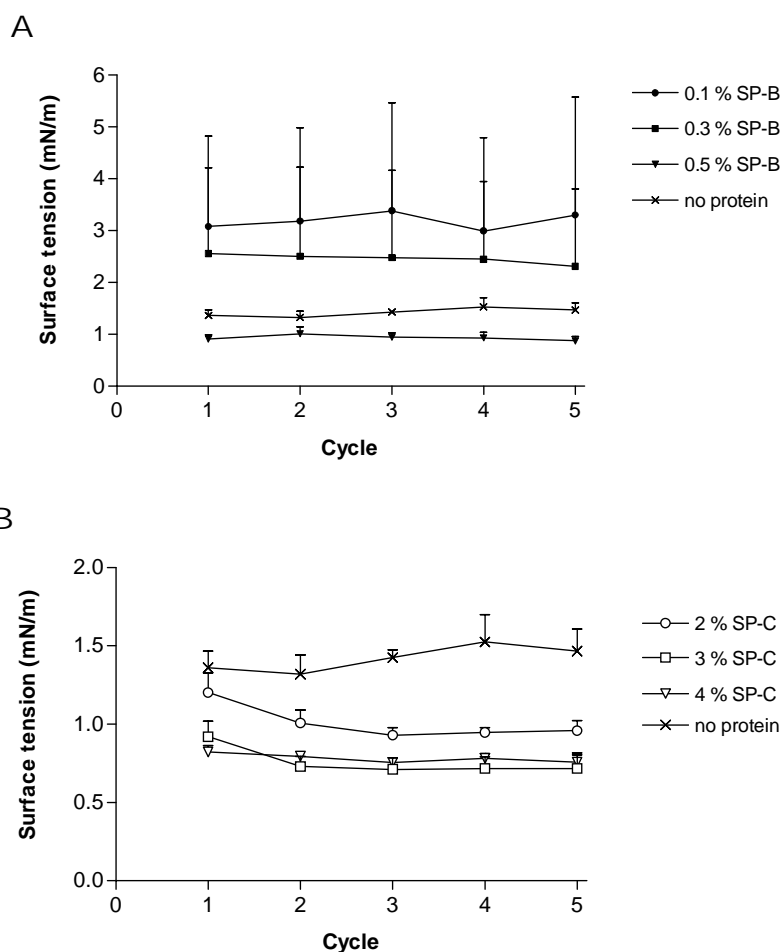


Figure 2. Concentration dependence of SP-B and SP-C on the minimum surface tensions during cycling in the presence of SUV.

Concentration curves of SP-B (A) and SP-C (B) are shown. Values shown are the average of at least three separate experiments \pm SEM.

The area reduction required to reach very low surface tensions can be calculated from area - surface tension isotherms. Also the compressibility at 15 mN/m can be determined from these isotherms. Both values are considered to be indicative for the enrichment in DPPC of the protein/lipid monolayer at the interface. The area reduction that is required to lower the surface tension from 20 mN/m to 2 mN/m and the compressibility at 15 mN/m were calculated for a number of SP-B and SP-C concentrations for the first, second and fourth cycle. These values are depicted in Table 1. Both values showed the same pattern: the SP-B containing samples had lower compressibility and required less area reduction than the SP-C containing samples. For both proteins the enrichment was essentially completed at the second cycle, although a slight indication for further refinement of the film was observed for most SP-B containing films.

4. Discussion

In this article we describe the effect of the inclusion of the hydrophobic surfactant proteins SP-B and SP-C in a DPPC/POPG lipid mixture, when spread at the interface of an air bubble in the captive bubble surfactometer. Both proteins showed a clear concentration dependence with maximum activity at 3 mol% SP-C and 0.5 mol% SP-B. Although the clearest differences were observed in the maximum surface tensions (Fig. 1), the γ_{\min} values were also concentration dependent (Fig. 2). Without surfactant proteins present, the γ_{\min} values were just above 1 mN/m, while significantly lower γ_{\min} values were observed when SP-B or SP-C was present. This could imply that the composition of the surface film was altered and the last traces of unsaturated lipids were removed by the proteins. Alternatively, the film structure, including the lipid reservoir, could be altered by the presence of SP-B or SP-C in such a way that the film can withstand these lower surface tensions (higher surface pressures). Increasing concentrations of protein led to decreasing minimal surface tensions during cycling. For SP-C, a plateau value is reached at 3 mol% SP-C. For SP-B, larger variations in minimal surface tensions at lower protein concentrations were measured when repeatedly doing the experiment. We cannot give a satisfactory explanation for these variations.

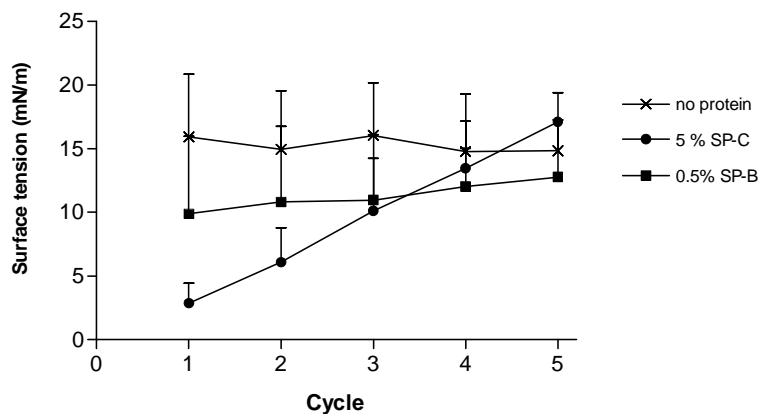


Figure 3. Minimum surface tensions of films containing SP-B, SP-C, or no protein during cycling in the absence of subphase vesicles.

Values shown are the average of at least three separate experiments \pm SEM.

An interesting feature was observed when no lipid vesicles were present in the subphase (Fig. 3). Upon compression of the air bubble it is assumed that mainly non-saturated lipids (here POPG) and the hydrophobic proteins will be squeezed out of the monolayer [160-162]. When no protein was present in the spread film either a near-zero minimum surface was reached or a high minimum surface tension of approximately 20 mN/m ('all-or-nothing'). The

Chapter 2

CBS offers a highly controlled experimental environment, but apparently small differences in the separate experiments determined whether POPG was properly squeezed out of the interface upon compression (resulting in the near-zero γ_{\min}). We do not have a logical explanation for this all-or-nothing behavior of pure lipid surface films. In contrast with these protein-free lipid films, γ_{\min} values covering the whole area in between the two extremes of 2 and 20 mN/m were observed in surface films containing SP-B or SP-C .

If SP-C was present in the surface film, the γ_{\min} increased step-wise upon each cycle (Fig. 3). This implies that when subphase lipid vesicles are not present, some of the squeezed-out protein and lipids cannot stay attached to the monolayer and are lost into the subphase. The graduality of the increase shows that during every cycle some more material is lost. This is supported by Wilhelmy balance monolayer studies in which it was observed that SP-C is partly squeezed out at a surface pressure of 55 mN/m (surface tension of 15 mN/m at 37 °C) together with 7 - 10 lipids per SP-C molecule [162]. A completely different behavior was observed when SP-B containing films were cycled without lipid vesicles in the subphase. Upon the first compression the film reached a γ_{\min} of approximately 10 mN/m. Contrary to the SP-C containing films, no significant increase in the γ_{\min} values was observed upon cycling. This implies that no material is irreversibly lost into the subphase from SP-B containing films. Apparently, SP-B does not require a lipid reservoir adsorbed from subphase vesicles to stay attached to the monolayer. Lipids excluded from the interface upon compression might suffice to form a mini lipid-reservoir in which SP-B is partly located. Recently the formation of disc-like protrusions of SP-B containing phospholipid film upon compression was described [163, chapter 4 of this thesis]. Although SP-B does not require subphase vesicles to stay attached to the monolayer, it does require lipid subphase vesicles to create stable films with very low minimum surface tensions (compare Fig. 1 and Fig. 3). This might be explained by the dimeric structure of SP-B. Both monomers of SP-B will interact with lipids because of their hydrophobicity. A likely localization of SP-B in CBS experiments might be between membranes: one monomer in the lipid monolayer at the interface and the other monomer in the lipid bilayer of the lipid reservoir. If lipid bilayer structures are not present (without injected subphase vesicles), SP-B might be forced into an irregular shape and lose some of its activity, resulting in the higher γ_{\min} values.

When the observed gradual loss of surface-active material from the surface film in experiments with a vesicle-free subphase (Fig. 3) is due to the loss of SP-C into the subphase, this seems to be contradictory to some experiments performed with spread films in a Wilhelmy balance [164,81,82]. In these experiments a monolayer of lipids and SP-C was spread and decreasing the surface area resulted in a collapse of the monolayer. The collapse occurred in domains rich in SP-C and the formation of bilayer lipid structures under these domains was visualized by fluorescence techniques and scanning force microscopy. The latter technique showed that phospholipid bilayers were stacked in these structures and piles of up to four bilayers were found. Upon expansion of the surface area these lipid stacks were inserted into the monolayer again. The discrepancy with our experiments could be due to the fact that we used a fast dynamic system of multiple compressions and expansions, whereas

Effect of SP-B and SP-C on spread surface films

Kramer *et al.* and von Nahmen *et al.* used a slower static system with a single compression. Alternatively, it could be due to the different lipid composition used in the experiments, since we used POPG as anionic lipid, while the saturated DPPG was used in the Wilhelmy balance studies.

Table 1. The percentage area reduction required to decrease the surface tension from 20 mN/m to 2 mN/m and the compressibility at 15 mN/m (in 10^{-3} m/mN) for spread films containing SP-B or SP-C. Protein concentrations are given as mol%.

	% area reduction			compressibility at 15 mN/m		
	1 st cycle	2 nd cycle	4 th cycle	1 st cycle	2 nd cycle	4 th cycle
no protein	27 ± 4.6	22 ± 5.2	22 ± 4.4	23 ± 5.0	15 ± 2.6	17 ± 4.4
0.1% SP-B	24 ± 5.5	19 ± 4.3	20 ± 6.8	33 ± 24	13 ± 7.0	16 ± 9.6
0.2% SP-B	23 ± 8.1	20 ± 5.0	15 ± 3.6	11 ± 5.5	11 ± 3.4	8.3 ± 2.1
0.3% SP-B	23 ± 8.2	20 ± 3.0	18 ± 2.7	10 ± 3.3	11 ± 1.1	8.7 ± 1.6
0.4% SP-B	28 ± 6.0	19 ± 4.8	16 ± 5.2	12 ± 3.6	8.8 ± 1.6	7.5 ± 2.0
0.5% SP-B	17 ± 8.3	17 ± 2.9	13 ± 5.6	9.2 ± 5.6	8.8 ± 1.7	6.3 ± 3.4
2% SP-C	27 ± 2.9	24 ± 1.1	21 ± 1.9	17 ± 5.3	14 ± 1.5	13 ± 2.6
2.5% SP-C	24 ± 5.5	22 ± 2.8	19 ± 1.6	13 ± 3.7	12 ± 1.5	11 ± 4.0
3% SP-C	28 ± 4.2	21 ± 2.2	19 ± 3.2	14 ± 4.4	13 ± 1.8	11 ± 3.4

More area reduction of the air bubble was required to decrease the surface tension from 20 mN/m to 2 mN/m upon compression when SP-C was present at the air/liquid interface than when SP-B was present (Table 1). When we regard these values as being indicative of the amount of DPPC present at the interface at 20 mN/m, this may suggest that SP-C is not as effective in DPPC enrichment as SP-B. However, part of the observed extra area reduction that was required might be caused by the squeeze-out of SP-C at a surface tension of 15 mN/m. At these surface tensions, SP-B is not present anymore in the monolayer [165] and therefore the extra area reduction is not required. In this model, SP-B is present in the lipid reservoir which is attached to the monolayer. A plateau at 15 mN/m in the surface tension - area isotherms should be observed when SP-C is squeezed out of the monolayer upon compression. Unfortunately, we were not able to clearly detect these plateaus due to the fast compression of the bubble in our experimental setup. Only a few video frames are available per compression and the bubble is sometimes forced into an irregular shape by the pressure applied to it. Since it is impossible to determine the area and the surface tension of deformed non-symmetrical bubbles, they were not used to calculate the isotherms.

It remains remarkable that two structurally completely different proteins possess so

Chapter 2

many overlapping activities. SP-B usually has a stronger effect on surface activity than SP-C, both on a molar or weight basis. This is not only observed in this study, but also in Wilhelmy balance, pulsating bubble surfactometer and other CBS studies [158,157,85,166,72]. However, it is unlikely that SP-C is only used as a back-up protein for SP-B or vice versa. Most of the model systems that are used to test these proteins are relatively simple, especially concerning the composition of the subphase vesicles and the spread film. The interaction of SP-B and SP-C with other lipids present in pulmonary surfactant or the interaction with SP-A might have to be tested to discover the molecular mechanism by which SP-B and SP-C fulfill their roles. For example, the importance of the lipid composition was recently shown by Nag *et al.* In these studies, SP-B could refine a lipid monolayer upon cycling when DPPC/POPG mixtures were used, but not when POPG was replaced by POPC [167].

Recently, SP-C knock-out mice have been produced [22,86]. Surprisingly, and contrary to SP-B knock-outs [168], these mice do not seem to experience any respiratory failures. Also the surfactant pool size and lipid composition were not altered by the lack of SP-C in the lungs. This could imply that in normal situations the specific functions of SP-C are not required or that they could be taken over by another protein, probably SP-B. It will be very interesting to see in the near future how these mice will react to respiratory stress situations, which might help to elucidate the *in vivo* role of SP-C in surfactant.

In summary, we tested the surface activity of SP-B and SP-C in a pressure driven captive bubble surfactometer. Maximum activity, both in lipid insertion and refinement, were observed for 0.5 mol% SP-B and 3 mol% SP-C. Minimum surface tensions upon compression of the air bubble were also affected by the presence of SP-B and SP-C. Remarkable differences were observed for SP-B and SP-C when no lipid vesicles were present in the subphase, and no lipid reservoir can be formed. Upon cycling, SP-C containing monolayers showed gradually increasing minimum surface tensions, indicating that the lipid reservoir is required to prevent loss of material from the monolayer. SP-B containing monolayers had reversible cycling dynamics but failed to reach near-zero minimum surface tensions, indicating that the lipid reservoir is required for stable minimum surface tensions.

Acknowledgments

We thank Barbara Hotter and Monika Walch for their help with the CBS experiments. This research was supported by the Netherlands Foundation for Chemical Research (S.O.N.).

Chapter 3

Effects of Cholesterol on Surface Activity and Surface Topography of Spread Surfactant Films

Robert V. Diemel ^{a,b}, Margot M.E. Snel ^c, Lambert M.G. van Golde ^a, Günther Putz ^b,
Henk P. Haagsman ^{a,d} and Joseph J. Batenburg ^a

^a Department of Biochemistry and Cell Biology, and ^d Department of the Science of Food of Animal Origin, Faculty of Veterinary Medicine, Graduate School of Animal Health, Utrecht University, Utrecht, The Netherlands

^b Department of Anaesthesiology and Critical Care Medicine, The Leopold-Franzens-University of Innsbruck, Innsbruck, Austria

^c Department of Interfaces, Faculty of Chemistry, Utrecht University, Utrecht, The Netherlands

Submitted for publication, 2001

Abstract

Pulmonary surfactant forms a monolayer of lipids and proteins at the alveolar air/liquid interface. Although cholesterol is a natural component of surfactant, its function in surface dynamics is unclear. To further elucidate the role of cholesterol in surfactant, we used a captive bubble surfactometer (CBS) to measure surface activity of spread films containing dipalmitoylphosphatidylcholine/1-palmitoyl-2-oleoyl-phosphatidylcholine/1-palmitoyl-2-oleoyl-phosphatidylglycerol (DPPC/POPC/POPG, 50/30/20, molar percentages), surfactant protein B (SP-B, 0.75 mol%) and/or SP-C (3 mol%) with up to 20 mol% cholesterol. A cholesterol concentration of 10 mol% was found to be optimal for reaching and maintaining low surface tensions in SP-B containing films, whereas it led to an increase in maximum surface tension in films containing SP-C. No effect of cholesterol on surface activity was found in films containing both SP-B and SP-C. Atomic force microscopy (AFM) was used, for the first time, to visualize the effect of cholesterol on topography of SP-B and/or SP-C containing films compressed to a surface tension of 22 mN/m. The protrusions found in the presence of cholesterol were homogeneously dispersed over the film, whereas in the absence of cholesterol protrusions tended to be more clustered into network structures. Furthermore, differential scanning calorimetry (DSC) showed that cholesterol broadened the phase transition and lowered the gel to liquid-crystalline phase transition enthalpy. The results of this study suggest that cholesterol causes a more homogeneous dispersion of the various surfactant film components. Furthermore, our data provide additional evidence that natural surfactant, containing SP-B and SP-C, is superior to surfactants lacking one of both components.

1. Introduction

Pulmonary surfactant is a mixture of lipids and proteins, synthesized and secreted by the alveolar type II epithelial cells. Its main function is to reduce the surface tension at the alveolar air/liquid interface. This is achieved by formation of a surface-active film that consists of a lipid monolayer highly enriched in dipalmitoylphosphatidylcholine (DPPC) and a bilayer or multilayer structures ('surface-associated reservoir') closely attached to the monolayer. The presence of a surfactant film prevents the alveoli from collapsing at end-expiration and makes breathing with minimal effort possible. The existence of such a film has been visualized *in vitro* by atomic force microscopy (AFM) and fluorescence light microscopy [13] and *in vivo* by electron microscopy [12]. Film compression during expiration might lead to a squeeze-out of non-DPPC [169,170], film expansion during inspiration to selective adsorption of DPPC [12], or just to an alteration of structure rather than a change in composition [171,172,13].

Important components for surfactant film formation and homeostasis are the small hydrophobic surfactant specific proteins B and C (SP-B and SP-C). SP-B is a 79 amino acid

amphipathic protein that is active as an 18 kDa dimer [35]. SP-B has a net positive charge that is thought to be essential for its interaction with negatively charged phospholipids [72,173,56]. The many different activities ascribed to SP-B include the ability to induce the formation of a monolayer film from vesicles [174], to facilitate respreading of films from the collapsed phase [15], to support membrane fusion and lysis [16], to aid in the formation of tubular myelin [17] and to increase surfactant reuptake by type II cells [18]. In addition, recent studies carried out with a captive bubble surfactometer (CBS) suggested that SP-B induces film refinement by selective removal of non-DPPC lipid upon cycling [175]. The importance of SP-B is further documented by the observation that homozygous SP-B knockout mice died of respiratory failure immediately after birth [47]. Moreover, blocking of SP-B with monoclonal antibodies in rabbits led to respiratory failure and the loss of surfactant activity [21].

SP-C is a 35 amino acid protein that is extremely hydrophobic. It is further characterized by one or two palmitoylated cysteines in its N-terminal part. The C-terminal amino acids form an α -helix rich in valines [75]. In a lipid environment the α -helical content increases and might even extend to the two palmitoylated cysteines. The activities of SP-C largely overlap those of SP-B, including promotion of lipid adsorption into the air/liquid interface [14], stabilization of the monolayer film [85], respreading of films from the collapsed phase [15] and surfactant reuptake by type II cells [18]. Upon compression of a lipid monolayer to a surface tension of 22 mN/m, SP-C has been shown to induce formation of protrusions with a height of multiples of lipid bilayers [13]. Surplus surfactant might be kept in close proximity to the monolayer in these protrusions, from which it might be inserted quickly back into the monolayer upon inspiration. In contrast to SP-B knockout mice, SP-C knockout mice survive, although their surfactant shows altered stability when measured in small captive bubbles [86].

Lipids are the main components of surfactant (see [176] for review). Most abundant and best characterized are the phospholipids DPPC and phosphatidylglycerol (PG). DPPC (40 to 50 wt% of the lipid pool) is responsible for keeping the surface tension near zero during compression. Negatively charged PG (5 to 10 wt%) is likely to interact with positive charges of SP-B and SP-C. The most important non-phospholipid in surfactant is cholesterol, present in amounts of 10 to 20 mol% (approximately 5 to 10 wt%) [177]. Even though the presence of cholesterol in surfactant has long been recognized, little is known about its function. Although it is presumed that in the presence of the hydrophobic surfactant proteins cholesterol is important for enhancing lipid adsorption into the monolayer, studies using a Langmuir-Wilhelmy surface balance [178,179] or pulsating bubble surfactometer (PBS) [180] showed that cholesterol also had deleterious effects, like increasing the minimum surface tension during compression or diminishing post-collapse respreading. In pure lipid mixtures, cholesterol has been shown to be beneficial by enhancing surface reentry and respreading of the monolayer upon dynamic compression beyond collapse, as measured by Wilhelmy balance [181].

To further elucidate the role of cholesterol in surfactant films we studied the effect of

Chapter 3

cholesterol on i) the minimum and maximum surface tensions under dynamic conditions in a CBS, ii) the topography of the surface-associated reservoir by AFM, and iii) the calorimetric properties of lipid/protein mixtures using DSC. For this purpose, we compared mixtures of lipids (DPPC, POPG, POPC) and proteins (SP-B and/or SP-C) with and without cholesterol.

2. Materials and Methods

2.1 Materials

1,2-dipalmitoyl-*sn*-glycero-3-phosphocholine (DPPC), 1-palmitoyl-2-oleoyl-*sn*-glycero-3-phosphocholine (POPC), 1-palmitoyl-2-oleoyl-*sn*-glycero-3-phospho-*rac*-(1-glycerol) (POPG) and cholesterol were obtained from Avanti Polar Lipids (Alabaster, AL, USA); HEPES was purchased from Life Technologies (Paisley, Scotland); EDTA and CaCl₂ were obtained from Baker Chemicals (Deventer, the Netherlands); chloroform (CHCl₃) and methanol (MeOH) from Labscan (Dublin, Ireland) were HPLC grade.

2.2 Biochemical assays

Bovine SP-B and porcine SP-C obtained from lung lavage were isolated and characterized according to standard procedures [158]. The protein concentration was determined by fluorescamine assay [182]. Concentrations of phospholipids [183] and cholesterol [184] were determined as described.

2.3 Vesicle preparation

Small unilamellar vesicles (SUV) were prepared as follows. Aliquots of lipids and/or SP-B or SP-C from stock solutions in CHCl₃/MeOH were dried under a continuous stream of nitrogen at room temperature. The resulting dry lipid/peptide film was rehydrated by adding subphase buffer (140 mM NaCl, 10 mM HEPES, 0.5 mM EDTA, 2.5 mM CaCl₂, pH 6.9), vortexing and incubation at 55 °C for 15 min. The multilamellar vesicles thus formed were sonicated five times for 20 s at 2 μm amplitude at 55 °C with 20 s intervals to obtain SUV. The SUV were cooled to 37 °C and used immediately.

2.4 Captive Bubble Sufactometry

The capability of the hydrophobic surfactant proteins to insert lipids into the air/liquid interface and to alter the lipid composition of this layer was determined using a pressure driven CBS [25,26]. We used a CBS since it has several advantages over PBS or Wilhelmy balance [24,25], especially when making dynamic compressions with spread film in which the composition is known [26]. In short, a bubble (0.50 cm²) was formed in subphase buffer by injecting air (28.5 μl) into the sample chamber at 1.0 bar and 37 °C. After that, a surfactant film containing 0.25 nmol lipids with or without hydrophobic surfactant proteins was spread at the air/liquid interface using a glass syringe (volume of 0.05 μl). Subsequently, the subphase was stirred for 30 min to enhance desorption of solvent. Next, the sample chamber

Effects of cholesterol on spread surfactant films

was perfused for 20 min with ten times subphase volume. Thereafter, 100 μl SUV of various lipid compositions (see below) were injected into the subphase (final concentration of 1 μmol lipid/ml) and stirring was continued for another 15 min. To study adsorption the bubble area was increased by sudden lowering of the pressure to 0.5 bar, where it was kept for 10 s. Subsequently, the pressure in the sample chamber was cycled five times within 1 min between two preset pressures of 0.5 and 2.8 bar to measure surface activity during dynamic cyclic compression and expansion of the bubble. The system pressure was kept constant (2.8 bar) at the end of the fifth compression over a period of 5 min to determine film stability. Finally, the pressure was cycled another five times and film stability was measured again. A video camera continuously monitored the shape and size of the bubble from which the surface tension values were calculated. During each second 25 video-frames were generated. Maximum surface tension was defined as the surface tension measured at the end of bubble expansion (just before onset of compression). Minimum surface tension was measured at the end of compression (just before onset of expansion). All measurements were carried out at least in four-fold.

2.5 CBS film and SUV composition

When spread films contained protein, a concentration of 0.75 mol% for SP-B and 3 mol% for SP-C was used. These concentrations were shown to have maximal activity in this experimental setup [57,185,26]. The lipid composition of films and vesicles was DPPC/POPC/POPG/cholesterol (50/30/20/x) in which x was 0, 5, 10 or 20 mol%. A mixture of DPPC/POPC/POPG/cholesterol (50/30/20/10), for instance, means that the relative molar percentage of the standard phospholipid mixture to cholesterol is 90 to 10. In this way the total amount of lipids was always kept constant.

2.6 Atomic Force Microscopy

For Langmuir-Blodgett transfer, films were prepared on a home-built teflon trough with an operational area of 66.5 cm^2 . The surface tension of the spread monolayer was measured with a platinum Wilhelmy plate connected to a microbalance (Cahn2000, Ankersmit, Oosterhout, the Netherlands). Before film spreading, a freshly cleaved mica sheet was dipped vertically into a subphase of demineralized water at room temperature (20 ± 3 °C). Films, composed of DPPC/POPC/POPG (50/30/20) plus 0.75 mol% SP-B and/or 3 mol% SP-C with or without cholesterol (10 mol%) in $\text{CHCl}_3/\text{MeOH}$, were formed by spreading aliquots onto the subphase. After the solvent had been allowed to evaporate for 5 min, the film was compressed at a rate of 8.6 % of the operational area per min, until a surface tension of 22 mN/m was reached. Subsequently, films were transferred onto a disc of mica (14 mm in diameter) at a rate of 2.0 mm/min at constant surface tension.

For AFM measurements, transferred films were mounted on the J-type scanner (150 $\mu\text{m} \times 150 \mu\text{m}$ scan range) of a Nanoscope III Multimode microscope (Digital Instruments, Santa Barbara, CA, USA) operating in contact mode in air. Scanning was performed using oxide-sharpened Si_3N_4 tips with a spring constant of 0.12 N/m. Scans were

Chapter 3

recorded at minimal force and the interaction force was dominated by strong adhesion of usually 15 nN. No indications tip induced film damage were found, as checked by zooming out after an area had been scanned.

2.7 Differential Scanning Calorimetry

DSC experiments were carried out using a Microcal MCS (Microcal Inc., Northampton, MA, USA). Samples used for DSC had the same composition as those used for AFM. In every case the DPPC concentration was 5 $\mu\text{mol/ml}$. Dried lipid/protein films were rehydrated in calcium-free subphase buffer and repeatedly freeze-thawed prior to use. Ten consecutive thermographs were made at a scan speed of 45 $^{\circ}\text{C}$ per hour over a temperature range from 15 to 70 $^{\circ}\text{C}$. Data were taken from the heating scans. Repeated scans of the same sample gave nearly identical thermographs. The enthalpy of the phase transition, determined from the area under the endotherm, was normalized to the enthalpy of DPPC.

2.8 Statistics

Data are presented as average \pm standard deviation, unless stated otherwise. For statistical analysis, the computer program SPSS version 9.0 was used (SPSS Inc., Chicago, IL, USA). The values of the heights of the protrusions observed with AFM were analyzed by Student's t-test. To compare minimum and maximum surface tension of CBS films data were analyzed by Repeated Measures analysis. Differences were considered significant at $P < 0.05$.

3. Results

3.1 Effect of cholesterol on surface tension: Captive Bubble Surfactometry

CBS experiments were performed using spread films to study the effect of cholesterol on film dynamics. Although in our previous studies a DPPC content of 80 % in film and vesicles was used, we expected this high DPPC concentration to mask the effect of cholesterol on surface tensions. Therefore, we used a standard phospholipid mixture of DPPC, POPC and POPG at a fixed molar percentage of 50/30/20 while the amount of cholesterol was varied (0, 5, 10 or 20 mol%).

Effect of cholesterol in the presence of SP-B. A concentration curve of cholesterol in films of standard mixture plus SP-B (0.75 mol%) showed that the maximum surface tension (Fig. 1A) decreased with increasing cholesterol concentrations, reaching the lowest values at 10 mol% cholesterol ($P = 0.013$). In most experiments maximum surface tension temporarily decreased after the stabilization period at high pressure following the 5th compression. For cholesterol concentrations up to 10 mol% the minimum surface tension (Fig. 1B) reached on the 2nd or 3rd compression was always < 5 mN/m, whereas minimum surface tension of films containing 20 mol% cholesterol was always > 15 mN/m. Although no statistically significant difference in minimum surface tensions was observed for 0, 5 and 10 mol% cholesterol for the first five cycles, initially stable films rapidly destabilized after the 5th compression when

Effects of cholesterol on spread surfactant films

no cholesterol was present. The observed increase in minimum surface tension in the absence of cholesterol could indicate an irreversible loss of surface-active material from the film.

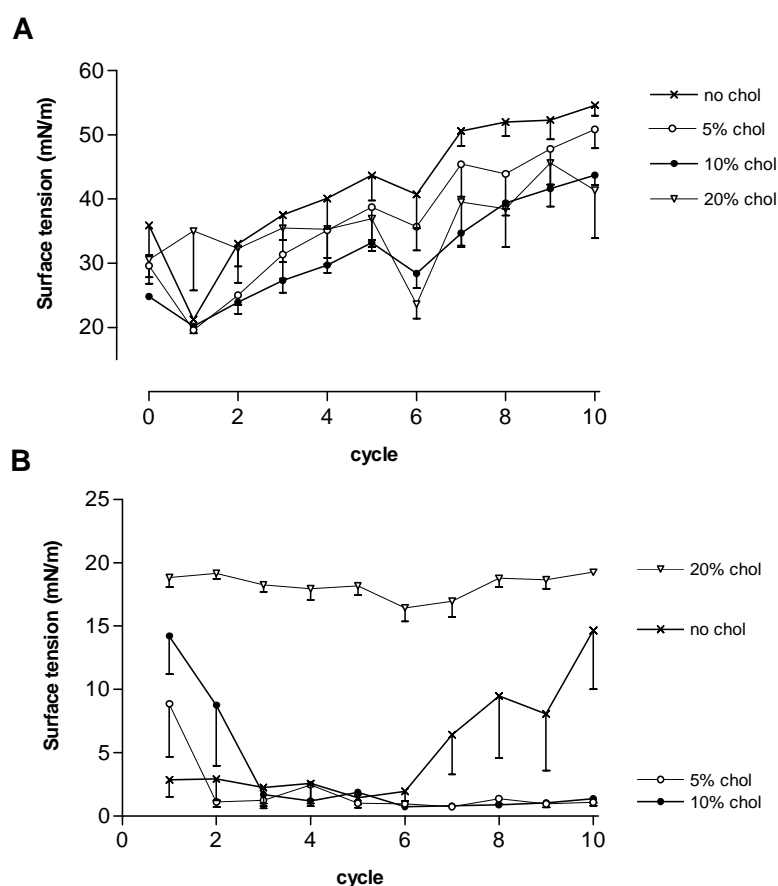


Figure 1. Maximum (A) and minimum (B) surface tensions during cycling of spread films of SP-B (0.75 mol%) and DPPC/POPC/POPG (50/30/20) with different concentrations of cholesterol (chol).

Protein/lipid mixtures (0.25 nmol), dissolved in $\text{CHCl}_3/\text{MeOH}$, were spread at the bubble interface in a CBS. After the subphase had been washed, SUV were injected; SUV had the same lipid composition as the film, but contained no protein. Subsequently, cycling was performed by varying the pressure between 0.5 and 2.8 bar. Values shown are the average of at least four separate experiments \pm SEM.

A film can be enriched in a specific component by bubble cycling when experiments are started with differences in concentration of that particular component between film and subphase. At an initial film concentration of 0 mol% cholesterol, the film can be enriched in cholesterol when injecting SUV containing 10 mol% cholesterol into the subphase. Similarly, a dilution of cholesterol in the film can be created by starting the experiments with 10 mol% cholesterol in the film and 0 mol% in the SUV. Surprisingly, no significant difference in minimum or maximum surface tension was found between experiments starting with 10 mol%

Chapter 3

cholesterol in the film only, in the subphase only, or in both the film and the subphase (Fig. 2).

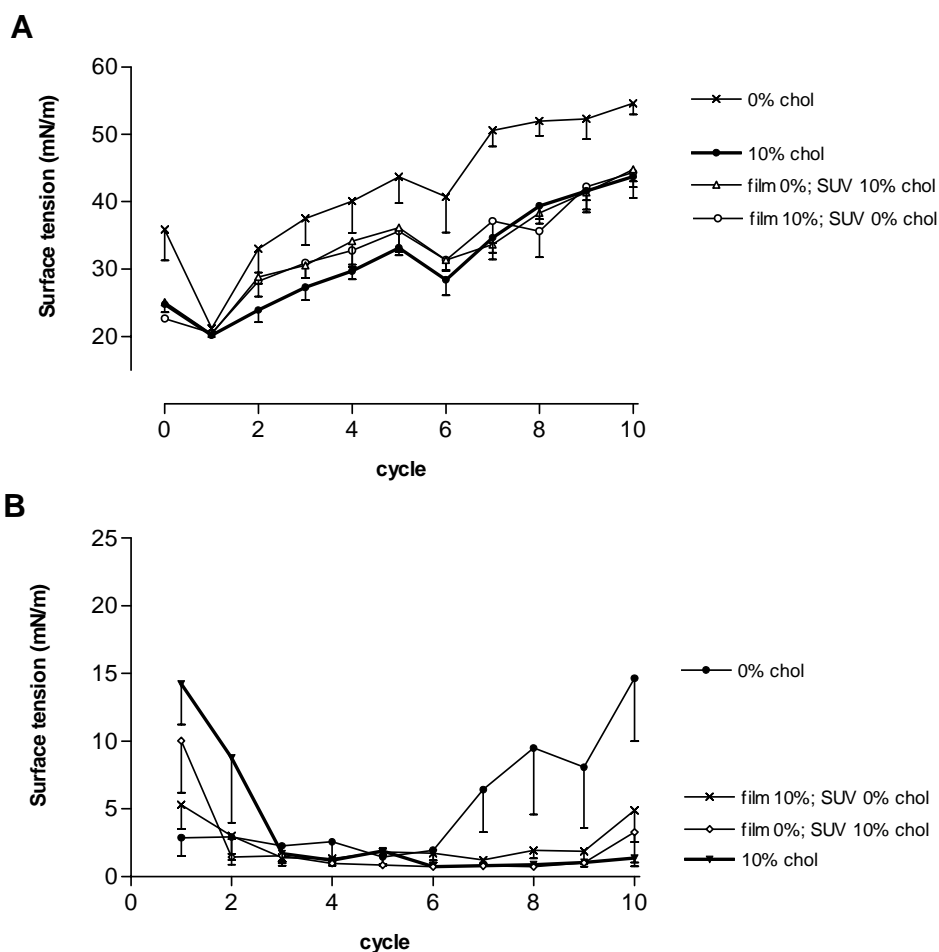


Figure 2. Maximum (A) and minimum (B) surface tensions during cycling of spread films of SP-B (0.75 mol%) and DPPC/POPC/POPG (50/30/20) during enrichment or dilution of the film with cholesterol (chol). Cholesterol was present in the film, in the subphase, in both or in neither of the two. Values shown are the average of at least four separate experiments \pm SEM.

Although it has been proposed for calf lung surfactant extract measured by CBS [171] and PBS [186] that films are stable even at less than 40 % DPPC, it is possible that some of our results might have been caused by an insufficient amount of DPPC. To investigate the effect of an increased amount of DPPC in the film on surface tension, experiments were performed with 20 mol% cholesterol in a DPPC/POPC/POPG (50/10/20) mixture (Fig. 3). In this lipid mixture the concentration of DPPC was truly 50 % instead of varying between 40 % and 48 % depending on the amount of added cholesterol. Moreover, the amount of POPC was decreased to 10 %. When 20 % cholesterol was present, minimum surface tension reached

Effects of cholesterol on spread surfactant films

with the 50/10/20 mixture was lower than with the 50/30/20 mixture ($P = 0.022$) (Fig. 3B). However, the 50/10/20 mixture with cholesterol never reached the low minimum surface tension observed for the 50/30/20 mixture without cholesterol ($P = 0.017$), although there is an equal amount of DPPC in both mixtures. When measuring maximum surface tension, however, no statistically significant difference was found between the 50/30/20 mixture without cholesterol and the 50/10/20 mixture with 20 % cholesterol (Fig. 3A). So, the presence of unsaturated phospholipids, like POPC, seems to be similarly important for high surface activity as the presence of a sufficiently large amount of DPPC, especially for achieving and maintaining low minimum surface tensions.

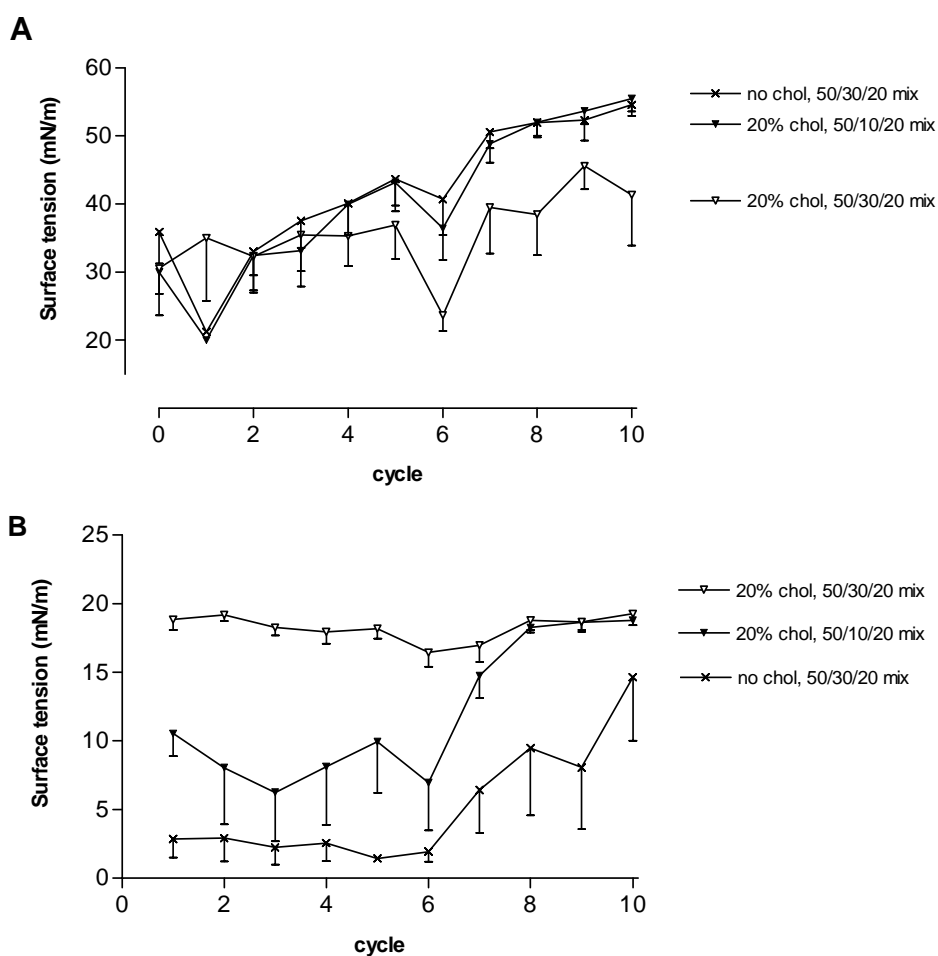


Figure 3. Maximum (A) and minimum (B) surface tensions during cycling of spread films of SP-B (0.75 mol%) and DPPC/POPC/POPG (50/30/20) or (50/10/20) plus 20 % cholesterol.

The influence of a larger amount of DPPC in films and vesicles was investigated. SUV and film had the same lipid composition. Values shown are the average of at least four separate experiments \pm SEM.

Effect of cholesterol in the presence of SP-C. The presence of 10 mol% cholesterol in SP-C containing films led to a significant increase of the maximum surface tension ($P = 0.033$)

Chapter 3

(Fig. 4A). The minimum surface tension (Fig. 4B) reached by these films was high (> 10 mN/m) and tended towards the equilibrium surface tension (approximately 25 mN/m [332]) during cycling, indicating an irreversible loss of active material from the surface film into the subphase. There was no statistically significant difference in minimum surface tension reached between films with and without cholesterol.

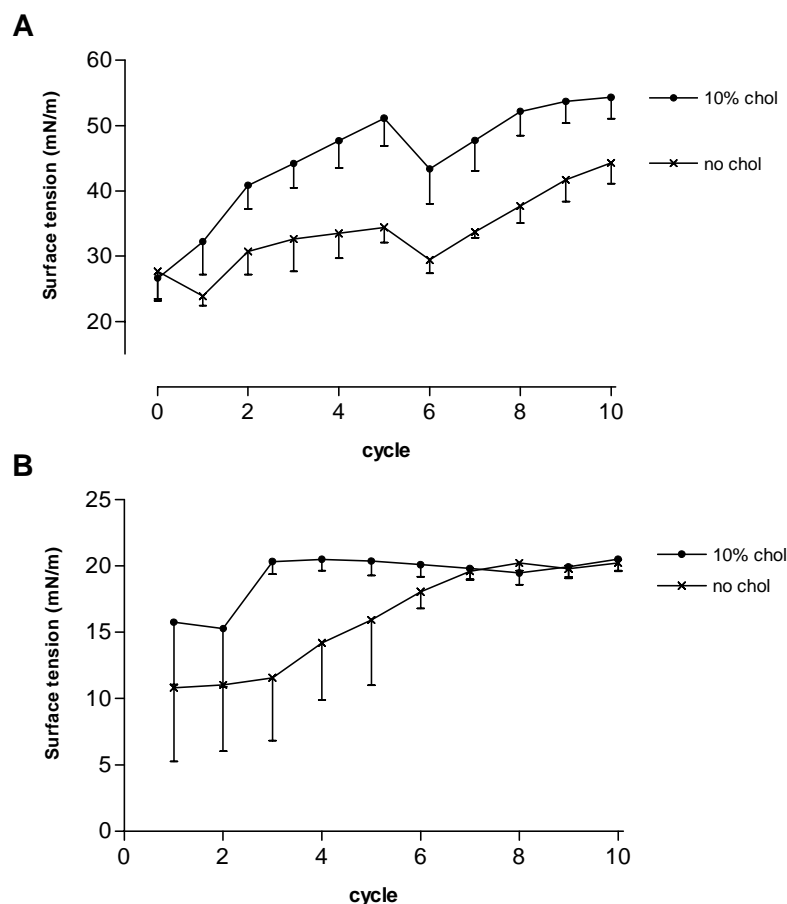


Figure 4. Maximum (A) and minimum (B) surface tensions during cycling of spread films of SP-C (3 mol%) and DPPC/POPC/POPG (50/30/20), with and without 10 % cholesterol (chol).

SUV and film had the same lipid composition. Values shown are the average of at least four separate experiments \pm SEM.

Effect of cholesterol in the presence of both SP-B and SP-C. Interestingly, the presence of 10 mol% cholesterol had no effect on minimum or maximum surface tension when both SP-B and SP-C were present in the film (Fig. 5). Moreover, compared to films containing either SP-B or SP-C (Figs. 1 and 4), films containing both proteins had lower minimum surface tensions and did not show an increase of maximum surface tension during cycling.

Effect of cholesterol in the absence of proteins. Both with and without cholesterol in the film, maximum surface tension in the absence of proteins rose to 59 mN/m at the first

Effects of cholesterol on spread surfactant films

bubble expansion and leveled off at 65 mN/m on the third expansion (not shown). Furthermore, minimum surface tension reached with repeated film compression was never lower than the equilibrium surface tension, independent of the presence of cholesterol. So, the presence of SP-B and/or SP-C is a requirement for obtaining and sustaining low maximum and minimum surface tension in this lipid mixture.

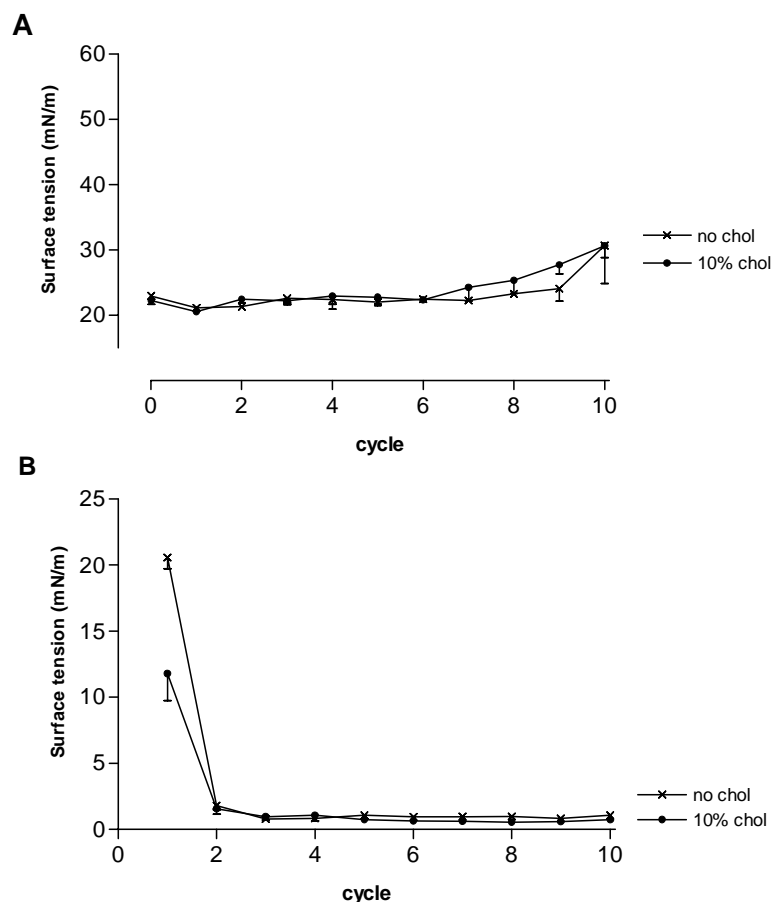


Figure 5. Maximum (A) and minimum (B) surface tensions during cycling of spread films of SP-B (0.75 mol%) + SP-C (3 mol%) and DPPC/POPC/POPG (50/30/20), with and without 10 % cholesterol (chol). SUV and film had the same lipid composition. Values shown are the average of at least four separate experiments \pm SEM.

Effect of cholesterol on lipid adsorption. To learn more about the processes during adsorption, the change in surface tension after sudden bubble expansion was recorded over a 5 s period. In the presence of SP-B, surface tensions observed before expansion were significantly lower in films containing 10 mol% cholesterol than in films without cholesterol (Fig. 6A). Even though films with cholesterol appeared to reach a higher surface tension than films without cholesterol one second after bubble expansion, this difference was not statistically significant. Although films containing SP-C as the only protein started at similar

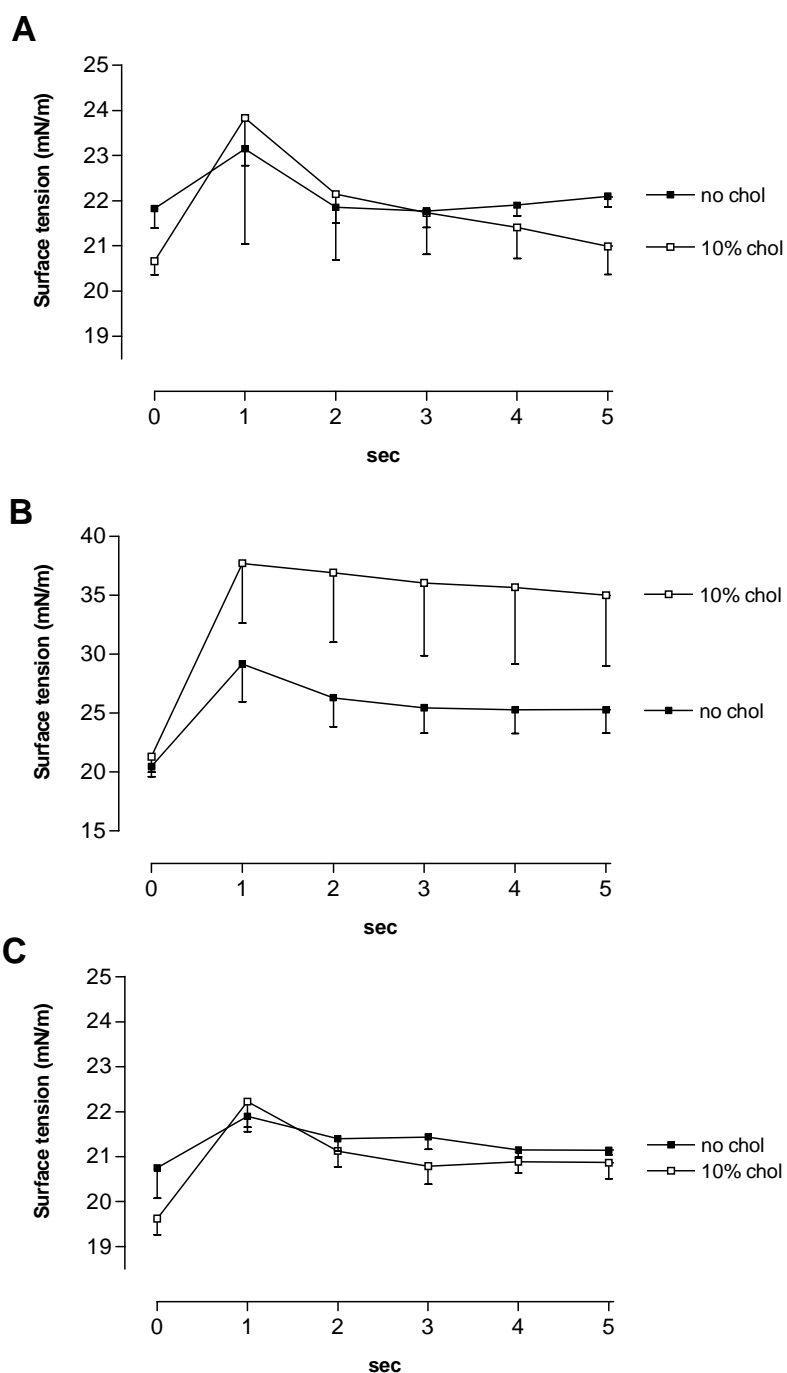


Figure 6. Adsorption during the first five seconds after sudden bubble expansion for films of DPPC/POPC/POPG (50/30/20) plus SP-B (A), SP-C (B), or SP-B + SP-C (C), with and without 10 % cholesterol (chol).

SUV and film had the same lipid composition. Values shown are the average of at least four separate experiments \pm SEM.

surface tensions independent of cholesterol concentration (Fig. 6B), the surface tension of cholesterol containing films rapidly rose to high values. Both in the presence and absence of

Effects of cholesterol on spread surfactant films

cholesterol, film formation was fastest when both SP-B and SP-C were present (Fig. 6C). In the absence of proteins the surface tension of films with or without cholesterol rose quickly from 25 to 59 mN/m within the first second and remained at that level (not shown). No extra information was obtained when adsorption was viewed frame-by-frame (25 video-frames per second) instead of second-by-second.

3.2 Effect of cholesterol on surface film topography: Atomic Force Microscopy

To obtain additional information about film structure below the equilibrium surface tension, surfactant films were compressed to a surface tension of 22 mN/m and film topography was visualized by atomic force microscopy. Films were composed of the standard mixture plus SP-B, SP-C or both proteins. Cholesterol was present in the films at a concentration of 0 or 10 mol%. In AFM and fluorescence microscopy studies dealing with SP-B and SP-C in DPPC/DPPG mixtures it was shown that at a surface tension of 22 mN/m the protrusions (white regions in the AFM images) contained lipid and protein in liquid expanded phase, while the monolayer (black regions in the AFM images) consisted solely of lipid in liquid condensed phase [13,81,163].

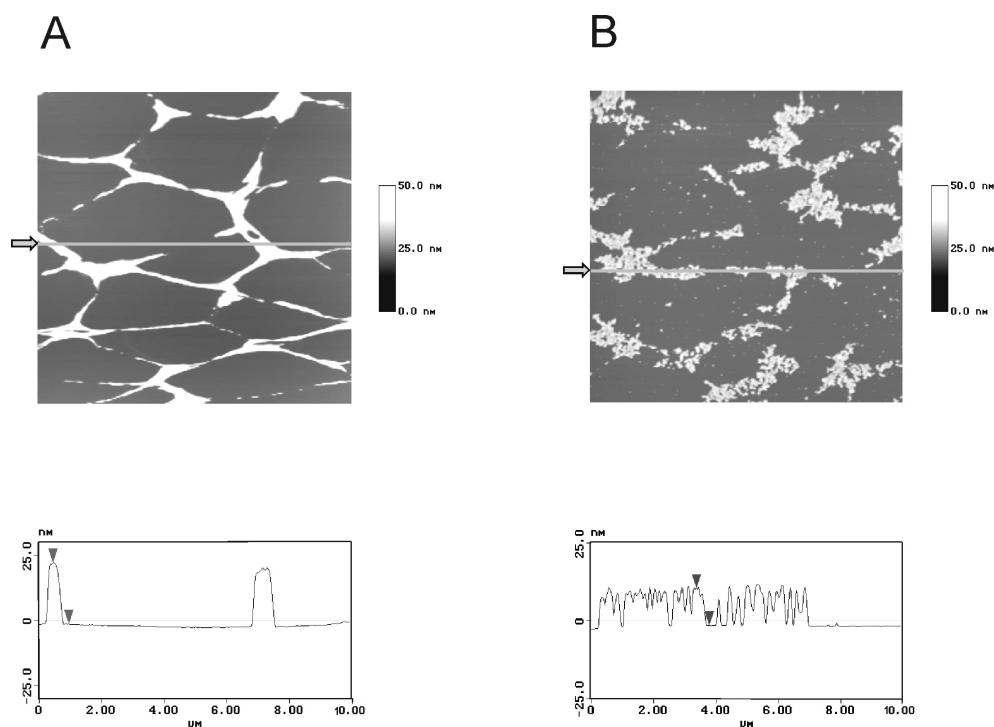


Figure 7. AFM topography of films of SP-B (0.75 mol%) and DPPC/POPC/POPG (50/30/20), without (A) and with (B) 10 % cholesterol.

Black regions represent lipid monolayer, while white regions are protrusions of lipids/protein. The average height of the protrusions was 24 ± 3 nm for (A) and 13 ± 2 nm for (B). The arrowheads on the height traces show the approximate height difference, which was 23.9 nm for (A) and 12.1 nm for (B). Scan area was $10 \mu\text{m} \times 10 \mu\text{m}$.

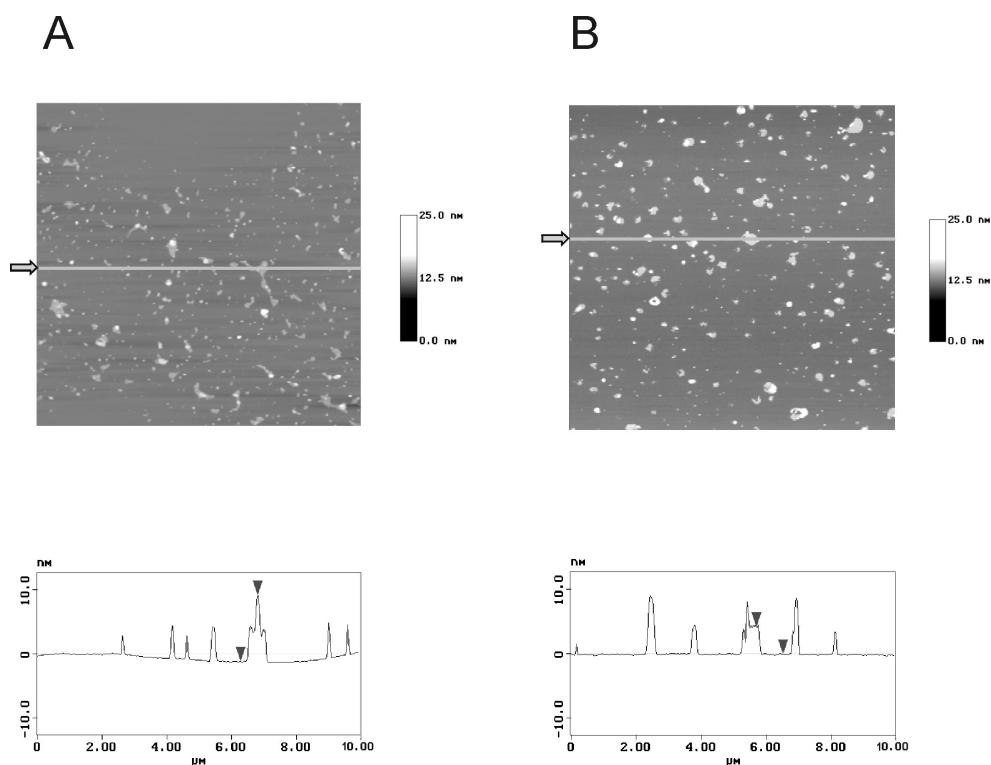


Figure 8. AFM topography of films of SP-C (3 mol%) and DPPC/POPC/POPG (50/30/20), without (A) and with (B) 10 % cholesterol.

The average height of the protrusions was typically 4 ± 1 nm for both (A) and (B), but protrusions of 8 nm height were observed as well. The arrowheads on the height traces show the approximate height difference, which was 8.8 nm for (A) and 4.1 nm for (B). Scan area was $10 \mu\text{m} \times 10 \mu\text{m}$.

Representative $10 \mu\text{m} \times 10 \mu\text{m}$ scans of mica-supported DPPC/POPC/POPG films with SP-B and/or SP-C are shown in Figs. 7-9, both in the absence and presence of cholesterol. For SP-B containing films the surface topography dramatically differed between films containing 0 % or 10 % cholesterol (Fig. 7). In the absence of cholesterol, continuous network structures were present, appearing as mountain ridges. Since addition of more surfactant proteins led to the formation of a larger amount of protrusions, we deduce, analogous to the work of Amrein, Sieber and collaborators [13,81,163], that the protrusions consist of protein and lipid. AFM allows very accurate measurements in the z direction, *i.e.* height. The height of the protein/lipid protrusions was almost exclusively 24 ± 3 nm. Since the shape of each individual AFM tip (up to 10 nm at the apex [188], 50 nm in radius [189]) is not known exactly, AFM does not allow very accurate measurements (a phenomenon known as tip convolution) in the x and y direction, *i.e.* protrusion widths. Nevertheless, widths of similar samples scanned with the same tip can be roughly compared with each other. The width of the ridges ranged between 100 and 400 nm and were approximately 200 nm in average. In contrast, films containing 10 % cholesterol showed non-continuous networks made up of small domains like pearls-on-a-string, with a height of typically 13 ± 2 nm. The average size of the

protrusions (*i.e.* the separate pearls on the string) was roughly 100 nm.

For SP-C containing films the difference in topography was less extreme than for films containing SP-B, but the same trend was observed: in cholesterol containing films the protrusions seemed to be homogeneously dispersed (Fig. 8B), while films without cholesterol also contained lipid areas without protrusions (Fig. 8A, *e.g.* upper part in the center). Both in the presence and absence of cholesterol the height of the protrusions was 4 ± 1 nm. Incidentally a height of 8 nm was observed. The shape of the protrusions was mostly non-circular. The size of the protrusions varied largely, being 100 nm on average, and were independent on the presence of cholesterol.

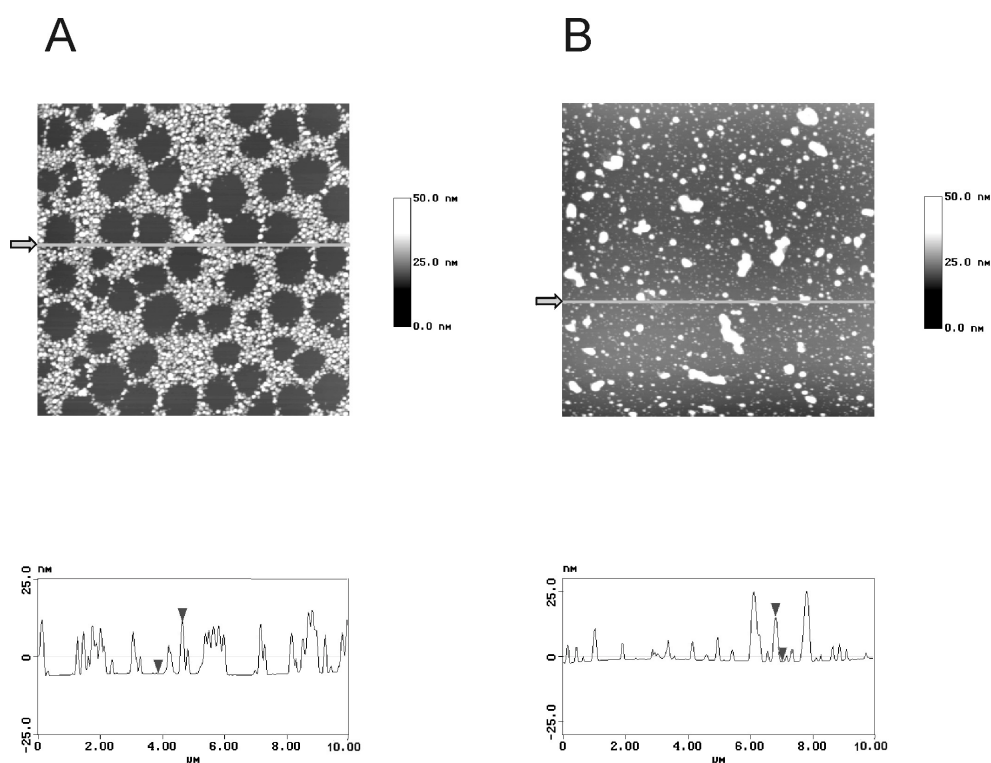


Figure 9. AFM topography of films of SP-B (0.75 mol%), SP-C (3 mol%) and DPPC/POPC/POPG (50/30/20), without (A) and with (B) 10 % cholesterol.

Heights of the protrusions ranged from 16 to 24 nm in steps of 4 nm in the absence of cholesterol (A). In the presence of cholesterol heights ranging from 16 to 34 nm in steps of 4 nm were found (B). The arrowheads on the height traces show the approximate height difference, which were 16.3 nm for (A) and 16.6 nm for (B). Scan area was $10 \mu\text{m} \times 10 \mu\text{m}$.

The structure of films containing both SP-B and SP-C was a combination of the film topography observed in the presence of the separate proteins (compare Fig. 9 with Figs. 7 and 8). In the absence of cholesterol there is a striking pattern of monolayer surrounded by many circular protrusions of lipids/proteins. This pattern is absent in the presence of cholesterol,

Chapter 3

although incidentally a region was found that contained both unorganized as well as organized structures. In the absence of cholesterol the height of the protrusions varied, ranging from 16 to 24 nm in steps of 4 nm, while in the presence of cholesterol higher protrusions of up to 34 nm were also found. The size of the protrusions (*i.e.* the separate pearls on the string) were approximately 100 nm, independent of the presence of cholesterol.

When no proteins were present, no differences in topography were found between the standard lipid mixture plus or minus cholesterol. The surfaces of these films were predominantly flat (results not shown). No phase separation was observed.

When the amount of white (protrusions) of the AFM images was determined, it was found that the total area of protrusions in SP-B films was significantly higher ($P < 0.001$) in the presence of cholesterol (15.6 ± 1.0 %) than in its absence (12.3 ± 1.3 %). In the case of SP-C a similar trend (but not statistically significant) was observed: 8.7 ± 1.4 % in the presence and 7.2 ± 2.0 % in the absence of cholesterol. However, when both proteins were present in the film the total area of protrusions was lower in the presence (19.1 ± 8.8 %) than in the absence (25.9 ± 6.5 %) of cholesterol ($P = 0.031$).

3.3 Effect of cholesterol on the calorimetric behavior of lipid/protein mixtures: Differential Scanning Calorimetry

The main gel to liquid-crystalline transition temperature (T_m), transition peak width at half-maximum transition ($T_{1/2}$), and phase transition enthalpy normalized to that of DPPC (ΔH) of the various lipid/protein mixtures are shown in Table 1; representative thermographs are depicted in Fig. 10. The addition of POPC and POPG to DPPC resulted in a substantial decrease in T_m . The gel to liquid-crystalline transition temperature is known to depend strongly on the length and degree of unsaturation of the fatty acid chains, as well as the nature of the phospholipid headgroups [337].

When cholesterol was added to the various samples, the most obvious effect was a substantial decrease of the phase transition enthalpy. In addition, the presence of cholesterol was observed to result in broadening of the lipid transition enthalpy peak, except for samples containing SP-C as the sole protein. Transition temperature was hardly affected by cholesterol. Interestingly, the presence of SP-B in the lipid vesicles led to phase separation of the lipids, indicated by the appearance of two transition peaks instead of one. This phase separation was not observed when both SP-B and SP-C were present. Furthermore, when examining the effect of the hydrophobic proteins, it was found that they altered transition temperature. When cholesterol was present, both SP-B and SP-C decreased reaction enthalpy when they were included into the film separately, but not when they were included together.

4. Discussion

Approximately 10 - 20 mol% of the surfactant lipids are non-phospholipid. However, the exact function of these neutral lipids (mainly cholesterol) in surfactant is not clear. In

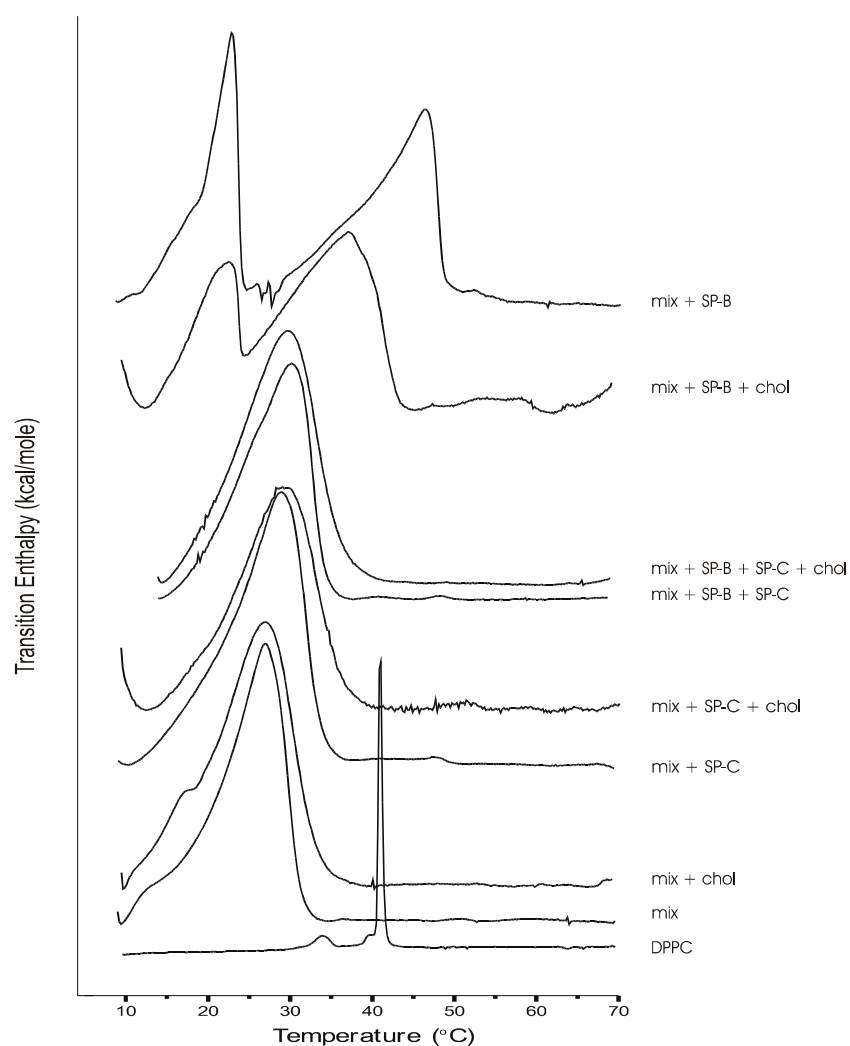


Figure 10. Differential scanning calorimetry thermograms of gel to liquid-crystalline phase transition of mixtures of DPPC/POPC/POPG (mix, 50/30/20) with and without SP-B (0.75 mol%), SP-C (3 mol%) and cholesterol (chol, 10 mol%).

The presence of cholesterol resulted in a broadening of the transition peak and a decrease of the transition enthalpy.

general, cholesterol is able to induce the liquid ordered phase, in which lipid acyl chains are extended and tightly packed as in the solid phase, although the lateral diffusion is almost as high as in the fluid phase. In this way cholesterol increases the fluidity of the lipid acyl chains below the transition temperature of that lipid, but rigidifies the acyl chains above the transition temperature [191,177]. The greatest rigidifying effect is exerted on fully saturated PC, with cholesterol packing in the intermolecular cavities of DPPC [192], and the least on PC containing a double bond in both acyl chains [193]. The fluidizing effect is achieved by direct interaction of cholesterol with the fatty acyl chains of the phospholipids, preventing them from crystallizing by coming too close together, thereby preventing possible phase transitions. In surfactant at physiological temperature, cholesterol is thought to act as a fluidizing agent,

Chapter 3

enhancing adsorption and respreading of lipid from collapsed phase [181,194]. This study shows that there is an ideal cholesterol concentration of 10 mol% for SP-B containing surfactant films. Furthermore, cholesterol was found to induce dramatic structural alterations in films containing SP-B and/or SP-C.

Table 1. Effect of cholesterol (10 mol%) on transition temperature (T_m), peak width at half-maximum transition ($T_{1/2}$), and phase transition energy (ΔH) of vesicles containing DPPC/POPC/POPG (50/30/20, molar percentages; mix), with and without SP-B (0.75 mol%) and/or SP-C (3.0 mol%)*

sample	T_m (°C)	$\Delta T_{1/2}$ (°C)	ΔH (%)
DPPC	41.0 ± 0.1	0.6 ± 0.0	100
mix	27.2 ± 0.4	7.9 ± 0.2	104 ± 1
mix + cholesterol	27.4 ± 0.3	10.1 ± 0.4	60 ± 4
mix + SP-B	23.3 ± 0.1	3.9 ± 0.4	44 ± 3
	46.5 ± 0.2	9.1 ± 1.2	64 ± 6
mix + SP-B + cholesterol	23.2 ± 0.9	6.3 ± 0.8	7 ± 1
	39.1 ± 1.9	11.7 ± 1.0	17 ± 1
mix + SP-C	29.2 ± 0.0	9.4 ± 0.3	101 ± 5
mix + SP-C + cholesterol	29.6 ± 0.7	8.7 ± 1.2	26 ± 1
mix + SP-B + SP-C	30.7 ± 0.1	9.5 ± 0.1	88 ± 3
mix + SP-B + SP-C + cholesterol	30.2 ± 0.1	10.5 ± 0.2	69 ± 1

* Data taken from the heating scan. DPPC concentration was always 5 $\mu\text{mol/ml}$. Dried lipid/protein films were rehydrated in calcium-free subphase buffer and repeatedly freeze-thawed prior to use. Ten consecutive thermographs were made at a scan speed of 45 °C per hour over a temperature range from 15 to 70 °C. In the presence of SP-B as the sole protein two transition peaks were observed.

In our CBS experiments cholesterol lowered maximum surface tension in the presence of SP-B. This effect was dependent on cholesterol concentration. On the one hand, too much cholesterol in the film destabilized the monolayer, preventing the film from reaching low minimum surface tensions (Fig. 1B). This is likely due to the fact that the cholesterol concentration in the film was higher than a critical level at which it can no longer be squeezed out rapidly, as was observed in DPPC/cholesterol monolayers [195]. On the other hand, a total absence of cholesterol led to a rise in minimum surface tension after six bubble compressions. Therefore, it is conceivable that the presence of cholesterol has a beneficial effect on film

stability by packing between the fatty acyl chains of DPPC, leading to an improved tolerance of high lateral pressures. Furthermore, maximum surface tension decreased with increasing cholesterol concentration, reaching the lowest value at 10 mol% in the presence of SP-B. These findings are different from those obtained in a PBS study [180] using DPPC/POPG/SP-B (70/30/0.4, mol/mol/mol) where both minimum and maximum surface tension were found to be higher after addition of 20 mol% cholesterol. In another study, using the Wilhelmy balance, cholesterol (up to 10 mol%) in the presence of SP-B increased minimum surface tension as well [178]. Surprisingly, we found that cholesterol increased both maximum and minimum surface tension in films containing SP-C (Fig. 4). One could speculate that cholesterol at this concentration fixes the orientation of the SP-C palmitoyl chains in the membrane, thereby decreasing the freedom to move between lipid layers of the surface-associated reservoir, and altering the monolayer lipid composition. It is thought that the SP-C is more favorably accommodated in fluid DPPC bilayers than in rigid gel phase DPPC [196,197]. Such a rigidifying effect of cholesterol on SP-C, however, is not readily observed from our DSC results (Fig. 10 and Table 1). Furthermore, in the presence of cholesterol SP-C containing films did not reach the same low surface tensions as films with SP-B. This is in line with another CBS study [185] in which it was shown that SP-C had less of a refining effect on surfactant films than SP-B. Thus, in the presence of SP-B the effect of cholesterol on surface activity is the opposite of that found for SP-C. When both SP-C and SP-B were present in the film an overall improvement on surface activity compared to that in the presence of either protein separately was obtained (compare Fig. 5 with Figs. 1 and 4) on which cholesterol addition had no effect. In our experiments performed at 37 °C only minor effects of cholesterol on adsorption were seen (Fig. 6), although the CBS method using spread films is accurate enough to measure small differences in surface tension. Moreover, the influence of surfactant proteins on adsorption seemed much more pronounced than the influence of cholesterol. Yet, in a study using a Wilhelmy balance as well as a PBS, both at 37 °C and at 23 °C, calf lung surfactant extract devoid of neutral lipids was reported to have hampered adsorption activity (higher maximum surface tensions) compared with CLSE [198]. In the same study neutral lipids were also reported to facilitate respreading. As leakage of film material is a problem often encountered in experiments with the PBS or the Wilhelmy balance [24,25,176], some of the previously reported detrimental effects attributed to cholesterol may instead have been related to film leakage.

In an effort to enrich or deplete the film in cholesterol, the lipid composition between the spread film and the subphase vesicles in the CBS was varied. Surface tensions reached during cholesterol enrichment or dilution of the film were found to be equal to those in experiments in which cholesterol was present in both film and subphase (Fig. 2). The experimental setup was such that bubble cycling was preceded by expansion of the bubble, during which material from the subphase will adsorb into the monolayer. So, it is conceivable that during bubble expansion cholesterol contained in subphase vesicles was inserted into a monolayer that started with 0 % cholesterol. Similarly, cholesterol contained in the initial film at *e.g.* 10 % could become diluted by subphase vesicles lacking cholesterol. Thus, at the time

Chapter 3

on which cycling started, films in enrichment and depletion experiments could have had equal composition as in experiments in which both film and subphase contained cholesterol. From this we conclude that cholesterol is able to adsorb from the subphase into the bubble surface and vice versa.

When spread films on a Langmuir-Willhelmy balance are compressed beyond the equilibrium surface tension, surfactant components leave the interface, forming structures connected to the monolayer. Therefore, parts of the film must undergo transformation from a monolayer into structures protruding into or out of the aqueous subphase. Other studies, using fluorescence microscopy, time-of-flight secondary ion mass spectrometry, and Brewster angle microscopy, showed that structures transferred from the air-water interface onto solid substrates are essentially identical to the structures in the monolayer itself [199,200]. To achieve a better understanding of the effect of cholesterol on formation of such structures, we used AFM to study, for the first time, surfactant films containing cholesterol which were compressed below the equilibrium surface tension. The most striking difference between AFM images of films containing and those lacking cholesterol is that protrusions in the presence of cholesterol appear more dispersed throughout the entire area and less clustered into network structures (Figs. 7-9). This homogenizing effect of cholesterol was observed for films containing SP-B, SP-C, as well as for films containing both proteins.

Another effect of cholesterol on these lipid/protein mixtures that may be important for surfactant action was seen by DSC (Table 1 and Fig. 10). In samples containing 10 % cholesterol the gel to liquid-crystalline phase transition enthalpy was decreased substantially with concomitant broadening of the endotherm, indicating a decrease in the cooperativity of the phase transition. It is known that at sufficiently high concentrations (32 mol% [201]) cholesterol can eliminate the lipid phase transition, resulting in a state of fluidity intermediate to either the gel or the liquid-crystalline phase over an increased temperature range [177]. DSC data also correlated well with AFM results in showing a lipid demixing effect of SP-B, indicated by the presence of two phase transition peaks using DSC and the mountain ridge-like protrusions observed by AFM. In the absence of cholesterol and in the presence of SP-B, phase transition temperature of the second peak was increased, possibly a result of SP-B induced alteration in packing of DPPC. When SP-C was present as well, the effect of SP-C dominated that of SP-B, since demixing was no longer seen. No experiments with cholesterol have been performed in the few studies dealing with DSC in the presence of hydrophobic surfactant proteins [202,203]. Furthermore, only saturated lipid systems were used in those studies. It was found that SP-B as well as SP-C in either DPPC or DPPG decreased transition enthalpy, while increasing transition temperature [202]. On the other hand, SP-C in DMPC was shown to decrease transition enthalpy as well as transition temperature [203].

In our AFM studies protrusion heights were often multiples of 4 - 4.5 nm, independent of the presence of cholesterol. The value found for bilayer height depends on the method of analysis, temperature and lipid unsaturation. The bilayer thickness of DPPC was found to be 3.7 nm [204] to 4.3 nm [328] in fluid liquid crystalline state and 4.7 nm in gel state [328], as determined by X-ray diffraction. In an AFM study using contact mode, films of SP-B in

DPPC/DPPG (4/1) transferred at 22 mN/m were found to have protrusions of 6 - 7 nm, thought to represent bilayers [163]. However, in another AFM study using contact mode, protrusions in films of SP-B peptide analogs in DPPG/POPG (3/1) transferred at 18 mN/m were found to be 10 - 40 nm, in steps of 5.0 nm [206]. Therefore, in our study we considered a height of 4 - 4.5 nm to represent the thickness of a bilayer. Thus, most protrusions found in films with SP-C were 1 bilayer in thickness, while those found in SP-B containing films were 3 - 6 bilayers thick. This finding is different from the scarce AFM information available on films containing SP-B or SP-C, since compression of films containing DPPC/DPPG (4/1) plus SP-C were found to result in the formation of protrusions with a height of multiples of bilayers [13], while the same lipid mixture plus SP-B resulted in protrusions of only one bilayer in thickness [163]. In line with our results, multilayered structures were found for SP-B analogs in DPPG/POPG [206]. The discrepancy between results is likely to be due to the differences in lipid mixtures used. Our highly unsaturated lipid mixture presumably led to altered fluidity and thereby to a different tendency to form protrusions during squeeze-out of film components. Unfortunately, the methods used in our studies do not provide information on whether cholesterol is present in the protrusions or located between DPPC in the condensed lipid domains.

Extrapolation of our AFM findings to the physiological situation is difficult since minimum surface tension in the lung is much lower than the minimum surface tension of 15 - 20 mN/m that we can achieve in the Langmuir-Wilhelmy balance during film transfer. Nevertheless, it is of interest that a dramatic alteration in surface topography like that observed after addition of cholesterol to films containing both SP-B and SP-C is not accompanied by measurable differences in surface activity in the CBS. Apparently, both types of structures allow rapid insertion and removal of lipids into and out of the monolayer. An explanation might be the small domain sizes of liquid expanded phase in both structures. From the broad and continuous network structures seen in the absence of cholesterol in films containing SP-B as the only protein (Fig. 7A) it is apparently more difficult to insert lipids into an expanding bubble, since maximum surface tension increases as cholesterol concentration decreases (Fig. 1A). However, it should be kept in mind that the CBS experiments were performed at 37 °C, while the AFM experiments were done at room temperature. This may have led to differences in lipid fluidity between the two types of measurements, possibly affecting surfactant activity or topography.

In summary, it is shown that cholesterol has remarkable effects on the biophysical activity of pulmonary surfactant. Surfactant films containing both cholesterol and SP-B have surface dynamics superior over those lacking cholesterol. Moreover, the presence of cholesterol in surfactant films leads to a dramatic alteration of the structural appearance. Our data provide additional evidence for the general concept that natural surfactant containing SP-B and SP-C is superior to surfactants lacking one of both components. Moreover, the combined presence of SP-B and SP-C in surfactant resulted in a negligible effect of cholesterol on surface tension, but to a profound effect of cholesterol on surface topography.

Chapter 3

Acknowledgments

We would like to thank Dr. Hilde Rinia and Prof. Dr. Ben de Kruijff from the Department of Biochemistry of Membranes of the Utrecht University for help with DSC experiments and fruitful discussion.

Chapter 4

Multilayer Formation upon Compression of Surfactant Monolayers depends on Protein Concentration as well as Lipid Composition: an Atomic Force Microscopy Study

Robert V. Diemel ^{a,b}, Margot M.E. Snel ^c, Alan J. Waring ^{d,e}, Frans J. Walther ^e,
Lambert M.G. van Golde ^a, Günther Putz ^b, Henk P. Haagsman ^{a,f}
and Joseph J. Batenburg ^a

^aDepartment of Biochemistry and Cell Biology, and ^fDepartment of the Science of Food of Animal Origin, Faculty of Veterinary Medicine, Graduate School of Animal Health, Utrecht University, Utrecht, The Netherlands

^bDepartment of Anaesthesiology and Critical Care Medicine,
The Leopold-Franzens-University of Innsbruck, Innsbruck, Austria

^cDepartment of Interfaces, Faculty of Chemistry, Utrecht University, Utrecht, The Netherlands

^dDepartment of Medicine, Division of Infectious Diseases, UCLA, Los Angeles, USA,
and ^eDepartment of Pediatrics, Division of Medical Genetics, Harbor-UCLA Research and Education Institute, Torrance, USA

Submitted for publication, 2001

Abstract

Pulmonary surfactant forms a surface-active layer of lipids and proteins at the alveolar air/liquid interface, consisting mainly of a monolayer at end-inspiration, and changing into multilayer structures upon expiration. From the latter structures, surface-active material can readily be reinserted into the monolayer upon inspiration. The determinants for the formation of multilayers were investigated by compressing films, beyond the squeeze-out plateau, to a surface tension of 22 mN/m. Atomic force microscopy (AFM) was used to visualize the topography of lipid films containing varying amounts of native SP-B. These films were compared with films containing synthetic peptides based on the N-terminus of human SP-B: monomeric mSP-B₁₋₂₅ or dimeric dSP-B₁₋₂₅. The formation of typical hexagonal network structures as well as the height of protrusions were shown to depend on the concentration of SP-B. Protrusions of bilayer height were formed from physiologically relevant concentrations of 0.2 - 0.4 mol% SP-B upwards. Much higher concentrations of SP-B₁₋₂₅ peptides were needed to obtain network structures, and protrusion heights were not equal to those found for films with native SP-B. A striking observation was that while protrusions formed in films of DPPC/DPPG (80/20) had single bilayer thickness, those formed in DPPC/POPG (80/20) had various heights of multilayers, whereas those seen in DPPC/POPC/DPPG (60/20/20) were mainly of bilayer height. For the first time direct observations by AFM show i) that a certain minimal concentration of SP-B is required for the formation of layered protrusions upon film compression, ii) that protrusion height depends on whether the phospholipids contain an unsaturated fatty acyl chain, and iii) that protrusion height also depends on whether the unsaturated acyl chain is present in phosphatidylcholine or in phosphatidylglycerol. Synthetic SP-B₁₋₂₅ based surfactants to be used clinically will therefore have to contain, in addition to DPPC, a high concentration of SP-B₁₋₂₅ peptides as well as unsaturated phospholipids, preferentially unsaturated PG.

1. Introduction

Pulmonary surfactant is a mixture of lipids and proteins, synthesized and secreted into the alveolar fluid by the alveolar type II epithelial cells. Its main function is to reduce the surface tension at the alveolar air/liquid interface, thus preventing the alveoli from collapsing at end-expiration and making breathing at minimal effort possible. This is achieved by the formation of a surface-active film that consists of a lipid monolayer highly enriched in dipalmitoylphosphatidylcholine (DPPC) and bilayer or multilayer structures ('surface-associated reservoir') closely attached to the monolayer. From such multilayer structures surfactant material can be readily incorporated into the monolayer film upon inspiration. The existence of a layered film has recently been visualized *in vitro* by atomic force and fluorescence light microscopy [13,163,206] and *in vivo* by electron microscopy [12]. Film compression during expiration might lead to a squeeze-out of non-DPPC [169,170], film

expansion during inspiration to selective adsorption of DPPC [12], or they might just lead to an alteration of structure rather than a change in composition [171,172,206,13].

Administration of exogenous surfactant is a successful strategy in treating premature infants suffering from respiratory distress syndrome (RDS) [207]. Moreover, surfactant therapy is also considered promising for adults with acute respiratory distress syndrome (ARDS) [10,11,208]. Presently, the majority of clinically used surfactants is derived from animals. In an effort to circumvent the possibility of zoonotic infections and to reduce the considerable costs of surfactant production, the use of surfactants containing artificial proteins and lipids is currently under consideration. With respect to the proteins, the hydrophobic surfactant protein B (SP-B) is known to fulfill a crucial role in the lung, since respiratory distress is always observed in SP-B deficient humans [209,19] and in homozygous SP-B knock-out mice [20]. SP-B is a 79 amino acid amphipathic protein, active as an 18 kDa dimer [35], and has a net positive charge that is thought to be essential for its interaction with negatively charged phospholipids such as phosphatidylglycerol (PG) [72,173,56]. The SP-B amino acid sequence among mammals has been highly conserved [210]. Because of the importance of SP-B for proper surfactant activity, synthetic peptides based on its sequence have been developed: mSP-B₁₋₂₅ is a monomeric synthetic peptide based on the N-terminal segment of human SP-B, while dSP-B₁₋₂₅ is the dimeric form of mSP-B₁₋₂₅ (Fig. 1). The structure and surface activity of these peptides have been investigated thoroughly, both *in vitro* and *in vivo*. The conformation of mSP-B₁₋₂₅ was found to be α -helical [211,212]. *In vitro* comparison of the surface activity of mSP-B₁₋₂₅ with that of dSP-B₁₋₂₅ in a captive bubble surfactometer (CBS) revealed that both peptides reduced the surface tension, with the dimeric peptide expressing better ability to lower surface tension than the monomeric peptide [53]. *In vivo* experiments showed that SP-B₁₋₂₅ peptides improved lung function in two animal models of surfactant deficiency [213-216]. With respect to the lipids (discussed in [176]), it has long been recognized that DPPC (40 to 50 wt% of the surfactant lipid pool) is responsible for keeping the surface tension near zero during expiration. Negatively charged PG (5 to 10 wt%) is likely to interact with the positive charges of SP-B. Lipids with unsaturated fatty acids are thought to be important for fluidizing the surfactant film.

Various established methods, among which captive bubble surfactometry, are available to obtain information on surfactant surface activity. In addition to these methods, growing interest has recently emerged in atomic force microscopy (AFM) [217], which yields information on surface topography, thereby providing new insight into the action of surfactant proteins and lipids during the breathing cycle. Although it has been found that upon compression material is squeezed-out of the monolayer to form protrusions connected to the monolayer [13,163], it is so far not clear which surfactant components determine the size and height of the protrusions. Therefore, in this study we used AFM to visualize the determinants for protrusion formation. For this purpose, we investigated monolayer films containing either bovine SP-B or an SP-B₁₋₂₅ peptide in the fully saturated lipid system DPPC/DPPG (80/20, mol/mol), or in the partially unsaturated mixtures DPPC/POPG (80/20) or DPPC/POPC/DPPG (60/20/20).

Chapter 4

Native human SP-B (residues 1-25):

NH₂ - F P I P L P Y C W L C R A L I K R I Q A M I P K G - X

Native bovine SP-B (residues 1-25):

NH₂ - F P I P **I** P Y C W L **L R T** L I K **K** I Q A **V** I P K G - X

Monomeric mSP-B₁₋₂₅:

NH₂ - F P I P L P Y C W L **A** R A L I K R I Q A M I P K G - COOH

Dimeric dSP-B₁₋₂₅:

NH₂ - F P I P L P Y C W L **A** R A L I K R I Q A M I P K G - COOH
|
S
|
S
|
NH₂ - F P I P L P Y C W L **A** R A L I K R I Q A M I P K G - COOH

Figure 1. Amino acid sequences of native SP-B and of SP-B derived synthetic peptides.

The differences in amino acid sequence between the various peptides are depicted in bold font. X represents the rest of the amino acids of native SP-B, which consists of 79 amino acids per monomer and is active as a dimer.

2. Materials and Methods

2.1 Materials

1,2-dipalmitoyl-*sn*-glycero-3-phosphocholine (DPPC), 1,2-dipalmitoyl-*sn*-glycero-3-(phospho-*rac*-(1-glycerol)) (DPPG), 1-palmitoyl-2-oleoyl-*sn*-glycero-3-phosphocholine (POPC) and 1-palmitoyl-2-oleoyl-*sn*-glycero-3-phospho-*rac*-(1-glycerol) (POPG) were obtained from Avanti Polar Lipids (Alabaster, AL, USA); chloroform (CHCl₃) and methanol (MeOH) from Labscan (Dublin, Ireland) were HPLC grade.

2.2 Biochemical assays

Bovine SP-B obtained from lung lavage was isolated and characterized according to standard procedures [158]. The protein concentration was determined by fluorescamine assay [182]. Concentrations of phospholipids were determined according to Rouser *et al.* [183]. The monomeric peptide mSP-B₁₋₂₅ was synthesized based on the N-terminal 25 amino acids of human SP-B with Cys-11 substituted for Ala [215] (Fig. 1). The dimeric version of the

Determinants for surfactant multilayer formation

peptide, dSP-B₁₋₂₅, was obtained by linking two monomer peptides through their only remaining cysteine, Cys-8 [53].

2.3 Surface pressure - area (Π - A) diagrams

Π - A curves were obtained using a home-built teflon trough with an operational area of 630 cm². Surface tension was measured with a platinum Wilhelmy plate connected to a microbalance (Cahn2000, Ankersmit, Oosterhout, the Netherlands). Films, composed of DPPC/DPPG (80/20, molar percentages), DPPC/POPG (80/20) or DPPC/POPC/DPPG (60/20/20) plus varying amounts of bovine SP-B or one of the SP-B₁₋₂₅ peptides, were formed by spreading aliquots in CHCl₃/MeOH onto the water subphase at 20 ± 3 °C. After the solvent had been allowed to evaporate for at least 5 min, films were compressed at a rate of 13.8 % of the operational area per min (28.8 Å² / molecule lipid · min) until film collapse (usually at a surface tension of 10 - 15 mN/m). Repeated measurements gave identical diagrams.

2.4 Atomic Force microscopy

For Langmuir-Blodgett transfer, films were prepared on a home-built teflon trough with an operational area of 66.5 cm². Surface tension was measured as described above. Before film spreading, a freshly cleaved mica sheet was dipped vertically into a subphase of demineralized water at room temperature (20 ± 3 °C). Films, having the same composition as described for the surface pressure - area curves, were formed by spreading aliquots onto the subphase. The films were compressed at a rate of 8.6 % of the operational area per min until a surface tension of 22 mN/m was reached. Subsequently, the films were transferred onto a disc of mica (14 mm in diameter) at a rate of 2.0 mm/min at constant surface tension.

For AFM measurements, transferred films were mounted on the J-type scanner (150 μm × 150 μm scan range) of a Nanoscope III Multimode microscope (Digital Instruments, Santa Barbara, CA, USA) operating in contact mode in air. Scanning was performed using oxide-sharpened Si₃N₄ tips with a spring constant of 0.12 N/m. The force with which the tip scanned the sample was set such that it was as small as possible while the image was stable and clear, which was usually at a force of 15 nN. Samples were checked for possible tip-induced deformation by zooming out after a region had been scanned. Since scanning in tapping mode did not give better images compared to those obtained in contact mode, we used contact mode because of its ease of handling.

2.5 Statistics

The computer program SPSS version 9.0 (SPSS Inc., Chicago, IL, USA) was used for statistical analysis by ANOVA with Bonferroni's post-hoc test. Differences were considered significant at $P < 0.05$.

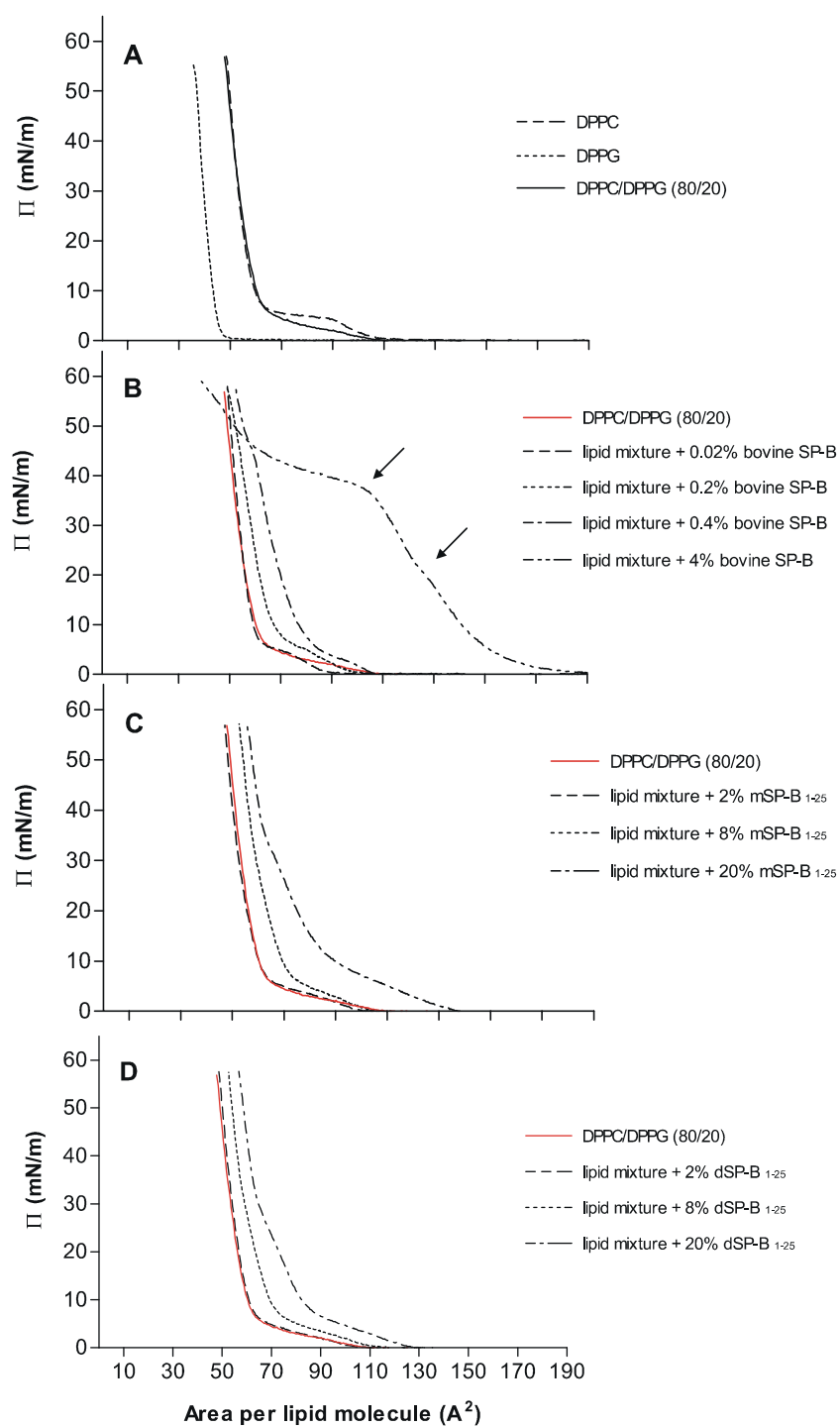


Figure 2. Pressure - Area isotherms of DPPC/DPPG films with and without native SP-B or SP-B₁₋₂₅ peptide. Compression isotherms of monolayers containing DPPC, DPPG or DPPC/DPPG (80/20, mol/mol) (A) plus 0.02 - 4 mol% bovine SP-B (B), 2 - 20 mol% mSP-B₁₋₂₅ (C), or 2 - 20 mol% dSP-B₁₋₂₅ (D) on a water subphase at 21 °C. The squeeze-out plateaus observed for bovine SP-B are indicated by arrows (B).

3. Results

Pressure - area isotherms were recorded to obtain information about the surface tension at which protrusion formation occurred. Lipid/protein monolayers were compressed by movement of a barrier in a Langmuir-Wilhelmy trough, which leads to a decrease in the area available to the film. Consequently, film surface pressure (π) was increased, and film surface tension (γ) was lowered. The relationship between π and γ is given by the equation $\pi = 72.5 - \gamma$, where 72.5 mN/m represents the surface tension of pure water at 21 °C. A typical pressure-area isotherm of pure lipid monolayers is depicted in Fig. 2A. The isotherm of DPPC/DPPG (80/20) shows phase behavior similar to that of pure DPPC. When bovine SP-B was added to DPPC/DPPG (Fig. 2B), two plateau regions were observed: the first at a surface pressure of approximately 23 mN/m and a second one, that was much more pronounced, at $\pi = 40$ mN/m. These plateaus were seen most clearly at higher protein concentrations and are in line with data found for porcine SP-B [163]. For monolayers containing 4 mol% SP-B the squeeze-out plateau was elongated and the monolayer could be compressed to very low areas, indicating massive squeeze-out. No additional plateaus were observed above $\pi = 48$ mN/m until onset of film collapse (at approximately $\pi = 59$ mN/m in our experimental setup), indicating that no extra squeeze-out occurred. For mSP-B₁₋₂₅ containing monolayers, isotherms of films with 2 mol% or less peptide were identical to isotherms of DPPC/DPPG (Fig. 2C). Furthermore, at increasing peptide concentrations no plateau like that observed at $\pi = 40$ mN/m for bovine SP-B was seen, but instead a region with a decreased slope was observed between surface pressures of 8 and 32 mN/m, comparable to the first faint plateau observed for bovine SP-B. The region with decreased slope was most clearly visible for monolayers containing as much as 20 mol% of the peptide. If protrusion formation occurs, it can be expected to be in this region. A similar region with decreased slope was seen for dSP-B₁₋₂₅ peptide containing monolayers (Fig. 2D). From Fig. 2 it is apparent that the compressibility of bovine SP-B containing monolayers is considerably higher than those containing SP-B₁₋₂₅ peptides at the same concentration. Since squeeze-out had fully occurred above a surface tension of 24 mN/m (*i.e.* below a surface pressure of 48 mN/m), determinants for protrusion formation were studied using monolayers compressed beyond this plateau to a surface tension of 22 mN/m.

Lipid/protein films, compressed to the desired surface tension, were deposited on mica and the topography was subsequently visualized by atomic force microscopy. Fig. 3 shows the effect of surface tension on film structure, using films of DPPC/DPPG/SP-B (80/20/4, mol/mol/mol). Films deposited at $\gamma = 62$ mN/m, *i.e.* when squeeze-out has not yet occurred, showed brighter islands (*i.e.* having a higher surface) surrounded by darker (*i.e.* lower) regions (Fig. 3A). According to other AFM studies [163,206] the bright islands at this surface tension correspond to liquid condensed (LC) phase while the dark regions consist of liquid expanded (LE) phase. The LC domains showed dark spots (readily seen at higher magnification, Fig. 3B), probably consisting of trapped LE phase. Upon compression of the monolayer (*i.e.* decreasing the surface tension) the amount of LC phase was increased (Fig. 3C). The

Chapter 4

difference in height between both lipid phases was found to be 1.2 ± 0.1 nm, which is similar to that found by others [163,206]. Film topography altered dramatically when films were compressed through the second plateau region of the isotherm to a surface tension of 22 mN/m (Fig. 3D). At this surface tension protrusions were formed that appeared as bright mountains amongst dark valleys consisting of monolayer. The height of the protrusions was 4.1 ± 1.1 nm. It has been shown for the same lipid/protein mixture that while the protrusions consist of proteins as well as lipids in LE phase, the lipid monolayer is in LC phase [163].

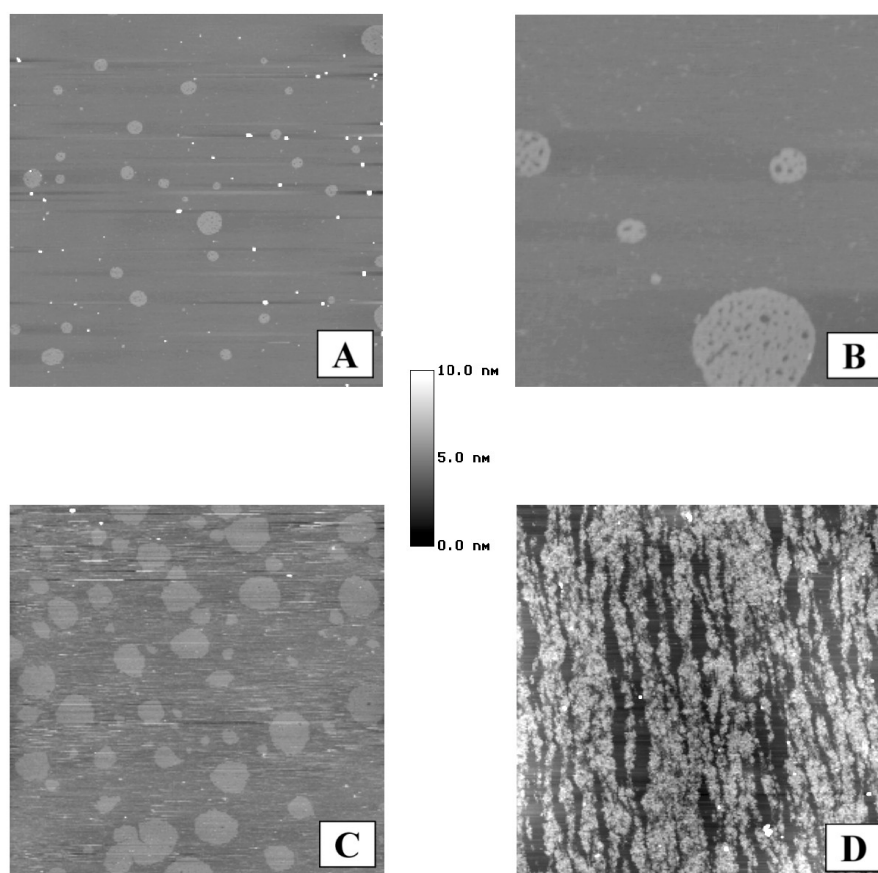


Figure 3. AFM topography of DPPC/DPPG films containing native SP-B compressed to varying surface tensions.

Films of DPPC/DPPG/bovine SP-B (80/20/4, molar percentages) were transferred onto mica at $\gamma = 62$ mN/m (scan area = $10 \times 10 \mu\text{m}$ in (A) and $2 \times 2 \mu\text{m}$ in (B)), $\gamma = 42$ mN/m (C) (scan area = $10 \times 10 \mu\text{m}$), and $\gamma = 22$ mN/m (D) (scan area = $10 \times 10 \mu\text{m}$).

To learn more about the origin and development of the protrusions, we made a concentration curve of bovine SP-B in DPPC/DPPG (80/20) films compressed to a surface

Determinants for surfactant multilayer formation

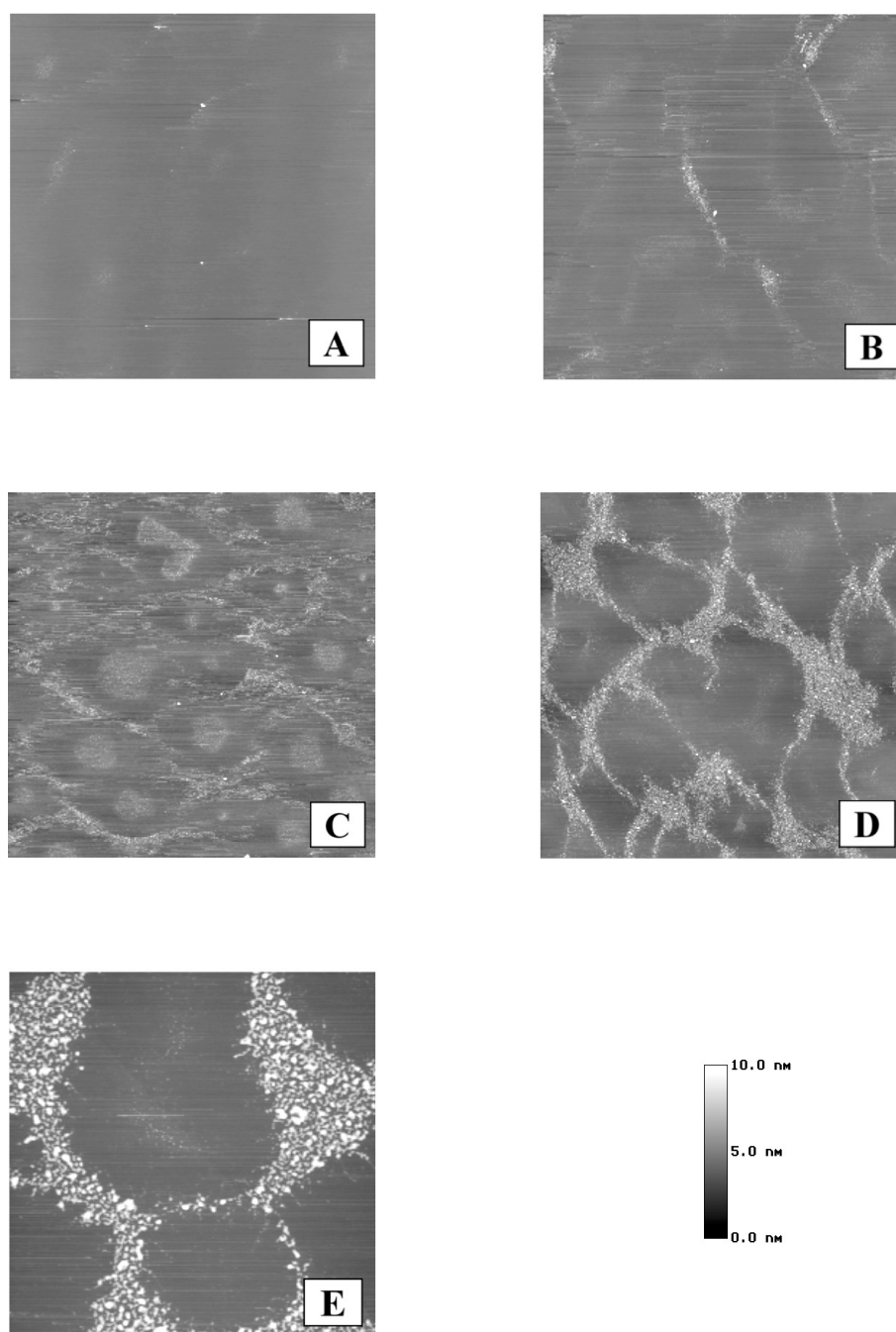


Figure 4. AFM topography of DPPC/DPPG films containing low to moderate amounts of native SP-B.

Films were transferred onto mica at $\gamma = 22$ mN/m, containing DPPC/DPPG (80/20, mol/mol) plus low to moderate bovine SP-B concentrations of 0.02 mol% (A), 0.1 mol% (B), 0.2 mol% (C), or 0.4 mol% (D); scan areas were $10 \times 10 \mu\text{m}$. Furthermore, a zoomed-in image of DPPC/DPPG/SP-B (80/20/0.4) is shown (E) at a scan area of $3 \times 3 \mu\text{m}$.

tension of 22 mN/m (Figs. 4 and 5). Although indications for protrusion formation were observed even at very low SP-B concentration (0.02 mol%), protrusion height differed

Chapter 4

statistically significant through the concentration curve: at very low concentration (0.02 mol%) heights were 0.5 ± 0.1 nm; at low to moderate concentration (0.1 - 0.2 mol%) heights were 2.0 ± 0.9 nm overall; at moderate to high concentrations (0.4 - 8 mol%) heights were 4.1 ± 1.1 nm overall; see Table 1 for protrusion heights of individual concentrations. Furthermore, upon increasing the protein concentration the protrusion regions became connected and started forming networks of small circular domains (readily observed as white dots in Fig. 4E). The typical hexagonal shape of the cells of the networks is best seen at a physiologically relevant SP-B concentration of 0.2 - 0.4 mol%. Although AFM determinations in the x and y direction are not as accurate as in the z direction, widths of samples scanned with the same tip can be roughly compared to each other. Protrusions were found to be disc-like in shape with a typical diameter of approximately 35 nm that did not change over the range of SP-B concentrations studied. An interesting observation was the presence of large circles of protruded material captured inside a hexagonal cell, most clearly seen in films containing 0.2 mol% SP-B (Fig. 4C). The height of these protrusions was 0.7 ± 0.1 nm, suggesting that they represent domains with different lipid orientation. One can speculate that these large circles consist of lipids with extended acyl chains, that have an increased height compared to the lipids around the circles, either because the latter have tilted chains, or because they are in a fluid state like the lipids in the networks. The large circles were not observed at high protein concentrations (2 - 8 mol%, Fig. 5) at which the monolayer domains were much smaller. Increasing the SP-B concentration led to a higher amount of protruded material until the monolayer had almost vanished and mostly protruded material was seen (Fig. 5E and F). Meanwhile, the network structures lost their typical hexagonal appearance. Importantly, when films contained no protein or peptide, protrusions were not observed upon compression to a surface tension of 22 mN/m (not shown).

AFM images of films containing SP-B₁₋₂₅ peptides differed dramatically from those containing bovine SP-B, in the sense that i) much higher peptide concentrations were needed to obtain the same kind of network structures, and ii) the height of the protrusions was considerably lower than that found for the native protein. Interestingly, monomeric mSP-B₁₋₂₅ and dimeric dSP-B₁₋₂₅ were found to have similar film topography (compare Figs. 6 and 7). Although protrusions were visible at 2 mol% of the SP-B₁₋₂₅ peptides (Figs. 6A and 7A), the first indication for structured networks is seen at a peptide concentration of 8 mol% (Figs. 6B and 7B). At an SP-B₁₋₂₅ concentration as high as 20 mol% hexagonal structures comparable to those of 0.4 mol% bovine SP-B were observed, although the size of the hexagonal cells were markedly larger in the case of dSP-B₁₋₂₅ than in that of mSP-B₁₋₂₅ or native SP-B (compare Fig. 7C with Figs. 6C and 4D). The overall height of the protrusions was 2.7 ± 1.3 nm for films containing 2 mol% or 8 mol% mSP-B₁₋₂₅ or 2 mol% dSP-B₁₋₂₅; see Table 1 for protrusion heights at individual concentrations. Surprisingly, protrusion height of films containing 20 mol% mSP-B₁₋₂₅ was significantly lower than that found at lower mSP-B₁₋₂₅ concentrations and for films containing dSP-B₁₋₂₅. Films containing 8 mol% or 20 mol% dSP-B₁₋₂₅ had overall protrusion heights of 3.5 ± 1.7 nm. Protrusion heights of films containing the SP-B₁₋₂₅ peptides were significantly lower than those containing 0.4 mol%

Determinants for surfactant multilayer formation

bovine SP-B, except for films with high concentrations (8 and 20 mol%) of dSP-B₁₋₂₅. Finally, the tendency to form the large circles of protruded material inside the network, as observed for 0.2 mol% bovine SP-B (Fig. 4C), was also seen for films containing 20 mol% dSP-B₁₋₂₅ (Fig. 7C and D).

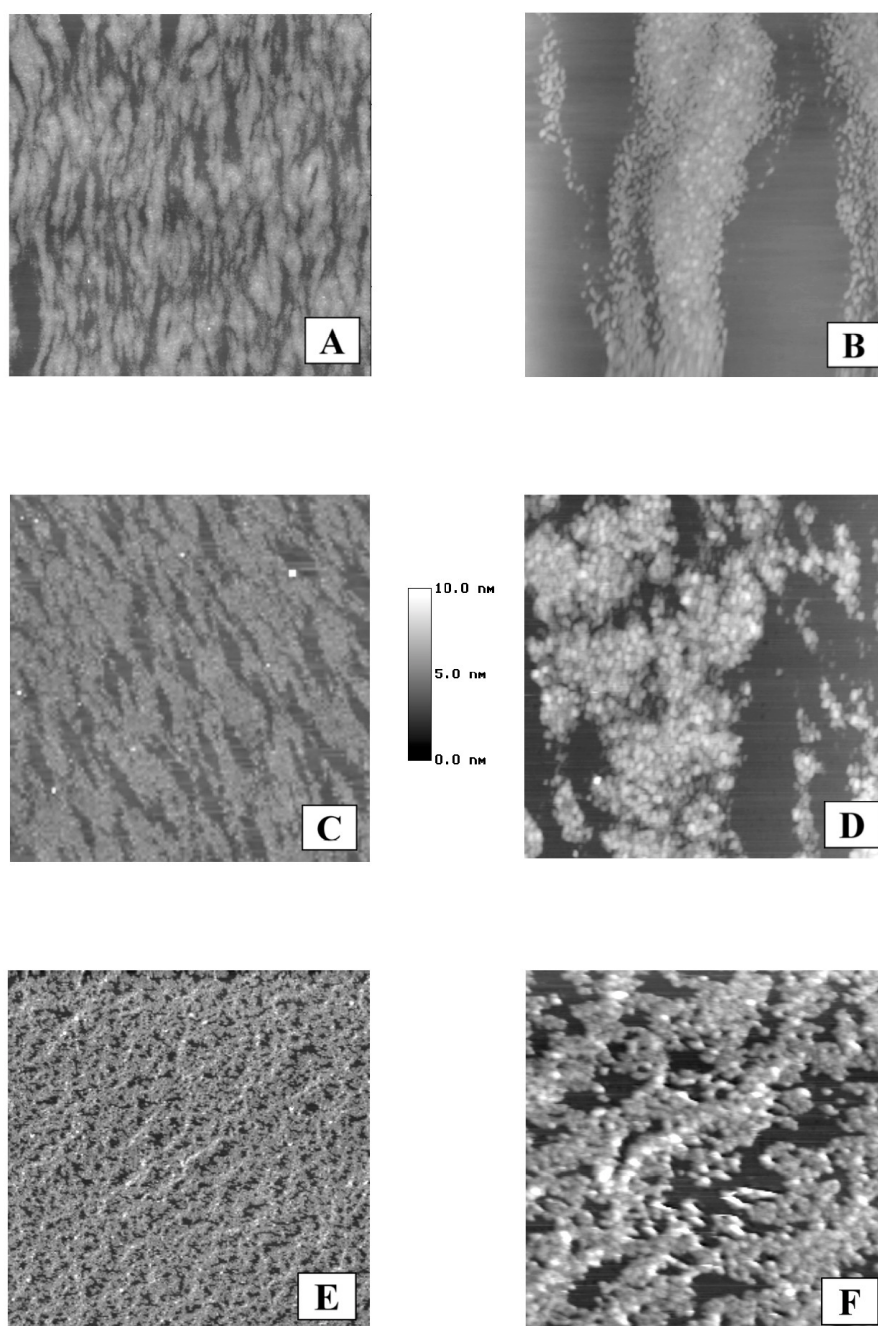


Figure 5. AFM topography of DPPC/DPPG films containing high amounts of native SP-B.

Films were transferred onto mica at $\gamma = 22$ mN/m, containing DPPC/DPPG (80/20, mol/mol) plus high concentrations of bovine SP-B of 2 mol% at a scan area of $10 \times 10 \mu\text{m}$ (A) and $2 \times 2 \mu\text{m}$ (B), 4 mol% at a scan area of $10 \times 10 \mu\text{m}$ (C) and $2 \times 2 \mu\text{m}$ (D), and 8 mol% at a scan area of $10 \times 10 \mu\text{m}$ (E) and $2 \times 2 \mu\text{m}$ (F).

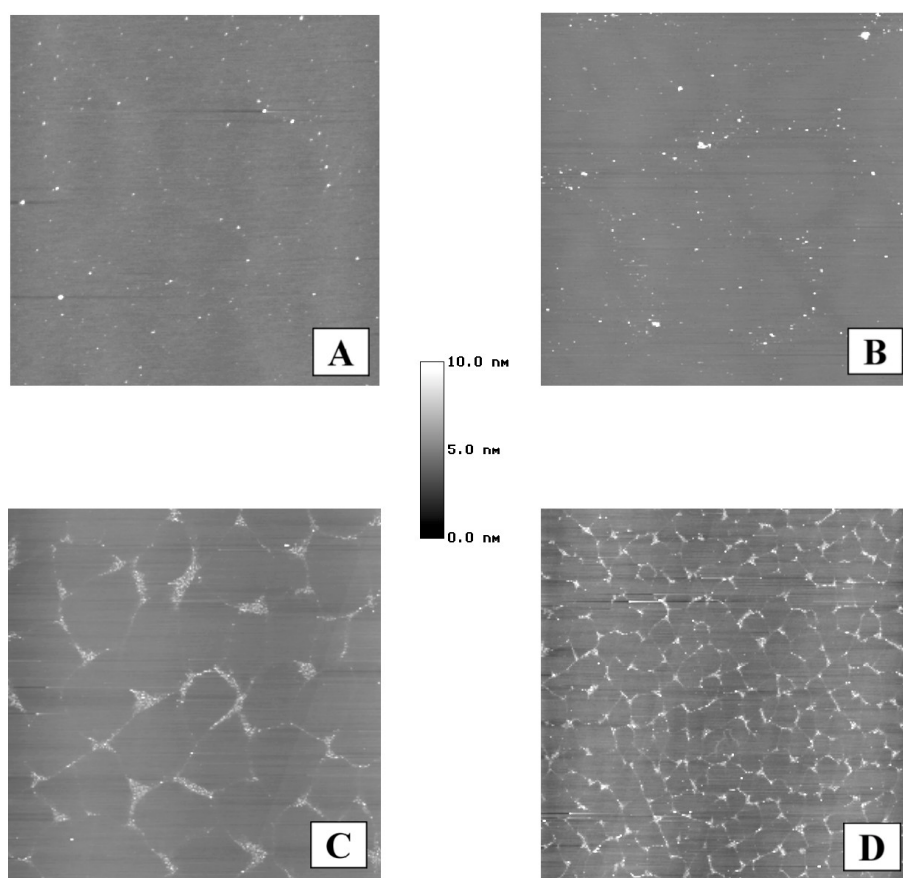


Figure 6. AFM topography of DPPC/DPPG films containing varying concentrations of monomeric SP-B₁₋₂₅ peptide.

Films were transferred onto mica at $\gamma = 22$ mN/m, containing DPPC/DPPG (80/20, mol/mol) plus the monomeric peptide mSP-B₁₋₂₅ at 2 mol% (A), 8 mol% (B), and 20 mol% (C), scanned at $10 \times 10 \mu\text{m}$. Furthermore, an image of DPPC/DPPG/mSP-B₁₋₂₅ (80/20/20) is shown at a scan area of $30 \times 30 \mu\text{m}$ (D).

The influence of lipid unsaturation on film topography was investigated by substituting DPPG by POPG. For these experiments, protein or peptide concentrations used were those previously observed to give clear network structures in the DPPC/DPPG (80/20) mixtures, *i.e.* 0.4 mol% bovine SP-B and 20 mol% of the SP-B₁₋₂₅ peptides. Compression isotherms (Fig. 8) clearly showed squeeze-out plateaus at approximately $\pi = 40$ mN/m ($\gamma = 32$ mN/m) for DPPC/POPG films containing either native SP-B or SP-B₁₋₂₅ peptide. Film appearance (Fig. 9) was similar for lipid mixtures containing either saturated or unsaturated PG (compare Fig. 9 with Figs. 4D, 6C and 7C). The size of the hexagonal cells was again larger in the case of dSP-B₁₋₂₅ than for mSP-B₁₋₂₅, albeit that the difference was less extreme than in the fully saturated lipid system. DPPC/POPG films containing low amounts of peptides, like 2 mol% mSP-B₁₋₂₅ or 1 mol% dSP-B₁₋₂₅, did not show network structures (Fig. 9D and E). A spectacular difference was found for the height of the protrusions: whereas in the case of a fully saturated lipid system compressed material always formed protrusions with a height of

Determinants for surfactant multilayer formation

approximately 4 nm, the exchange of DPPG for POPG resulted in the presence of protrusions of up to 24 nm. This was found for bovine SP-B as well as the SP-B₁₋₂₅ peptides. Mostly, protrusions of 4, 8, 12, 16, 20 and 24 nm were found. Occasionally, higher protrusions of up to 60 nm were seen.

Table 1. AFM measurements of protrusion height of compressed films containing DPPC/DPPG (80/20) plus varying amounts of native SP-B or SP-B₁₋₂₅ peptides. The number of protrusion height determinations is denoted by *n*.

protein or peptide (mol%)		protrusion height (nm)
<u>bovine SP-B</u>		
0.02	(<i>n</i> =12)	0.5 ± 0.1 ^a
0.1	(<i>n</i> =18)	2.0 ± 1.0 ^b
0.2	(<i>n</i> =10)	2.1 ± 0.8 ^b
0.4	(<i>n</i> =21)	4.3 ± 1.5 ^c
2	(<i>n</i> =9)	3.6 ± 0.8 ^c
4	(<i>n</i> =19)	4.1 ± 1.1 ^c
8	(<i>n</i> =20)	4.3 ± 0.9 ^c
<u>mSP-B₁₋₂₅</u>		
2	(<i>n</i> =18)	2.4 ± 0.9 ^{d, f}
8	(<i>n</i> =59)	2.8 ± 1.4 ^{d, f}
20	(<i>n</i> =75)	2.0 ± 0.9 ^{e, f}
<u>dSP-B₁₋₂₅</u>		
2	(<i>n</i> =34)	2.7 ± 1.3 ^{d, f}
8	(<i>n</i> =46)	3.5 ± 2.0 ^d
20	(<i>n</i> =39)	3.4 ± 1.4 ^d

^a Value differs significantly from those observed for all other concentrations of native SP-B ($P < 0.05$).

^b Values differ significantly from those observed for other concentrations of native SP-B ($P < 0.05$), but not from each other.

^c Values differ significantly from those observed for other concentrations of native SP-B ($P < 0.05$), but not from each other.

^d Value does not differ significantly from those observed for other SP-B₁₋₂₅ peptides, except for 20 mol% mSP-B₁₋₂₅.

^e Value differs significantly from that for other SP-B₁₋₂₅ peptides ($P < 0.05$).

^f Values differ significantly ($P < 0.05$) from that observed for 0.4 mol% bovine SP-B.

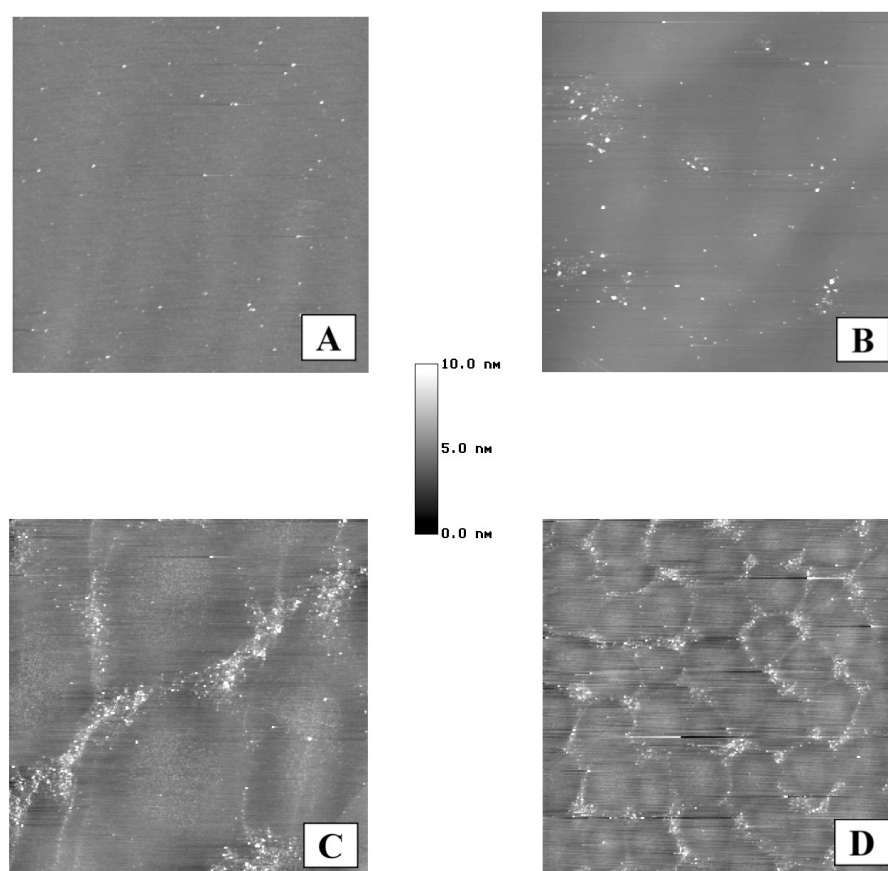


Figure 7. AFM topography of DPPC/DPPG films containing varying concentrations of dimeric SP-B₁₋₂₅ peptide. Films were transferred onto mica at $\gamma = 22$ mN/m, containing DPPC/DPPG (80/20, mol/mol) plus the dimeric peptide dSP-B₁₋₂₅ at 2 mol% (A), 8 mol% (B), and 20 mol% (C), scanned at $10 \times 10 \mu\text{m}$. Furthermore, an image of DPPC/DPPG/dSP-B₁₋₂₅ (80/20/20) is shown at a scan area of $30 \times 30 \mu\text{m}$ (D).

In a subsequent set of experiments the topography of films consisting of DPPC/POPC/DPPG (60/20/20, molar percentages) instead of DPPC/POPG (80/20) was investigated. In this way it was studied whether the increased height of the protrusions was dependent on the presence of the unsaturated acyl chain in phosphatidylglycerol, or could also be brought about by an unsaturated acyl chain in an equal number of the phosphatidylcholine molecules. Compression isotherms of DPPC/POPC/DPPG films containing proteins or peptides (Fig. 10) did not show the pronounced plateaus as observed for films of DPPC/POPG at the same protein or peptide concentration (Fig. 8), although to some degree isotherm flattening was observed, albeit at higher surface pressure (at $\pi = 42$ mN/m) than in the films of the other lipid mixtures. DPPC/POPC/DPPG films containing 20 mol% SP-B₁₋₂₅ peptides (Fig. 11) appeared different from those formed in the two other lipid mixtures at the same peptide concentration, but resembled films of lower peptide concentration. Moreover, network structures were not visible in films with 20 mol% mSP-B₁₋₂₅. Surprisingly, it was found for

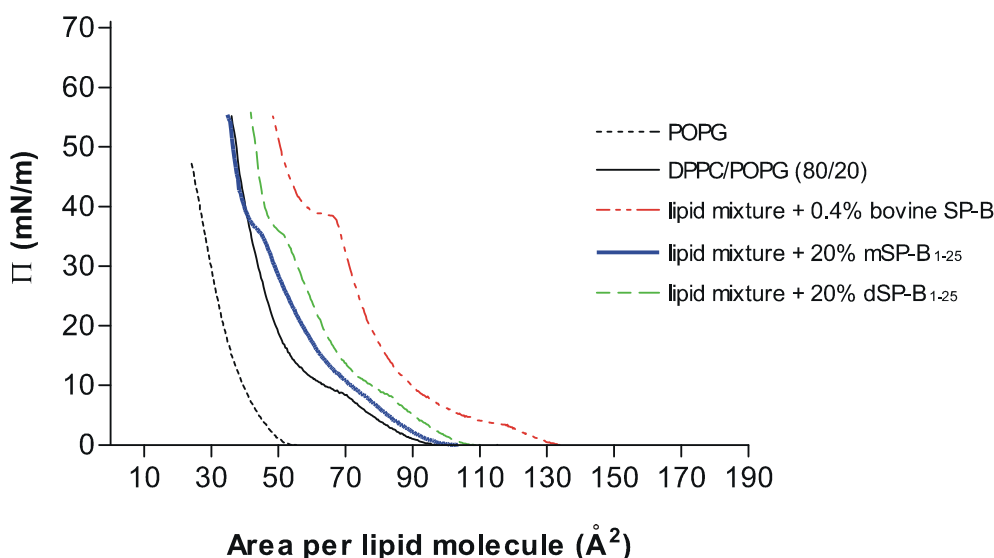


Figure 8. Pressure - Area isotherms of DPPC/POPG films with and without native SP-B or SP-B₁₋₂₅ peptide. Compression isotherm of monolayers containing POPG, or DPPC/POPG (80/20, mol/mol) plus 0.4 mol% bovine SP-B, 20 mol% mSP-B₁₋₂₅, or 20 mol% dSP-B₁₋₂₅.

films with 0.4 mol% bovine SP-B or 20 mol% SP-B₁₋₂₅ peptides that the heights of the protrusions formed were mainly 4.4 ± 0.7 nm, which is lower than the heights found for films containing DPPC/POPG. Heights of 8 - 32 nm were also observed, but this was less common and was seen only for films containing bovine SP-B and dimeric peptide.

4. Discussion

Surfactants based on synthetic peptides are of growing interest to clinical use, because of their low risk of containing biohazardous contaminants and their relative ease of production. Before clinical application of artificial surfactant, detailed knowledge about biophysical activity of their synthetic peptides and lipids is required. Here we describe the effect of synthetic peptides based on the N-terminal 25 amino acids of human SP-B on the topography of supported DPPC/DPPG (80/20) films and compare it with the effect of bovine SP-B, which is present in a large number of commercially available surfactants. Moreover, the effect of lipid acyl chain unsaturation and the effect of the nature of the phospholipid that contains an unsaturated acyl chain on the formation of multilayered surfactant protrusions was investigated using films with DPPC/POPG (80/20) or DPPC/POPC/DPPG (60/20/20) as lipid components. Our findings suggest that the molecular composition of mixed lipid/protein monolayers plays an important role in surfactant film topography.

Compression isotherms of monolayers of DPPC/DPPG (80/20) with bovine SP-B (0.02 - 4 mol%) showed two squeeze-out plateaus of which the plateau starting at

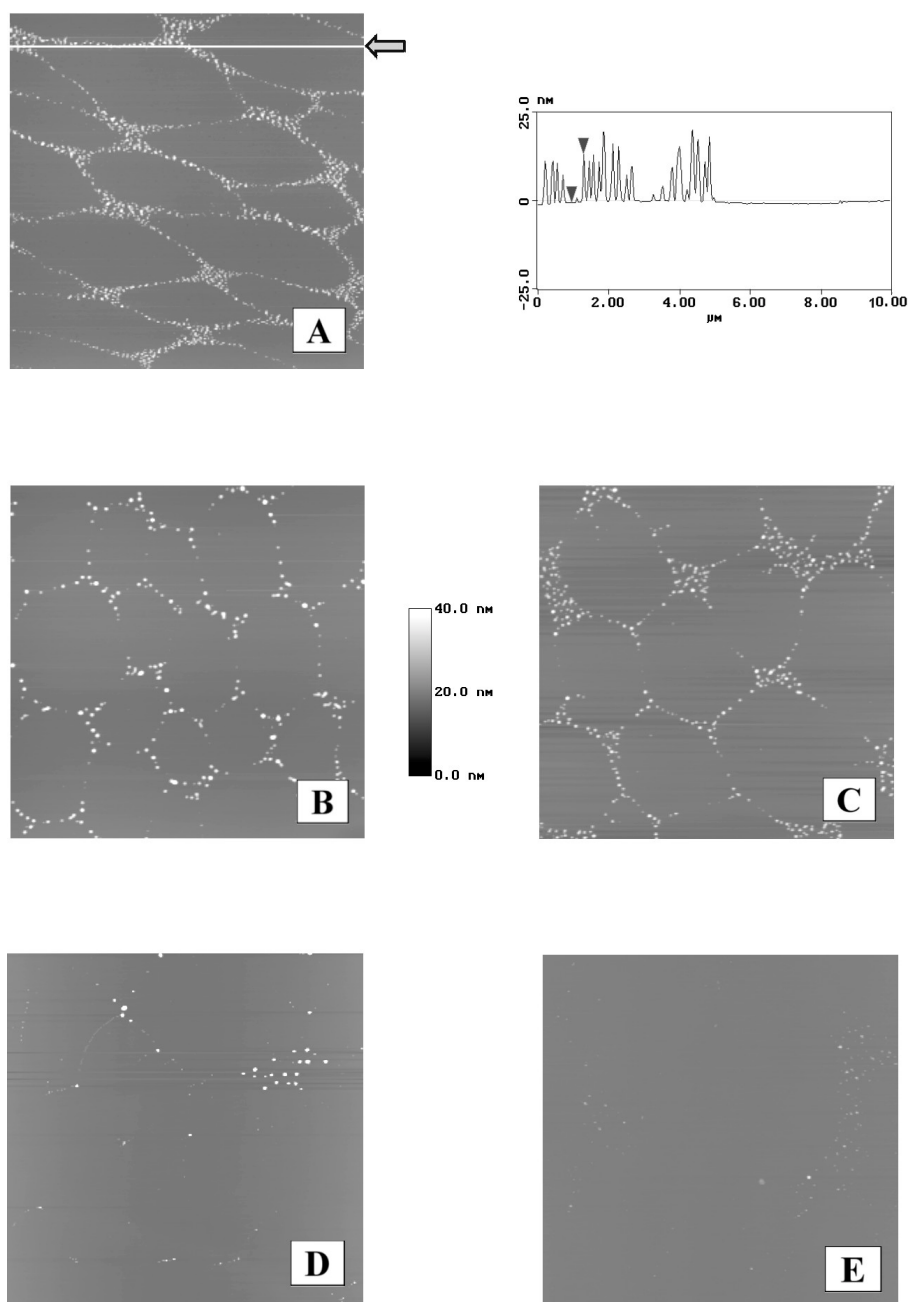


Figure 9. AFM topography of DPPC/POPG films containing native SP-B, mSP-B₁₋₂₅ or dSP-B₁₋₂₅.

Films were transferred onto mica at $\gamma = 22$ mN/m, containing DPPC/POPG (80/20, mol/mol) plus 0.4 mol% bovine SP-B (A), 20 mol% mSP-B₁₋₂₅ (B), 20 mol% dSP-B₁₋₂₅ (C), 2 mol% mSP-B₁₋₂₅ (D), or 1 mol% dSP-B₁₋₂₅ (E), scanned at $10 \times 10 \mu\text{m}$. The height trace is that of the white line in image A. The arrowheads on the height trace show the approximate height difference, which was 15.7 nm.

$\gamma = 32$ mN/m was broadened as protein concentration increased (Fig. 2). It should be noted that we define squeeze-out as exclusion of fluid lipid and protein from the monolayer into the

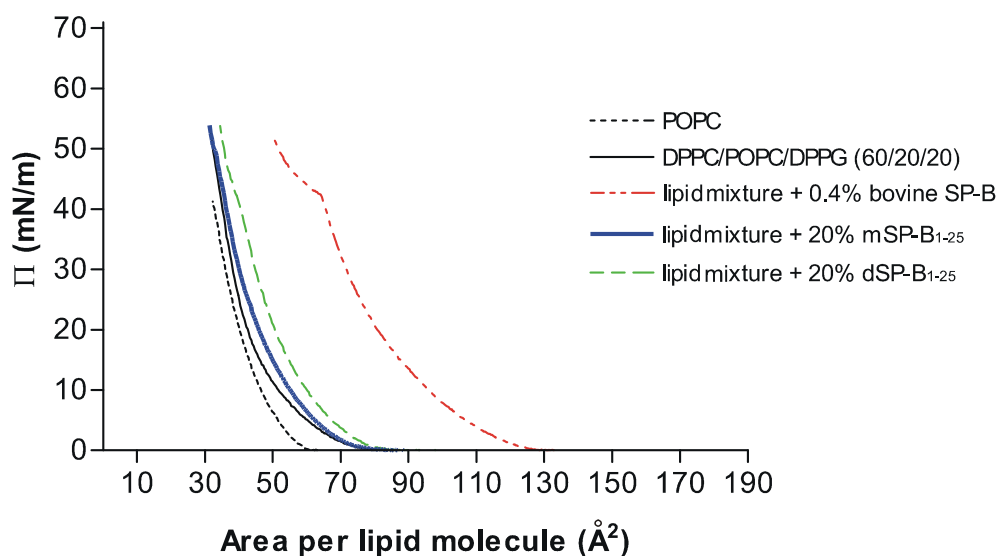


Figure 10. Pressure - Area isotherms of DPPC/POPC/DPPG films with and without native SP-B or SP-B₁₋₂₅ peptide.

Compression isotherm of monolayers containing POPC, or DPPC/POPC/DPPG (60/20/20, mol/mol/mol) with 0.4 mol% bovine SP-B, 20 mol% mSP-B₁₋₂₅, or 20 mol% dSP-B₁₋₂₅.

surface-associated reservoir, and not as exclusion out of layered structures and into an aqueous subphase. AFM measurements showed that increasing concentrations of bovine SP-B in DPPC/DPPG films resulted in the formation of more protrusions. At SP-B levels of 0.2 - 0.4 mol% the protrusions appeared as small disc-like domains which formed network structures, which is in agreement with results from AFM studies in which porcine SP-B was used [163]. Interestingly, similar SP-B concentrations were found to show optimal activity *in vitro*, as measured by CBS (0.5 - 0.75 mol%) [57,185], spreading trough (0.2 mol%) [57], and lipid mixing assays (0.2 mol%) [173,218,219]. Moreover, it is comparable to the amount of SP-B reported in bronchoalveolar lavage fluid, ranging from 0.02 mol% [57] to 0.9 mol% [220]. Ultimately, addition of more protein will stop leading to formation of extra protrusions, due to the fact that there is no more lipid available. This probably occurs in films with more than 4 mol% SP-B.

The protrusion height in experiments with films containing DPPC/DPPG (80/20) and a concentration of native SP-B \geq 0.4 mol% was 4.0 - 4.3 nm (Table 1). This is lower than in AFM studies using porcine SP-B in DPPC/DPPG (80/20), in which protrusions with a height of 6 - 7 nm after film compression to a surface tension of 22 mN/m were reported [163]. Although the same lipid mixture and protein were used, and although both in our study and in the study by [163] contact mode AFM in air was used, subtle differences in film compression rate, temperature, brand of microscope and force of scanning may result in differences in measured protrusion height. In another study using contact mode AFM,

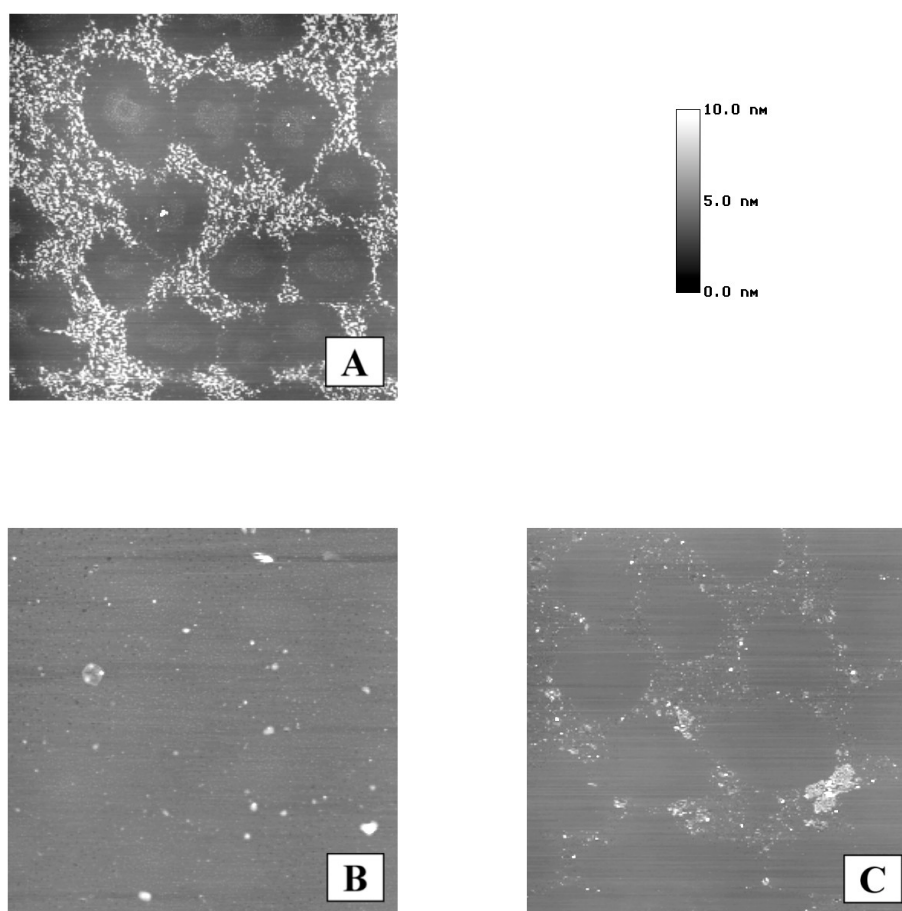


Figure 11. AFM topography of DPPC/POPC/DPPG films containing native SP-B, mSP-B₁₋₂₅ or dSP-B₁₋₂₅. Films were transferred onto mica at $\gamma = 22$ mN/m, containing DPPC/POPC/DPPG (60/20/20, mol/mol/mol) plus 0.4 mol% bovine SP-B (A), 20 mol% mSP-B₁₋₂₅ (B), or 20 mol% dSP-B₁₋₂₅ (C), scanned at 10×10 μm .

compression of mSP-B₁₋₂₅ in a lipid mixture of DPPG/POPG (3/1), transferred at $\gamma = 18$ mN/m, was found to result in protrusions of 10 - 40 nm, in steps of 5.0 nm [206]. Furthermore, X-ray diffraction determination of bilayer thickness showed heights of 3.7 nm [204] to 4.3 nm [328] for DPPC in fluid liquid crystalline state, and 4.7 nm for DPPC in gel state [328]. Since our observed heights were found to be reproducible along the concentration curve from 0.4 mol% bovine SP-B upwards, we believe that the height of 4 nm represents the dimensions of a protruded bilayer. Since protrusion heights of ≤ 2 nm were found for SP-B concentrations of ≤ 0.2 mol%, these protrusions are not made up of bilayers. This means that low amounts of protein relative to lipid can not induce and sustain protrusions of bilayers, but will probably partly reorient the lipids and lift them out of the monolayer. The molecular organization of such protruded material is not clear. We suggest that surfactants used for therapy containing SP-B as the sole protein should contain more than 0.2 mol% of the protein in order to ensure sufficient formation of surface-associated reservoir.

Compression isotherms of DPPC/DPPG monolayers containing the peptides mSP-B₁₋₂₅ and dSP-B₁₋₂₅ (Figs. 2C and D) did not have the pronounced squeeze-out plateau observed for bovine SP-B at $\pi = 40$ mN/m (Fig. 2B), even when they were used at high concentrations, but showed a region of decreased slope comparable to the faint plateau of bovine SP-B observed at $\pi = 25$ mN/m. The absence of a plateau suggests that squeeze-out in SP-B₁₋₂₅ peptide containing films took place in a different way than in films with the native protein. The compressibility of DPPC/DPPG films containing native SP-B (Fig. 2A) was higher than that observed for films containing SP-B₁₋₂₅ peptides (Figs. 2C and D). This may reflect a more pronounced fluidizing effect of full-length SP-B compared to SP-B₁₋₂₅ peptides. Alternatively, it could mean that native SP-B is better able to stack the lipids in multilayers. This observation was confirmed by AFM measurement which showed that much higher SP-B₁₋₂₅ peptide concentrations were needed to form structures similar to those seen with native SP-B. Furthermore, the height of the protrusions was significantly smaller than that obtained with native SP-B, except when high concentrations (8 and 20 mol%) of dimeric peptide were included in the film. From this we conclude that, although SP-B₁₋₂₅ peptides are able to form network structures, they are not as effective in doing so as native SP-B is.

Interestingly, structures observed for films of DPPC/DPPG (80/20) containing mSP-B₁₋₂₅ peptides and those containing dSP-B₁₋₂₅ of roughly the same weight% (*i.e.* at roughly the same amount of N-termini) were not the same (compare for instance 20 mol% mSP-B₁₋₂₅ (Fig. 6C) with 8 mol% dSP-B₁₋₂₅ (Fig. 7B)). Similar structures for mSP-B₁₋₂₅ and dSP-B₁₋₂₅ were only observed when compared at equimolar peptide concentrations, both in films of DPPC/DPPG and in films of DPPC/POPG. This indicates that dimerization of mSP-B₁₋₂₅ does not result in an increased tendency to form protrusions. However, in DPPC/POPC/DPPG films the dimeric peptide did show a higher tendency to form protrusion networks than the monomeric peptide did (compare Fig. 11B with Fig. 11C). We have no explanation for this observation.

We found that the presence of unsaturated lipid acyl chains resulted in formation of multilayered structures. Multilayers were previously observed in studies using electron microscopy [12,221]. These findings are in accordance with a recent AFM study, using monomeric SP-B₁₋₂₅ in DPPG/POPG (3/1) [206], in which multilayered structures were reported as well. Presumably, unsaturated lipids are able to easily form curved protrusions during surface compression, because of their fluid and flexible character, while mixtures containing only saturated lipids (*e.g.* DPPC/DPPG) will be tightly packed and resist squeeze-out into protrusions. It has been shown in a number of studies that SP-B specifically interacts with PG [72,219,173,56,222]. The high number of multilayered protrusions found in DPPC/POPG lipid mixtures compared with the single bilayer protrusions found in DPPC/POPC/DPPG suggests that SP-B preferentially interacts with POPG rather than with POPC or DPPG.

It is of interest to consider whether surface activity measured by CBS is correlated with surface topography visualized by AFM. Our AFM observation that a higher concentration of SP-B₁₋₂₅ peptide than of native SP-B was needed for the formation of network structures is in

Chapter 4

line with a recent CBS study [53]. In that study it was shown that spread DPPC/POPG (80/20) films containing SP-B₁₋₂₅ peptides were in general less surface active than those containing native human SP-B. This suggests that surface topography measured by AFM can give an indication for surface activity measured by CBS. However, in the same CBS study it was reported that spread DPPC/POPG (80/20) films containing 1 mol% dSP-B₁₋₂₅ i) had a better surface activity (*i.e.* lower surface tensions) than spread films containing 2 mol% of mSP-B₁₋₂₅, and ii) reached equally low minimum surface tensions as spread films containing 0.5 mol% native human SP-B. Those CBS findings can not be readily correlated to the AFM results described in this article, since we found that the appearance of DPPC/POPG films containing 1 mol% dSP-B₁₋₂₅ (Fig. 9E) was similar to that of films containing 2 mol% mSP-B₁₋₂₅ (Fig. 9D), but was very different from that of films containing 0.4 mol% native bovine SP-B (Fig. 4D). On the other hand, differences between both SP-B₁₋₂₅ peptides were seen in DPPC/POPC/DPPG films, since films containing mSP-B₁₋₂₅ (Fig. 11B) did not have network structures, while those containing dSP-B₁₋₂₅ did (Fig. 11C). These data suggest that there may not always be a clear correlation between surface topography measured by AFM and surface activity measured by CBS. However, it should be kept in mind that the CBS experiments were performed at 37 °C, while our AFM experiments were carried out at room temperature. This may have led to differences in lipid fluidity between films in the two types of measurements, possibly affecting surfactant activity or topography. Obviously, to make a firmly founded comparison between AFM and CBS results, the experimental conditions should be kept the same.

We conclude i) that proteins are required to form protrusions of material that is squeezed out of the surfactant monolayer upon compression, and that protrusions of bilayer height are formed at a physiologically relevant concentration of 0.4 mol% SP-B, ii) that peptides based on the first 25 amino acids of the N-terminus of SP-B are also able to induce protrusion formation, but only at much higher concentrations, and iii) that determinants for protrusion height are lipid unsaturation as well as lipid headgroup, since in the presence of unsaturated lipid, protrusions of multiples of bilayers are found to be formed most clearly in the presence of POPG. Synthetic SP-B₁₋₂₅ based surfactants to be used clinically will therefore have to contain, in addition to DPPC, a high concentration of SP-B₁₋₂₅ peptides as well as unsaturated phospholipids, preferentially unsaturated PG.

Acknowledgments

We like to thank Dr. Anja ten Brinke for inspiring discussions about this work.

Chapter 5

Functional Tests for the Characterization of Surfactant Protein B (SP-B) and a Fluorescent SP-B Analog

Robert V. Diemel ^{a,b}, Dietmar Bader ^a, Monika Walch ^a, Barbara Hotter ^a, Lambert M.G. van Golde ^b, Anton Amann ^a, Henk P. Haagsman ^{b,c} and Günther Putz ^a

^a Department of Anaesthesiology and Critical Care Medicine,

The Leopold-Franzens-University of Innsbruck, Innsbruck, Austria

^b Department of Biochemistry and Cell Biology, and ^c Department of the Science of Food of Animal Origin, Faculty of Veterinary Medicine, Graduate School of Animal Health, Utrecht University, Utrecht, The Netherlands

Archives of Biochemistry and Biophysics, 2001, **385**: 338-347

Abstract

Surfactant protein B (SP-B) enhances lipid insertion into the alveolar air/liquid interface upon inhalation. The aim of this study was (i) to apply a palette of tests for a detailed biochemical and biophysical characterization of SP-B and (ii) to use these tests to compare native SP-B with a fluorescent (Bodipy) SP-B analog. The method of labeling was fast and resulted in a covalent fluorophore - protein bond. The ability of both proteins to spread a surfactant film on top of a buffer surface was determined in a spreading tray using the Wilhelmy plate technique to allow detection of alterations in surface tension and calculation of spreading velocities. In a captive bubble surfactometer surface tensions of spread films were measured. Similar biophysical properties were found for both native and Bodipy-labeled SP-B. It is concluded that the combination of tests used allows detection of small differences in structure and activity between the two proteins.

1. Introduction

Pulmonary surfactant is a mixture of lipids and proteins which is synthesized and secreted by the alveolar type II epithelial cells. Its main function is to reduce the surface tension at the air/liquid interface of the lung by forming a surface-active film, thereby preventing the alveoli from collapsing at the end of exhalation (see reviews [223,224] for surfactant composition and functions). Important components of pulmonary surfactant are the small hydrophobic proteins surfactant protein B (SP-B) and C (SP-C), which are closely associated with surfactant phospholipids. Both proteins have been demonstrated to enhance lipid insertion into the monolayer at the air/liquid interface, thereby maintaining a relatively low surface tension upon inhalation. In addition, SP-B and SP-C influence the molecular ordering of the phospholipid monolayer. Furthermore, SP-B is required for the formation of tubular myelin, an extracellular surfactant reservoir.

SP-B is a 79-residue polypeptide that has a net positive charge. These positive charges are essential for its interaction with negatively charged phospholipids [72,173]. *In vivo*, mature SP-B is active as a dimer with a molecular mass of 17.4 kDa, calculated from the amino acid sequence. An indication that dimerization of SP-B is required for optimal surfactant activity comes from a study in which SP-B mutant mice expressing only SP-B monomer were bred [52,20]: although these mice were able to survive, lung compliance and surface properties of the surfactant were altered. The importance of SP-B is further stressed by the observation that homozygous SP-B knock-out mice died of respiratory failure immediately after birth [20]. Furthermore, blocking of SP-B with monoclonal antibodies in rabbits led to respiratory failure and the loss of surfactant activity [21,225].

Since SP-B is essential for a properly functioning respiratory system and its amount in patients with acute respiratory distress syndrome (ARDS) is decreased [226-228], it might be taken as a marker for the distribution of exogenously instilled surfactant. Monitoring the

distribution of administered surfactant can be carried out most conveniently if one or more of its components are labeled, for instance fluorescently or radioactively. When labeling SP-B, procedures should be available to test if the labeled protein is as active as the native one. Therefore, we selected functional tests that were already available and combined them with newly developed procedures to be able to make a full characterization of SP-B as well as a fluorescently (Bodipy) labeled SP-B analog. Although surfactant components have been labeled before, only in a few cases was the label bound to SP-B [229-232], and labeled SP-B was never fully characterized. Moreover, the labeling procedures used were time-consuming. In our study the method of labeling was fast and resulted in a covalent fluorophore-protein bond. When compared with native SP-B it was found that Bodipy-labeled SP-B was labeled at specific sites. The primary and secondary structure of both native and labeled SP-B were determined by amino acid sequencing and circular dichroism. Furthermore, a fluorescent vesicle mixing assay was used to test the ability of both proteins to bring vesicular membranes in close proximity. With the aid of a glass spreading tray the capability to spread a surfactant film on top of a buffer surface was determined, as well as the spreading velocity at which this process took place. A captive bubble surfactometer was used to investigate the ability of both proteins to transport lipids into the air/water interface of an air bubble in buffer. Moreover, using a recently developed technique for the spreading of a surfactant film [26], it was possible to determine the surface tension during dynamic bubble compression and expansion precisely. Since even minor differences between native and Bodipy-labeled SP-B could be detected when applying these techniques, it is concluded that this combination of tests allows for detection of small differences in structure and activity between the two proteins.

2. Materials and Methods

2.1. Materials

1,2-dipalmitoyl-*sn*-glycero-3-phosphocholine (DPPC) and 1-palmitoyl-2-oleoyl-*sn*-glycero-3-(phospho-*rac*-(1-glycerol)) (POPG) were obtained from Avanti Polar Lipids (Alabaster, AL, USA). Trifluoroacetic acid (TFA) (Pierce, Rockford, IL, USA), methanol (MeOH) (Scharlau, Barcelona, Spain), chloroform (B&J, Miskogon, MI, USA), dimethylsulfoxide (DMSO) (Sigma, St. Louis, MI, USA) and butanol, dichloromethane and triethylamine (Fluka, Buchs, Switzerland) were HPLC grade. 2-(4,4-difluoro-5,7-dimethyl-4-bora-3a,4a-diaza-*s*-indacene-3-dodecanoyl)-1-hexadecanoyl-*sn*-glycero-3-phosphocholine (Bodipy[®]-PC), *N*-(4,4-difluoro-5,7-dimethyl-4-bora-3a,4a-diaza-*s*-indacene-3-propionyl)cysteic acid succinimidyl ester (Bodipy[®] FL CASE) and 1-hexadecanoyl-2-(1-pyrenedecanoyl)-*sn*-glycero-3-phosphocholine (pyrene-PC) were obtained from Molecular Probes Europe (Leiden, the Netherlands). HEPES, KCl, NaCl and EDTA were obtained from Sigma. For SDS-PAGE the molecular weight standards from Gibco (Gibco Life Technologies, Gaithersburg, MD, USA) and Biorad (Biorad, Hercules, CA, USA) were used. Alveofact[®] was purchased from Thomae (Biberach, Germany). Water was filter-purified in our lab (Modulab

Chapter 5

Water Systems, Lowell, MA, USA). Agarose (SeaKem ME agarose, FMC Bioproducts, Rockland, ME, USA) was extracted as described [25].

2.2. Isolation and fluorescent labeling of SP-B

SP-B was isolated from bovine lung lavage. Bovine lungs were obtained from a slaughterhouse, and isolation and characterization of SP-B was performed using standard procedures [158]. The amount of protein was determined by fluorescamine assay [182], or by Pierce Micro BCA assay when Bodipy-labeled SP-B was measured and directly compared to non-labeled SP-B; both assays used bovine serum albumin as standard. To determine the amount of lipid phosphorus, the Rouser assay [183] was used.

Purified bovine SP-B (50 μg = 2.9 nmol) dissolved in dichloromethane/MeOH/0.1 M HCl (30/65/5, v/v/v) was dried under a stream of N_2 and redissolved in 40 μl DMSO. Then, 770-fold molar excess triethylamine in 20 μl DMSO and 16-fold molar excess Bodipy FL CASE in 20 μl DMSO were added and the mixture was incubated at room temperature for 30 min. Bodipy FL CASE reacts with free amino-groups, resulting in the formation of an amide-bond. The reaction mixture containing Bodipy-labeled SP-B, excess of unreacted Bodipy and trace components of non-labeled SP-B was separated on a HP 1100 Series HPLC (Hewlett Packard, Geneva, Switzerland) using an HP reversed phase rp-C18 Zorbac column (2.1 \times 150 mm, 5 μm particle size, 300 \AA poresize). A 15 min gradient of methanol from 70 to 100 vol% was run in water with a constant amount of TFA (0.1 vol%). The flow velocity was 0.2 ml/min at an oven temperature of 40 $^\circ\text{C}$. Absorbance (diode array detector at 190 - 950 nm) and fluorescence ($\lambda_{\text{ex}} = 488 \text{ nm}$, $\lambda_{\text{em}} = 512 \text{ nm}$) were measured. Peaks were analyzed by Tricine/SDS-PAGE in the absence of reducing agents and stained with silver nitrate. For Western Blot analysis, rabbit anti-sheep SP-B polyclonal antibodies were used (gift of Dr. Hawgood, San Francisco, USA). Western Blot detection was done using the ECL kit (Amersham, Buckinghamshire, England).

2.3. Amino acid sequencing

To determine the amino acid that reacted with the fluorescent label, 1.9 μg Bodipy-labeled SP-B was subjected to N-terminal sequence analysis (25 amino acids) using an Applied Biosystems Procise ABI protein sequencer (Perkin Elmer Biosystems, Foster City, CA, USA). For comparison, the N-terminal 25 amino acids of native SP-B were determined as well.

2.4. Electrospray Ionization Mass Spectrometry (ESI-MS)

Electrospray ionization mass spectra were recorded using a Micromass Q-ToF quadrupole time-of-flight mass spectrometer (Micromass, Cheshire, UK) equipped with a nanospray source. Samples were introduced using the “Z-spray” nanoflow electrospray source, using in-house pulled electrospray needles. The needles were made of borosilicate glass capillaries (Kwik-Fil, World Precision Instruments, Sarasota, FL, USA) using a P-97 puller (Sutter Instruments, Novato, CA, USA). The needles were gold-coated using an Edwards

Scancoat six Pirani 501. The standard mass range scanned was 700 - 4000 Thompson. The raw mass spectra were processed (averaged and smoothed) using MassLynx software (version 3.1). Deconvolution of the spectra was accomplished using MaxEnt. Mass analysis was performed with 2.9 μ M SP-B dissolved in MeOH/water (9/1, v/v) without further dilution.

2.5. Circular dichroism (CD)

CD spectra were obtained using a J600 spectropolarimeter (JASCO, Tokyo, Japan) in a 1 mm cell at 25 °C. Pure protein was dissolved in MeOH/water (9/1, v/v) at 300 μ g/ml. Scan speed was 20 nm/min with a resolution of 0.2 nm. Ten to forty consecutive scans from 260 to 195 nm were averaged and the protein-free MeOH/water spectrum was subtracted to yield the protein spectrum.

2.6. Pyrene-PC vesicle mixing assay

The ability of SP-B to induce vesicle mixing was measured by the pyrene-PC assay [218], with a few modifications concerning vesicle composition and fluorescence ratio. Lipids (DPPC/POPG, 8/2, mol/mol) with or without SP-B or pyrene-PC were dissolved in CHCl_3 /MeOH (1/1, v/v) and subsequently dried under a stream of N_2 . The lipid/protein films were then hydrated in buffer (25 mM HEPES, 0.20 mM EGTA, pH 7.0) at 60 °C. The suspensions were sonicated three times for 20 s at 2 microns amplitude (Soniprep 150, MSE Scientific Instruments, Crawley, England) resulting in SUVs. All vesicles were prepared freshly each day and kept on ice until use. Phospholipid SUVs (300 nmol lipid) were mixed with pyrene-containing SUVs (15 nmol lipid containing 10 mol% pyrene-PC, supplemented with 0.4 mol% native or Bodipy-labeled SP-B) in buffer at a final volume of 2 ml. The fusion reaction was initiated by addition of 20 μ l 0.3 M CaCl_2 . Fluorescence emission spectra ($\lambda_{\text{ex}} = 343$ nm, $\lambda_{\text{em}} = 360 - 550$ nm) were recorded under continuous stirring at 37 °C on a LS-50 luminescence spectrometer (Perkin Elmer, Beaconsfield, England). The excimer to monomer (E/M) fluorescence ratio was calculated by dividing the fluorescence emission intensity at 471 nm by the intensity at 396 nm.

2.7. Spreading tray

A glass tray (24 \times 30 cm, Duran Schott, Mainz, Germany) was filled with subphase buffer (140 mM NaCl, 10 mM HEPES, 0.5 mM EDTA, 2.5 mM CaCl_2 , pH 6.9) and covered with a 14 mm thick plexiglass lid to maintain humidity near saturation. The tray was placed in a waterbath which was kept at 37 °C. Before each measurement the buffer surface was cleaned by aspiration. Between measurements the tray was washed with detergent and rinsed with distilled water 3 times. After droplet formation the sample was gently put onto the buffer surface through a 42 \times 9 mm hole in the middle of the plexiglass lid by a multichannel pipette (5 \times 6 μ l). Just underneath the buffer surface a 1 % (w/v) agarose disc (3 - 4 mm thick, 54 mm in diameter) was placed to serve as a ramp for the surfactant sample. More peripherally in the lid, 4 holes were drilled (*a*, *b*, *c* and *d*, 18 \times 5 mm; distance *a* - *b* was 5 cm and *c* - *d* was 8 cm, measured at the center of each hole) through which roughened platinum plates (10 \times 15 mm)

Chapter 5

were dipped into the buffer (Fig. 1). These platinum plates were positioned in such a way that surfactant reaches the most peripheral plates (*b* and *d*) before reaching the tray edge. The plates were connected to 4 force-displacement transducers (type FT 03, Grass, Quincy, MA, USA) that measured the change in surface tension using the Wilhelmy plate technique. Surface tension calibration of the sensors was done using methanol, water and 10 % (w/v) sodium dodecyl sulphate (standard surface tensions at 37 °C of 20.9, 69.9 and 39.7 mN/m, respectively). Spreading velocity was expressed as the distance (cm) traveled by the surfactant sample between two platinum plates (*a - b* or *c - d*), divided by the time (s) required for the samples to spread between these plates and lower the surface tension. The moment that the surface tension measured at plates *a* or *c* reached 65 mN/m was taken as the starting point of the experiment. The time until the surface tension decreased to 65 mN/m at plates *b* or *d* was used to calculate spreading velocity. Since spreading velocity from *a* to *b* was not found to be statistically different than from *c* to *d*, both velocities were averaged. Raw data passed an A/D converter (resolution 12 bit, input range ± 12 V, sampling rate 200 Hz, homemade) that was connected to a computer (Hewlett Packard Vectra VL5/166.Series.5 D4593A) and the surface tension was recorded using a computer program developed in our lab. Data were filtered using computer program Matlab (The Math works Inc., Natick, MA, USA), applying wavelet family db8.

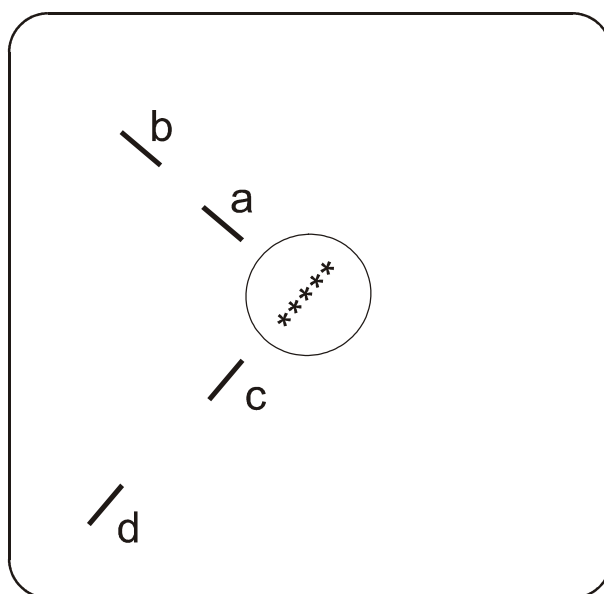


Figure 1. Glass spreading tray.

Droplets of sample (*****) were gently put on top of a buffer (140 mM NaCl, 10 mM HEPES, 0.5 mM EDTA, 2.5 mM CaCl₂, pH 6.9) surface by multichannel pipette. An agarose disc, placed just underneath the buffer surface, served as a ramp. Surfactant spreading velocity was expressed as the distance (cm) traveled by the surfactant sample between two platinum plates (*a - b* or *c - d*), divided by the time (s) required for the samples to spread between these plates and lower the surface tension.

For the spreading experiments, multilamellar vesicles (MLVs) containing hydrophobic surfactant protein - phospholipid mixtures were prepared as follows. Aliquots of phospholipid solutions ($\text{CHCl}_3/\text{MeOH}$, 1/1, v/v) and Bodipy-labeled or native SP-B ($\text{MeOH}/\text{water}/\text{TFA}$, 90/10/0.1, v/v/v) were mixed and the resulting DPPC/POPG/SP-B (80/20/0.2, mol/mol/mol) solution was dried under a stream of N_2 . Since butanol was found to be the only organic solvent in which lyophilization could be performed without solvent spraying, SP-B was redissolved in butanol (1 ml) and water (2 ml) was added. Since contact time at room temperature with liquid butanol was very short, chemical modifications like butylation that can be found especially at high temperatures [233] are not to be expected. After vigorous mixing on a vortexer the sample was instantly frozen in liquid nitrogen and freeze-dried overnight. Just before a spreading experiment, saline was added to a final concentration of $41.7 \mu\text{g}$ phospholipid/ μl and the sample was thoroughly mixed by repeatedly pipetting the suspension up and down using a $200 \mu\text{l}$ tip, resulting in MLVs. The same procedure was used for bovine lung surfactant extract (BLSE) in butanol (obtained during a step of the SP-B isolation procedure [158]). For each spreading experiment $1250 \mu\text{g}$ (phospholipid basis) surfactant was used.

2.8. Captive bubble surfactometer (CBS)

Quantitative measurements of the surface tension in a dynamic system were done using a captive bubble surfactometer, that was constructed and refined in our laboratory [26]. In short, a bubble (0.50 cm^2) was formed in the sample chamber containing subphase buffer by injecting air ($28.5 \mu\text{l}$) at 1.0 bar and 37°C . Stock solutions of DPPC/POPG (80/20, mol/mol) with varying amounts of SP-B (0.01 - 1.5 mol%) were prepared in $\text{CHCl}_3/\text{MeOH}$ (1/1, v/v). From these stock solutions $0.05 \mu\text{l}$ (0.25 nmol lipids) was spread at the air/water interface using a glass syringe (7000.5, blunt tip, Hamilton, Bonaduz, Switzerland). The subphase was stirred for 60 min to enhance desorption of solvent, after which the sample chamber was perfused for 30 min with ten times subphase volume. Subsequently, $30 \mu\text{l}$ SUVs (DPPC/POPG, 8/2, mol/mol) were injected into the subphase (final concentration of 1 mg DPPC/ml) and stirring was continued for another 15 min. The bubble area was increased by sudden lowering of the pressure to 0.5 bar for 10 s to study adsorption. The pressure in the sample chamber was then cycled five times within 1 min between two preset pressures of 0.5 and 2.8 bar to measure the film surface activity during dynamic cyclic area changes. The system pressure was kept constant (2.8 bar) at the end of the fifth compression over a period of 5 min to determine film stability after cyclic area changes. Finally, the pressure was cycled another five times and film stability was measured again. A video camera continuously monitored the shape of the bubble, from which the surface tension values were calculated. Maximum surface tension was defined as the surface tension measured at the end of bubble expansion (just before the onset of compression). Minimum surface tension was measured at the end of compression, just before the onset of bubble expansion.

For statistical analysis, the computer program SPSS version 9.0 was used (SPSS Inc., Chicago, IL, USA). To compare minimum and maximum surface tension of films containing

Chapter 5

0.75 mol% native or Bodipy-labeled SP-B, data were analyzed by Repeated Measures analysis. Differences were considered significant at $P < 0.05$.

3. Results

3.1. Fluorescent labeling of SP-B

Fluorescent labeling of SP-B resulted in a mixture of Bodipy-labeled SP-B and unreacted Bodipy. Reaction components were separated by reversed phase HPLC, resulting in the elution of unreacted Bodipy in the void peak. A protein eluted at a solvent mixture of MeOH/water/TFA (90/10/0.1, v/v/v) as a single peak (214 nm) at 38.0 min (Fig. 2). This peak coincided with a fluorescence peak ($\lambda_{\text{ex}} = 488 \text{ nm}$, $\lambda_{\text{em}} = 512 \text{ nm}$), indicating that it contained Bodipy-labeled SP-B. A control run of sham-treated SP-B resulted in the elution of a protein peak at 36.2 min. There was no fluorescence visible during this run. The degree of labeling was determined spectrophotometrically and was found to be 3.0 ± 0.3 labels per SP-B dimer ($n = 5$; ϵ for Bodipy FL CASE = 68000 l/mol/cm).

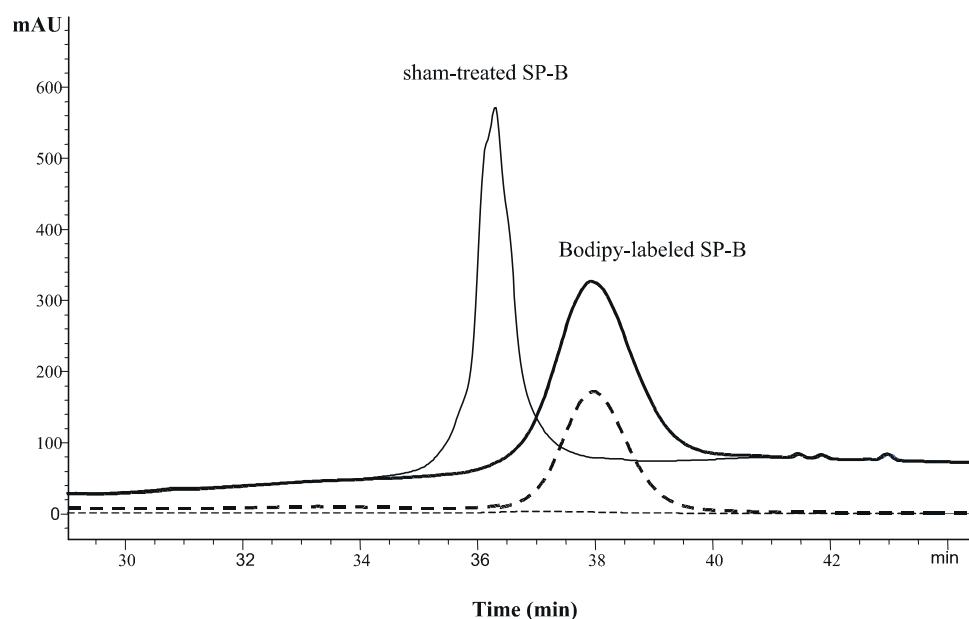


Figure 2. HPLC chromatogram of the elution of Bodipy-labeled SP-B and sham-treated SP-B.

Protein (5 μg) with or without Bodipy treatment (as described in section 2.2) was applied to an rp-C18 column. A methanol gradient from 70 to 100 vol% was run in water with a constant amount of 0.1 vol% TFA. Consecutive runs of Bodipy-labeled SP-B (bold lines) and sham-treated SP-B (normal lines), shown for fluorescence ($\lambda_{\text{ex}} = 488 \text{ nm}$, $\lambda_{\text{em}} = 512 \text{ nm}$; dashed lines) and peptide bond absorbance (214 nm; solid lines), resulted in different retention times. The run with Bodipy-labeled SP-B showed quantitative labeling since no peak at 36.2 min was observed. Absorbance/fluorescence is expressed in arbitrary units (AU).

Characterization of Bodipy-labeled SP-B

The 38.0 min HPLC peak, sham-treated and non-treated native SP-B were subjected to Tricine/SDS-PAGE (Fig. 3). The same gel was viewed by ultraviolet illumination (365 nm) and only the 38.0 min peak showed fluorescence; sham-treated and native SP-B did not. Due to the weak fluorescence signal upon UV illumination the gel had to be overloaded with protein. The relative mobility of SP-B in this analysis ranged from 16 to 29 kDa. Western Blot analysis showed that dimeric SP-B is the major component of all three samples.

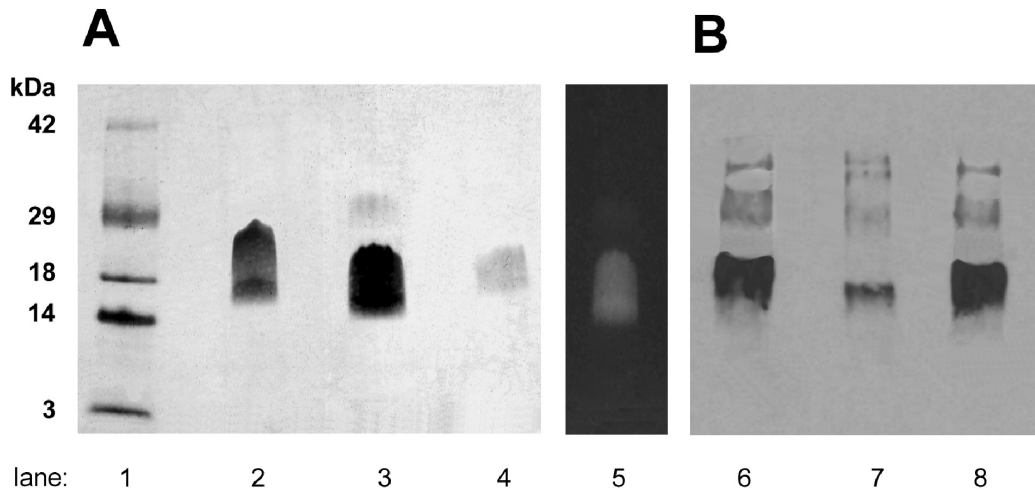


Figure 3. Tricine/SDS-PAGE gel (A) and Western Blot (B) under non-reducing conditions.

(A) Lane 1: molecular mass marker; lane 2: sham-treated SP-B; lane 3: Bodipy-labeled SP-B; lane 4: native SP-B; lane 5: lane 3 illuminated by UV light (365 nm). In each lane 2 μ g protein was applied. (B) Lane 6: sham-treated SP-B; lane 7: Bodipy-labeled SP-B; lane 8: native SP-B. In each lane 0.5 μ g protein was applied.

3.2. Amino acid sequencing

Part of the primary structure of both native and labeled SP-B was obtained by amino acid sequencing. The N-terminal 25 amino acids of purified bovine SP-B matched the known sequence exactly (SWISS-PROT protein sequence database, <http://www.expasy.ch>, P15781). One-third of the sequenced Bodipy-labeled SP-B sample turned out to be blocked at positions 16 (for 84 % of the SP-B dimers), 17 (82 %) and 24 (80 %), which are all of the lysines in the bovine SP-B sequence from the database. This blocking is most probably due to the presence of the label. The remaining two-thirds of the sample could not be sequenced because it was blocked at the N-terminus, implying that this part of the protein is also labeled with Bodipy. Moreover, it is highly likely that the NH_2 -group of lysine of this part of the sample is labeled with Bodipy as well.

All of the amino acids of Bodipy-labeled SP-B that were not blocked matched the native sequence. Truncated SP-B isoforms were not detected by N-terminal amino acid sequencing.

Chapter 5

3.3. ESI-MS

Two major species were observed in the ESI mass spectrum of SP-B (Fig. 4A) with charge states ranging between 11 and 6. Using the deconvolution software a molecular mass of the main component of 17487 ± 10 Da was determined. For the minor component a molecular mass of 17216 ± 10 Da was established, presumably a truncated form of SP-B. Mass/charge ratios between 7 and 11 were best visible.

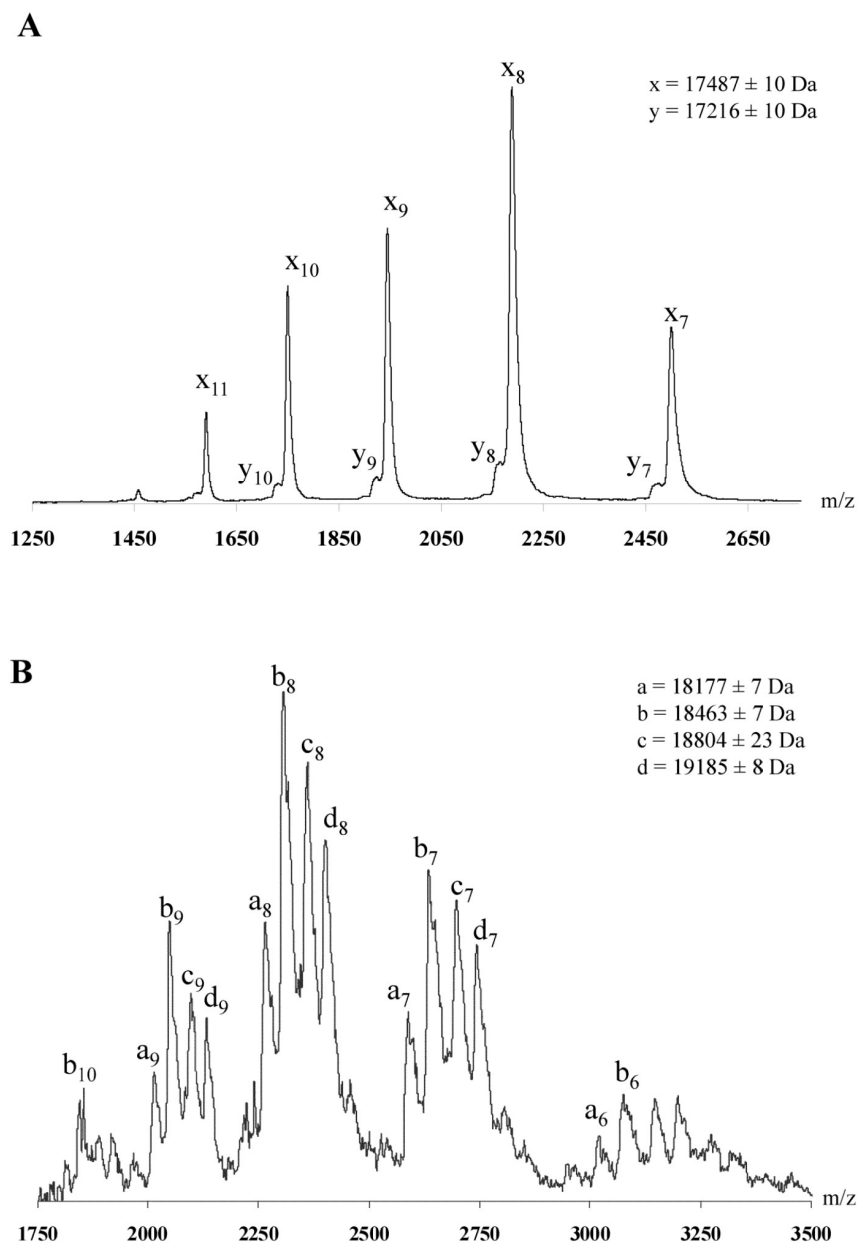


Figure 4. ESI mass spectrum of native bovine SP-B (A) and Bodipy-labeled SP-B (B).

(A) Mass analysis was performed with $2.9 \mu\text{M}$ SP-B dissolved in MeOH/water (9/1, v/v). The major species observed had a mass of 17487 Da. Mass/charge (m/z) ratios between 7 and 11 are shown. (B) Four species were found with approximate mass differences of 350 Da, indicating that SP-B dimer is labeled with one to four Bodipy molecules. Mass/charge ratios between 6 and 10 are shown.

The ESI mass spectrum of Bodipy-labeled SP-B (Fig. 4B) clearly revealed four major species, indicating that SP-B dimer is labeled with one to four Bodipy molecules. Repetitive differences of approximately 350 Da were found. Mass/charge ratios between 6 and 10 were best visible.

3.4. CD

Information about the protein's secondary structure was obtained by circular dichroism. CD spectra of native and labeled SP-B were very similar (Fig. 5), having a minimum in ellipticity at 208 nm and a shoulder at 222 nm and crossing the x-axis at 202 nm, a typical shape of proteins with a mainly α -helical structure. Comparison of the spectra with reference spectra yielded 45 - 55 % α -helix and 25 - 35 % β -sheet. Differences between the spectra below 195 nm were mainly due to apparatus imperfections at these wavelengths.

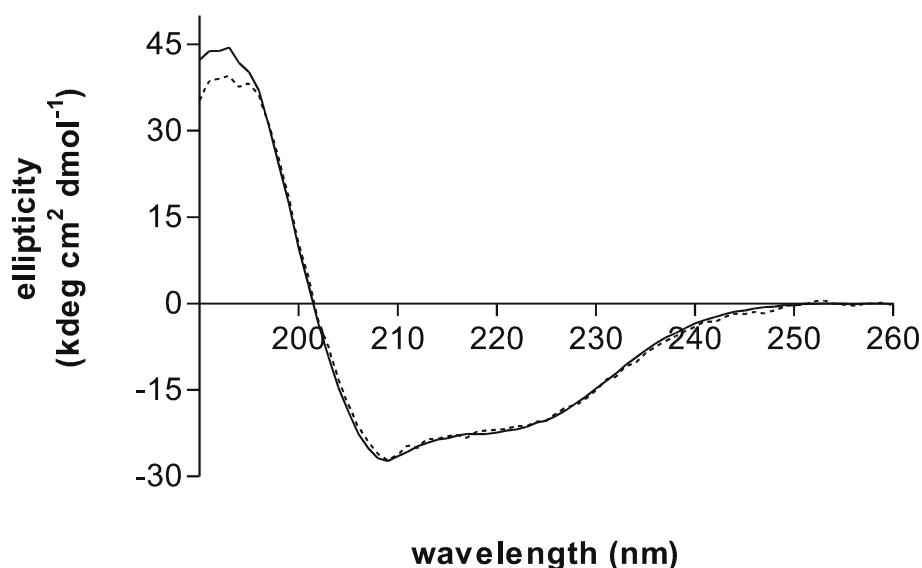


Figure 5. CD spectra of native and Bodipy-labeled SP-B.

Native (solid line) and labeled (dashed line) SP-B were measured at a concentration of 300 $\mu\text{g/ml}$ in MeOH/water (9/1, v/v). Ten to forty consecutive scans from 260 to 195 nm were averaged and the protein-free MeOH/water spectrum was subtracted to yield the protein spectrum.

3.5. Pyrene-PC vesicle mixing assay

The pyrene-PC assay measures the ability of SP-B to bring vesicles into close contact resulting in mixing of the vesicle lipids. When donor vesicles containing pyrene-PC are mixed with acceptor vesicles (initiated by the addition of calcium ions), pyrene-PC gets diluted, leading to more monomeric fluorescence and less excimeric fluorescence. For phospholipid vesicles containing native SP-B the excimer to monomer value of pyrene-PC fluorescence intensities (E/M) at 471/396 nm decreased from 0.93 ± 0.32 (before calcium was added) to

Chapter 5

0.20 ± 0.02 after calcium was added (Fig. 6). For Bodipy-labeled SP-B containing vesicles the E/M ratio decreased from 0.50 ± 0.05 to 0.18 ± 0.02 ($n = 5$ experiments), indicating that labeled SP-B is able to mix vesicles equally well as native SP-B. The difference in E/M ratio between labeled and native SP-B before calcium addition is due to the decrease of excimer peak of vesicles containing Bodipy-labeled SP-B. This is caused by energy transfer from pyrene to Bodipy, which can only happen if these fluorophores are in close proximity. As a control, Bodipy-PC was added to lipid SUVs containing pyrene-PC and the same energy transfer phenomenon was observed. Control vesicles containing only lipids and pyrene-PC showed a decrease in E/M ratio from 0.93 ± 0.18 to 0.48 ± 0.16 .

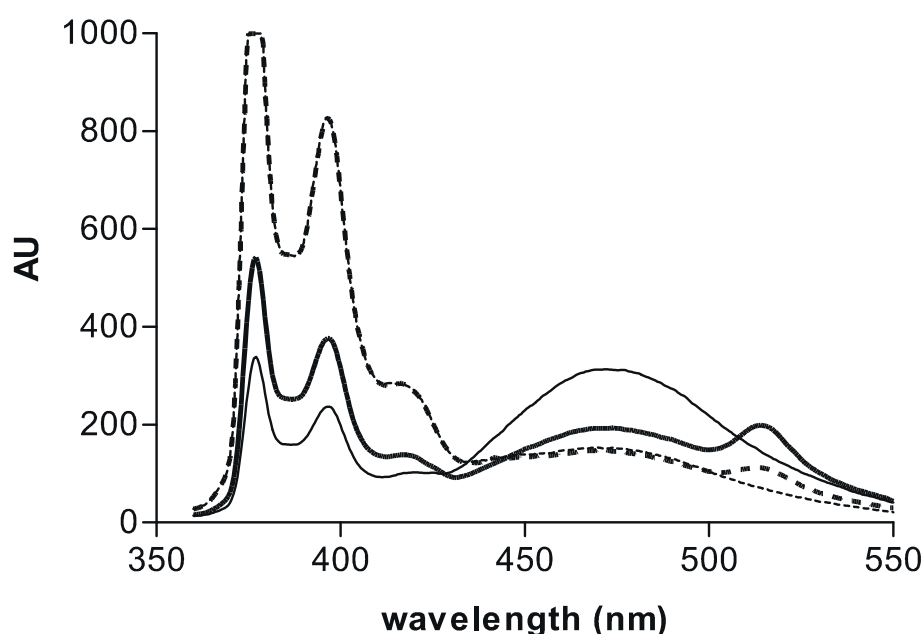


Figure 6. Vesicle mixing induced by native and Bodipy-labeled SP-B.

Phospholipid SUVs (DPPC/POPG, 8/2 mol/mol, 300 nmol lipid) were mixed with pyrene-containing SUVs (15 nmol lipid containing 10 mol% pyrene-PC, supplemented with 0.4 mol% native or Bodipy-labeled SP-B) in buffer (25 mM HEPES, 0.20 mM EGTA, pH 7.0). The fusion reaction proceeded after addition of 0.3 M CaCl_2 (solid lines before calcium addition; dashed lines after calcium addition ($n = 5$)). Fluorescence emission spectra were recorded under continuous stirring at 37 °C; fluorescence is expressed in arbitrary units (AU). The change in excimer to monomer fluorescence ratio, calculated by dividing the fluorescence intensity at 471 nm by the intensity at 396 nm, is proportional to the ability to mix lipid vesicles. Labeled SP-B (bold lines) and native SP-B (normal lines) were equivalently able to mix vesicles.

3.6. Spreading tray

The ability of SP-B to spread a surfactant film was measured in a square glass spreading tray filled with buffer. Spreading velocity was expressed as the distance (cm) traveled by the surfactant sample between two platinum plates, divided by the time (s) required for the samples to spread between the plates and lower the surface tension to 65 mN/m. No

statistical difference in spreading velocity was found between MLVs containing native SP-B (DPPC/POPG/SP-B, 80/20/0.2, mol/mol/mol; 1250 μ g lipid and 58 μ g SP-B) and MLVs containing Bodipy-labeled SP-B of the same concentration (Fig. 7). Spreading velocity was not increased by changing the concentration of SP-B in artificially mixed MLVs to 1 mol% or the amount of phospholipids to 2500 μ g. Addition of bovine SP-C (2 mol%) to the lipid/SP-B MLVs did not alter the velocity either. Importantly, MLVs containing lipids only were not able to spread a film. This means that the presence of hydrophobic surfactant proteins is a prerequisite for these spreading experiments.

Furthermore, addition of 0.2 mol% of neither Bodipy-labeled nor native SP-B influenced the spreading velocity of BLSE (which contains phospholipids, SP-B and SP-C (100/0.02/0.25, mol/mol/mol)). Interestingly, when comparing natural with artificially mixed surfactants, it was found that the spreading velocity of the natural surfactants BLSE (with or without Bodipy-labeled SP-B supplementation) and Alveofact (containing lipids, SP-B and SP-C [234,235]) was significantly higher than the velocity of artificially mixed MLVs containing DPPC, POPG and SP-B ($P = 0.001$).

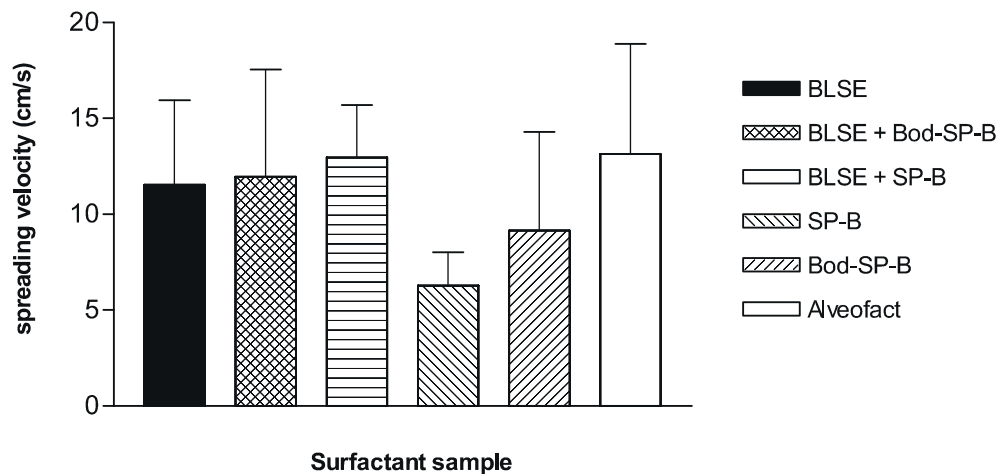


Figure 7. Spreading of MLVs of natural and artificial surfactants in a glass tray.

Each sample contained 1250 μ g surfactant on PL basis. Data are expressed as mean \pm S.D. ($n = 5$ to 11). Bod-SP-B = Bodipy-labeled SP-B; see text for further abbreviations. No difference in spreading velocity was found between artificially mixed MLVs (DPPC/POPG, 80/20, mol/mol) containing native or Bodipy-labeled SP-B (0.2 mol%). Addition of 0.2 mol% Bodipy-labeled or native SP-B to MLVs of BLSE did not alter spreading velocity. Spreading velocity of the natural surfactants BLSE and Alveofact was higher than that of artificially mixed MLVs containing DPPC, POPG and SP-B. Surfactants containing only lipids were not able to spread on a buffer surface.

3.7. CBS

The ability of SP-B to insert lipids into the air/water interface and thereby lower the surface tension was measured by a pressure driven CBS using the spread film technique. The

surface tension of film containing protein and DPPC/POPG (8/2, mol/mol) reached one second after a sudden increase of bubble area (γ_{Ads1}) was significantly lower when the protein concentration was increased, both for native and Bodipy-labeled SP-B (Fig. 8). No further decrease in surface tension was observed for protein concentrations higher than 0.75 mol%. The small but consistent difference in γ_{Ads1} values between native and labeled SP-B showed that Bodipy-labeled SP-B was not as active as native protein of the same concentration.

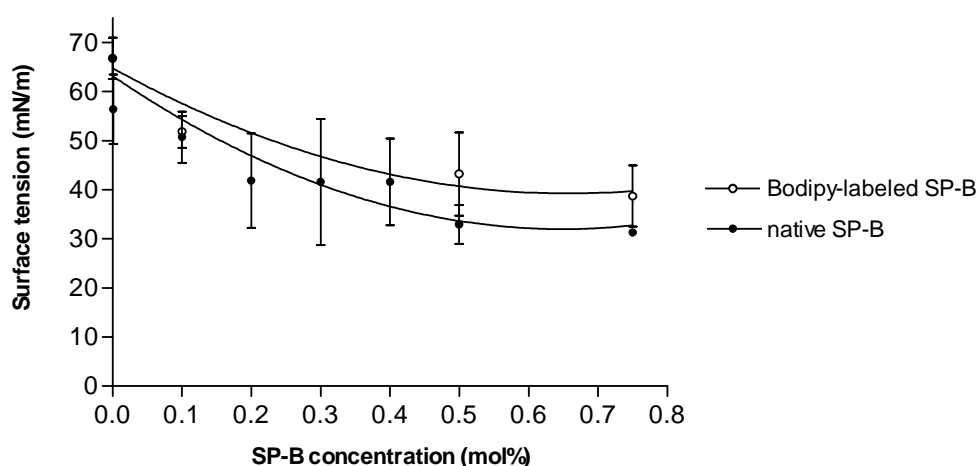


Figure 8. Surface tension reached one second after sudden bubble expansion (γ_{Ads1}).

DPPC/POPG (80/20, mol/mol) mixtures containing various amounts of either native or Bodipy-labeled SP-B (0.01 - 0.75 mol%) were spread at the surface of a 0.50 cm² air bubble at 37 °C. SUVs of the same lipid composition were injected into the subphase with a final concentration of 1 mg DPPC/ml. The bubble area was suddenly increased by reducing the system pressure from 1.0 to 0.5 bar. Data are expressed as mean \pm S.D. (n = 3 to 6). Surface activity of Bodipy-labeled SP-B showed the same trend as native SP-B: in both cases an increase in the protein concentration led to a lowering of γ_{Ads1} .

During cycling, the minimum surface tension of spread films containing 0.75 mol% protein was always less than 2 mN/m (Fig. 9A). Minimum surface tensions during cycling seemed slightly higher for Bodipy-labeled SP-B than for the native protein, although this difference was not significant ($P = 0.050$).

Maximum surface tension of spread films containing 0.75 mol% Bodipy-labeled SP-B showed the same trend as films containing native SP-B. Contrary to minimum surface tension, a statistically significant difference between labeled and native SP-B was found for the maximum surface tension ($P = 0.040$) (Fig. 9B).

On the first compression during rapid cycling, the compressibility at 15 mN/m for spread films containing 0.75 mol% Bodipy-labeled SP-B was significantly higher than for films containing the native protein, 0.0208 ± 0.0177 vs. 0.0069 ± 0.0057 m/mN.

Control experiments with sham-treated SP-B showed that the reduced activity found

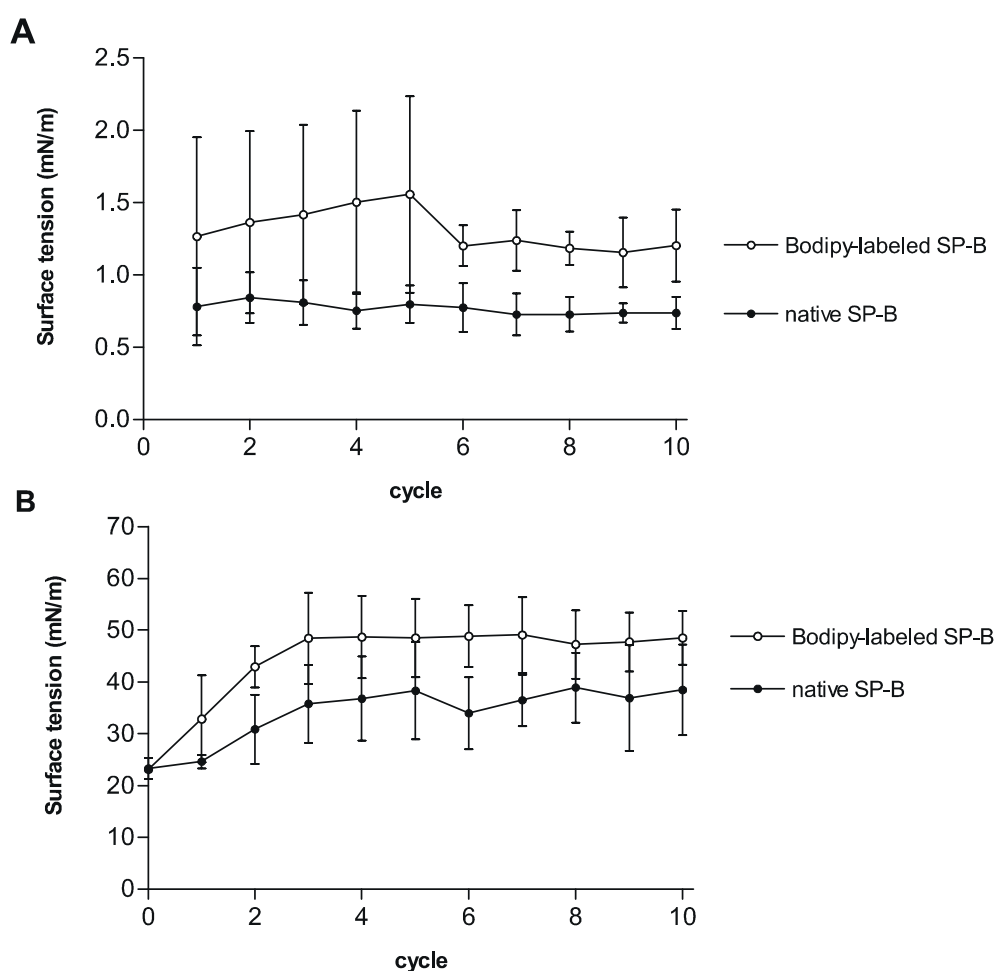


Figure 9. Minimum (A) and maximum (B) surface tension of films containing 0.75 mol% SP-B during cyclic area changes.

The bubble was cycled 5 times between two preset pressures of 0.5 and 2.8 bar within 1 min. After the system pressure had been kept constant over a period of 5 min at a pressure of 2.8 bar at the end of the fifth compression, the bubble was cycled another five times. Data are expressed as mean \pm S.D. ($n = 3$ to 10). Minimum and maximum surface tension of spread films of phospholipids (DPPC/POPG, 80/20, mol/mol) plus 0.75 mol% labeled SP-B were comparable to films with native SP-B.

for Bodipy-labeled SP-B compared to native SP-B was not due to the labeling procedure itself, because no differences in γ_{Ads1} , compressibility, minimum and maximum surface tension values were observed between native and sham-treated SP-B. The activity of Bodipy-labeled SP-B was fully preserved after two weeks storage at -20 °C.

4. Discussion

In order to determine the activity of a protein accurately and to be able to compare it to an analogous protein that has been labeled with a fluorescent or radioactive group, a wide

Chapter 5

range of functional tests has to be available. It was our goal to develop and select such tests for surfactant protein B. Furthermore, the biochemical and biophysical activity of SP-B was compared to a fluorescently labeled analog. Both proteins were found to have similar structure and activity; only small differences were detected.

The labeling procedure described here is fast: one hour after pipetting the reaction components together, the reaction mixture was separated and Bodipy-labeled SP-B was isolated from the reaction products and ready to be used for activity assays. In contrast, previously described assays for fluorescent labeling of SP-B took 12 to 36 h, not including chromatographic separation of the reaction products [229-232]. Unfortunately, in earlier studies little attention was given to characterization of the labeled protein. The scarce information available either positively identified labeled SP-B by mass spectrometry [230], or claimed that the lytic effect on liposomes was indistinguishable from unlabeled protein [231], or did not characterize the labeled protein at all [229]. In only one study the effect of radioactive labeling on SP-B surface activity was determined, using pulsating bubble surfactometry, and found to be comparable with the native protein [232]. In our study, during HPLC separation of the labeling reaction components almost no protein eluted at the retention time of sham-treated SP-B (Fig. 2), indicating that all SP-B molecules were labeled. When the primary structure was analyzed and compared to that of the native protein, it was found that the majority of SP-B was labeled at the free amino groups of the N-terminus and/or lysines. Labeling efficiency was high: 80 % of the protein was labeled at all 3 lysines and two-thirds of the protein was labeled at the N-terminus. The degree of labeling was 3.0 (determined spectrophotometrically). This is high compared to 1.4 [229] and 1.6 [231] dye molecules per molecule SP-B. Mass spectrometrical analysis using small amounts of sample showed four molecular species, indicating that SP-B dimer was labeled with one to four Bodipy molecules. Repetitive mass differences of approximately 350 Da were found, which is lower than the mass of a Bodipy molecule after labeling (425 Da). We cannot give a satisfactory explanation for this difference. The analysis of the secondary structure by circular dichroism revealed that both proteins contained equal amounts of α -helices and β -sheets, 45 - 55 and 25 - 35 % respectively. This is in agreement with previously found values of 40 - 60 % α -helix and 20 - 25 % β -sheet [158,61,39,236].

In this study we introduced a spreading tray to obtain information about the ability of a surfactant to distribute over an aqueous surface, for instance like the premature lung of an RDS patient before surfactant therapy. For spreading experiments SP-B was lyophilized, mixed with lipids and subsequently suspended in water to obtain MLVs. The spreading velocity of natural surfactant was found to be 12 cm/s. This is 4 cm/s higher than the velocity of artificially mixed MLVs containing DPPC, POPG and SP-B. For the spreading of surfactant on an aqueous layer, lipids alone were found to be insufficient; hydrophobic surfactant proteins were indispensable. Four different concentrations ranging from 0.1 to 1.0 mol% were tested and the optimal SP-B concentration in MLVs was found to be 0.2 mol%. This is in agreement with other studies that have reported that SP-B enhances lipid mixing between vesicles, particularly at concentrations around 0.2 mol% [173,218,219]. This percentage is

higher than the native concentration of SP-B present in BLSE (0.02 mol% compared to total phospholipid; $n = 3$ determinations). In previous studies using pig surfactant, calculated molar amounts of SP-B were 0.01 - 0.04 mol% [159] and 0.9 mol% [220]. The SP-B:SP-C molar ratio in BLSE of 2:25 found in this study is the same as the ratio found in [159], but is considerably different from the 2:5 ratio found in another porcine lung surfactant study [220]. Spreading velocity of SP-B containing MLVs was not increased by the addition of various amounts of SP-C, or by altering the concentration of lipids or SP-B.

A captive bubble surfactometer was used to investigate the ability of Bodipy-labeled SP-B to transport lipids into the air/water interface of an air bubble in buffer. It was shown that labeled SP-B catalyzes the adsorption and spreading of phospholipids in a concentration-dependent manner. Successive rapid cyclic area changes did not affect the lipid adsorption process. Minimum surface tension was unaltered during cycling, suggesting that labeled SP-B remained associated with the film. However, a small but consistent difference between labeled and native SP-B was found for the maximum surface tension (Fig. 9B). A difference was also found for the surface tension reached one second after sudden bubble expansion throughout the concentration curve (Fig. 8). The scattering of γ_{Ads1} within a concentration, observed between 0.1 and 0.5 mol% SP-B, could indicate that these are critical concentrations at which the protein is barely associated (or not) with the film after rapid bubble area increase. During cycling, such scattering within a concentration remained, from which we conclude that proteins that were not immediately associated with the film were irreversibly lost from the surface. At a concentration of 0.5 - 0.75 mol% SP-B in lipid films a plateau was reached. Further increase of the amount of the protein did not alter surface tension for either native or labeled SP-B, indicating that this is the maximum amount of SP-B that can be associated with the film; excess SP-B will be irreversibly lost to the buffer. Alternatively, when the maximum spreading speed is related to lipid viscosity, the effect of further increase of the SP-B concentration above 0.75 mol% could be too small to be measured.

The difference in surface activity between Bodipy-labeled and unlabeled SP-B observed during CBS experiments might be explained by a slight Bodipy-induced conformational change, not detectable by circular dichroism. Since it has been found for SP-B-like peptides that positively charged residues were essential for activity [45] and since cationic SP-B is known to interact preferably with negatively charged phospholipids [237], an alternative explanation for the small difference in activity might be the replacement of the positively charged ϵ -amino group of lysine by a neutral peptide bond during labeling with Bodipy. Our use of the negatively charged Bodipy FL CASE fluorophore (because of its superior separation on HPLC compared to a neutral Bodipy analog) did not impair SP-B surface activity, as shown by vesicle mixing, spreading tray and CBS results. In previous studies it was found that the positive net charge of SP-B is important for interaction with negatively charged phospholipids [72,173]. Furthermore, it is suggested that SP-B penetrates the acyl chain region of the monolayer only to a small extent [238,239]. On the other hand, our results suggest that the source of biophysical effects of SP-B on lipid systems may be

Chapter 5

dependent on both hydrophobic as well as electrostatic interactions with the lipids. To avoid labeling SP-B lysines, the pH should be kept below 10, the pK of lysin. To label SP-B N-terminally the pH should be kept above 8, the pK of the N-terminus. Unfortunately, it is difficult to estimate pH in an organic solvent. Therefore, it is impossible to adjust the pH to the desired value for our labeling reaction. Since a basic environment is a prerequisite for our labeling reaction, the only alternative is to increase the pH of the reaction mixture by adding a small amount of triethylamine.

In conclusion, we have shown that a range of tests including several new techniques gives us the ability to fully characterize the biochemical and biophysical properties of SP-B. Furthermore, using these tests the activity of native SP-B could be accurately compared to a fluorescently labeled analog. Bodipy-labeled SP-B was found to remain surface active. Since differences between native and Bodipy-labeled SP-B are minimal, Bodipy-labeled SP-B can be used for *in vitro* as well as for *in vivo* investigations. Possible *in vitro* applications of fluorescent SP-B analogs for biophysical studies could be: further studies of protein - lipid interactions using fluorescent SP-B and/or lipid analogs, visualization of SP-B in surfactant films by a combination of atomic force microscopy and fluorescence microscopy, or determination of the role of SP-B in surface dynamics by fluorescent Wilhelmy balance or captive bubble surfactometer experiments. *In vivo*, Bodipy-labeled SP-B might be helpful to follow surfactant distribution in models of ARDS.

Acknowledgments

We gratefully thank Peter Hamm, Hubert Staud and Fritz Zschiegner of the Department of Anaesthesiology and Critical Care Medicine of the University of Innsbruck for their technical support with the spreading tray and Dr. Herbert Lindner of the Institute of Medical Chemistry and Biochemistry for amino acid sequencing. Prof. Albert Heck of the Department of Biomolecular Mass Spectrometry and Dr. Maurits de Planque of the Department of Biochemistry of Membranes of the Utrecht University are acknowledged for their help with MS and CD, respectively. This research was supported by the *Fonds zur Förderung der Wissenschaftlichen Forschung* (FWF) (#P11527-MED).

Chapter 6

***In vitro* and *in vivo*-Intrapulmonary Distribution of Fluorescently Labeled Surfactant**

Robert V. Diemel ^{a,b}, Monika Walch ^a, Henk P. Haagsman ^{b,c} and Günther Putz ^a

^aDepartment of Anaesthesiology and Critical Care Medicine,

The Leopold-Franzens-University of Innsbruck, Innsbruck, Austria

^bDepartment of Biochemistry and Cell Biology, and ^cDepartment of the Science of Food of Animal Origin, Faculty of Veterinary Medicine, Graduate School of Animal Health, Utrecht University, Utrecht, The Netherlands

Critical Care Medicine, 2002, in press

Chapter 6

Abstract

Objective: To determine the distribution of endotracheally administered surfactant at the alveolar level in an animal model of acute respiratory distress syndrome (ARDS).

Design: Prospective, randomized animal study.

Setting: Research laboratory of an university hospital.

Subjects: Seventy-one male Sprague-Dawley rats, weighing 330 - 370 g.

Intervention: To measure surfactant distribution *in vitro*, a glass trough mimicking dichotomic lung anatomy was used to determine the spreading properties of bovine lung surfactant extract (BLSE) supplemented with fluorescent Bodipy-labeled surfactant protein B (SP-B). To measure surfactant distribution *in vivo*, rats were anesthetized and lipopolysaccharide (LPS) was aerosolized (12 mg/kg body weight) to induce ARDS-like lung injury; in control rats buffered saline was aerosolized. Twenty-four hours later rats were anesthetized, tracheotomized and mechanically ventilated ($P_{\text{peak}} = 20$ mbar; PEEP = 6 mbar; $t_{\text{insp}} = t_{\text{exp}} = 0.6$ sec; $\text{FiO}_2 = 50\%$). Surfactant (BLSE, supplemented with fluorescently labeled SP-B; 50 mg/kg body weight) was applied as a bolus; in control rats, saline was administered as a bolus. Rats were ventilated for 5, 15, 30 or 60 min ($n = 8$ or 9 for each group). Then, lungs were excised and sliced. Lung slices, divided into aerated (open), underinflated (dystelectatic) or collapsed (atelectatic) alveolar areas, were examined by both light and fluorescence microscopy.

Results: *In vitro* experiments revealed that surfactant spread independent of glass trough geometry and lowered the surface tension to equilibrium values (25 mN/m) within a few seconds. *In vivo* experiments showed that administered surfactant distributed preferentially into underinflated and aerated alveolar areas. Furthermore, surfactant distribution was not affected by length of mechanical ventilation.

Conclusions: Using conventional mechanical ventilation in LPS induced lung injury, surfactant preferentially distributed into underinflated and aerated alveolar areas. Since surfactant rarely reached collapsed alveolar areas, methods aiding in alveolar recruitment (*e.g.* open lung concept or body positioning) should precede surfactant administration.

1. Introduction

Pulmonary surfactant is a mixture of lipids and proteins, synthesized and secreted by the alveolar type II epithelial cells. Its main function is to reduce the surface tension at the air/liquid interface of the lung by formation of a surface-active film. The presence of surfactant prevents the alveoli from collapsing at end-expiration and makes breathing with minimal effort possible. In addition, lung surfactant plays a substantial role in the lung's host defense system.

An important component of lung surfactant is the small hydrophobic surfactant protein B. This dimeric protein, which is closely associated with surfactant phospholipids, enhances

lipid insertion into the monolayer at the air/liquid interface and influences the molecular ordering of the phospholipid monolayer (see [223,224] for reviews). The observation that homozygous SP-B knock-out mice died of respiratory failure immediately after birth (see [20] for review) emphasizes the importance of SP-B. Moreover, blocking of SP-B with monoclonal antibodies in immature newborn rabbits led to respiratory failure and loss of surfactant activity [225].

In premature newborns, a deficiency of surfactant is the primary cause of neonatal respiratory distress syndrome. Therefore, these infants are treated with exogenous surfactant, resulting in a dramatic decrease in mortality (see [240] for review). In adult patients with acute lung injury, secondary changes in the endogenous surfactant system have been found: the amount of surfactant specific proteins in bronchoalveolar lavage (BAL) was considerably reduced, the total amount and composition of phospholipids in BAL was altered and the biophysical activity of surfactant lavaged from ARDS lungs was decreased compared to that of healthy persons [226-228]. These surfactant alterations are thought to contribute to ARDS. Therefore, also in adult patients administration of exogenous surfactant has been suggested as a beneficial therapeutic strategy [241].

The results obtained thus far with surfactant replacement therapy in ARDS patients are inconclusive. In an earlier series of clinical investigations either lung function and mortality remained largely unchanged [242,243]. In a more recent series of clinical investigations it was shown that gas exchange improved more than twofold after surfactant instillation, but the effect was lost within a few hours and a repeat dose of surfactant was required to improve gas exchange again [10]. Furthermore, it was found that mortality dropped significantly after repetitive doses of natural surfactant [11]. Yet, it was found by others [244] that neither gas exchange improved nor survival rate increased when a synthetic surfactant devoid of proteins was administered. The causes of these contradicting results are subject of discussion [245,234,235].

Although the distribution of exogenous surfactant in ARDS models has been investigated before [246-250], the tracer used was never labeled covalently to a surfactant protein. Furthermore, global (lobar) rather than local (alveolar) distribution was studied. Therefore, the aim of this study was to determine the distribution of endotracheally administered surfactant at the alveolar level in a rat model of ARDS caused by exposure to lipopolysaccharide (LPS) aerosols [251].

2. Materials and Methods

2.1. Materials

1,2-dipalmitoyl-*sn*-glycero-3-phosphocholine (DPPC) and 1-palmitoyl-2-oleoyl-*sn*-glycero-3-(phospho-*rac*-(1-glycerol)) (POPG) were obtained from Avanti Polar Lipids (Alabaster, AL, USA). Methanol (MeOH) (Scharlau, Barcelona, Spain), chloroform (B&J, Miskegon, MI, USA), dimethylsulfoxide (Sigma, St. Louis, MI, USA), butanol and

Chapter 6

triethylamine (Fluka, Buchs, Switzerland) were HPLC grade. N-(4,4-difluoro-5,7-dimethyl-4-bora-3a,4a-diaza-s-indacene-3-propionyl)cysteic acid succinimidyl ester (Bodipy[®] FL CASE, Lot no. 4481-1) was obtained from Molecular Probes Europe (Leiden, the Netherlands). HEPES, KCl, NaCl, phosphate buffered saline and EDTA were obtained from Sigma. Water was filter purified (Modulab Water Systems, Lowell, MA, USA). Agarose (SeaKem ME agarose, FMC Bioproducts, Rockland, ME, USA) was extracted as described [25]. Alveofact[®] was purchased from Thomae (Biberach, Germany).

SP-B was isolated from bovine bronchoalveolar lavage fluid. Bovine lungs were obtained from a slaughterhouse, and isolation and characterization of SP-B was performed as described [158]. Bovine lung surfactant extract (BLSE; containing surfactant lipids, SP-B and SP-C) is obtained during a step of this SP-B isolation procedure. The amount of protein was determined [182] using bovine serum albumin (BSA) as standard. Furthermore, the amount of phospholipids was determined [183].

2.2. Fluorescent Labeling of SP-B

Bovine lung surfactant extract was supplemented with Bodipy-labeled SP-B as a marker for surfactant distribution. SP-B was considered an ideal marker, because i) SP-B is a natural component of surfactant and ii) SP-B is a prerequisite for a properly functioning surfactant system. Labeling of SP-B with Bodipy FL CASE and full characterization of Bodipy-labeled SP-B is described elsewhere [57, chapter 5]. In short, a 770-fold molar excess of triethanolamine and a 16-fold molar excess of Bodipy FL CASE were added to 50 μ g purified bovine SP-B dissolved in dimethylsulfoxide. After 30 min of incubation the reaction products were separated by reversed phase HPLC. Bodipy-labeled SP-B closely resembled native SP-B both in structure and biophysical activity.

2.3. Captive Bubble Surfactometer

Important biophysical parameters to verify constant quality of a surfactant preparation can be obtained in a captive bubble surfactometer (CBS) [26]. Therefore, in parallel to the *in vivo* experiments, quality control experiments were performed with freeze-dried BLSE. CBS experiments were done with adsorbed films (1 mg phospholipid per ml saline (n = 12)). The area of a 20 μ l air bubble was increased by a sudden lowering of the pressure from 1.0 to 0.5 bar to study adsorption. After 1 min the pressure was stepwise increased to 2.8 bar, where it was kept constant for 5 min to determine film stability. Then, the bubble was cycled nine times within 2 min between two preset pressure values of 0.5 and 2.8 bar to measure surface activity of the film during dynamic cyclic area changes. Alveofact suspensions (bovine lung surfactant extract, 1 mg phospholipid/ml) were used as a control.

2.4. In Vitro Distribution: Lung Spreading Trough

The ability of surfactant to spread in the lung as a function of geometry was determined in a spreading trough (custom-made by Swarovski, Wattens, Austria), which is a two-dimensional anatomical replica of the first three generations of a human lung's

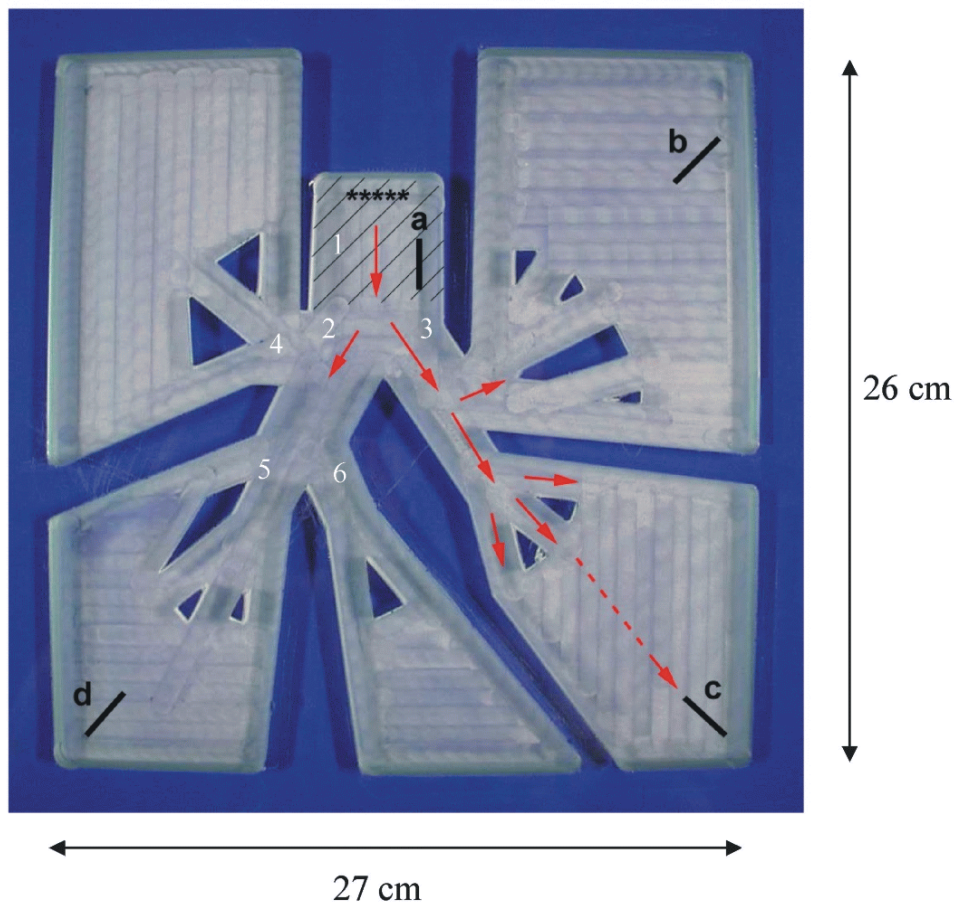


Figure 1. Glass lung spreading trough: a two dimensional anatomical replica of the first three generations of a human lung's tracheobronchial tree.

a, b, c, d: position of platinum plates; *****: site of application of surfactant sample; cross hatched area: agarose (covered with thin layer of subphase buffer); 1: trachea; 2: right main bronchus; 3: left main bronchus; 4: right upper lobe bronchus; 5: right lower lobe bronchus; 6: right middle lobe bronchus.

tracheobronchial tree (Fig. 1). The trough was filled with subphase buffer (140 mM NaCl, 10 mM HEPES, 0.5 mM EDTA, 2.5 mM CaCl₂, pH 6.9) and covered with a plexiglass lid to maintain humidity near saturation at 37 °C. At the tracheal position of the trough, just underneath the buffer surface, a 1 % (w/v) agarose slab (3 - 4 mm thick, position *a*) was placed to serve as a ramp for the surfactant sample. In the lid, 4 holes were drilled (18 × 5 mm) through which roughened platinum plates were dipped into the buffer. Each plate was connected to a force-displacement transducer (type FT 03, Grass, Quincy, MA, USA) to measure surface tension (Wilhelmy plate technique). After droplet formation (multichannel pipettor), the sample was gently applied onto the buffer surface. The moment that the surface tension measured at position *a* had reached 65 mN/m (from 69.9 mN/m) was taken as the starting point of the experiment. Lung surfactant spreading was defined as the surface tension

Chapter 6

reached at positions *b*, *c* or *d* within five seconds after sample application.

Multilamellar vesicles (MLVs) of BLSE supplemented with native or Bodipy-labeled SP-B were prepared as follows: 58 μg SP-B was mixed with BLSE (1250 μg on phospholipid basis) in butanol and a double volume of water was added subsequently. After vigorous mixing on a vortex mixer the sample was instantaneously frozen in liquid nitrogen, freeze-dried overnight and stored at $-20\text{ }^{\circ}\text{C}$. On the day of a spreading experiment, freeze-dried surfactant was suspended in saline to a final concentration of 41.7 mg phospholipid/ml.

2.5. *In Vivo* Distribution: Animal experimental design

Animals. Male albino Sprague-Dawley rats (Him:OFA/SPF) obtained from the Forschungsinstitut für Versuchstierzucht und -haltung (University of Vienna, Himberg, Austria) were housed in Macrolon cages on dust-free pine shavings. Until treatment, the rats (330 - 370 g) were kept at a regular 12-h light/dark cycle with a temperature of $22 \pm 2\text{ }^{\circ}\text{C}$. Food (Altromin1324ff, Lage, Germany) and acidified water were given ad libitum. Animal studies were approved by both the Committee for Animal Experiments of the University of Innsbruck and the Austrian Ministry for Science and Traffic (permission GZ66.011/82-Pr/4/98). Care and handling of animals were in accord with National Institutes of Health guidelines.

Preparation of aerosols for induction of lung injury. Lung injury induced by intratracheal aerosolization of LPS causes lung damage with a clinical picture comparable to that of ARDS in human patients [251]. LPS from *Salmonella enteritidis* obtained from Sigma (Lot no. 55F4013) was dissolved in LPS-free phosphate-buffered saline at pH 7.4. For aerosolization, a miniature nebulizer (PennCentury, Philadelphia, PA, USA) consisting of a 0.5 ml syringe (1750 TLL Hamilton, Bonaduz, Switzerland) in combination with a nozzle mounted on top of a stainless steel tube (length 5.5 cm, diameter 1 mm) was used. This nebulizer allows aerosolization of a small volume (0.2 ml).

Anaesthesia and induction of lung injury. Rats were anaesthetized by inhalation of ether vapor. With the rat fixed in supine position the trachea was intubated with the aerosolizer tube and LPS (12 mg/kg) was aerosolized in the trachea just above the bifurcation. Subsequently, the rats were housed in their cages.

Anaesthesia, surgical procedures and mechanical ventilation. Rats were anesthetized by ketamine (100 mg/kg i.m.; Ketazol[®], Gräub, Berne, Switzerland) and xylazine (7 mg/kg i.m.; Rompun[®], Bayer, Leverkusen, Germany). Respiratory frequency was determined from radiologic observation of chest movements during a 30 sec period. After tracheotomy, rats were intubated with a home-made steel tube (12 mm length, 1 mm diameter). Neuromuscular blockade was induced by pancuroniumbromide (0.6 mg/kg injected into the tail vein; Pavulon[®], Organon Teknika, Boxtel, the Netherlands) and pressure controlled mechanical ventilation initiated ($P_{\text{peak}} = 20\text{ mbar}$; PEEP = 6 mbar; $t_{\text{insp}} = t_{\text{exp}} = 0.6\text{ sec}$; $\text{FiO}_2 = 50\%$; Babylog 8000, Dräger, Austria) in supine position. Either two or four rats were ventilated simultaneously, always evenly divided between LPS-treatment and control. For blood gas analysis, a catheter (polyethylene, 0.9 mm diameter) was inserted into the carotid artery and

In vitro and in vivo distribution of labeled surfactant

12.5 IU heparin (Immuno, Vienna, Austria) was injected. Blood was analyzed using an AVL 995 automatic blood gas system and an AVL 912 CO-Oxylite (AVL Medical Instruments, Graz, Austria).

Computed Tomography (CT). CT scans (1 mm slice thickness) were recorded by a HiSpeed Advantage (General Electric Medical Systems, Milwaukee, WI, USA) at 120 kV and 200 mAs using a computational lung algorithm.

Compliance. A volume - pressure diagram was recorded using a home-made pressure driven hydraulic piston (pressure sensor range 0 - 200 mbar). While rats were kept in deep anaesthesia and full muscle relaxation their lungs were inflated with 100 % oxygen in steps of 0.5 ml until a pressure of 25 mbar was reached; subsequently, the lungs were deflated in 0.5 ml steps. The time typically required for a full inflation - deflation cycle was 35 - 40 s. Airway pressure was continuously measured. Compliance was defined as the volume of oxygen insufflated at a pressure of 25 mbar.

Surfactant administration. To study the distribution of exogenously administered surfactant, BLSE (50 mg phospholipid/kg body weight) supplemented with Bodipy-labeled SP-B (143 $\mu\text{g}/\text{kg}$, approximately $\frac{1}{4}$ of the endogenous amount) was instilled as a bolus (0.5 ml in saline) into the trachea just above the bifurcation.

General experimental protocol. On day 1, rats were anaesthetized and LPS was aerosolized intratracheally. In control rats, phosphate buffered saline was aerosolized instead of LPS. On day 2, twenty-four hours after the induction of lung injury, rats were anaesthetized with ketamine/xylazine and lung CT scans were recorded. After tracheotomy had been performed and mechanical ventilation had been initiated, a blood sample (0.5 ml) was withdrawn from the carotid artery and lung compliance was measured. Then, BLSE supplemented with Bodipy-labeled SP-B was administered. To facilitate surfactant spreading into underinflated and collapsed alveolar areas, lungs were inflated three times to 20 mbar for 3 s periods after surfactant administration. Subsequently, the rats were mechanically ventilated for 5, 15, 30 or 60 minutes ($n \geq 8$ rats per group). Subsequently, the chest was opened and the rat lungs were excised. In control rats, saline was administered instead of surfactant.

Histology and microscopy. The excised lungs were fixed for 12 h at atmospheric pressure in fixation buffer (2 % (w/v) para-formaldehyde and 10 % (w/v) sucrose in 0.1 M Na-phosphate, pH 7.35) at room temperature. Subsequently, the lungs were washed overnight in sucrose buffer (30 % (w/v) sucrose in 0.1 M Na-phosphate, pH 7.35) at 4 °C. Lungs were stored at -20 °C in Tissue-Tek[®] OCT Compound (Sakura, Zoeterwoude, the Netherlands) until use. Each left lung was cut vertically into four equal pieces, at approximately $\frac{1}{4}$, $\frac{1}{2}$ and $\frac{3}{4}$ of the ventral-to-dorsal distance. Then, each piece was further sliced longitudinally (10 μm thickness) using a Frigocut 2800 cryostatic microtome (Reichert-Jung, Vienna, Austria), with the chamber at -25 °C and the cutting block at -17 °C. One of two successive slices was hematoxylin-eosin stained. The other slice was covered with a droplet of Vectashield[®] H-1000 mounting medium (Vector Laboratories, Burlingame, CA, USA) to prevent fluorescence photobleaching. Slices were examined by both light microscopy and

Chapter 6

fluorescence microscopy (Polyvar, Reichert-Jung; fluorescence excitation filter 455 - 490 nm, dichroic mirror 500 nm, emission filter 515 nm) at 400 × magnification. To determine the accuracy of an eye-based classification of lung areas (open, dystelectatic or atelectatic), photos of 281 slices were taken on PAN F 50 film (Ilford Imaging, Dreieich, Germany) and the tissue/air ratios (black/white ratio of the photo films) were determined using the computer program Photoshop[®] version 3.0 (Adobe Systems, San Jose, CA, USA). For statistical analysis of the distribution of Bodipy-labeled SP-B, slices were randomly chosen and examined by fluorescence microscopy. Each slice was divided into open (aerated), dystelectatic (underinflated) and atelectatic (collapsed) alveolar areas, as judged by eye. Next, a 100-cell counting grid was inserted. Then, 10 atelectatic, 10 dystelectatic and 10 open lung areas were randomly selected and the number of grid cells containing a fluorescence signal was counted. In case the area of interest contained airway structures or blood vessel, the counting grid was moved to a different position. To see if administered surfactant distributed preferentially into specific areas, the number of grid-cells containing fluorescent signals in a given alveolar area was standardized for the presence of air and tissue. This was done by dividing this number by the tissue/air ratio of that respective area.

Bronchoalveolar lavage. Rat lungs were lavaged using six volumes of 10 ml saline. BAL fluid was centrifuged (142 g, 10 min, 4 °C) and the supernatant was taken for determination of total protein by Pierce Micro BCA assay using BSA as standard. BAL pellet was resuspended in saline and aliquots were cytocentrifuged and stained with May-Grünwald and Giemsa solution (Merck, Darmstadt, Germany) for cell count. Three hundred cells were counted and the percentage of present alveolar macrophages, lymphocytes and polymorphonuclear neutrophils was determined.

Thin layer chromatography (TLC). TLC was performed [252] to check for lipid degradation of BLSE during storage. Furthermore, the amount of lipid phosphorus in TLC spots was determined [253].

2.6. Statistics

For statistical analysis, the computer program SPSS[®] version 9.0 was used (SPSS Inc., Chicago, IL, USA). Data were compared by ANOVA with Bonferroni posthoc test, Mann-Whitney test or Kruskal-Wallis test as indicated. Differences were considered significant at $P < 0.05$.

3. Results

3.1. BLSE quality control

Throughout the *in vivo* experiments (90 days) BLSE was stored at -20 °C until use and aliquots were repeatedly tested for material deterioration. No changes in phospholipid composition were found by thin layer chromatography (Table 1; n = 4 experiments). Furthermore, the surface activity, tested in a captive bubble surfactometer (n = 12), showed

In vitro and in vivo distribution of labeled surfactant

no differences with regard to film formation as well as minimum and maximum surface tension reached during cycling. Similarly, the spreading properties, tested in a square glass tray ($n \geq 9$; for method see [57]), remained unchanged.

Table 1. Quality control of BLSE during the 90-day period of *in vivo* experiments

	day -30	day 1 (begin)	day 30	day 90 (end)
<u>TLC: PL composition (mol%)^a</u>				
PC	81	79	76	80
PG	11	13	12	9
PE	3	3	3	4
PI	0.1	1	2	2
PS	0	0.2	0.2	0
lyso-PC	1	1	2	2
sphingomyelin	3	3	3	3
other	0.7	0.4	0.5	0.1
<u>CBS: surface tension (mN/m)^a</u>				
1 st cycle				
E _{Ads 1} , 0.5 bar	24.1 ± 1.7		23.8 ± 0.2	23.4 ± 1.1
C1, 2.8 bar	6.5 ± 0.4		9.8 ± 5.9	9.2 ± 2.8
2 nd cycle				
E2, 0.5 bar	27.4 ± 0.9		25.3 ± 0.9	25.6 ± 2.3
C2, 2.8 bar	3.9 ± 1.1		2.6 ± 0.1	1.9 ± 1.0
<u>Square glass tray^a</u>				
final surface tension (mN/m) (n=20)		27.4 ± 5.4		26.2 ± 3.4
spreading velocity (cm/s) (n=9)		11.2 ± 2.2		11.9 ± 6.0

^a no statistically significant difference was found within the 90-day period by means of Mann-Whitney test.

Definition of abbreviations: TLC = thin layer chromatography; PL = phospholipid; PC = phosphatidylcholine; PG = phosphatidylglycerol; PE = phosphatidylethanolamine; PI = phosphatidylinositol; PS = phosphatidylserine; CBS = captive bubble surfactometer; E_{Ads 1} = maximum surface tension of film reached one second after first bubble expansion; E2 = maximum surface tension of film reached at 2nd bubble expansion; Cx = minimum surface tension of film reached at xth bubble compression.

3.2. In vitro distribution of fluorescently labeled surfactant

A spreading trough was used to test whether spreading of surfactant throughout the

Chapter 6

first three generations of the airway depended on geometry. It was found that the surface tension reached five seconds after sample application to the buffer surface was the same at positions *a*, *b*, *c* and *d* for each surfactant tested (Table 2). Moreover, when comparing the surfactant mixtures it was found that the final surface tensions reached at positions *a*, *b*, *c* and *d* by BLSE and Alveofact (both containing SP-B and SP-C) were equally low at 26 mN/m ($P = 1.0$).

Table 2. Surfactant spreading ability related to lung geometry ^a. Surface tension (mN/m) \pm S.D. for $n \geq 4$ experiments.

	sensor position <i>a</i>	sensor position <i>b</i>	sensor position <i>c</i>	sensor position <i>d</i>	overall mean
BLSE	26.3 \pm 1.0	27.7 \pm 2.0	23.3 \pm 0.8	25.6 \pm 0.4	25.7 \pm 2.9 ^b
BLSE supplemented with Bodipy-labeled SP-B	31.6 \pm 1.0	30.6 \pm 1.5	28.8 \pm 0.7	29.7 \pm 1.3	30.2 \pm 2.7 ^c
BLSE;BSA(10 mg/ml) in subphase buffer	22.8 \pm 1.0	26.9 \pm 1.4	24.4 \pm 1.1	25.8 \pm 1.9	25.0 \pm 2.9 ^b
Alveofact	23.3 \pm 0.8	27.7 \pm 1.7	24.9 \pm 1.5	27.6 \pm 2.3	25.9 \pm 5.9 ^b
MLV (lipids)	69.9 \pm 1.0	69.9 \pm 1.0	69.9 \pm 1.0	69.9 \pm 1.0	69.9 \pm 1.0 ^d
MLV (lipids+SP-B)	55.6 \pm 4.0	54.9 \pm 5.3	52.7 \pm 3.7	52.6 \pm 3.9	53.9 \pm 4.3 ^e
MLV (lipids+ Bodipy-labeled SP-B)	52.3 \pm 3.3	51.8 \pm 3.2	49.4 \pm 4.3	49.2 \pm 1.9	50.7 \pm 3.5 ^e

^a no statistically significant difference among sensor positions was found for each tested surfactant by means of Kruskal-Wallis test.

^b no statistically significant difference among these three surfactants was found by means of ANOVA test.

^c $P < 0.01$ for BLSE supplemented with Bodipy-labeled SP-B vs all other surfactants by means of ANOVA test.

^d significantly different from all other surfactants ($P < 0.001$) by means of ANOVA test.

^e no statistically significant difference was found between both surfactants, but each was significantly different from all other surfactants ($P < 0.001$) by means of ANOVA test.

BLSE supplemented with Bodipy-labeled SP-B was also able to lower the surface tension to a comparably low value. In a subsequent series of experiments BLSE was spread on buffer to which bovine serum albumin had been added (10 mg/ml). This protein concentration is similar to that found in ARDS patients (0.5 - 4 mg/ml in BAL fluid [254-256] and 12 mg/ml in alveolar epithelial lining fluid [254]; the protein concentration in BAL fluid of healthy persons is around 0.1 mg/ml). The surface tension reached five seconds after sample application did not differ between BSA containing buffer and buffer alone. This shows that administered surfactant is able to spread on an aqueous surface even when a plasma protein is present at a concentration similar to that found in ARDS patients. In another set of experiments where MLVs consisting solely of lipids were applied onto the buffer

In vitro and in vivo distribution of labeled surfactant

surface, the need of surfactant proteins for surfactant spreading was shown. These lipid MLVs were not able to spread a film, as indicated by the absence of a drop in surface tension. In contrast, when SP-B or Bodipy-labeled SP-B were added to these MLVs, surface tension decreased by approximately 20 mN/m. From the results above it was concluded that both BLSE and Alveofact were able to quickly cover the entire air/water interface and lower the surface tension independent of airway branching. Furthermore, it was concluded that *in vitro* spreading of BLSE was not impaired by supplementation with Bodipy-labeled SP-B. Therefore, this fluorescently labeled surfactant could be used to follow its distribution *in vivo*.

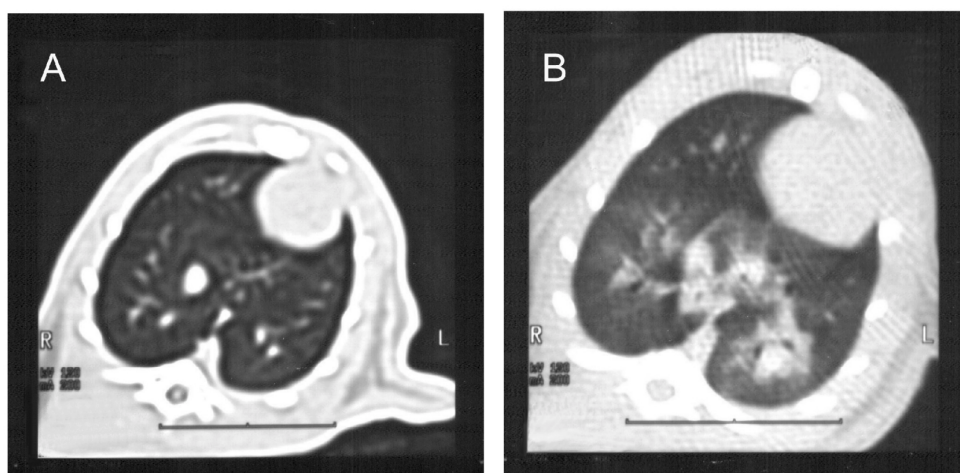


Figure 2. Representative CT scans of lungs of a control (A) and an LPS-exposed (B) rat.

3.3. In vivo distribution of fluorescently labeled surfactant

Development of ARDS in rats. LPS exposure to rats resulted in lung damage (Table 3). Measurements of total protein concentration and differential cell count in BAL showed that proteinaceous edema and inflammation had occurred. Furthermore, in LPS-exposed rats respiratory frequency was higher ($P < 0.05$) and compliance was lower ($P < 0.001$) than in control rats, and both arterial oxygenation and ventilation were impaired ($P < 0.001$). CT scans of the chest revealed that LPS exposure had caused formation of lung edema and dense areas. The left lung was generally found to be more affected than the right lung (Fig. 2). These findings were confirmed by histological evaluation of hematoxylin-eosin stained lung slices which showed a high percentage of atelectatic and dystelectatic regions (40 - 90 % of total lung area analyzed), a high content of polymorphonuclear (PMN) infiltrates, thickening of the alveolar-capillary membrane and accumulation of erythrocytes outside larger pulmonary blood vessels. In contrast, histological evaluation of control lungs showed little atelectatic and dystelectatic regions, no PMN infiltration and neither thickening of the alveolar-capillary membrane nor accumulation of erythrocytes outside blood vessels.

Chapter 6

Surfactant distribution. Analysis of lung slices by light microscopy showed that mean tissue/air ratios were different for aerated (open), underinflated (dystelectatic) and collapsed (atelectatic) areas (0.5, 1.0 and 1.5, respectively; $P < 0.001$ by means of Kruskal-Wallis test), confirming that judgement of lung tissue by eye according to these categories was legitimate. A hematoxylin-eosin-stained lung slice of an LPS-exposed rat showing the different lung tissue aeration states is depicted in Fig. 3.

For LPS-exposed and surfactant-treated rats the number of grid cells containing a fluorescent signal was found to be independent of the ventral-to-dorsal distance (data not shown), but dependent on type of alveolar area. When slices were examined by microscope, fluorescent signals were predominantly seen in dystelectatic and to a lesser extent in open lung areas (Fig. 4). They were rarely seen in atelectatic areas. This observation was statistically confirmed when the number of grid cells containing fluorescence per alveolar area was expressed as a function of lung tissue aeration (Fig. 5, $P < 0.001$). The number of grid cells containing a fluorescent signal was not found to be significantly different among the four periods of mechanical ventilation (5, 15, 30 and 60 min) studied.

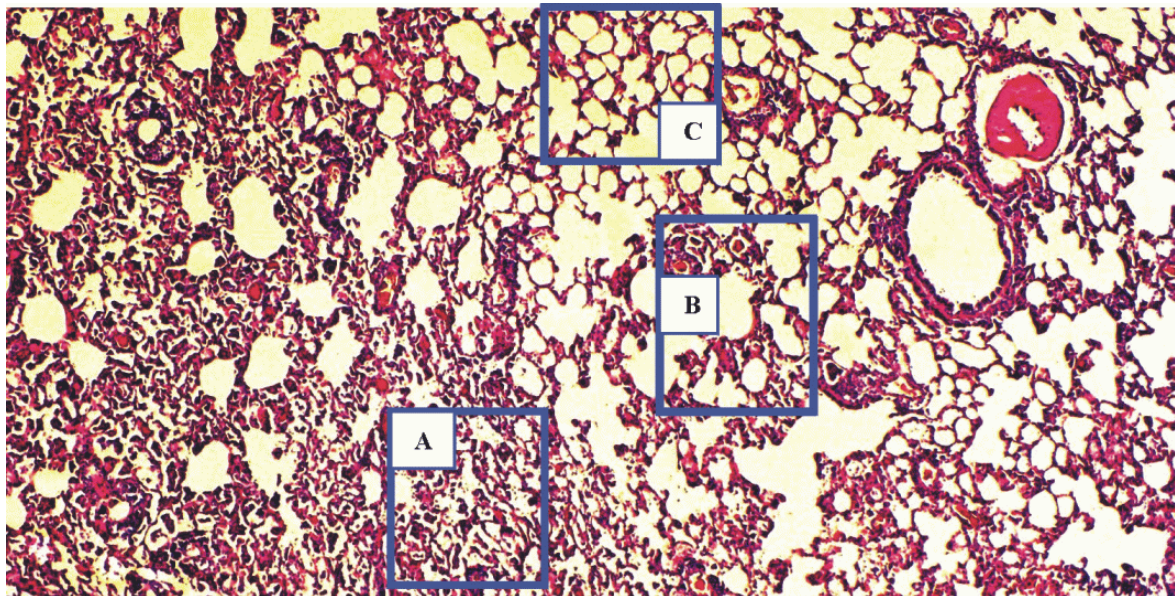


Figure 3. Slice of the left lung lobes of an LPS-exposed rat.

Examples of open (A), dystelectatic (B) and atelectatic (C) lung areas are shown. Tissue/air ratios of A, B and C were 0.5, 1.0 and 1.5, respectively. Lung slices were HE stained and are shown at $400\times$ magnification.

4. Discussion

The aim of this study was to follow the distribution of surfactant that was intratracheally administered into rat lungs suffering from ARDS-like injury. Prior to the *in*

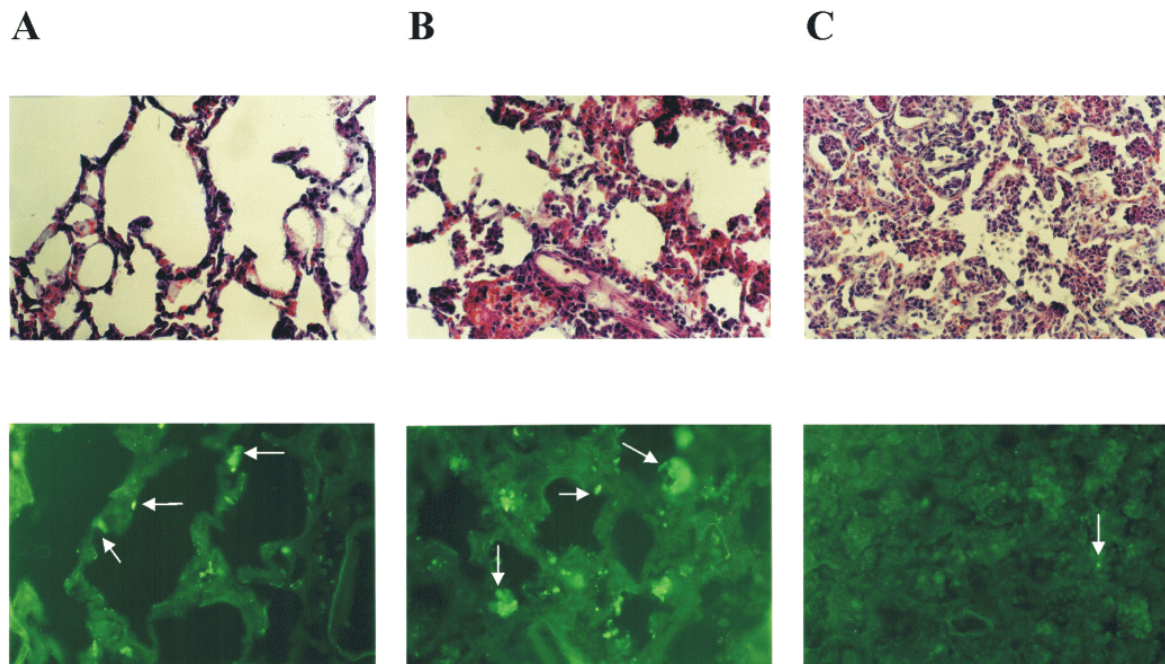


Figure 4. Slices of the left lungs of LPS-exposed rats after endotracheal administration of BLSE supplemented with Bodipy-labeled SP-B.

Top row: light microscopy (hematoxylin-eosin staining); bottom row: fluorescence microscopy. Slices of open (A), dystelelectatic (B), and atelectatic (C) alveolar areas are depicted. Arrows indicate fluorescence signals caused by deposition of Bodipy-labeled SP-B. Slices are shown at $400\times$ magnification.

in vivo experiments, surfactant distribution was measured *in vitro* in a two-dimensional anatomical glass replica of the first three generations of a human lung's tracheobronchial tree (Fig. 1; Table 2). Previously, the *in vitro* spreading velocities of Alveofact, BLSE and BLSE supplemented with Bodipy-labeled SP-B in a square glass tray were found to be equal [57]. In the spreading experiments performed in this study the three surfactants compared reduced the surface tension to near equilibrium (approximately 25 mN/m) independent of trough geometry. These results demonstrated that BLSE supplemented with Bodipy-labeled SP-B can be used as a marker to investigate surfactant distribution *in vivo*.

Intratracheal aerosolization of LPS was chosen as a model for ARDS, because ARDS frequently occurs in conjunction with sepsis caused by infection with bacteria producing the pathogen LPS. In agreement with [251], this approach resulted in lung damage comparable to that seen in ARDS (Table 3). According to [257], the LPS-exposed rats would have to be classified as having severe lung injury.

The optimal dose of exogenous surfactant for treatment of ARDS patients is unknown. Usually doses of 50 - 200 mg/kg are used in human and animal studies. Although higher doses are considered as being necessary to overcome inhibitory effects of plasma proteins on surfactant activity, we decided against a high dose strategy because it was recently shown for

Chapter 6

LPS-induced lung injury that treatment of rats with Curosurf[®] (62.5 mg/kg) improved lung function and decreased mortality [258]. Furthermore, promising results in humans have also been obtained at low doses (50 mg/kg) [243,208,259].

Table 3. Clinical comparison of LPS-exposed and control rats

	LPS-exposed	Control
<u>BAL</u>		
Total protein ($\mu\text{g/ml}$) ^a	160.0 \pm 18.9	124.3 \pm 70.4
Cells		
Total amount ml ⁻¹ BAL (\times 1000) ^b	2228 \pm 1036	113 \pm 26
Macrophages (%) ^b	20.4 \pm 3.9	80.0 \pm 17.3
PMNs (%) ^b	79.5 \pm 4.1	19.4 \pm 18.0
Lymphocytes (%) ^c	0.2 \pm 0.3	0.6 \pm 0.9
<u>Respiratory frequency (min⁻¹)^a</u>	102 \pm 8	79 \pm 4
<u>Blood gasses during ventilation</u>		
Pa _{O₂} (mm Hg) ^b	160 \pm 11	273 \pm 5
Pa _{CO₂} (mm Hg) ^b	48 \pm 3	34 \pm 2
<u>Compliance (ml at 25 mbar)^b</u>	12.0 \pm 0.3	15.3 \pm 0.4

^a $P < 0.05$ for LPS-exposed vs control by means of Mann-Whitney test.

^b $P < 0.001$ for LPS-exposed vs control by means of Mann-Whitney test.

^c no statistically significant difference between LPS-exposed and control rats found by means of Mann-Whitney test.

When slices of LPS-exposed and surfactant treated rat lungs were examined using a fluorescence microscope, fluorescent signals were readily observed at the alveolar level as well as in some airways (Fig. 4). Although visualization of labeled SP-B in the alveolar lining layer of thin lung slices is beyond the resolution of a fluorescence microscope, this finding strongly suggests that fluorescently labeled surfactant had entered the most peripheral parts of the lung by spreading along the airway surface. Moreover, the possibility exists that some of the signals observed may even represent fluorescently labeled surfactant taken up by either type II cells or macrophages. This would not disprove our assumption. Instead, it would only add further evidence to our observation that surfactant had reached the alveolus. Based on the half-lives of SP-B in rabbit [260] and mouse lung [261] of 7 h and 28 h, respectively, we

estimate that in our series of experiments SP-B clearance was less than 10 % within one hour. Since no statistical differences in total fluorescent signals were observed within the observation period of 5 to 60 min, it is reasonable to assume that the major portion of the administered SP-B visible by fluorescence microscopy was part of the alveolar lining layer.

Interestingly, fluorescent signals were mostly detected in lung regions representing underinflated (dystelelectatic), as well as aerated (open) alveolar areas (Fig. 5). In contrast, only little fluorescence was detected in regions defined as collapsed (atelectatic) areas. This finding indicates that surfactant instilled into sick lungs, known for both their patchy distribution as well as their inhomogeneous extent of tissue damage, rather distributes in a nonuniform than in a uniform way. In particular, surfactant appears to spread preferentially into ventilated rather than unventilated lung areas. This is in contrast to [249], who showed by immunohistochemical localization of surfactant protein C (SP-C) that instilled surfactant predominantly distributed to collapsed alveolar spaces. However, appearance and distribution pattern of SP-C varied substantially among animals. One possible explanation for the disparate result is that the pathologic changes seen in a lung injury model induced by repeated lavage used [249] (*e.g.* surfactant depletion, air trapping by foamy liquid) are usually less severe than those seen by aerosolization of LPS used in this study (*e.g.* evasion of polymorphonuclear leukocytes, high permeability, alveolar edema, surfactant inhibition). In fact, surfactant depleted lungs can be easily rescued and appropriate gas exchange re-instituted just by simple lung volume recruitment maneuvers [262], indicating that ventilation is quite homogeneously distributed. Therefore, surfactant in lavaged lungs is likely to spread more evenly. Another explanation is that dystelelectatic and atelectatic alveoli were not discerned in [249]. This raises the possibility that at least part of the signal attributed to collapsed (atelectatic) alveoli in fact originated from underinflated (dystelelectatic) alveolar areas.

Another interesting aspect raised by the inhomogeneous distribution of lung surfactant observed in this study is the possible response of the injured lung to mechanical ventilation. In an attempt to open up the lung and facilitate surfactant spreading, we inflated the lungs three times to 20 mbar over a 3 s period after surfactant administration. This moderate form of lung volume recruitment was chosen because of ease of application and lack of hemodynamic interference. It was furthermore chosen because the aim of this study was to investigate intrapulmonary surfactant distribution rather than effects of aggressive volume recruitment maneuvers recommended to open up severely consolidated lungs [263-265]. Nevertheless, though, the results of our study are of importance for several reasons. First, the results provide evidence that ventilated lung areas receive surfactant (Fig. 4) and can be expected to respond to and benefit from moderate recruitment maneuvers and appropriate mechanical ventilation between upper and lower inflection point of the respiratory pressure - volume curve. With regard to the underinflated lung areas, the decrease in surface tensile force will move them out of the flatter part towards the steep part of the pressure - volume curve. Thereby it might help protect against shear stress, prevent alveolar collapse and avoid propagation of ventilator-induced lung injury [266]. With regard to the aerated lung

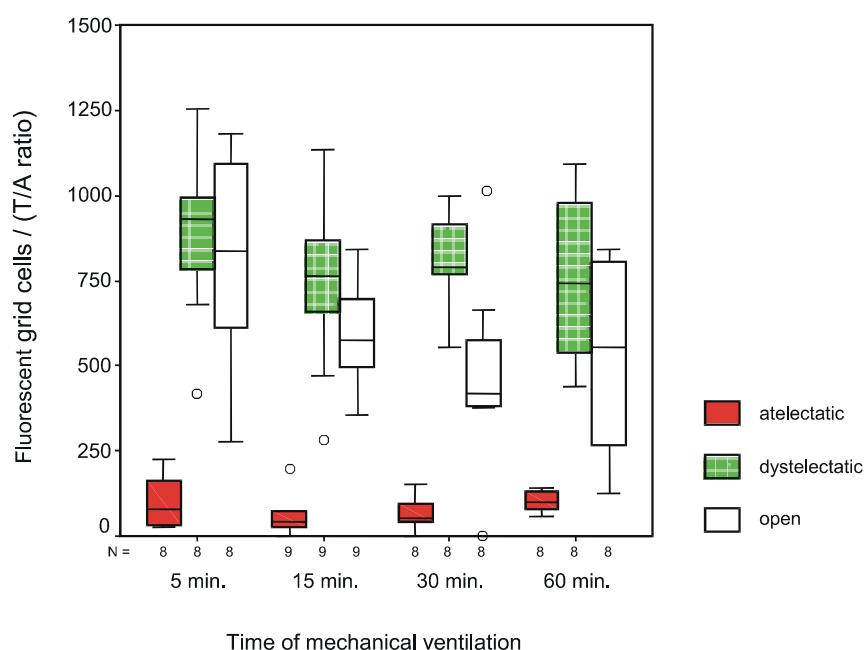


Figure 5. Boxplots of the number of fluorescence containing grid cells determined in open, dystelectatic, and atelectatic areas in the left lungs of rats having LPS-induced lung failure resembling ARDS.

The number of grid cells containing a fluorescent signal was corrected for the amount of tissue (T) and air (A) present per slice area. Circles represent outliers. Intratracheally administered surfactant preferentially distributed into dystelectatic and open alveolar areas ($P < 0.001$ by means of Kruskal-Wallis test).

areas, the decrease in surface tensile force will move them up higher towards the more flat portion of the inspiratory pressure - volume curve. Therefore, application of excessively high transpulmonary pressures will tend to overdistend aerated lung units and increase their risk for barotrauma. However, if transpulmonary pressures larger than 30 to 35 cm of water are avoided, aerated lung areas should not be overdistended [267] and the risk for barotrauma be negligible. In fact, surfactant replacement might even help reduce occurrence of pneumothorax [268]. In our series of experiments a pneumothorax never occurred. Second, in our study only small amounts of exogenously administered surfactant reached collapsed areas. This finding was independent of length of mechanical ventilation (up to 60 min). It suggests that atelectatic lung units can not readily benefit from surfactant replacement therapy unless these structures are opened up and conditioned such that an air/water interface is formed prior to surfactant instillation. In contrast to aerated and underinflated lung regions, such collapsed areas might benefit from aggressive lung volume recruitment maneuvers aimed at opening the alveoli up and keeping them open [263-265]. If such an approach appears too invasive, body positioning could be considered as an alternative. In a case report it was recently shown by quantitative analysis of CT that conditioning of the lungs by changes in body positioning prior to surfactant replacement helped improve gas exchange by expansion of underinflated and collapsed lung areas [269].

Finally, intrapulmonary surfactant distribution has thus far been investigated only on a macroscopic scale (small pieces of lung) [246-250] but not on a microscopic scale (alveolus). Moreover, the results were inconclusive. While [248,250] found that exogenous surfactant spread homogeneously throughout the entire lung, other groups [246,247] observed a more inhomogeneous distribution. These results, when compared to those obtained in our study, may be different for various reasons. First, markers used in those studies were either not derived from natural surfactant components or they were just added to surfactant without knowing the component(s) to which the label was attached [246-248,250]. Second, we found that the boundary between open and atelectatic lung areas can be as small as a few alveoli. Consequently, homogenization of lung lobes or pieces will not allow a sufficiently detailed analysis of a particular lung area.

5. Conclusion

It is concluded that the direct observation of a natural component of lung surfactant is a valuable approach to study surfactant distribution. The results obtained in this study suggest that exogenous surfactant instilled into lungs with ARDS-like injury distributes preferentially into underinflated (dystelelectatic) and aerated (open) lung areas. Therefore, these lung regions might benefit the most from surfactant replacement therapy. Furthermore, we have shown that when using conventional mechanical ventilation, instilled surfactant can in general not reach collapsed (atelectatic) alveolar areas in sufficiently large amounts. Therefore, collapsed regions will not readily benefit from surfactant therapy unless they are opened up prior to surfactant administration.

Acknowledgments

We gratefully acknowledge the following people from the university of Innsbruck: Dr. J. Kellner and H. Staud for assistance during the animal experiments and P. Hamm, W. Goldschmied, Dr. A. Amann and Dr. D. Bader for technical support (Department of Anaesthesiology and Critical Care Medicine); W. Salvenmoser (Institute of Zoology and Limnology), Prof. F. Offner (Institute of Pathological Anatomy), Dr. S. Eschertzhuber and Dr. M. Frick (Institute of Physiology and Balneology), Prof. K. Pfaller (Institute of Anatomy and Histology), Dr. M. Freund (Department of Radiodiagnostics) and Mag. G. Eibl (Institute of Biostatistics and Documentation) for invaluable practical tips and technical support.

Chapter 7

Summarizing Discussion

Rob Diemel

1. General overview

1.1 Surfactant in the healthy lung

The lung contains a large inner surface - 1 cm³ lung tissue has a total gas-exchange surface of 300 cm² - that is in direct contact with the environment. Mammalian lungs are composed of bronchi and bronchioli (functioning as connective tubes) that ultimately end in alveoli (the smallest compartments in the lung). It is in the alveoli where the gas-exchange (oxygen entering and carbon dioxide leaving the blood stream) takes place. The roughly spherically shaped alveoli have a high curvature, similar to an air-bubble surrounded by water. The law of LaPlace, $\Delta P = 2\gamma / r$, dictates that the pressure difference (ΔP) over an air/water interface is equal to twice the surface tension (γ) at the air/water interface, divided by the bubble radius (r). During expiration lung volume and thus bubble radius decreases, leading to a higher pressure difference. This means that more energy would be required to reopen the lung upon inspiration, if surface tension would not vary. Fortunately, though, energy expenditure is kept low and lung collapse is prevented by a substance called surfactant, which covers the surface of the alveoli and the rest of the airway system and lowers the surface tension.

Pulmonary surfactant is a mixture of lipids and proteins, synthesized and secreted into the alveolar fluid by the alveolar type II epithelial cells. Its main function, lowering the surface tension at the alveolar air/liquid interface, is achieved by formation of a surface-active film that consists of a lipid monolayer highly enriched in dipalmitoyl-phosphatidylcholine (DPPC; 40 to 50 wt% of the lipid pool). DPPC has a gel to liquid-crystalline transition temperature (T_m) of 41.5 °C. Therefore, at a physiological temperature of 37 °C it is in an ordered gel state. Because DPPC contains two saturated acyl chains, it can be tightly packed in the monolayer. This tight packing is crucial at end-expiration when the alveolus is compressed to a minimal area. Lipids with unsaturated fatty acids have a T_m well below 37 °C and are therefore in a fluid state at physiological temperature. These unsaturated lipids are considered to be important for surfactant function, since fluidization of the surfactant film prevents the film from becoming too rigid to withstand dynamic compression and expansion, which would be the case if the film were composed of saturated lipids only. These data have led to the hypothesis that upon compression the monolayer is enriched in saturated DPPC, necessary to achieve low surface tensions, while the fluid lipids and proteins are squeezed out of the monolayer, forming bilayer or multilayer structures ('surface-associated reservoir') that stay connected to the monolayer. From such layered protrusions, surfactant material can be readily incorporated into the monolayer film upon inspiration. The existence of a layered film has been visualized *in vivo* by electron microscopy and recently *in vitro* by atomic force and fluorescence light microscopy.

Components important for surfactant film formation and homeostasis are the small hydrophobic surfactant specific proteins B and C (SP-B and SP-C). SP-B is a 79 amino acid amphipathic protein that is active as an 17.4 kDa dimer. Its amino acid sequence among mammals is highly conserved (see chapter 1), indicating that it has a highly important

function in the lung. Secondary structure analysis and homology with related proteins, especially members of the saposin-like family, predict an SP-B structure that contains four amphipathic α -helices. These helices are thought to interact with the surfactant lipids by a specific interaction between the positive charges of SP-B and anionic lipids like phosphatidylglycerol (PG; 5 to 10 wt% of the surfactant lipid pool). The many different activities ascribed to SP-B include the ability to induce the formation of a monolayer film from vesicles, to facilitate respreading of films from the collapsed phase, to induce film refinement by selective removal of non-DPPC lipid upon compression, to support membrane fusion and lysis, to aid in the formation of tubular myelin and to increase surfactant reuptake by type II cells. SP-B deficiency in humans causes lethal respiratory distress syndrome. Moreover, mice in which the SP-B gene has been knocked out die of respiratory failure immediately after birth. Since SP-B deficiency is mostly accompanied by not fully processed SP-C, it is thought that another role of SP-B is to participate in the processing of SP-C proprotein. In addition to the traditional role as a surface tension lowering agent, the results of preliminary studies suggest that SP-B also has a function as an anti-inflammatory agent and as a protector against oxygen-induced lung injury (see chapter 1).

SP-C is a 35 amino acid protein of 4.2 kDa that is extremely hydrophobic. It is further characterized by one or two palmitoylated cysteines at positions 5 and 6 of its N-terminal part. Its two conserved positively charged amino acids at positions 11 and 12 are thought to interact with negatively charged lipid head groups. The C-terminal amino acids form an α -helix rich in valines, able to span a lipid bilayer. In a lipid environment the α -helical content increases and might even extend to the two palmitoylated cysteines. Interestingly, the activities of SP-C largely overlap those of SP-B. This includes promotion of lipid adsorption into the air/liquid interface, stabilization of the monolayer film, respreading of films from the collapsed phase and surfactant reuptake by type II cells. Quite surprisingly, in contrast to SP-B null-mutant mice, SP-C knockout (*i.e.* -/-) mice survive. Surfactant pool sizes, surfactant synthesis and lung morphology of SP-C (-/-) mice were similar to those in SP-C (+/+) mice. However, their surfactant showed altered stability when measured in small captive bubbles, indicating that SP-C plays a role in the stabilization of surfactant at low lung volumes. This correlates with findings that SP-C deficiency in humans is not necessarily lethal, but is accompanied with increased mortality due to the development of interstitial lung disease.

Lipids are the main components of surfactant (90 wt%). Most abundant and best characterized are the previously mentioned phospholipids DPPC and PG. The most important non-phospholipid in surfactant is cholesterol, present in amounts of 10 to 20 mol% (approximately 5 to 10 wt%). Even though the presence of cholesterol in surfactant has long been recognized, little is known about its function. It is presumed that in the presence of the hydrophobic surfactant proteins and at physiological temperature, cholesterol acts as a fluidizing agent, enhancing adsorption and respreading of lipid from collapsed phase. In general, cholesterol is able to induce a liquid ordered phase, in which the lipid acyl chains are extended and tightly packed as in the solid phase, but have a lateral diffusion that is almost

Chapter 7

as high as in the fluid phase. In this way cholesterol increases the fluidity of the lipid acyl chains below the transition temperature of that lipid, but rigidifies the acyl chains above the transition temperature. The rigidifying effect of cholesterol is exerted on DPPC by its packing into the intermolecular cavities of DPPC. The fluidizing effect is achieved by direct interaction of cholesterol with the fatty acyl chains of the phospholipids, hindering close packing of the phospholipids.

1.2 Surfactant in the diseased lung

Among the many lung diseases, two are directly related to surfactant: respiratory distress syndrome (RDS) in premature newborns and acute respiratory distress syndrome (ARDS) in adults. Since surfactant is produced from the 26th week of gestation onwards, the primary cause of RDS in prematurely born children is a lethal deficiency of surfactant. As part of the treatment, exogenous surfactant is instilled into the lungs of these infants, resulting in a dramatic increase in survival rate. In adult patients with acute lung injury, secondary changes in the endogenous surfactant system have been found: the amount of surfactant specific proteins in bronchoalveolar lavage (BAL) was considerably reduced and the total amount of phospholipids in BAL was decreased by 70 % compared to healthy persons. Also, the composition of the phospholipid fraction in BAL was changed: the amount of DPPC, necessary to reach minimal surface tension, was decreased while the amount of lyso-PC was increased. Furthermore, the amount of negatively charged phospholipids was markedly altered. Finally, the biophysical activity of surfactant lavaged from ARDS patients was decreased: maximum and especially minimum surface tension were increased compared to that of healthy persons. These surfactant alterations are thought to contribute to ARDS. Therefore, also in adult patients administration of exogenous surfactant has been suggested as a beneficial therapeutic strategy. Unfortunately, the results obtained for ARDS patients thus far are conflicting. In an earlier series of clinical investigations either lung function improved and mortality dropped significantly after surfactant instillation, or it remained largely unchanged. In a more recent series of clinical investigations it was shown that gas exchange improved more than twofold after surfactant instillation, but the effect was lost within a few hours and a repeat dose of surfactant was required to improve gas exchange again. Furthermore, it was found that mortality dropped significantly after repetitive doses of natural surfactant. From literature data it is unclear whether administered surfactant is able to reach diseased parts of the lung. It is conceivable, that administered surfactant might only spread into healthy lung regions that already contain active surfactant.

In this thesis attention is focused mainly on SP-B, i) to obtain more knowledge on surfactant action in the healthy lung by investigating its surface activity *in vitro* by captive bubble surfactometry (CBS) and atomic force microscopy (AFM), and ii) to study its usefulness *in vivo* in the diseased lung as a marker for surfactant distribution in rat lungs having ARDS-like injury.

2. Results described in this thesis

2.1 Surface activity measurements of lipid films with SP-B and SP-C: captive bubble surfactometry (CBS)

In chapters 2, 3 and 5 the captive bubble surfactometer is used to obtain information about the surface activity of individual surfactant components. Events taking place in the captive bubble surfactometer are considered to be the most accurate *in vitro* imitation of the events taking place in an alveolus with regard to surfactant surface dynamics. Its mode of action is described below. Alternative methods to obtain information about surfactant surface dynamics are i) the pulsating bubble surfactometer (PBS), in which the air-bubble is not completely enclosed as in the CBS, but is in open connection with a small capillary, and ii) the Langmuir-Wilhelmy balance, a teflon trough that is filled with buffer on which a surfactant monolayer is present; by movement of a teflon barrier positioned in the trough surface tension can be altered. Both PBS and Langmuir-Wilhelmy balance are proven to provide less accurate information than usually obtained by the use of CBS, since both of the former devices can be subject to film leakage [24,176]. Moreover, measurements by Langmuir-Wilhelmy balance can not be performed under dynamic conditions.

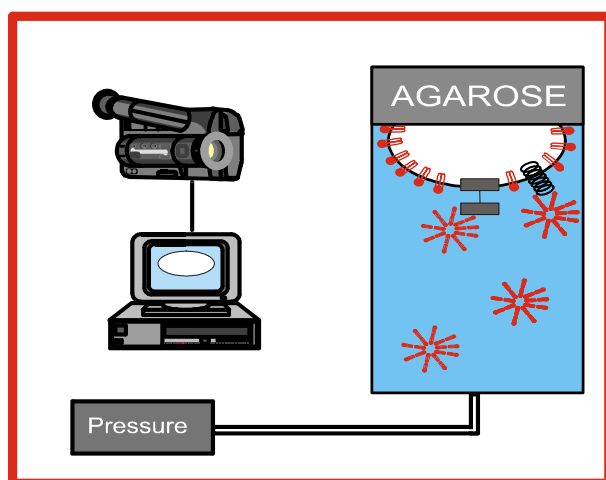


Figure 1: Captive Bubble Surfactometry (CBS).

An air-bubble is trapped underneath the ceiling of a cuvette that is filled with buffer. The pressure inside the cuvette can be altered, thereby changing the shape of the bubble and concomitantly the surface tension at the air/liquid interface. The bubble shape is monitored by a camera that is connected to a video-recorder and a computer. Values of parameters such as bubble area and surface tension are obtained by home-built computer software.

The captive bubble surfactometer consists of a cuvette that contains an air bubble (in our case with a typical area of 0.5 cm^2) trapped in buffer underneath an agarose ceiling (Fig. 1). Using the spread film technique [26], a known amount of surfactant material (lipids and protein(s)) is spread at the bubble air/liquid interface by microsyringe. Subsequently, surfactant lipids are injected as small unilamellar vesicles into the buffer to function as a lipid reservoir. After that, the pressure inside the system is changed: first, pressure is instantly decreased from atmospheric pressure (1.0 bar) to 0.5 bar, where it remains for 10 seconds.

Chapter 7

During this period the bubble area is increased and lipids can adsorb from the subphase into the air/liquid interface. This process is mediated by the proteins residing at the interface. Second, pressure is slowly (few seconds) increased to 2.8 bar, thereby decreasing the bubble area. During this period (“expiration”) surfactant material is squeezed out of the monolayer at the interface, forming protrusions (surface associated reservoir) connected to the monolayer (chapters 3 and 4 describe the visualization of these protrusions by atomic force microscopy). During compression, the monolayer becomes enriched in DPPC. The surface tension at minimum bubble size is called minimum surface tension (γ_{\min}). Third, pressure is slowly (over a period of a few seconds) decreased to 0.5 bar, thereby increasing the bubble area. During this period (“inspiration”), lipids and proteins are reinserted from the protrusions into the monolayer at the interface. The surface tension at maximum bubble size is called maximum surface tension (γ_{\max}). Subsequently, the pressure inside the cuvette is repeatedly decreased and increased to cycle bubble area (“breathing”). This is followed by a 5 minute period at 2.8 bar to determine film stability. Finally, bubble cycling and stabilization are repeated once more. The variation of the pressure inside the cuvette leads to alterations of bubble shape, which is continuously monitored by a camera. With the use of a frame-grabber, home-built software can convert side-view bubble images into desired parameters such as surface tension and bubble area.

Chapter 2 describes the effect that SP-B and SP-C have on surface activity of spread films in the CBS. Surface tension was found to depend on the amount of protein present in the film. The lowest surface tensions were reached with DPPC/POPG (80/20) films containing 0.5 - 0.75 mol% SP-B (see also chapter 5) or 3 mol% SP-C. These concentrations are similar to the amounts obtained by bronchoalveolar lavage. In additional experiments, the need for surfactant material in vesicular structures in the subphase was demonstrated: the presence of MLV or SUV in the subphase led to lower γ_{\max} and γ_{\min} than surface tensions reached in the absence of lipid vesicles. No clear difference between SUV and MLV was observed. Furthermore, we found only small differences in surface activity between both proteins: when no lipids were present in the subphase, minimum surface tension of films containing SP-B never reached low values and remained at approximately 10 mN/m, while minimum surface tension of films containing SP-C started at 3 mN/m and increased to 17 mN/m within 5 cycles. From this it can be concluded, that lipids excluded from the monolayer might form a mini lipid-reservoir that is sufficient for SP-B to stay attached to the monolayer, while it is not sufficient for SP-C to stay attached. Nevertheless, SP-B does need subphase lipid vesicles to create stable films with very low γ_{\min} . Therefore, the overall conclusion drawn from the experiments described in chapter 2 is that the presence of a (surface associated) lipid reservoir is required for films containing either SP-B or SP-C to reach and maintain low surface tensions. Because of its more standardized size compared to MLV, we used SUV in the further CBS studies that are described in chapters 3 and 5.

Chapter 3 describes the effect of cholesterol on both surfactant surface tension and surface topography. To best observe an effect of cholesterol, films contained lower amounts of DPPC than the films described in chapters 2 and 5. Films were composed of

DPPC/POPC/POPG (50/30/20, molar percentages) plus 0.75 mol% SP-B and/or 3.0 mol% SP-C. Moreover, these films contained up to 20 mol% cholesterol. Striking differences in the effects of cholesterol on surface activity of films containing SP-B and those containing SP-C were observed. Increasing concentrations of cholesterol led to decreasing maximum and minimum surface tensions when SP-B was present as the sole protein in the films, with an optimal cholesterol concentration of 10 mol%. On the other hand, the presence of 10 mol% cholesterol worsened surface activity of films containing SP-C as the sole protein. Yet, the presence of cholesterol had no effect on surface activity of films containing both SP-B and SP-C. Interestingly, both minimum and maximum surface tension were the lowest when the film contained both hydrophobic proteins, providing further evidence to the general idea that natural surfactant containing SP-B and SP-C is superior to synthetic surfactants that lack one of both components. Unfortunately, there is no easy explanation for the CBS results obtained in chapter 3. The complex lipid mixture used in our study made it especially difficult to draw conclusions concerning mechanisms. Moreover, although AFM and differential scanning calorimetry showed that cholesterol has a homogenizing effect on the film, it did not provide us with enough solid evidence to build a model for the action of cholesterol in surfactant. As a result, the best that we could do is to describe the effects that we have found. This is the first time that the influence of cholesterol on surfactant function has been investigated by CBS. Previous studies on the role of cholesterol in surfactant using the PBS or the Langmuir-Wilhelmy balance have not led to the production of a conclusive model concerning the effect of cholesterol. Although we have described effects of cholesterol under dynamic conditions, its interaction with other membrane components will require further study. Since cholesterol is present in considerable amount in the lungs of all analyzed mammals [177,176], it must have an important function in the surfactant system. The observation of increased levels of cholesterol in lungs of fish and amphibians compared to that of mammals [177], together with the report that cholesterol levels are altered with changing body temperature [270], suggest that cholesterol also has a crucial role in proto-surfactant (*i.e.* the surfactant present in species that are less evolved than mammals).

2.2 Surface topography of lipid films containing SP-B and SP-C: Atomic Force Microscopy (AFM)

Chapters 5 and 6 describe the use of AFM to visualize surfactant film topography of compressed monolayer films. Samples were prepared using the Langmuir-Blodgett transfer technique (Fig. 2). In this technique a small disc of mica acts as a support for the surfactant film. After the mica has been dipped into the water that is contained in a teflon trough, a solution of lipids and protein in MeOH/CHCl₃ (1/1) is spread onto the water surface. After the solvent has been allowed to evaporate for at least 5 minutes, a teflon barrier is moved mechanically to compress the film to a desired surface tension (in our case usually to $\gamma = 22$ mN/m). Subsequently, the mica disc is moved upwards out of the water, resulting in transfer of the film from the air/water interface onto the mica support.

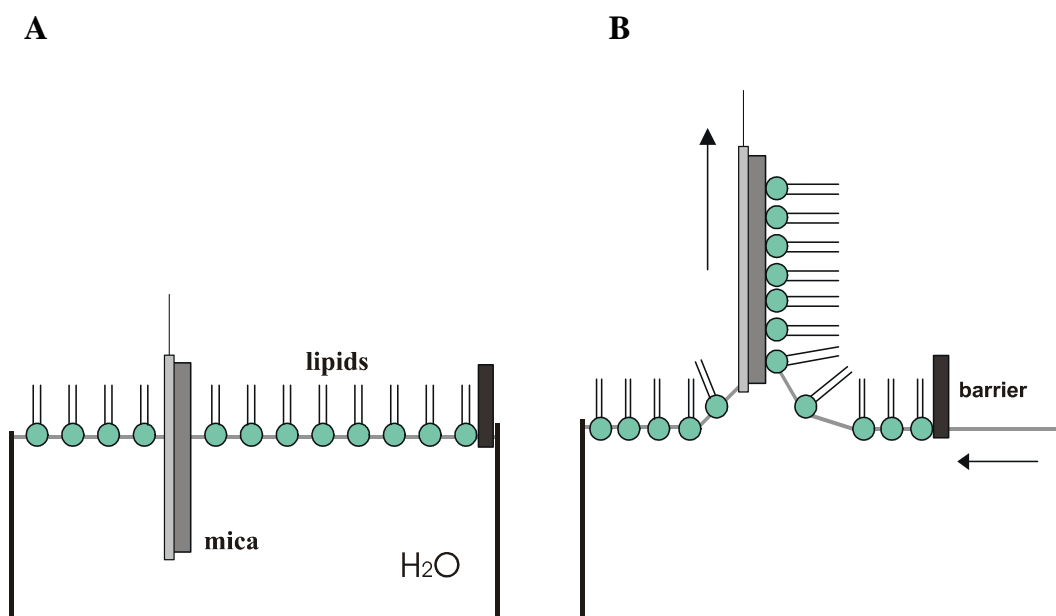


Figure 2: Langmuir-Blodgett transfer.

A disc of mica is dipped into water contained in a teflon trough (A). Subsequently, a film, in this figure made up of solely lipids, is spread onto the water surface. The resulting monolayer is oriented such that the hydrophobic fatty acids face the air, while the hydrophilic lipid headgroups face the water. After that, the teflon barrier is moved to compress the film to a desired surface tension. The mica disc is subsequently moved upwards out of the water at constant surface pressure, resulting in film transfer onto the mica (B).

A few hours later the sample is mounted on top of an AFM scanner. AFM is a fairly new technique, first described in 1986 [217], that allows measurements of height differences as small as that of a single molecule. The action of an atomic force microscope on a surfactant film is depicted in Fig. 3: a sharp tip with a radius of 5 to 50 nm scans in the x and y direction over the film. A laser beam that is continuously directed on the cantilever connected to the tip is reflected on the cantilever and ultimately enters a detector. When the tip encounters an area of increased height, such as a protrusion that is formed as a result of monolayer compression, the deflection of the tip into the z direction results in an altered route of the laser beam, leading to a shift in the spot where the laser beam hits the detector. From this, the difference in height can be calculated by computer software. It has been shown that structures transferred from the air/water interface onto solid substrates are essentially identical to the structures in the monolayer itself [200,199].

In chapter 3 the same lipid/protein mixtures as described above for CBS were used: DPPC/POPC/POPG (50/30/20) plus 0.75 mol% SP-B and/or 3.0 mol% SP-C. Furthermore, films contained either 0 mol% or 10 mol% cholesterol. The differences in film topography between films containing and those lacking cholesterol were stunning. The protrusions observed in films containing cholesterol were homogeneously dispersed over the film, whereas protrusions seen in films without cholesterol tended to be more clustered into network structures. The most clear effects of cholesterol on film topography were observed

for films containing SP-B. Our results suggest that cholesterol causes a more homogeneous dispersion of the various surfactant components over the entire film.

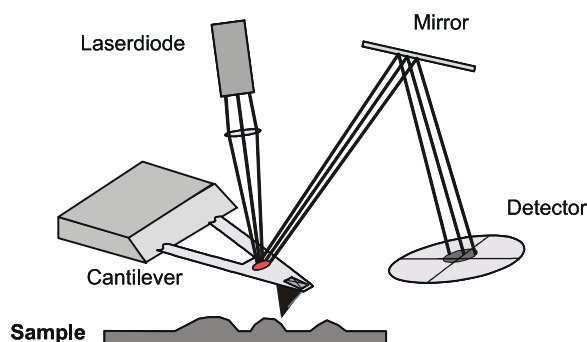


Figure 3: Atomic Force Microscopy (AFM).

A sharp tip scans the surface of a sample (in our case a compressed surfactant monolayer). A laser beam is directed on the cantilever, from which it is reflected to a detector. When the tip encounters an area of increased height, the cantilever to which the tip is connected is deflected upwards. As a result, the laser beam follows an alternative route and enters the detector on a different spot. Computer software translates detector output into sample height differences.

Protrusions heights of multiples of 4 - 4.5 nm were found upon compression of DPPC/POPC/POPG films containing SP-B and/or SP-C, independent of cholesterol concentration, as described in chapter 3. For SP-C in the fully saturated DPPC/DPPG (80/20) system, formation of protrusions with heights of multiples of 5.5 nm have been reported [13,81,163]. In both these and our own AFM studies, films were compressed to a surface tension of 22 mN/m. Since the height of a bilayer is reported to be 4 to 5.5 nm, depending on the lipid composition as well as the method of determination, it is deduced that multiples of bilayers are protruded. However, protrusions reported for DPPC/DPPG films containing SP-B had heights of a single bilayer instead of multilayers [163]. To study whether the proteins or the lipids determine the height of the protrusions formed, we investigated the determinants for protrusion formation (chapter 4).

In chapter 4 we describe a concentration curve of bovine SP-B in DPPC/DPPG films. Protrusions of single bilayer thickness were shown to be formed, but only above a certain concentration of SP-B in the film. This concentration was found to be between 0.2 and 0.4 mol%, which is similar to the amount of SP-B found to have optimal activity in *in vitro* assays [57,173,218,219] and is roughly comparable to the amount of SP-B present in bronchoalveolar lavage fluid (ranging from 0.02 [57] to 0.9 mol% [220]). The protrusions formed networks consisting of cells with a hexagonal shape, which is a typical structure found upon compression of films containing hydrophobic surfactant protein(s). Similar network shape was observed for films containing synthetic peptide based on the 25 N-terminal amino acids of human SP-B (either monomeric or dimeric SP-B₁₋₂₅), but much higher concentrations (20 mol%) were needed to obtain such structures. Furthermore, the protrusions formed in the presence of SP-B₁₋₂₅ peptides were not as high as those found for the native protein. In a second set of experiments, the influence of phospholipid on protrusion formation was studied. Films containing SP-B protein or peptide at concentrations found to

Chapter 7

be optimal for protrusion formation (*i.e.* 0.4 mol% bovine SP-B and 20 mol% mSP-B₁₋₂₅ or dSP-B₁₋₂₅) were compressed to $\gamma = 22$ mN/m. First, films containing DPPC/POPG (80/20) were tested. Remarkably, in these protein/lipid and peptide/lipid mixtures protrusions with heights of multiples of 4 nm were observed, indicating that in this lipid mixture protrusions with multilayer height instead of a single bilayer height were formed. Then, to find out whether the unsaturated lipid acyl chain or the negative charge of POPG was responsible for the formation of multilayered protrusions, protein and peptide were incorporated in films of DPPC/POPC/DPPG (60/20/20). Compression of these films resulted in the formation of protrusions of mainly bilayer height, although occasionally multilayered structures were also observed. From these AFM data we conclude i) that a certain minimal concentration of SP-B is required for the formation of layered protrusions upon film compression, ii) that protrusion height depends on whether the phospholipids contain an unsaturated fatty acyl chain, and iii) that protrusion height also depends on the presence of a negative charge on the phospholipid that contains the unsaturated acyl chain. Our conclusions are in line with other studies (not using AFM) in which it was reported that it are mainly the unsaturated lipids and the hydrophobic proteins that are squeezed-out of the monolayer upon compression [160-162]. Interestingly, we have also found multilayered protrusions instead of single bilayer protrusions in SP-B and/or SP-C containing films of DPPC/POPC/POPG (50/30/20), as described in chapter 3. Moreover, multilayered protrusions were recently found in an AFM study using synthetic monomeric SP-B peptide containing films of DPPC/POPG (3/1) as well [206]. These results indicate that POPG could play a crucial role in multilayer formation.

Fig. 4 depicts a model that combines the findings from our AFM studies. For clarity reasons, we show a simplified representation of the events happening at film compression, depicting a protrusion of a single bilayer only. In this figure the hydrophobic surfactant proteins are located at the sites of the protrusion. This is based on fluorescence microscopy studies that showed that the surfactant proteins were present in the liquid expanded phase of the protrusions [163,13]. It can be argued that compression of a protein/lipid film leads to the formation of domains of increased order, consisting mainly of saturated lipids, surrounded by regions containing “contaminants” like proteins and unsaturated lipids that are forced out of the ordered domains. For films containing surfactant proteins such separation of film components results in formation of hexagonal cells in which the borders contain SP-B and/or SP-C plus unsaturated lipids. At these sites SP-B and SP-C are able to form and maintain protrusions. Based on the results described in chapter 4, SP-B in Fig. 4 is located near unsaturated phospholipids containing a negative charge. Likewise, we assume that the two positively charged N-terminal amino acids of SP-C will also be in the vicinity of negatively charged lipids. Although SP-C is depicted to be surrounded by saturated lipids, this does not exclude the possibility that unsaturated lipids are present in the direct proximity of SP-C, since the lipid determinants for protrusion formation in SP-C containing films are not yet known.

Interestingly, in recent studies performed at collapse pressure (*i.e.* at a surface tension below approximately 12 mN/m) it was reported that films, already showing the typical

network structures of protrusions, reversibly fold into the subphase (a process known as buckling). In this way all surfactant components will be retained near the interface. This observation was made in a fluorescence microscopy study using films of DPPG/POPG/palmitic acid (68/22/8) plus synthetic SP-B₁₋₇₈ [271]. Buckling was furthermore reported in two studies using both fluorescence microscopy as well as AFM, using DPPG [172] or DPPG/POPG (3/1) [172,206] films containing the synthetic peptides SP-B₁₋₂₅ or SP-B₁₋₇₈. Film buckling could be interpreted as the next step in a multi-step process of film compression to extremely low surface tensions, in which first protrusions are formed upon compression of the film from $\gamma = 72$ to 12 mN/m, followed by buckling upon further compression towards 0 mN/m.

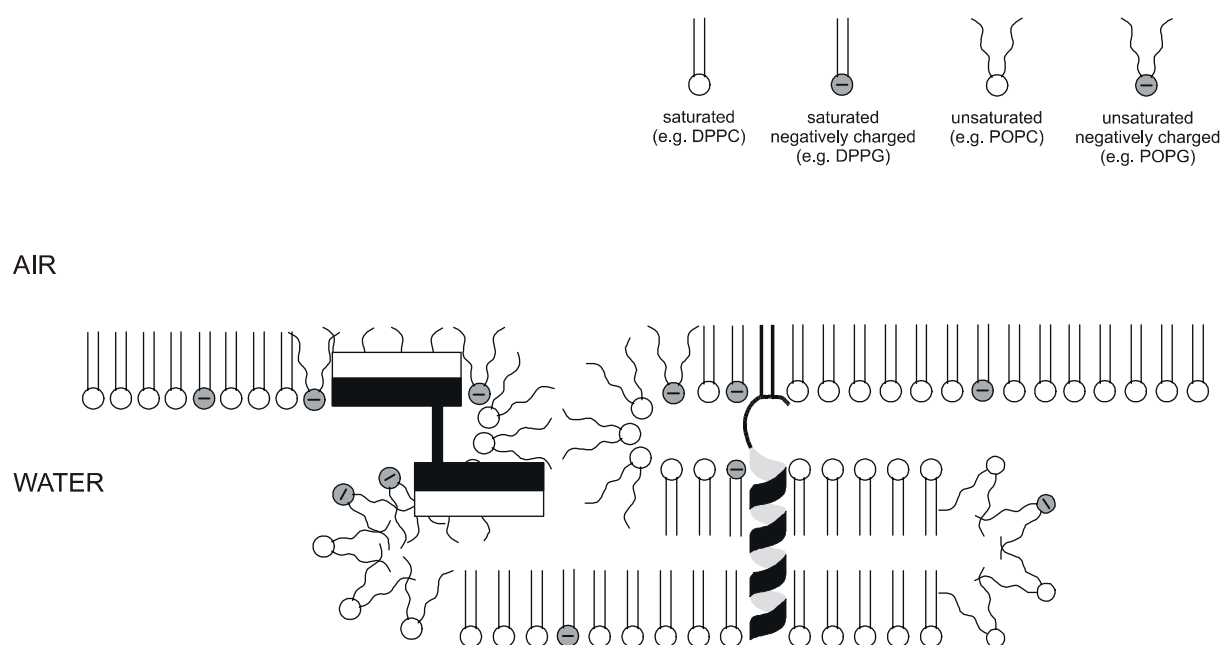


Figure 4: A model for a protrusion formed upon compression of a surfactant monolayer.

For clarity reasons, phospholipids are depicted in four variants: those with saturated acyl chains, those with unsaturated acyl chains, those which are negatively charged, and those which are zwitter-ionic. The structure of SP-B has been depicted in a very simplified form as black/white rods, indicative of its amphiphatic character and its dimeric form. The size of SP-B is not drawn to scale. SP-C is represented as an α -helix with a non-coiled N-terminal part that contains two palmitic acid residues. As our studies have indicated, in the formation and/or maintenance of protrusions SP-B preferentially interacts with unsaturated phospholipids with a negatively charged headgroup.

2.3 The distribution of surfactant during replacement therapy in an rat model of ARDS

In chapters 5 and 6 SP-B was chosen as a marker for the distribution of surfactant into lungs with ARDS-like injury. For this purpose SP-B was labeled covalently with the

Chapter 7

fluorescent tag Bodipy[®] FL CASE at specific sites (chapter 5). When SP-B was incubated in dimethylsulfoxide in the presence of triethylamine and excess of Bodipy, virtually 100 % of the SP-B molecules became labeled within 30 minutes. This is much faster than the 12 to 36 hours described for fluorescent labeling studies thus far [229-232]. Moreover, every SP-B molecule was labeled with three fluorophore molecules on average, which is higher than reported in other studies [229,231]. Due to the high degree of labeling and the stability of the Bodipy FL CASE fluorophore, samples could be stored in MeOH/water (90/10) in the dark at -20 °C for over 1 year with the preservation of fluorescence as well as maintenance of full surface activity in the captive bubble surfactometer (unpublished data). Because of the bulky character of the Bodipy molecule it could be argued that an average labeling of three fluorophore molecules per SP-B dimer might alter its structure and/or deteriorate its activity. Since the labeled protein was destined to be administered into lungs as a supplement of total hydrophobic lung surfactant extract, we considered it to be of utmost importance that SP-B activity would be (at least for a substantial part) preserved. Otherwise, administered surfactant could potentially contain material with a partially misfolded and/or inactive component, probably resulting in altered spreading properties when compared to that of surfactant preparations generally used for replacement therapy. Fortunately, however, the properties of Bodipy-labeled SP-B turned out to be almost the same as those of the native protein. First, its secondary structure, measured by circular dichroism, did not differ from that of native SP-B. Second, labeled SP-B induced vesicle mixing equally well as non-labeled SP-B. Third, its spreading velocity on a surface of buffered water in a square glass tray was the same as that of natural SP-B. Fourth, in a two-dimensional anatomical replica of a human tracheobronchial tree, multilamellar lipid vesicles containing either labeled or native SP-B spread equally well on the buffer surface and spreading was independent of trough geometry. Moreover, vesicles of bovine lung surfactant extract (BLSE) supplemented with Bodipy-labeled SP-B spread equally into all regions of the trough, lowering surface tension to a value comparable to that of both non-supplemented BLSE and the commercial surfactant Alveofact[®]. Finally, the ability of Bodipy-labeled SP-B to decrease both minimum and maximum surface tension in films of DPPC/POPG (80/20) in a captive bubble surfactometer did not differ from that of native or sham-treated SP-B. To the best of our knowledge, no labeled surfactant component has so far been studied as intensely as this Bodipy-labeled SP-B. In most studies the label is simply mixed with surfactant without knowing the component to which it becomes attached, *e.g.* [272-275].

Since Bodipy-labeled SP-B resembled native bovine SP-B both in structure and activity and since supplementation of BLSE with labeled SP-B did not impair its *in vitro* spreading properties, we felt confident to use this fluorescent SP-B analog as a marker for *in vivo* distribution of surfactant in lungs that had ARDS-like injury (chapter 6). Since it was the goal of this study to determine surfactant distribution under standardized settings, not to obtain the highest survival rate by optimizing treatment for the individual rat, surfactant administration and ventilatory settings were set equal for each rat. Lipopolysaccharide was aerosolized in seventy-one rats, resulting in lung damage that would be classified as ARDS,

according to a lung injury score used to categorize injury in human lungs [257]. Lung damage included increased levels of total protein in bronchoalveolar lavage, increased respiratory frequency, decreased compliance (a measure for lung elasticity), and impaired gas exchange. Moreover, histological evaluation of stained lung slices revealed inflammation and proteinaceous edema, the latter being confirmed by chest CT scans. LPS-exposed lungs showed a high percentage of collapsed (atelectatic) and underinflated (dystelectatic) alveolar regions (40 - 90 % of total lung area analyzed). Twenty-four hours after LPS exposure, rats were fully anesthetized and treated with surfactant: BLSE (50 mg on phospholipid base per kg body weight) supplemented with Bodipy-labeled SP-B ($\frac{1}{4}$ of the endogenous amount) was administered as a bolus into the trachea, followed by sustained inflations to open the lung and facilitate surfactant spreading. Subsequently, rats were mechanically ventilated for either 5, 15, 30 or 60 minutes, followed by lung excision. Lung slices were examined by both light- and fluorescence microscopy, revealing that surfactant distributed preferentially into aerated and underinflated alveolar areas. Remarkably, only minor amounts reached collapsed alveolar regions, indicating that these severely damaged lung areas did not readily benefit from therapeutic surfactant administration. Moreover, surfactant distribution was found to be independent of length of mechanical ventilation of up to one hour. A consequence of our findings is that during conventional ventilation at high transpulmonary pressures, healthy lung regions could become overdistracted, eventually leading to barotrauma. However, if transpulmonary pressures are kept below 30 to 35 cm of water, as was the case in our study, overdistracted of aerated lung areas will not be a problem [267]. Unfortunately, spreading of exogenous surfactant into aerated areas does not greatly improve the clinical situation, as these regions already participate in gas exchange. A second consequence of our findings is that underinflated alveolar areas will probably benefit from distribution of administered surfactant into these areas, because they will be moved out of the flat bottom part of the pressure-volume curve into the steep part. It is in the steep part that only a small increase in airway pressure (*i.e.* energy) generates a large increase in lung volume. As a result, exogenous surfactant spreading into underinflated areas can prevent alveolar collapse and protect against shear stress (*i.e.* lung damage induced by repetitive alveolar area changes beyond and below the alveolar distension during normal breathing in healthy persons). The small amounts of fluorescent surfactant found in collapsed alveolar regions indicates that atelectatic lung regions do not benefit from surfactant replacement therapy at conditions used in these experiments. Based on the results obtained in our study we, as well as other authors [263], believe that efforts should be made to open up the lung prior to surfactant administration. In our study we chose a moderate form of lung volume recruitment. The use of more aggressive lung volume recruitment maneuvers has also been recommended [263-265], although a risk of ventilator-induced lung injury exists when such methods are applied together with lung surfactant.

Many factors determine whether surfactant replacement therapy will be successful [245,207]. Most importantly, the dose given and the number of doses administered are thought to influence therapy outcome. To be on the safe side, the doses given in many clinical

Chapter 7

trials are rather high (up to 400 mg/kg) [207]. The need for such high doses is not firmly established and studies in animals [258] and in humans [243,259,208] have shown that repeated administration of a low dose of 50 mg/kg can be more beneficial than a single high dose. Furthermore, changing of body position prior to surfactant replacement therapy is 1) a way to treat gravity induced consolidation of the patient lungs caused by ARDS and prolonged ventilation in supine position and 2) has been shown to improve gas exchange by expansion of underinflated and collapsed lung areas [269]. Further possible causes for the varying outcome between several surfactant replacement therapy studies is that protein composition and surface activity among these surfactants varied. Other contributions to the differences observed could be variations in timing of surfactant application and the mode of application.

3. Conclusions and suggestions for further research

Our observation that surfactant replacement therapy in ARDS lungs under standard mechanical ventilation and without change of body position is primarily beneficial for underinflated lung areas and only to minor amounts for collapsed lung areas (chapter 6) indicates that as much alveolar area as possible should be recruited prior to surfactant instillation. Unfortunately, damage in ARDS lungs is never homogeneous, making the introduction of a standard treatment protocol hardly feasible. Although research on surfactant replacement therapy is considerable, more knowledge is needed on parameters such as dose, mode of application and mode of ventilation. For this purpose, the use of animal models of lung diseases may be sufficient, although results of such studies have to be confirmed by clinical investigations on humans. To see differences in treatment outcome that are statistically significant, multi-center clinical trials should be performed preferentially. When synthetic surfactants are to be used for treatment, in addition to DPPC they should contain high amounts of peptide as well as negatively charged unsaturated phospholipid like POPG.

The data described in chapters 2, 3 and 4 add to the knowledge on surfactant surface activity obtained in other CBS studies (*e.g.* [157,26,25,85,86,171,167,222,175, 53,221]) and in the still few AFM studies performed with surfactant [13,81,206,163]. From these and other studies it could be deduced that i) SP-B might function as the key-player in altering the composition and structure of the surfactant film during compression and expansion, thereby reaching and maintaining low surface tensions, while ii) the presence of SP-C seems to be of special importance at low lung volumes, stabilizing phospholipid films and thereby preventing collapse. The proposed role for SP-C can also be deduced from a study [86] in which films of surfactant from SP-C knockout mice (that have normal levels of SP-B) were unstable when measured in small captive bubbles. Moreover, SP-C mutations in humans are associated with lung disease and, as a result, to a shortened life expectancy [276,277]. The proposed role for SP-B is in accordance with the observation that SP-B knock-out mice (also having diminished levels of mature SP-C) die from respiratory failure immediately after birth

[47]. The role of the surfactant lipids, mainly DPPC, is to form structures that can be compressed to low surface tensions. We and others have shown that the unsaturated lipids function as film fluidizers, and are preferentially situated at locations where surfactant material is protruded out of the film. In this process, POPG seems to have a preferential interaction with SP-B.

Special interest for future research can be directed towards i) the structural determinants for the function of SP-B and SP-C, and ii) the influence of lipid headgroup and acyl chain saturation on the surfactant film. To address i), the use of peptides based on a part of the mature protein amino acid sequence will be helpful. A possible candidate is SP-B₁₋₇₈, a monomeric synthetic peptide based on human dimeric SP-B. Furthermore, synthetic peptides based on native SP-C are available for study. To address ii), the influence of negatively charged lipids like phosphatidylserine or phosphatidylinositol, both present in surfactant in minor amounts, on protrusion formation in films containing SP-B, SP-C, or both proteins can be investigated at various surface tensions. In addition to this, lipid acyl chain unsaturation should be studied. To facilitate data interpretation, it will be advisable to use simple secondary or ternary lipid mixtures. The use of a fluorescence microscope or a mass spectrometer can provide us with important additional data on the whereabouts of labeled surfactant components during various stages of film compression. In conclusion, we expect that the combination of CBS and AFM will give us powerful tools to obtain information on surfactant surface activity and surface topography.

Acknowledgment

I like to thank Margot Snel and Paul Deley for their preparation of the raw versions of figures 3 and 1+4, respectively.

References

REFERENCE LIST

1. von Neergaard, K. 1929. Neue Auffassungen über einen Grundbegriff der Atemmechanik. *Z. Gesamte Exp. Med.* 66:373-394.
2. Pattle, R.E. 1955. Properties, function and origin of the alveolar lining. *Nature* 175:1125-1126.
3. Clements, J.A. 1957. Surface tension of lung extracts. *Proc. Soc. Exp. Biol. Med.* 95:170-172.
4. Clements, J.A., E.S. Brown, and R.P. Johnson. 1958. Pulmonary surface tension and the mucus lining of the lungs: some theoretical considerations. *J. Appl. Physiol.* 12:262-268.
5. Avery, M.E. and J. Mead. 1959. Surface properties in relation to atelectasis and hyaline membrane disease. *Am. J. Dis. Child* 97:517-523.
6. Klaus, M.H., J.A. Clements, and R.J. Havel. 1961. Composition of surface-active material isolated from beef lung. *Proc. Natl. Acad. Sci. USA* 47:1858-1859.
7. Gluck, L., E.K. Motoyama, H.L. Smits, and M.V. Kulovich. 1967. The biochemical development of surface activity in mammalian lung. I. The surface-active phospholipids; the separation and distribution of surface-active lecithin in the lung of the developing rabbit fetus. *Pediatr. Res.* 1:237-246.
8. King, R.J., D.J. Klass, E.G. Gikas, and J.A. Clements. 1973. Isolation of apoproteins from canine surface active material. *Am. J. Physiol.* 224:788-795.
9. Fujiwara, T., H. Maeta, S. Chida, T. Morita, Y. Watabe, and T. Abe. 1980. Artificial surfactant therapy in hyaline-membrane disease. *Lancet* 1:55-59.
10. Walmrath, D., A. Günther, H.A. Ghofrani, R. Schermuly, T. Schneider, F. Grimminger, and W. Seeger. 1996. Bronchoscopic surfactant administration in patients with severe adult respiratory distress syndrome and sepsis. *Am. J. Respir. Crit. Care Med.* 154:57-62.
11. Gregory, T.J., K.P. Steinberg, R.G. Spragg, J.E. Gadek, T.M. Hyers, W.J. Longmore, M.A. Moxley, G.Z. Cai, R.D. Hite, R.M. Smith, L.D. Hudson, C. Crim, P. Newton, B.R. Mitchell, and A.J. Gold. 1997. Bovine surfactant therapy for patients with acute respiratory distress syndrome. *Am. J. Respir. Crit. Care Med.* 155:1309-1315.
12. Schürch, S., R. Qanbar, H. Bachofen, and F. Possmayer. 1995. The surface-associated surfactant reservoir in the alveolar lining. *Biol. Neonate* 67 (Suppl. 1):61-76.
13. Amrein, M., A. von Nahmen, and M. Sieber. 1997. A scanning force- and fluorescence light microscopy study of the structure and function of a model pulmonary surfactant. *Eur. Biophys. J.* 26:349-357.
14. Curstedt, T., H. Jörnvall, B. Robertson, T. Bergman, and P. Berggren. 1987. Two hydrophobic low-molecular-mass protein fractions of pulmonary surfactant. Characterization and biophysical activity. *Eur. J. Biochem.* 168:255-262.
15. Taneva, S.G. and K.M.W. Keough. 1994. Dynamic surface properties of pulmonary surfactant proteins SP-B and SP-C and their mixtures with dipalmitoylphosphatidylcholine. *Biochemistry* 33:14660-14670.
16. Poulain, F.R., L. Allen, M.C. Williams, R.L. Hamilton, and S. Hawgood. 1992. Effects of surfactant

References

- apolipoproteins on liposome structure: implications for tubular myelin formation. *Am. J. Physiol.* 262:L730-L739.
17. Suzuki, Y., Y. Fujita, and K. Kogishi. 1989. Reconstitution of tubular myelin from synthetic lipids and proteins associated with pig pulmonary surfactant. *Am. Rev. Respir. Dis.* 140:75-81.
 18. Horowitz, A.D., B. Moussavian, and J.A. Whitsett. 1996. Roles of SP-A, SP-B, and SP-C in modulation of lipid uptake by pulmonary epithelial cells in vitro. *Am. J. Physiol.* 270:L69-L79.
 19. Noguee, L.M., G. Garnier, H.C. Dietz, L. Singer, A.M. Murphy, D.E. deMello, and H.R. Colten. 1994. A mutation in the surfactant protein B gene responsible for fatal neonatal respiratory disease in multiple kindreds. *J. Clin. Invest.* 93:1860-1863.
 20. Weaver, T.E. and D.C. Beck. 1999. Use of knockout mice to study surfactant protein structure and function. *Biol. Neonate* 76 (Suppl. 1):15-18.
 21. Robertson, B., T. Kobayashi, M. Ganzuka, G. Grossmann, W.Z. Li, and Y. Suzuki. 1991. Experimental neonatal respiratory failure induced by a monoclonal antibody to the hydrophobic surfactant-associated protein SP-B. *Pediatr. Res.* 30:239-243.
 22. Glasser, S.W., M.S. Burhans, M. Ikegami, T.R. Korfhagen, and J.A. Whitsett. 2000. In vivo analysis of the SP-C gene. *Appl. Cardiopulm. Pathophysiol.* 9:221-221.
 23. Glasser, S.W., M. Ikegami, G. Ross, P.D. Sly, C.L. Na, T.R. Korfhagen, and J.A. Whitsett. 2001. Altered stability of pulmonary surfactant in SP-C deficient mice. *Am. J. Respir. Crit. Care Med.* 163:A328.
 24. Putz, G., J. Goerke, H.W. Taeusch, and J.A. Clements. 1994. Comparison of captive and pulsating bubble surfactometers with use of lung surfactants. *J. Appl. Physiol.* 76:1425-1431.
 25. Putz, G., J. Goerke, S. Schürch, and J.A. Clements. 1994. Evaluation of pressure-driven captive bubble surfactometer. *J. Appl. Physiol.* 76:1417-1424.
 26. Putz, G., M. Walch, M. van Eijk, and H.P. Haagsman. 1998. A spreading technique for forming film in a captive bubble. *Biophys. J.* 75:2229-2239.
 27. Crouch, E.C. 1998. Collectins and pulmonary host defense. *Am. J. Respir. Cell Mol. Biol.* 19:177-201.
 28. Haagsman, H.P. 1998. Interactions of surfactant protein A with pathogens. *Biochim. Biophys. Acta* 1408:264-277.
 29. Reid, K.B. 1998. Interactions of surfactant protein D with pathogens, allergens and phagocytes. *Biochim. Biophys. Acta* 1408:290-295.
 30. Malhotra, R., J. Haurum, S. Thiel, J.C. Jensenius, and R.B. Sim. 1993. Pollen grains bind to lung alveolar type II cells (A549) via lung surfactant protein A (SP-A). *Biosci. Rep.* 13:79-90.
 31. Wang, J.Y., U. Kishore, B.L. Lim, P. Strong, and K.B. Reid. 1996. Interaction of human lung surfactant proteins A and D with mite (*Dermatophagoides pteronyssinus*) allergens. *Clin. Exp. Immunol.* 106:367-373.
 32. Phizackerley, P.J., M.H. Town, and G.E. Newman. 1979. Hydrophobic proteins of lamellated osmiophilic bodies isolated from pig lung. *Biochem. J.* 183:731-736.

References

33. Possmayer, F. 1988. A proposed nomenclature for pulmonary surfactant-associated proteins. *Am. Rev. Respir. Dis.* 138:990-998.
34. Glasser, S.W., T.R. Korfhagen, T. Weaver, T. Pilot-Matias, J.L. Fox, and J.A. Whitsett. 1987. cDNA and deduced amino acid sequence of human pulmonary surfactant-associated proteolipid SPL(Phe). *Proc. Natl. Acad. Sci. USA* 84:4007-4011.
35. Hawgood, S., B.J. Benson, J. Schilling, D. Damm, J.A. Clements, and R.T. White. 1987. Nucleotide and amino acid sequences of pulmonary surfactant protein SP 18 and evidence for cooperation between SP 18 and SP 28-36 in surfactant lipid adsorption. *Proc. Natl. Acad. Sci. USA* 84:66-70.
36. Jacobs, K.A., D.S. Phelps, R. Steinbrink, J. Fisch, R. Kriz, L. Mitsock, J.P. Dougherty, H.W. Tausch, and J. Floros. 1987. Isolation of a cDNA clone encoding a high molecular weight precursor to a 6-kDa pulmonary surfactant-associated protein. *J. Biol. Chem.* 262:9808-9811.
37. Warr, R.G., S. Hawgood, D.I. Buckley, T.M. Crisp, J. Schilling, B.J. Benson, P.L. Ballard, J.A. Clements, and R.T. White. 1987. Low molecular weight human pulmonary surfactant protein (SP5): isolation, characterization, and cDNA and amino acid sequences. *Proc. Natl. Acad. Sci. USA* 84:7915-7919.
38. Glasser, S.W., T.R. Korfhagen, T.E. Weaver, J.C. Clark, T. Pilot-Matias, J. Meuth, J.L. Fox, and J.A. Whitsett. 1988. cDNA, deduced polypeptide structure and chromosomal assignment of human pulmonary surfactant proteolipid, SPL(pVal). *J. Biol. Chem.* 263:9-12.
39. Cruz, A., C. Casals, and J. Pérez-Gil. 1995. Conformational flexibility of pulmonary surfactant proteins SP-B and SP-C, studied in aqueous organic solvents. *Biochim. Biophys. Acta* 1255:68-76.
40. Pilot-Matias, T.J., S.E. Kister, J.L. Fox, K. Kropp, S.W. Glasser, and J.A. Whitsett. 1989. Structure and organization of the gene encoding human pulmonary surfactant proteolipid SP-B. *DNA* 8:75-86.
41. Lin, S., K.S. Phillips, M.R. Wilder, and T.E. Weaver. 1996. Structural requirements for intracellular transport of pulmonary surfactant protein B (SP-B). *Biochim. Biophys. Acta* 1312:177-185.
42. Oosterlaken-Dijksterhuis, M.A., M. van Eijk, B.L. van Buel, L.M.G. van Golde, and H.P. Haagsman. 1991. Surfactant protein composition of lamellar bodies isolated from rat lung. *Biochem. J.* 274:115-119.
43. Noguee, L.M. 1998. Genetics of the hydrophobic surfactant proteins. *Biochim. Biophys. Acta* 1408:323-333.
44. Floros, J. and P. Kala. 1998. Surfactant proteins: molecular genetics of neonatal pulmonary diseases. *Annu. Rev. Physiol.* 60:365-384.
45. Cochrane, C.G. and S.D. Revak. 1991. Pulmonary surfactant protein B (SP-B): structure-function relationships. *Science* 254:566-568.
46. Pérez-Gil, J., K. Nag, S.G. Taneva, and K.M.W. Keough. 1992. Pulmonary surfactant protein SP-C causes packing rearrangements of dipalmitoylphosphatidylcholine in spread monolayers. *Biophys. J.* 63:197-204.
47. Clark, J.C., S.E. Wert, C.J. Bachurski, M.T. Stahlman, B.R. Stripp, T.E. Weaver, and J.A. Whitsett. 1995. Targeted disruption of the surfactant protein B gene disrupts surfactant homeostasis, causing respiratory failure in newborn mice. *Proc. Natl. Acad. Sci. USA* 92:7794-7798.
48. Kishimoto, Y., M. Hiraiwa, and J.S. O'Brien. 1992. Saposins: structure, function, distribution, and molecular genetics. *J. Lipid Res.* 33:1255-1267.

References

49. Patthy,L. 1991. Homology of the precursor of pulmonary surfactant-associated protein SP-B with prosaposin and sulfated glycoprotein 1. *J. Biol. Chem.* 266:6035-6037.
50. Johansson,J., T.Curstedt, and H.Jörnvall. 1991. Surfactant protein B: disulfide bridges, structural properties, and kringle similarities. *Biochemistry* 30:6917-6921.
51. Hawgood,S., M.Derrick, and F.Poulain. 1998. Structure and properties of surfactant protein B. *Biochim. Biophys. Acta* 1408:150-160.
52. Beck,D.C., M.Ikegami, C.L.Na, S.Zaltash, J.Johansson, J.A.Whitsett, and T.E.Weaver. 2000. The role of homodimers in surfactant protein B function in vivo. *J. Biol. Chem.* 275:3365-3370.
53. Veldhuizen,E.J.A., A.J.Waring, F.J.Walther, J.J.Batenburg, L.M.G.van Golde, and H.P.Haagsman. 2000. Dimeric N-terminal segment of human surfactant protein B (dSP-B(1-25)) has enhanced surface properties compared to monomeric SP-B(1-25). *Biophys. J.* 79:377-384.
54. Olafson,R.W., U.Rink, S.Kielland, S.H.Yu, J.Chung, P.G.Harding, and F.Possmayer. 1987. Protein sequence analysis studies on the low molecular weight hydrophobic proteins associated with bovine pulmonary surfactant. *Biochem. Biophys. Res. Commun.* 148:1406-1411.
55. Yu,S.H., W.Chung, R.W.Olafson, P.G.Harding, and F.Possmayer. 1987. Characterization of the small hydrophobic proteins associated with pulmonary surfactant. *Biochim. Biophys. Acta* 921:437-448.
56. Baatz,J.E., B.Elledge, and J.A.Whitsett. 1990. Surfactant protein SP-B induces ordering at the surface of model membrane bilayers. *Biochemistry* 29:6714-6720.
57. Diemel,R.V., D.Bader, M.Walch, B.Hotter, L.M.G.van Golde, A.Amann, H.P.Haagsman, and G.Putz. 2001. Functional tests for the characterization of surfactant protein B (SP- B) and a fluorescent SP-B analog. *Arch. Biochem. Biophys.* 385:338-347.
58. Holtschmidt,H., K.Sandhoff, H.Y.Kwon, K.Harzer, T.Nakano, and K.Suzuki. 1991. Sulfatide activator protein. Alternative splicing that generates three mRNAs and a newly found mutation responsible for a clinical disease. *J. Biol. Chem.* 266:7556-7560.
59. Vaccaro,A.M., R.Salvioli, A.Barca, M.Tatti, F.Ciaffoni, B.Maras, R.Siciliano, F.Zappacosta, A.Amoresano, and P.Pucci. 1995. Structural analysis of saposin C and B. Complete localization of disulfide bridges. *J. Biol. Chem.* 270:9953-9960.
60. Curstedt,T., J.Johansson, S.J.Barros, B.Robertson, G.Nilsson, M.Westberg, and H.Jörnvall. 1988. Low-molecular-mass surfactant protein type 1. The primary structure of a hydrophobic 8-kDa polypeptide with eight half-cystine residues. *Eur. J. Biochem.* 172:521-525.
61. Andersson,M., T.Curstedt, H.Jörnvall, and J.Johansson. 1995. An amphipathic helical motif common to tumourolytic polypeptide NK-lysin and pulmonary surfactant polypeptide SP-B. *FEBS Lett.* 362:328-32
62. Hagen,F.S., F.J.Grant, J.L.Kuijper, C.A.Slaughter, C.R.Moomaw, K.Orth, P.J.O'Hara, and R.S.Munford. 1991. Expression and characterization of recombinant human acyloxyacyl hydrolase, a leukocyte enzyme that deacylates bacterial lipopolysaccharides. *Biochemistry* 30:8415-8423.
63. Staab,J.F., D.L.Ginkel, G.B.Rosenberg, and R.S.Munford. 1994. A saposin-like domain influences the intracellular localization, stability, and catalytic activity of human acyloxyacyl hydrolase. *J. Biol. Chem.* 269:23736-23742.

References

64. Stamme,C. and J.R.Wright. 1999. Surfactant protein A enhances the binding and deacylation of E. coli LPS by alveolar macrophages. *Am. J. Physiol.* 276:L540-L547.
65. Borron,P., J.C.McIntosh, T.R.Korfhagen, J.A.Whitsett, J.Taylor, and J.R.Wright. 2000. Surfactant-associated protein A inhibits LPS-induced cytokine and nitric oxide production in vivo. *Am. J. Physiol.* 278:L840-L847.
66. van Rozendaal,B.A.W.M., C.H.van de Lest, M.van Eijk, L.M.G.van Golde, W.F.Voorhout, H.P.van Helden, and H.P.Haagsman. 1999. Aerosolized endotoxin is immediately bound by pulmonary surfactant protein D in vivo. *Biochim. Biophys. Acta* 1454:261-269.
67. Kaser,M.R. and G.G.Skouteris. 1997. Inhibition of bacterial growth by synthetic SP-B1-78 peptides. *Peptides* 18:1441-1444.
68. Pena,S.V., D.A.Hanson, B.A.Carr, T.J.Goralski, and A.M.Krensky. 1997. Processing, subcellular localization, and function of 519 (granulysin), a human late T cell activation molecule with homology to small, lytic, granule proteins. *J. Immunol.* 158:2680-2688.
69. Leippe,M., E.Tannich, R.Nickel, G.van der Goot, F.Pattus, R.D.Horstmann, and H.J.Muller-Eberhard. 1992. Primary and secondary structure of the pore-forming peptide of pathogenic *Entamoeba histolytica*. *EMBO J.* 11:3501-3506.
70. Leippe,M., S.Ebel, O.L.Schoenberger, R.D.Horstmann, and H.J.Muller-Eberhard. 1991. Pore-forming peptide of pathogenic *Entamoeba histolytica*. *Proc. Natl. Acad. Sci. USA* 88:7659-7663.
71. Vaccaro,A.M., R.Salvioli, M.Tatti, and F.Ciaffoni. 1999. Saposins and their interaction with lipids. *Neurochem. Res.* 24:307-314.
72. Yu,S.H. and F.Possmayer. 1992. Effect of pulmonary surfactant protein B (SP-B) and calcium on phospholipid adsorption and squeeze-out of phosphatidylglycerol from binary phospholipid monolayers containing dipalmitoylphosphatidylcholine. *Biochim. Biophys. Acta* 1126:26-34.
73. Glasser,S.W., T.R.Korfhagen, C.M.Perme, T.J.Pilot-Matias, S.E.Kister, and J.A.Whitsett. 1988. Two SP-C genes encoding human pulmonary surfactant proteolipid. *J. Biol. Chem.* 263:10326-10331.
74. Keller,A., W.Steinhilber, K.P.Schafer, and T.Voss. 1992. The C-terminal domain of the pulmonary surfactant protein C precursor contains signals for intracellular targeting. *Am. J. Respir. Cell Mol. Biol.* 6:601-608.
75. Johansson,J., T.Szyperski, T.Curstedt, and K.Wuthrich. 1994. The NMR structure of the pulmonary surfactant-associated polypeptide SP-C in an apolar solvent contains a valyl-rich alpha-helix. *Biochemistry* 33:6015-6023.
76. Pastrana,B., A.J.Mautone, and R.Mendelsohn. 1991. Fourier transform infrared studies of secondary structure and orientation of pulmonary surfactant SP-C and its effect on the dynamic surface properties of phospholipids. *Biochemistry* 30:10058-10064.
77. Vandenbussche,G., A.Clercx, T.Curstedt, J.Johansson, H.Jörnvall, and J.M.Ruysschaert. 1992. Structure and orientation of the surfactant-associated protein C in a lipid bilayer. *Eur. J. Biochem.* 203:201-209.
78. Linder,M.E., P.Middleton, J.R.Hepler, R.Taussig, A.G.Gilman, and S.M.Mumby. 1993. Lipid modifications of G proteins: alpha subunits are palmitoylated. *Proc. Natl. Acad. Sci. USA* 90:3675-3679.

References

79. Morello, J.P. and M. Bouvier. 1996. Palmitoylation: a post-translational modification that regulates signalling from G-protein coupled receptors. *Biochem. Cell Biol.* 74:449-457.
80. Kabore, A.F., S.J. Russo, W.-J. Wang, and M.F. Beers. 2000. Palmitoylation of proSP-C is not required for its intracellular targeting and proteolytic processing. *Am. J. Respir. Crit. Care Med.* 161:A41.
81. von Nahmen, A., M. Schenk, M. Sieber, and M. Amrein. 1997. The structure of a model pulmonary surfactant as revealed by scanning force microscopy. *Biophys. J.* 72:463-469.
82. von Nahmen, A., A. Post, H.-J. Galla, and M. Sieber. 1997. The phase behavior of lipid monolayers containing pulmonary surfactant protein C studied by fluorescence light microscopy. *Eur. Biophys. J.* 26:359-369.
83. Creuwels, L.A.J.M., R.A. Demel, L.M.G. van Golde, and H.P. Haagsman. 1995. Characterization of a dimeric canine form of surfactant protein C (SP-C). *Biochim. Biophys. Acta* 1254:326-332.
84. Creuwels, L.A.J.M., E.H. Boer, R.A. Demel, L.M.G. van Golde, and H.P. Haagsman. 1995. Neutralization of the positive charges of surfactant protein C. Effects on structure and function. *J. Biol. Chem.* 270:16225-16229.
85. Qanbar, R., S. Cheng, F. Possmayer, and S. Schürch. 1996. Role of the palmitoylation of surfactant-associated protein C in surfactant film formation and stability. *Am. J. Physiol.* 271:L572-L580.
86. Glasser, S.W., M.S. Burhans, T.R. Korfhagen, C.L. Na, P.D. Sly, G.F. Ross, M. Ikegami, and J.A. Whitsett. 2001. Altered stability of pulmonary surfactant in SP-C-deficient mice. *Proc. Natl. Acad. Sci. USA* 98:6366-6371.
87. White, R.T., D. Damm, J. Miller, K. Spratt, J. Schilling, S. Hawgood, B. Benson, and B. Cordell. 1985. Isolation and characterization of the human pulmonary surfactant apoprotein gene. *Nature* 317:361-363.
88. Katyal, S.L., G. Singh, and J. Locker. 1992. Characterization of a second human pulmonary surfactant-associated protein SP-A gene. *Am. J. Respir. Cell Mol. Biol.* 6:446-452.
89. Floros, J., R. Steinbrink, K. Jacobs, D. Phelps, R. Kriz, M. Recny, L. Sultzman, S. Jones, H.W. Taeusch, and H.A. Frank. 1986. Isolation and characterization of cDNA clones for the 35-kDa pulmonary surfactant-associated protein. *J. Biol. Chem.* 261:9029-9033.
90. Benson, B., S. Hawgood, J. Schilling, J.A. Clements, D. Damm, B. Cordell, and R.T. White. 1985. Structure of canine pulmonary surfactant apoprotein: cDNA and complete amino acid sequence. *Proc. Natl. Acad. Sci. USA* 82:6379-6383.
91. Sano, K., J. Fisher, R.J. Mason, Y. Kuroki, J. Schilling, B. Benson, and D. Voelker. 1987. Isolation and sequence of a cDNA clone for the rat pulmonary surfactant-associated protein (PSP-A). *Biochem. Biophys. Res. Commun.* 144:367-374.
92. Boggaram, V., K. Qing, and C.R. Mendelson. 1988. The major apoprotein of rabbit pulmonary surfactant. Elucidation of primary sequence and cyclic AMP and developmental regulation. *J. Biol. Chem.* 263:2939-2947.
93. Korfhagen, T.R., M.D. Bruno, S.W. Glasser, P.J. Ciruolo, J.A. Whitsett, D.L. Lattier, K.A. Wikenheiser, and J.C. Clark. 1992. Murine pulmonary surfactant SP-A gene: cloning, sequence, and transcriptional activity. *Am. J. Physiol.* 263:L546-L554.

References

94. van Eijk,M., H.P.Haagsman, T.Skinner, A.Archibold, K.B.Reid, and P.R.Lawson. 2000. Porcine lung surfactant protein D: complementary DNA cloning, chromosomal localization, and tissue distribution. *J. Immunol.* 164:1442-1450.
95. Voss,T., H.Eistetter, K.P.Schafer, and J.Engel. 1988. Macromolecular organization of natural and recombinant lung surfactant protein SP 28-36. Structural homology with the complement factor C1q. *J. Mol. Biol.* 201:219-227.
96. Haagsman,H.P., R.T.White, J.Schilling, K.Lau, B.J.Benson, J.Golden, S.Hawgood, and J.A.Clements. 1989. Studies of the structure of lung surfactant protein SP-A. *Am. J. Physiol.* 257:L421-L429.
97. Haas,C., T.Voss, and J.Engel. 1991. Assembly and disulfide rearrangement of recombinant surfactant protein A in vitro. *Eur. J. Biochem.* 197:799-803.
98. Voss,T., K.Melchers, G.Scheirle, and K.P.Schafer. 1991. Structural comparison of recombinant pulmonary surfactant protein SP-A derived from two human coding sequences: implications for the chain composition of natural human SP-A. *Am. J. Respir. Cell Mol. Biol.* 4:88-94.
99. Brodsky,D.B., K.R.Leonard, and K.B.Reid. 1976. Circular-dichroism and electron-microscopy studies of human subcomponent C1q before and after limited proteolysis by pepsin. *Biochem. J.* 159:279-286.
100. Thiel,S. and K.B.Reid. 1989. Structures and functions associated with the group of mammalian lectins containing collagen-like sequences. *FEBS Lett.* 250:78-84.
101. Drickamer,K. 1988. Two distinct classes of carbohydrate-recognition domains in animal lectins. *J. Biol. Chem.* 263:9557-9560.
102. Muramoto,K. and H.Kamiya. 1990. The positions of the disulfide bonds and the glycosylation site in a lectin of the acorn barnacle *Megabalanus rosa*. *Biochim. Biophys. Acta* 1039:52-60.
103. Giga,Y., A.Ikai, and K.Takahashi. 1987. The complete amino acid sequence of echinoidin, a lectin from the coelomic fluid of the sea urchin *Anthodidaris crassispira*. Homologies with mammalian and insect lectins. *J. Biol. Chem.* 262:6197-6203.
104. Munakata,H., R.B.Nimberg, G.L.Snider, A.G.Robins, H.Van Halbeek, J.F.Vliegthart, and K.Schmid. 1982. The structure of the carbohydrate units of the 36K glycoprotein derived from the lung lavage of a patient with alveolar proteinosis by high resolution 1H-NMR spectroscopy. *Biochem. Biophys. Res. Commun.* 108:1401-1405.
105. Haagsman,H.P., R.H.Elfring, B.L.van Buel, and W.F.Voorhout. 1991. The lung lectin surfactant protein A aggregates phospholipid vesicles via a novel mechanism. *Biochem. J.* 275:273-276.
106. van Iwaarden,J.F., J.A.van Strijp, H.Visser, H.P.Haagsman, J.Verhoef, and L.M.G.van Golde. 1992. Binding of surfactant protein A (SP-A) to herpes simplex virus type 1-infected cells is mediated by the carbohydrate moiety of SP-A. *J. Biol. Chem.* 267:25039-25043.
107. Stahlman,M.T., M.E.Gray, G.F.Ross, W.M.Hull, K.Wikenheiser, S.Dingle, K.R.Zelenski-Low, and J.A.Whitsett. 1992. Human surfactant protein-A contains blood group A antigenic determinants. *Pediatr. Res.* 31:364-371.
108. Persson,A.V., K.Rust, D.Chang, M.Moxley, W.Longmore, and E.C.Crouch. 1988. CP4: a pneumocyte-derived collagenous surfactant-associated protein. Evidence for heterogeneity of collagenous surfactant

References

- proteins. *Biochemistry* 27:8576-8584.
109. Persson,A.V., D.Chang, K.Rust, M.Moxley, W.Longmore, and E.C.Crouch. 1989. Purification and biochemical characterization of CP4 (SP-D), a collagenous surfactant-associated protein. *Biochemistry* 28:6361-6367.
 110. Phelps,D.S. and H.W.Taeusch. 1985. A comparison of the major surfactant-associated proteins in different species. *Comp. Biochem. Physiol. B* 82:441-446.
 111. Crouch,E.C., K.Rust, A.Persson, W.Mariencheck, M.Moxley, and W.Longmore. 1991. Primary translation products of pulmonary surfactant protein D. *Am. J. Physiol.* 260:L247-L253.
 112. Rust,K., L.Grosso, V.Zhang, D.Chang, A.Persson, W.Longmore, G.Z.Cai, and E.C.Crouch. 1991. Human surfactant protein D: SP-D contains a C-type lectin carbohydrate recognition domain. *Arch. Biochem. Biophys.* 290:116-126.
 113. Lu,J., A.C.Willis, and K.B.Reid. 1992. Purification, characterization and cDNA cloning of human lung surfactant protein D. *Biochem. J* 284:795-802.
 114. Crouch,E.C., K.Rust, R.Veile, K.H.Donis, and L.Grosso. 1993. Genomic organization of human surfactant protein D (SP-D). SP-D is encoded on chromosome 10q22.2-23.1. *J. Biol. Chem.* 268:2976-2983.
 115. Shimizu,H., J.H.Fisher, P.Papst, B.Benson, K.Lau, R.J.Mason, and D.R.Voelker. 1992. Primary structure of rat pulmonary surfactant protein D. cDNA and deduced amino acid sequence. *J. Biol. Chem.* 267:1853-1857.
 116. Lim,B.L., J.Lu, and K.B.Reid. 1993. Structural similarity between bovine conglutinin and bovine lung surfactant protein D and demonstration of liver as a site of synthesis of conglutinin. *Immunology* 78:159-165.
 117. Holmskov,U., R.Malhotra, R.B.Sim, and J.C.Jensenius. 1994. Collectins: collagenous C-type lectins of the innate immune defense system. *Immunol. Today* 15:67-74.
 118. Strang,C.J., H.S.Slayter, P.J.Lachmann, and A.E.Davis. 1986. Ultrastructure and composition of bovine conglutinin. *Biochem. J.* 234:381-389.
 119. Hartshorn,K., D.Chang, K.Rust, M.White, J.Heuser, and E.C.Crouch. 1996. Interactions of recombinant human pulmonary surfactant protein D and SP-D multimers with influenza A. *Am. J. Physiol.* 271:L753-L762.
 120. Schürch,S., F.Possmayer, S.Cheng, and A.M.Cockshutt. 1992. Pulmonary SP-A enhances adsorption and appears to induce surface sorting of lipid extract surfactant. *Am. J. Physiol.* 263:L210-L218.
 121. Walker,S.R., M.C.Williams, and B.Benson. 1986. Immunocytochemical localization of the major surfactant apoproteins in type II cells, Clara cells, and alveolar macrophages of rat lung. *J. Histochem. Cytochem.* 34:1137-1148.
 122. Williams,M.C., S.Hawgood, and R.L.Hamilton. 1991. Changes in lipid structure produced by surfactant proteins SP-A, SP-B, and SP-C. *Am. J. Respir. Cell Mol. Biol.* 5:41-50.
 123. Voorhout,W.F., T.Veenendaal, H.P.Haagsman, A.J.Verkleij, L.M.G.van Golde, and H.J.Geuze. 1991. Surfactant protein A is localized at the corners of the pulmonary tubular myelin lattice. *J. Histochem.*

References

- Cytochem.* 39:1331-1336.
124. deMello,D.E., D.S.Phelps, G.Patel, J.Floros, and D.Lagunoff. 1989. Expression of the 35kDa and low molecular weight surfactant-associated proteins in the lungs of infants dying with respiratory distress syndrome. *Am. J. Pathol.* 134:1285-1293.
 125. Kuroki,Y., R.J.Mason, and D.R.Voelker. 1988. Alveolar type II cells express a high-affinity receptor for pulmonary surfactant protein A. *Proc. Natl. Acad. Sci. USA* 85:5566-5570.
 126. Wright,J.R., J.D.Borchelt, and S.Hawgood. 1989. Lung surfactant apoprotein SP-A (26-36 kDa) binds with high affinity to isolated alveolar type II cells. *Proc. Natl. Acad. Sci. USA* 86:5410-5414.
 127. Wright,J.R., R.E.Wager, S.Hawgood, L.Dobbs, and J.A.Clements. 1987. Surfactant apoprotein Mr = 26,000-36,000 enhances uptake of liposomes by type II cells. *J. Biol. Chem.* 262:2888-2894.
 128. Dobbs,L.G., J.R.Wright, S.Hawgood, R.Gonzalez, K.Venstrom, and J.Nellenbogen. 1987. Pulmonary surfactant and its components inhibit secretion of phosphatidylcholine from cultured rat alveolar type II cells. *Proc. Natl. Acad. Sci. USA* 84:1010-1014.
 129. Rice,W.R., G.F.Ross, F.M.Singleton, S.Dingle, and J.A.Whitsett. 1987. Surfactant-associated protein inhibits phospholipid secretion from type II cells. *J. Appl. Physiol.* 63:692-698.
 130. Korfhagen,T.R., M.D.Bruno, G.F.Ross, K.M.Huelsman, M.Ikegami, A.H.Jobe, S.E.Wert, B.R.Stripp, R.E.Morris, S.W.Glasser, C.J.Bachurski, H.S.Iwamoto, and J.A.Whitsett. 1996. Altered surfactant function and structure in SP-A gene targeted mice. *Proc. Natl. Acad. Sci. USA* 93:9594-9599.
 131. Crouch,E.C., A.Persson, D.Chang, and D.Parghi. 1991. Surfactant protein D. Increased accumulation in silica-induced pulmonary lipoproteinosis. *Am. J. Pathol.* 139:765-776.
 132. Kuroki,Y., M.Shiratori, Y.Ogasawara, A.Tsuzuki, and T.Akino. 1991. Characterization of pulmonary surfactant protein D: its copurification with lipids. *Biochim. Biophys. Acta* 1086:185-190.
 133. Ogasawara,Y., Y.Kuroki, and T.Akino. 1992. Pulmonary surfactant protein D specifically binds to phosphatidylinositol. *J. Biol. Chem.* 267:21244-21249.
 134. Persson,A.V., B.J.Gibbons, J.D.Shoemaker, M.A.Moxley, and W.J.Longmore. 1992. The major glycolipid recognized by SP-D in surfactant is phosphatidylinositol. *Biochemistry* 31:12183-12189.
 135. Kuroki,Y., S.Gasa, Y.Ogasawara, M.Shiratori, A.Makita, and T.Akino. 1992. Binding specificity of lung surfactant protein SP-D for glucosylceramide. *Biochem. Biophys. Res. Commun.* 187:963-969.
 136. Botas,C., F.Poulain, J.Akiyama, C.Brown, L.Allen, J.Goerke, J.A.Clements, E.Carlson, A.M.Gillespie, C.Epstein, and S.Hawgood. 1998. Altered surfactant homeostasis and alveolar type II cell morphology in mice lacking surfactant protein D. *Proc. Natl. Acad. Sci. USA* 95:11869-11874.
 137. Korfhagen,T.R., V.Sheftelyevich, M.S.Burhans, M.D.Bruno, G.F.Ross, S.E.Wert, M.T.Stahlman, A.H.Jobe, M.Ikegami, J.A.Whitsett, and J.H.Fisher. 1998. Surfactant protein-D regulates surfactant phospholipid homeostasis in vivo. *J. Biol. Chem.* 273:28438-28443.
 138. McCormack,F.X. 1998. Structure, processing and properties of surfactant protein A. *Biochim. Biophys. Acta* 1408:109-131.

References

139. Wang,Z., O.Gurel, J.E.Baatz, and R.H.Notter. 1996. Acylation of pulmonary surfactant protein-C is required for its optimal surface active interactions with phospholipids. *J. Biol. Chem.* 271:19104-19109.
140. van Rozendaal,B.A.W.M., L.M.G.van Golde, and H.P.Haagsman. 2001. Localization and functions of SP-A and SP-D at mucosal surfaces. *Pediatr. Pathol. Mol. Med.* 20:319-339.
141. Tino,M.J. and J.R.Wright. 1998. Interactions of surfactant protein A with epithelial cells and phagocytes. *Biochim. Biophys. Acta* 1408:241-263.
142. Daniels,C.B., S.Orgeig, and A.W.Smits. 1995. The evolution of the vertebrate pulmonary surfactant system. *Physiol. Zool.* 68:539-566.
143. Daniels,C.B., O.V.Lopatko, and S.Orgeig. 1998. Evolution of surface activity related functions of vertebrate pulmonary surfactant. *Clin. Exp. Pharmacol. Physiol.* 25:716-721.
144. Sullivan,L.C., C.B.Daniels, I.D.Phillips, S.Orgeig, and J.A.Whitsett. 1998. Conservation of surfactant protein A: evidence for a single origin for vertebrate pulmonary surfactant. *J. Mol. Evol.* 46:131-138.
145. Takahashi,H., H.Komano, N.Kawaguchi, N.Kitamura, S.Nakanishi, and S.Natori. 1985. Cloning and sequencing of cDNA of *Sarcophaga peregrina* humoral lectin induced on injury of the body wall. *J. Biol. Chem.* 260:12228-12233.
146. Travis,J. 1993. Tracing the immune system's evolutionary history. *Science* 261:164-165.
147. Drickamer,K. 1999. C-type lectin-like domains. *Curr. Opin. Struct. Biol.* 9:585-590.
148. Drickamer,K. and R.B.Dodd. 1999. C-type lectin-like domains in *Caenorhabditis elegans*: predictions from the complete genome sequence. *Glycobiology* 9:1357-1369.
149. Weis,W.I., M.E.Taylor, and K.Drickamer. 1998. The C-type lectin superfamily in the immune system. *Immunol. Rev.* 163:19-34.
150. Zeng,X., K.E.Yutzey, and J.A.Whitsett. 1998. Thyroid transcription factor-1, hepatocyte nuclear factor-3beta and surfactant protein A and B in the developing chick lung. *J. Anat.* 193:399-408.
151. Johnston,S.D., C.B.Daniels, D.Cenzato, G.C.Packard, J.A.Whitsett, and S.Orgeig. 2001. The pulmonary surfactant system matures upon pipping in the freshwater turtle *Chelydra serpentina*. *Submitted for publication.*
152. Miller,L.D., S.E.Wert, and J.A.Whitsett. 2001. Surfactant proteins and cell markers in the respiratory epithelium of the amphibian, *Ambystoma mexicanum*. *Comp. Biochem. Physiol. A* 129:141-149.
153. Grossmann,G. and B.Robertson. 1975. Lung expansion and the formation of the alveolar lining layer in the fullterm newborn rabbit. *Acta Paediatr. Scand.* 64:7-16.
154. Pérez-Gil,J. and K.M.W.Keough. 1998. Interfacial properties of surfactant proteins. *Biochim. Biophys. Acta* 1408:203-217.
155. Vandenbussche,G., A.Clercx, M.Clercx, T.Curstedt, J.Johansson, H.Jörnvall, and J.M.Ruyschaert. 1992. Secondary structure and orientation of the surfactant protein SP-B in a lipid environment. A Fourier transform infrared spectroscopy study. *Biochemistry* 31:9169-9176.

References

156. Longo, M.L., A.M. Bisagno, J.A. Zasadzinski, R. Bruni, and A.J. Waring. 1993. A function of lung surfactant protein SP-B. *Science* 261:453-456.
157. Putz, G., M. Walch, M. van Eijk, and H.P. Haagsman. 1999. Hydrophobic lung surfactant proteins B and C remain associated with surface film during dynamic cyclic area changes. *Biochim. Biophys. Acta* 1453:126-134.
158. Oosterlaken-Dijksterhuis, M.A., H.P. Haagsman, L.M.G. van Golde, and R.A. Demel. 1991. Characterization of lipid insertion into monomolecular layers mediated by lung surfactant proteins SP-B and SP-C. *Biochemistry* 30:10965-10971.
159. van Eijk, M., C.G.M. de Haas, and H.P. Haagsman. 1995. Quantitative analysis of pulmonary surfactant proteins B and C. *Anal. Biochem.* 232:231-237.
160. Pastrana-Rios, B., C.R. Flach, J.W. Brauner, A.J. Mautone, and R. Mendelsohn. 1994. A direct test of the "squeeze-out" hypothesis of lung surfactant function. External reflection FT-IR at the air/water interface. *Biochemistry* 33:5121-5127.
161. Taneva, S.G. and K.M.W. Keough. 1994. Pulmonary surfactant proteins SP-B and SP-C in spread monolayers at the air-water interface: I. Monolayers of pulmonary surfactant protein SP-B and phospholipids. *Biophys. J.* 66:1137-1148.
162. Taneva, S.G. and K.M.W. Keough. 1994. Pulmonary surfactant proteins SP-B and SP-C in spread monolayers at the air-water interface: II. Monolayers of pulmonary surfactant protein SP-C and phospholipids. *Biophys. J.* 66:1149-1157.
163. Krol, S., M. Ross, M. Sieber, S. Kunneke, H.-J. Galla, and A. Janshoff. 2000. Formation of three-dimensional protein-lipid aggregates in monolayer films induced by surfactant protein B. *Biophys. J.* 79:904-918.
164. Kramer, A., A. Wintergalen, M. Sieber, H.-J. Galla, M. Amrein, and R. Guckenberger. 2000. Distribution of the surfactant-associated protein C within a lung surfactant model film investigated by near-field optical microscopy. *Biophys. J.* 78:458-465.
165. Taneva, S.G. and K.M.W. Keough. 1994. Pulmonary surfactant proteins SP-B and SP-C in spread monolayers at the air-water interface: III. Proteins SP-B plus SP-C with phospholipids in spread monolayers. *Biophys. J.* 66:1158-1166.
166. Yu, S.H. and F. Possmayer. 1990. Role of bovine pulmonary surfactant-associated proteins in the surface-active property of phospholipid mixtures. *Biochim. Biophys. Acta* 1046:233-241.
167. Nag, K., J.G. Munro, K. Inchley, S. Schürch, N.O. Petersen, and F. Possmayer. 1999. SP-B refining of pulmonary surfactant phospholipid films. *Am. J. Physiol.* 277:L1179-L1189.
168. Tokieda, K., J.A. Whitsett, J.C. Clark, T.E. Weaver, K. Ikeda, K.B. McConnell, A.H. Jobe, M. Ikegami, and H.S. Iwamoto. 1997. Pulmonary dysfunction in neonatal SP-B-deficient mice. *Am. J. Physiol.* 273:L875-L882.
169. Bangham, A.D., C.J. Morley, and M.C. Phillips. 1979. The physical properties of an effective lung surfactant. *Biochim. Biophys. Acta* 573:552-556.
170. Clements, J.A. 1977. Functions of the alveolar lining. *Am. Rev. Respir. Dis.* 115:67-71.

References

171. Crane, J.M. and S.B.Hall. 2001. Rapid compression transforms interfacial monolayers of pulmonary surfactant. *Biophys. J.* 80:1863-1872.
172. Lipp, M.M., K.Y.C.Lee, D.Y.Takamoto, J.A.Zasadinski, and A.J.Waring. 1998. Coexistence of buckled and flat monolayers. *Phys. Rev. Lett.* 81:1650-1653.
173. Pérez-Gil, J., C.Casals, and D.Marsh. 1995. Interactions of hydrophobic lung surfactant proteins SP-B and SP-C with dipalmitoylphosphatidylcholine and dipalmitoylphosphatidylglycerol bilayers studied by electron spin resonance spectroscopy. *Biochemistry* 34:3964-3971.
174. Oosterlaken-Dijksterhuis, M.A., H.P.Haagsman, L.M.G.van Golde, and R.A.Demel. 1991. Interaction of lipid vesicles with monomolecular layers containing lung surfactant proteins SP-B or SP-C. *Biochemistry* 30:8276-8281.
175. Veldhuizen, E.J.A., J.J.Batenburg, L.M.G.van Golde, and H.P.Haagsman. 2000. The role of surfactant proteins in DPPC enrichment of surface films. *Biophys. J.* 79:3164-3171.
176. Veldhuizen, R.A., K.Nag, S.Orgeig, and F.Possmayer. 1998. The role of lipids in pulmonary surfactant. *Biochim. Biophys. Acta* 1408:90-108.
177. Orgeig, S. and C.B.Daniels. 2001. The roles of cholesterol in pulmonary surfactant: insights from comparative and evolutionary studies. *Comp. Biochem. Physiol. A* 129:75-89.
178. Suzuki, Y. 1982. Effect of protein, cholesterol, and phosphatidylglycerol on the surface activity of the lipid-protein complex reconstituted from pig pulmonary surfactant. *J. Lipid Res.* 23:62-69.
179. Taneva, S.G. and K.M.W.Keough. 1997. Cholesterol modifies the properties of surface films of dipalmitoylphosphatidylcholine plus pulmonary surfactant-associated protein B or C spread or adsorbed at the air-water interface. *Biochemistry* 36:912-922.
180. Yu, S.H. and F.Possmayer. 1994. Effect of pulmonary surfactant protein A (SP-A) and calcium on the adsorption of cholesterol and film stability. *Biochim. Biophys. Acta* 1211:350-358.
181. Notter, R.H., S.A.Tabak, and R.D.Mavis. 1980. Surface properties of binary mixtures of some pulmonary surfactant components. *J. Lipid Res.* 21:10-22.
182. Böhlen, P., S.Stein, W.Dairman, and S.Udenfriend. 1973. Fluorometric assay of proteins in the nanogram range. *Arch. Biochem. Biophys.* 155:213-220.
183. Rouser, G., S.Fleischer, and A.Yamamoto. 1970. Two dimensional thin layer chromatographic separation of polar lipids and determination of phospholipids by phosphorus analysis of spots. *Lipids* 5:494-496.
184. Allain, C.C., L.S.Poon, C.S.Chan, W.Richmond, and P.C.Fu. 1974. Enzymatic determination of total serum cholesterol. *Clin. Chem.* 20:470-475.
185. Veldhuizen, E.J.A., R.V.Diemel, G.Putz, L.M.G.van Golde, J.J.Batenburg, and H.P.Haagsman. 2001. Effect of the hydrophobic surfactant proteins on the surface activity of spread films in the captive bubble surfactometer. *Chem. Phys. Lipids* 110:47-55.
186. Holm, B.A., Z.Wang, E.A.Egan, and R.H.Notter. 1996. Content of dipalmitoyl phosphatidylcholine in lung surfactant: ramifications for surface activity. *Pediatr. Res.* 39:805-811.

References

187. Goerke, J. and J.A. Clements. 1986. Alveolar surface tension and lung surfactant. *In Handbook of Physiology - The Respiratory System*. P.T. Macklem and J. Mead, editors. American Physiological Society, Bethesda, MD. 247-61.
188. Sheng, S., D.M. Czajkowsky, and Z. Shao. 1999. AFM tips: how sharp are they? *J. Microsc.* 196:1-5.
189. Zasadzinski, J.A., C.A. Helm, M.L. Longo, A.L. Weisenhorn, S.A. Gould, and P.K. Hansma. 1991. Atomic force microscopy of hydrated phosphatidylethanolamine bilayers. *Biophys. J.* 59:755-760.
190. Presti, F.T. 1985. The role of cholesterol in regulating membrane fluidity. *In Membrane fluidity in biology*. R. Aloia and J.M. Boggs, editors. Academic Press, New York. 97-146.
191. McElhaney, R.N. 1982. The use of differential scanning calorimetry and differential thermal analysis in studies of model and biological membranes. *Chem. Phys. Lipids* 30:229-259.
192. Shah, D.O. and J.H. Schulman. 1967. Influence of calcium, cholesterol, and unsaturation on lecithin monolayers. *J. Lipid Res.* 8:215-226.
193. Guyer, W. and K. Bloch. 1983. Phosphatidylcholine and cholesterol interactions in model membranes. *Chem. Phys. Lipids* 33:313-322.
194. Daniels, C.B., H.A. Barr, J.H. Power, and T.E. Nicholas. 1990. Body temperature alters the lipid composition of pulmonary surfactant in the lizard *Ctenophorus nuchalis*. *Exp. Lung Res.* 16:435-449.
195. Yu, S.H. and F. Possmayer. 1998. Interaction of pulmonary surfactant protein A with dipalmitoylphosphatidylcholine and cholesterol at the air/water interface. *J. Lipid Res.* 39:555-568.
196. Johansson, J., T. Szyperski, and K. Wuthrich. 1995. Pulmonary surfactant-associated polypeptide SP-C in lipid micelles: CD studies of intact SP-C and NMR secondary structure determination of depalmitoyl-SP-C(1-17). *FEBS Lett.* 362:261-265.
197. Johansson, J. 1998. Structure and properties of surfactant protein C. *Biochim. Biophys. Acta* 1408:161-172.
198. Wang, Z., S.B. Hall, and R.H. Notter. 1995. Dynamic surface activity of films of lung surfactant phospholipids, hydrophobic proteins, and neutral lipids. *J. Lipid Res.* 36:1283-1293.
199. Galla, H.-J., N. Bourdos, A. von Nahmen, M. Amrein, and M. Sieber. 1998. The role of pulmonary surfactant protein C during the breathing cycle. *Thin Solid Films* 327:632-635.
200. Leufgen, K.M., H. Rulle, A. Benninghoven, M. Sieber, and H.-J. Galla. 1996. Imaging time-of-flight secondary-ion-mass spectrometry (TOF-SIMS) allows to visualize and analyze coexisting phases in Langmuir-Blodgett films. *Langmuir* 12:1708-1711.
201. Demel, R.A. and B. de Kruijff. 1976. The function of sterols in membranes. *Biochim. Biophys. Acta* 457:109-132.
202. Shiffer, K., S. Hawgood, H.P. Haagsman, B. Benson, J.A. Clements, and J. Goerke. 1993. Lung surfactant proteins, SP-B and SP-C, alter the thermodynamic properties of phospholipid membranes: a differential calorimetry study. *Biochemistry* 32:590-597.
203. Simatos, G.A., K.B. Forward, M.R. Morrow, and K.M.W. Keough. 1990. Interaction between perdeuterated dimyristoylphosphatidylcholine and low molecular weight pulmonary surfactant protein SP-C. *Biochemistry*

References

- 29:5807-5814.
204. Lewis, B.A. and D.M.Engelman. 1983. Lipid bilayer thickness varies linearly with acyl chain length in fluid phosphatidylcholine vesicles. *J. Mol. Biol.* 166:211-217.
205. Marsh, D. 1990. Handbook of lipid bilayers. CRC, Boca Raton, FL, USA.
206. Takamoto, D.Y., M.M.Lipp, A. von Nahmen, K.Y.Lee, A.J.Waring, and J.A.Zasadzinski. 2001. Interaction of lung surfactant proteins with anionic phospholipids. *Biophys. J.* 81:153-169.
207. Robertson, B. and H.L.Halliday. 1998. Principles of surfactant replacement. *Biochim. Biophys. Acta* 1408:346-361.
208. Seeger, W., A.Günther, and D.Walmrath. 2000. Alterations of pulmonary surfactant in ARDS - Effects of a transbronchial surfactant application. *Appl. Cardiopulm. Pathophysiol.* 9:295-297.
209. Tredano, M., R.M.van Elburg, A.G.Kaspers, L.J.Zimmermann, C.Houdayer, P.Aymard, W.M.Hull, J.A.Whitsett, J.Elion, M.Griese, and M.Bahuau. 1999. Compound SFTPB 1549C => GAA (121ins2) and 457delC heterozygosity in severe congenital lung disease and surfactant protein B (SP-B) deficiency. *Hum. Mutat.* 14:502-509.
210. Haagsman, H.P. and R.V.Diemel. 2001. Surfactant-associated proteins: functions and structural variation. *Comp. Biochem. Physiol. A* 129:91-108.
211. Gordon, L.M., K.Y.Lee, M.M.Lipp, J.A.Zasadzinski, F.J.Walther, M.A.Sherman, and A.J.Waring. 2000. Conformational mapping of the N-terminal segment of surfactant protein B in lipid using ¹³C-enhanced Fourier transform infrared spectroscopy. *J. Pept. Res.* 55:330-347.
212. Gordon, L.M., S.Horvath, M.L.Longo, J.A.Zasadzinski, H.W.Taeusch, K.Faull, C.Leung, and A.J.Waring. 1996. Conformation and molecular topography of the N-terminal segment of surfactant protein B in structure-promoting environments. *Protein Sci.* 5:1662-1675.
213. Gupta, M., J.M.Hernandez-Juviel, A.J.Waring, R.Bruni, and F.J.Walther. 2000. Dimeric versus monomeric SP-B1-25 peptide and lung function in preterm rabbits. *Am. J. Respir. Crit. Care Med.* 161:A656.
214. Walther, F.J., J.M.Hernandez-Juviel, M.Gupta, R.Bruni, and A.J.Waring. 2000. The effect of synthetic surfactants with dimeric and monomeric SP-B1-25 peptide on lung function in lavaged rats. *Am. J. Respir. Crit. Care Med.* 161:A656.
215. Waring, A.J., H.W.Taeusch, R.Bruni, J.D.Amirkhanian, B.R.Fan, R.Stevens, and J.Young. 1989. Synthetic amphipathic sequences of surfactant protein-B mimic several physicochemical and in vivo properties of native pulmonary surfactant proteins. *Pept. Res.* 2:308-313.
216. Gupta, M., J.M.Hernandez-Juviel, A.J.Waring, R.Bruni, and F.J.Walther. 2000. Comparison of functional efficacy of surfactant protein B analogues in lavaged rats. *Eur. Respir. J.* 16:1129-1133.
217. Binnig, G., C.F.Quate, and C.Gerber. 1986. Atomic force microscope. *Phys. Rev. Lett.* 56:930-933.
218. Oosterlaken-Dijksterhuis, M.A., M.van Eijk, L.M.G.van Golde, and H.P.Haagsman. 1992. Lipid mixing is mediated by the hydrophobic surfactant protein SP-B but not by SP-C. *Biochim. Biophys. Acta* 1110:45-50.
219. Creuwels, L.A.J.M., L.M.G.van Golde, and H.P.Haagsman. 1996. Surfactant protein B: effects on lipid

References

- domain formation and intermembrane lipid flow. *Biochim. Biophys. Acta* 1285:1-8.
220. Johansson, J. and T. Curstedt. 1997. Molecular structures and interactions of pulmonary surfactant components. *Eur. J. Biochem.* 244:675-693.
221. Schürch, S., F.H. Green, and H. Bachofen. 1998. Formation and structure of surface films: captive bubble surfactometry. *Biochim. Biophys. Acta* 1408:180-202.
222. Rodriguez-Capote, K., K. Nag, S. Schürch, and F. Possmayer. 2001. Surfactant protein interactions with neutral and acidic phospholipid films. *Am. J. Physiol.* 281:L231-L242.
223. Creuwels, L.A.J.M., L.M.G. van Golde, and H.P. Haagsman. 1997. The pulmonary surfactant system: biochemical and clinical aspects. *Lung* 175:1-39.
224. Goerke, J. 1998. Pulmonary surfactant: functions and molecular composition. *Biochim. Biophys. Acta* 1408:79-89.
225. Kobayashi, T., K. Nitta, R. Takahashi, K. Kurashima, B. Robertson, and Y. Suzuki. 1991. Activity of pulmonary surfactant after blocking the associated proteins SP-A and SP-B. *J. Appl. Physiol.* 71:530-536.
226. Veldhuizen, R.A., L.A. McCaig, T. Akino, and J.F. Lewis. 1995. Pulmonary surfactant subfractions in patients with the acute respiratory distress syndrome. *Am. J. Respir. Crit. Care Med.* 152:1867-1871.
227. Gregory, T.J., W.J. Longmore, M.A. Moxley, J.A. Whitsett, C.R. Reed, A.A. Fowler, L.D. Hudson, R.J. Maunder, C. Crim, and T.M. Hyers. 1991. Surfactant chemical composition and biophysical activity in acute respiratory distress syndrome. *J. Clin. Invest.* 88:1976-1981.
228. Hallman, M., R. Spragg, J.H. Harrell, K.M. Moser, and L. Gluck. 1982. Evidence of lung surfactant abnormality in respiratory failure. Study of bronchoalveolar lavage phospholipids, surface activity, phospholipase activity, and plasma myoinositol. *J. Clin. Invest.* 70:673-683.
229. Horowitz, A.D. 1995. Exclusion of SP-C, but not SP-B, by gel phase palmitoyl lipids. *Chem. Phys. Lipids* 76:27-39.
230. Nag, K., S.G. Taneva, J. Pérez-Gil, A. Cruz, and K.M.W. Keough. 1997. Combinations of fluorescently labeled pulmonary surfactant proteins SP-B and SP-C in phospholipid films. *Biophys. J.* 72:2638-2650.
231. Chang, R., S. Nir, and F.R. Poulain. 1998. Analysis of binding and membrane destabilization of phospholipid membranes by surfactant apoprotein B. *Biochim. Biophys. Acta* 1371:254-264.
232. Breslin, J.S. and T.E. Weaver. 1992. Binding, uptake, and localization of surfactant protein B in isolated rat alveolar type II cells. *Am. J. Physiol.* 262:L699-L707.
233. Taneva, S.G., J. Stewart, L. Taylor, and K.M.W. Keough. 1998. Method of purification affects some interfacial properties of pulmonary surfactant proteins B and C and their mixtures with dipalmitoylphosphatidylcholine. *Biochim. Biophys. Acta* 1370:138-150.
234. Haagsman, H.P., M. van Eijk, M. Walch, and G. Putz. 1997. Protein composition and surface activity of commercial surfactant preparations. *Am. J. Respir. Crit. Care Med.* 155:A213-A213.
235. Bernhard, W., J. Mottaghian, A. Gebert, G.A. Rau, H. von der Hardt, and C.F. Poets. 2000. Commercial versus native surfactants. Surface activity, molecular components, and the effect of calcium. *Am. J. Respir. Crit.*

References

- Care Med.* 162:1524-1533.
236. Pérez-Gil,J., A.Cruz, and C.Casals. 1993. Solubility of hydrophobic surfactant proteins in organic solvent/water mixtures. Structural studies on SP-B and SP-C in aqueous organic solvents and lipids. *Biochim. Biophys. Acta* 1168:261-270.
 237. Johansson,J., M.Gustafsson, M.Palmblad, S.Zaltash, B.Robertson, and T.Curstedt. 1998. Synthetic surfactant protein analogues. *Biol. Neonate* 74 (Suppl. 1):9-14.
 238. Morrow,M.R., J.Pérez-Gil, G.Simatos, C.Boland, J.Stewart, D.Absolom, V.Sarin, and K.M.W.Keough. 1993. Pulmonary surfactant-associated protein SP-B has little effect on acyl chains in dipalmitoylphosphatidylcholine dispersions. *Biochemistry* 32:4397-4402.
 239. Cruz,A., L.A.Worthman, A.G.Serrano, C.Casals, K.M.W.Keough, and J.Pérez-Gil. 2000. Microstructure and dynamic surface properties of surfactant protein SP-B/dipalmitoylphosphatidylcholine interfacial films spread from lipid-protein bilayers. *Eur. Biophys. J.* 29:204-213.
 240. Jobe,A.H. 1993. Pulmonary surfactant therapy. *N. Engl. J. Med.* 328:861-868.
 241. Kollef,M.H. and D.P.Schuster. 1995. The acute respiratory distress syndrome. *N. Engl. J. Med.* 332:27-37.
 242. Weg,J.G., R.A.Balk, R.S.Tharratt, S.G.Jenkinson, J.B.Shah, D.Zaccardelli, J.Horton, and E.N.Pattishall. 1994. Safety and potential efficacy of an aerosolized surfactant in human sepsis-induced adult respiratory distress syndrome. *JAMA* 272:1433-1438.
 243. Spragg,R.G., N.Gilliard, P.Richman, R.M.Smith, R.D.Hite, D.Pappert, B.Robertson, T.Curstedt, and D.Strayer. 1994. Acute effects of a single dose of porcine surfactant on patients with the adult respiratory distress syndrome. *Chest* 105:195-202.
 244. Anzueto,A., R.P.Baughman, K.K.Guntupalli, J.G.Weg, H.P.Wiedemann, A.A.Raventos, F.Lemaire, W.Long, D.S.Zaccardelli, and E.N.Pattishall. 1996. Aerosolized surfactant in adults with sepsis-induced acute respiratory distress syndrome. Exosurf Acute Respiratory Distress Syndrome Sepsis Study Group. *N. Engl. J. Med.* 334:1417-1421.
 245. Lewis,J.F. and R.A.Veldhuizen. 1995. Factors influencing efficacy of exogenous surfactant in acute lung injury. *Biol. Neonate* 67 (Suppl. 1):48-60.
 246. Lewis,J.F. and L.McCaig. 1993. Aerosolized versus instilled exogenous surfactant in a nonuniform pattern of lung injury. *Am. Rev. Respir. Dis.* 148:1187-1193.
 247. van der Bleek,J., F.B.Plotz, F.M.van Overbeek, A.Heikamp, H.Beekhuis, R.H.Wildevuur, A.Okken, and S.Bambang Oetomo. 1993. Distribution of exogenous surfactant in rabbits with severe respiratory failure: the effect of volume. *Pediatr. Res.* 34:154-158.
 248. Segerer,H., W.van Gelder, F.W.Angenent, L.J.van Woerkens, T.Curstedt, M.Obladen, and B.Lachmann. 1993. Pulmonary distribution and efficacy of exogenous surfactant in lung-lavaged rabbits are influenced by the instillation technique. *Pediatr. Res.* 34:490-494.
 249. Bambang Oetomo,S., L.de Ley, T.Curstedt, J.G.ter Haar, C.Schoots, C.R.Wildevuur, and A.Okken. 1991. Distribution of endotracheally instilled surfactant protein SP-C in lung-lavaged rabbits. *Pediatr. Res.* 29:178-181.

References

250. Segerer, H., A. Scheid, M. H. Wagner, M. Lekka, and M. Obladen. 1996. Rapid tracheal infusion of surfactant versus bolus instillation in rabbits: effects on oxygenation, blood pressure and surfactant distribution. *Biol. Neonate* 69:119-127.
251. van Helden, H.P., W.C. Kuijpers, D. Steenvoorden, C. Go, P.L. Bruijnzeel, M. van Eijk, and H.P. Haagsman. 1997. Intratracheal aerosolization of endotoxin (LPS) in the rat: a comprehensive animal model to study adult (acute) respiratory distress syndrome. *Exp. Lung Res.* 23:297-316.
252. Touchstone, J.C., J.C. Chen, and K.M. Beaver. 1980. Improved separation of phospholipids in thin layer chromatography. *Lipids* 15:61-62.
253. Bartlett, G.R. 1959. Phosphorus assay in column chromatography. *J. Biol. Chem.* 234:466-468.
254. Holter, J.F., J.E. Weiland, E.R. Pacht, J.E. Gadek, and W.B. Davis. 1986. Protein permeability in the adult respiratory distress syndrome. Loss of size selectivity of the alveolar epithelium. *J. Clin. Invest.* 78:1513-1522.
255. Martin, T.R., G.D. Rubenfeld, J.T. Ruzinski, R.B. Goodman, K.P. Steinberg, D.J. Leturcq, A.M. Moriarty, G. Raghu, R.P. Baughman, and L.D. Hudson. 1997. Relationship between soluble CD14, lipopolysaccharide binding protein, and the alveolar inflammatory response in patients with acute respiratory distress syndrome. *Am. J. Respir. Crit. Care Med.* 155:937-944.
256. Siler, T.M., J.E. Swierkosz, T.M. Hyers, A.A. Fowler, and R.O. Webster. 1989. Immunoreactive interleukin-1 in bronchoalveolar lavage fluid of high-risk patients and patients with the adult respiratory distress syndrome. *Exp. Lung Res.* 15:881-894.
257. Murray, J.F., M.A. Matthay, J.M. Luce, and M.R. Flick. 1988. An expanded definition of the adult respiratory distress syndrome. *Am. Rev. Respir. Dis.* 138:720-723.
258. van Helden, H.P., W.C. Kuijpers, P.E. Langerwerf, R.C. Langen, H.P. Haagsman, and P.L. Bruijnzeel. 1998. Efficacy of Curosurf in a rat model of acute respiratory distress syndrome. *Eur. Respir. J.* 12:533-539.
259. Spragg, R.G., J.F. Lewis, W. Wurst, and F.E. Rathgeb. 2000. First clinical and early clinical experience with a recombinant SP-C based surfactant. *Appl. Cardiopulm. Pathophysiol.* 9:301-303.
260. Ueda, T., M. Ikegami, M. Henry, and A.H. Jobe. 1995. Clearance of surfactant protein B from rabbit lungs. *Am. J. Physiol.* 268:L636-L641.
261. Ikegami, M., T.R. Korfhagen, M.D. Bruno, J.A. Whitsett, and A.H. Jobe. 1997. Surfactant metabolism in surfactant protein A-deficient mice. *Am. J. Physiol.* 272:L479-L485.
262. Baum, M., G. Putz, N. Mutz, C. Putensen, G. Klima, and H. Benzer. 1989. Influence of high frequency ventilation at different end-expiratory lung volumes on the development of lung damage during lung lavage in rabbits. *Br. J. Anaesth.* 63:65S-70S.
263. Lachmann, B. 1992. Open up the lung and keep the lung open. *Intensive Care Med.* 18:319-321.
264. Hartog, A., G.F. Vazquez de Anda, D. Gommers, U. Kaisers, and B. Lachmann. 2000. At surfactant deficiency, application of "the open lung concept" prevents protein leakage and attenuates changes in lung mechanics. *Crit. Care Med.* 28:1450-1454.
265. Amato, M.B., C.S. Barbas, D.M. Medeiros, R.B. Magaldi, G.P. Schettino, G. Lorenzi-Filho, R.A. Kairalla,

References

- D.Deheinzelin, C.Munoz, R.Oliveira, T.Y.Takagaki, and C.R.Carvalho. 1998. Effect of a protective-ventilation strategy on mortality in the acute respiratory distress syndrome. *N. Engl. J. Med.* 338:347-354.
266. Dos Santos,C.C. and A.S.Slutsky. 2000. Invited review: mechanisms of ventilator-induced lung injury: a perspective. *J. Appl. Physiol.* 89:1645-1655.
267. Tobin,M.J. 2001. Advances in mechanical ventilation. *N. Engl. J. Med.* 344:1986-1996.
268. Kresch,M.J. and J.M.Clive. 1998. Meta-analyses of surfactant replacement therapy of infants with birth weights less than 2000 grams. *J. Perinatol.* 18:276-283.
269. Putz,G., C.Hörmann, W.Koller, and G.Schön. 1996. Surfactant replacement therapy in acute respiratory distress syndrome from viral pneumonia. *Intensive Care Med.* 22:588-590.
270. Lopatko,O.V., S.Orgeig, D.Palmer, S.Schürch, and C.B.Daniels. 1999. Alterations in pulmonary surfactant after rapid arousal from torpor in the marsupial *Sminthopsis crassicaudata*. *J. Appl. Physiol.* 86:1959-1970.
271. Ding,J., D.Y.Takamoto, A.von Nahmen, M.M.Lipp, K.Y.Lee, A.J.Waring, and J.A.Zasadzinski. 2001. Effects of lung surfactant proteins, sp-b and sp-c, and palmitic acid on monolayer stability. *Biophys. J.* 80:2262-2272.
272. Gilliard,N., D.Pappert, T.A.Merritt, G.Heldt, and R.G.Spragg. 1991. Radiolabeling of the hydrophobic components of lung surfactant with 3-(trifluoromethyl)-3-(m-[125I]iodophenyl)diazirine. *Anal. Biochem.* 193:310-315.
273. Bambang Oetomo,S., J.Lewis, M.Ikegami, and A.H.Jobe. 1990. Surfactant treatments alter endogenous surfactant metabolism in rabbit lungs. *J. Appl. Physiol.* 68:1590-1596.
274. Gilliard,N., P.M.Richman, T.A.Merritt, and R.G.Spragg. 1990. Effect of volume and dose on the pulmonary distribution of exogenous surfactant administered to normal rabbits or to rabbits with oleic acid lung injury. *Am. Rev. Respir. Dis.* 141:743-747.
275. Davis,J.M., G.A.Russ, L.Metlay, B.Dickerson, and B.S.Greenspan. 1992. Short-term distribution kinetics of intratracheally administered exogenous lung surfactant. *Pediatr. Res.* 31:445-450.
276. Amin,R.S., S.E.Wert, R.P.Baughman, J.F.Tomashefski, Jr., L.M.Nogee, A.S.Brody, W.M.Hull, and J.A.Whitsett. 2001. Surfactant protein deficiency in familial interstitial lung disease. *J. Pediatr.* 139:85-92.
277. Nogee,L.M., A.E.Dunbar, III, S.E.Wert, F.Askin, A.Hamvas, and J.A.Whitsett. 2001. A mutation in the surfactant protein C gene associated with familial interstitial lung disease. *N. Engl. J. Med.* 344:573-579.
278. Bourbon,J.R. and B.Chailley-Heu. 2001. Surfactant proteins in the digestive tract, mesentery, and other organs: evolutionary significance. *Comp. Biochem. Physiol. A* 129:151-163.
279. Bernhard,W., A.Gebert, G.Vieten, G.A.Rau, J.M.Hohlfeld, A.D.Postle, J.Freihorst. 2001. Pulmonary surfactant in birds: coping with surface tension in a tubular lung. *Am. J. Physiol.* 281:R327-R337.

Abbreviations

LIST OF ABBREVIATIONS

AFM	atomic force microscopy
ARDS	acute respiratory distress syndrome
BAL	bronchoalveolar lavage
BLSE	bovine lung surfactant extract
Bodipy FL CASE	<i>N</i> -(4,4-difluoro-5,7-dimethyl-4-bora-3a,4a-diaza- <i>s</i> -indacene-3-propionyl) cysteic acid succinimidyl ester
Bodipy-PC	2-(4,4-difluoro-5,7-dimethyl-4-bora-3a,4a-diaza- <i>s</i> -indacene-3-dodecanoyl)-1-hexadecanoyl- <i>sn</i> -glycero-3-phosphocholine
BSA	bovine serum albumin
CBS	captive bubble surfactometry
CD	circular dichroism
CHCl ₃	chloroform
CT	computed tomography
DMSO	dimethylsulfoxide
DPPC	1,2-dipalmitoyl- <i>sn</i> -glycero-3-phosphocholine
DPPG	1,2-dipalmitoyl- <i>sn</i> -glycero-3-(phospho- <i>rac</i> -(1-glycerol))
DSC	differential scanning calorimetry
EDTA	ethylenediamine tetraacetate
ESI-MS	electrospray ionization mass spectrometry
HEPES	<i>N</i> -(2-hydroxyethyl)piperazine- <i>N'</i> -2-ethanesulfonic acid
HPLC	high performance liquid chromatography
LPS	lipopolysaccharide
MeOH	methanol
MLV	multilamellar vesicles
PBS	pulsating bubble surfactometry
PL	phospholipids
PMN	polymorphonuclear neutrophil
POPC	1-palmitoyl-2-oleoyl- <i>sn</i> -glycero-3-phosphocholine
POPG	1-palmitoyl-2-oleoyl- <i>sn</i> -glycero-3-(phospho- <i>rac</i> -(1-glycerol))
pyrene-PC	1-hexadecanoyl-2-(1-pyrenedecanoyl)- <i>sn</i> -glycero-3-phosphocholine
SP-A (B/C/D)	surfactant protein A (B/C/D)
SUV	small unilamellar vesicles
TFA	trifluoroacetic acid
TLC	thin layer chromatography
γ	surface tension
γ_{Ads1}	surface tension reached one second after sudden bubble area increase
γ_{max}	maximal surface tension
γ_{min}	minimal surface tension
π	surface pressure

SAMENVATTING VOOR LEKEN EN ONNOZELEN

Algemene inleiding

De longen verzorgen de gas-uitwisseling tussen buitenlucht en bloed. Om deze functie goed te kunnen uitoefenen bevatten de longen van zoogdieren vele vertakkingen (generaties). Zo vertakt de luchtpijp zich in 2 bronchiën, verbindingsstukken met een iets kleinere diameter. Elke bronchus vertakt zich in meerdere bronchioli, die op hun beurt weer iets nauwer zijn. Ook deze bronchioli vertakken zich verder, om (na zo'n 23 generaties van vertakkingen) uiteindelijk uit te monden in de longblaasjes. De longblaasjes, ook wel alveoli genoemd, zijn de kleinste eenheden van de long. Het is in deze minuscule longdelen waar de gas-uitwisseling plaatsvindt: zuurstof diffundeert door zowel de wand van een longblaasje als de wand van een bloedvatje en wordt zodoende opgenomen in een rode bloedcel. Via de tegenovergestelde weg verlaat koolstofdioxide het bloed. Door de vele vertakkingen is het inwendig oppervlak van de long enorm groot: het inwendig oppervlak van de long van een volwassen mens heeft ruwweg de grootte van een tennisveld.

Een longblaasje bestaat voor het grootste deel uit cellen die de (ongeveer cirkelvormige) structuur van het longblaasje gestalte geven. Het overige deel van de cellen produceert een substantie die 'surfactant' genoemd wordt. Dit surfactant komt, via enkele tussenstappen, uiteindelijk terecht op een dunne waterlaag die over de longcellen ligt, alwaar het een film vormt waarvan de dikte slechts 1 molecuul is. Deze monolaag bevindt zich precies op het grensvlak tussen water en lucht aan de binnenkant van de longen.

Tijdens uitademen wordt de longinhoud kleiner. Omdat surfactant de oppervlaktespanning aan het lucht/water grensvlak verlaagt, kunnen de longblaasjes tijdens de uitademing zeer plat kunnen worden zonder samen te klappen. Daardoor kan ademhaling plaatsvinden zonder een al te grote investering van energie.

Het belang van surfactant tijdens de ademhaling blijkt uit de verschillende longziekten die er mee in verband kunnen worden gebracht, zoals RDS bij te vroeg geboren kinderen en ARDS bij volwassenen. Bij te vroeg geboren baby's is geen surfactant in de longen aanwezig, omdat surfactant pas vanaf de 26^e week van de zwangerschap door de baby-longen wordt geproduceerd. Hierdoor krijgen kinderen die vóór de 26^e week worden geboren zeer zware ademhalingsproblemen, hetgeen meestal resulteert in overlijden. Dit syndroom (= een complex ziektebeeld met velerlei symptomen) heet respiratory distress syndrome (RDS). Gelukkig echter is er sinds 1981 een therapie die tot zeer hoge overlevingskansen leidt: RDS patiëntjes krijgen surfactant toegediend dat uit dierenlongen is geïsoleerd. Er bestaat namelijk nauwelijks verschil in surfactant samenstelling tussen verschillende zoogdiersoorten. De toediening van dierlijk surfactant wordt gecontinueerd totdat de baby's zelf surfactant produceren. Bij volwassenen bestaat een soortgelijk syndroom, genaamd acute respiratory distress syndrome (ARDS). Bij deze patiënten is er weliswaar al surfactant aanwezig in de longen, maar de hoeveelheid is minder dan bij gezonde mensen en de samenstelling ervan is anders. Een ernstige probleem met ademen is het belangrijkste symptoom van ARDS. De oorzaak is zowel een vermindering van de hoeveelheid zuurstof in het bloed (hypoxemie) als

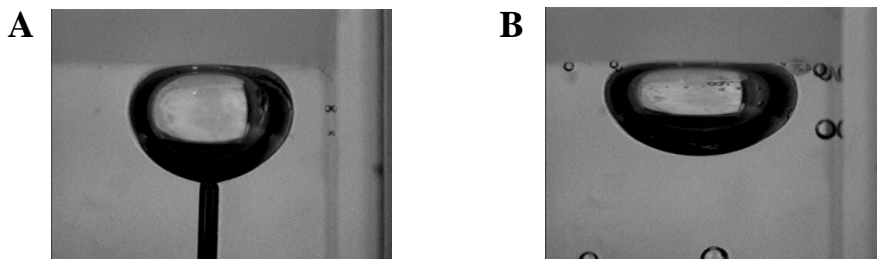
Samenvatting

de aanwezigheid van eiwitrijke vloeistof (oedeem) op de plaatsen in de long waar normaal gesproken alleen lucht zou moeten zijn. Oedeem wordt meestal veroorzaakt door vergrote permeabiliteit van de bloedvaten, waardoor eiwitten uit de bloedbaan in de longen terecht komen. ARDS kan het resultaat zijn van velerlei soorten long-beschadiging. Voorbeelden van aandoeningen die leiden tot verhoogd risico voor het ontwikkelen van ARDS zijn: zware longontsteking, ernstig trauma met bloedverlies (b.v. na een auto-ongeluk), bijna-verdrinking, ernstige bloedvergiftiging, inademing van toxische stoffen, of het in de longen krijgen van de maaginhoud. De overlevingskans van een ARDS patiënt is slechts 20 - 50 %. Alleen al in de USA schat men dat er per jaar circa 100.000 mensen aan de gevolgen van ARDS overlijden. ARDS patiënten verblijven vaak op de intensive care afdeling, waar ze onder volledige narcose mechanisch worden beademend met een verhoogd percentage zuurstof. Tevens wordt de druk in de longen aan het eind van uitademing hoog gehouden (PEEP = positive end-expiratory pressure), zodat wordt voorkomen dat nog meer oedeem de longen bereikt. Analooq aan de behandeling van te vroeg geboren kinderen met RDS, worden er bij volwassen ARDS patiënten klinische testen uitgevoerd waarbij dierlijk surfactant wordt toegediend. Deze behandeling is een stuk minder succesvol dan die bij baby's, met name veroorzaakt door de complexiteit van het ziektebeeld van ARDS. Tevens zijn er bij het toedienen van surfactant vele variabelen die de introductie van een standaard behandeling bemoeilijken, zoals daar zijn: de dosis toegediend surfactant, het aantal toedieningen, de wijze van toediening (grote druppels in de keel of verneveling in de bronchi), en de componenten waaruit het toegediende surfactant dient te bestaan.

Surfactant bestaat voor 90 % uit verschillende soorten lipiden (= vet-bevattende moleculen). Voor de overige 10 % bevat het vier verschillende soorten eiwitten die alleen voorkomen in surfactant in de long en in vergelijkbare slijmlagen (zoals b.v. in de darm). Één lipide, genaamd DPPC, is in de long in een grotere relatieve hoeveelheid aanwezig dan in andere delen van het lichaam. DPPC is een verzadigd lipide, wat betekent dat de vetzuurstaarten recht zijn en geen dubbele bindingen bevatten. Daardoor kunnen DPPC moleculen erg dicht op elkaar gepakt worden aan het water/lucht grensvlak van het longblaasje. Een monolaag die rijk is aan DPPC moleculen weerstaat een zeer lage oppervlaktespanning, met als gevolg dat de longblaasjes vrijwel helemaal leeggeblazen kunnen worden zonder dat ze samenklappen. Twee van de vier surfactant eiwitten, SP-A en SP-D (zie Fig. 1 op pag. 11 voor een schematische weergave van hun structuur), zijn hydrofiel ('water-minnend'). Aan deze eiwitten, die betrokken zijn bij de verdediging tegen ziektekiemen, heb ik geen onderzoek verricht. Mijn research omvatte verdere opheldering van het werkingsmechanisme van de hydrofobe ('water-hatende') surfactant eiwitten SP-B en SP-C (zie Fig. 2 op pag. 12). Zowel SP-B als SP-C zijn betrokken bij de verlaging van de oppervlaktespanning aan het water/lucht grensvlak door te zorgen voor een snel transport van lipiden in en uit monolaag. Omdat de longblaasjes tijdens uitademing steeds kleiner worden, wordt de monolaag alsmaar dichter op elkaar gepakt, totdat er een punt bereikt wordt dat de druk zo hoog is dat er materiaal uit de monolaag uit geperst wordt. SP-B en SP-C zorgen er voor dat dit materiaal in een reservoir in de buurt van de monolaag wordt gehouden, zodat het

tijdens het inademen weer snel in de monolaag kan geraken.

De vorm en hoogte van de surfactant uitstulpingen die tijdens de uitademing ontstaan kunnen worden bepaald door middel van een 'atomic force microscope' (AFM), zie Fig. 3 op pag. 123. Dit apparaat scant met een uiterst scherpe tip het oppervlak van een sample af. Zodoende krijg je een topografische kaart van het sample, waarin alle hoge delen wit worden afgebeeld en alle lage delen zwart (zie bijvoorbeeld Fig. 9 op pag. 51). De hoogte van de uitstulpingen zegt iets over het de manier waarop ze zijn ontstaan. Soms is de hoogte zo groot als een bilaag (= dubbele monolaag), maar we ontdekten dat er meervouden van bilagen (= multilagen) uit de monolaag geperst worden tijdens uitademing indien de film onverzadigde lipiden (= lipiden die een knik in de vetzuurstaart hebben i.p.v. een rechte vetzuurstaart) bevat.



Figuur 1. Videobeelden van een luchtbel tijdens de vorming van een surfactant film aan het lucht/water grensvlak in een CBS.

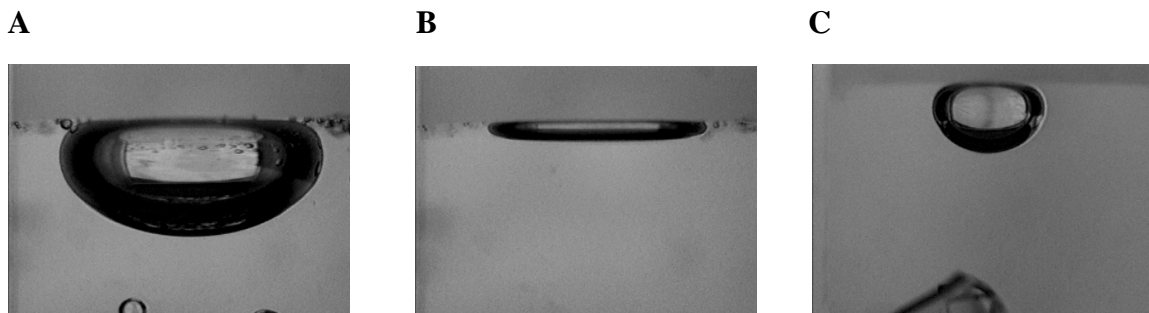
A: Luchtbel vóór film spreiding. Na contact te hebben gemaakt met de luchtbel zullen lipiden en eiwitten aan het lucht/water grensvlak gespoten worden (het uiteinde van de injectienaald is zichtbaar). De luchtbel heeft op dit moment nog een oppervlaktespanning van 72 mN/m. **B:** Luchtbel na film spreiding. Doordat nu aan het lucht/water grensvlak lipiden en eiwitten aanwezig zijn, is de oppervlaktespanning lager geworden (circa 22 mN/m), wat resulteert in een luchtbel met een plattere vorm. De breedte van de plaatjes komt overeen met 1 cm.

Een apparaat dat de werking van een longblaasje kan imiteren onder dynamische condities is een 'captive bubble surfactometer' (CBS), zie Fig. 1 op pag. 119. De CBS bestaat uit een glazen rechthoekig buisje (cuvet) dat is afgesloten van de buitenlucht. De cuvet is gevuld met een waterige buffer en bevat een kleine luchtbel die een ronde vorm heeft (oppervlaktespanning van ongeveer 72 mN/m). Als door middel van een injectiespuit met dunne naald surfactant aan de buitenkant van de bel aan het water/lucht grensvlak wordt gespreid (zie figuur 1A), daalt de oppervlaktespanning naar van 72 to 22-50 mN/m (afhankelijk van de samenstelling van het surfactant; Fig. 1B), en daarmee verandert het uiterlijk van de luchtbel tot een iets plattere vorm. Daarna wordt de druk in de cuvet gevarieerd. Bij lage druk is de luchtbel weliswaar groot (Fig. 2A), maar nog steeds enigszins plat. De oppervlaktespanning is daarom relatief laag (22 - 50 mN/m) vergeleken met een

Samenvatting

luchtbel waar die geen surfactant aan het grensvlak heeft (72 mN/m). Als de druk vervolgens wordt vergroot, wordt de luchtbel uiterst plat indien het aanwezige surfactant van goede kwaliteit is (Fig. 2B). De oppervlaktespanning is dan zeer laag (kleiner dan 1 mN/m). Deze situatie is vergelijkbaar met die van een longblaasje tijdens het einde van een uitademing. Echter, functioneert het surfactant niet naar behoren, dan krijgt de luchtbel een ronde vorm en is de oppervlaktespanning relatief hoog (circa 20 mN/m; Fig. 2C). Door de druk in de cuvet meerdere keren achter elkaar te vergroten en verkleinen ('cyclen') wordt in de CBS de ademhaling nagebootst.

Uit klinisch onderzoek bij mensen met ernstige ademhalingsproblemen blijkt dat mensen die een mutatie hebben in het gen dat voor SP-B codeert niet levensvatbaar zijn. Klinisch bekende mutaties in de genen coderend voor SP-C, SP-A of SP-D zijn niet expliciet levensbedreigend. Uit wetenschappelijke studies met muizen waarin het volledige gen dat voor SP-B codeert is weggehaald (de zogenaamde SP-B knock-out muizen) blijkt dat deze muizen niet in staat zijn te overleven. Daardoor zijn deze muizen geschikt om het effect van een behandeling met b.v. synthetische surfactant eiwitten te testen. De informatie die uit zulk onderzoek voortkomt zal leiden tot een verbeterde interpretatie van klinische ziektebeelden bij de mens en kan uiteindelijk resulteren in het redden van mensenlevens.



Figuur 2. Videobeelden van de luchtbel tijdens het cyclen.

A: Doordat de druk in de cuvet tot een half atmosfeer verlaagd is, heeft de luchtbel de maximale grootte. De oppervlaktespanning van deze luchtbel bedraagt 30 mN/m. **B en C:** Doordat de druk in de cuvet 2.8 maal de atmosferische druk bedraagt, is de grootte van de luchtbel minimaal. Aangezien het surfactant bij situatie B veel DPPC bevat dat zich aan het lucht/water grensvlak bevindt, wordt een zeer lage oppervlaktespanning (1 mN/m) bereikt. Bij situatie C bevat de bel weinig DPPC, waardoor de oppervlaktespanning (bij dezelfde druk als B) relatief hoog is: 20 mN/m.

Resultaten beschreven in dit proefschrift

Het proefschrift begint met een overzichtsartikel ('review') dat werd geschreven naar aanleiding van een congres dat het thema "de evolutie van ademen" had. In dit artikel (hoofdstuk 1) wordt de functie en de structurele variatie van de vier surfactant eiwitten beschreven. Vooral de aminozuursamenstelling van de hydrofobe eiwitten SP-B en SP-C blijkt gedurende de evolutie zeer geconserveerd te zijn gebleven. Dit gebrek aan variatie

tussen verschillende diersoorten duidt er op dat de structuur van deze eiwitten geperfectioneerd is en dat ze een cruciale functie vervullen.

Door te variëren in de samenstelling van surfactant dat wordt getest in de CBS, kun je achterhalen welke bestanddelen verantwoordelijk zijn voor het verkrijgen van een lage oppervlaktespanning. Op deze manier kan achterhaald worden welke moleculaire mechanismen zich afspelen tijdens de ademhaling. In hoofdstuk 2 van dit proefschrift wordt het maken van concentratie-reeksen van SP-B en SP-C beschreven. Zodoende werd de eiwit concentratie bepaald waarbij de optimale activiteit werd gevonden. Tevens bleek dat het noodzakelijk is om extra lipiden in de buffer te spuiten alvorens met het cyclen van de luchtbel te beginnen. Dit is een aanwijzing dat lipiden nodig zijn voor de vorming van een reservoir in de nabijheid van de monolaag.

De CBS werd ook gebruikt voor de experimenten beschreven in hoofdstuk 3. Zodoende werd het effect van cholesterol op surfactant activiteit en topografie onderzocht. Cholesterol is normaliter in surfactant weliswaar in kleine hoeveelheid aanwezig (5 à 10 % van de lipiden), maar bij diersoorten die hun lichaamstemperatuur kunnen aanpassen aan de buitentemperatuur varieert het gehalte cholesterol enorm. Omdat bij hogere temperaturen membranen vloeibaarder worden, lijkt het er op dat cholesterol in surfactant van koudbloedigen nodig is voor de aanpassing van de vloeibaarheid van de film aan de buitentemperatuur. Het effect van cholesterol op de oppervlaktespanning was nog nooit in een dynamisch systeem als de CBS gemeten. Voor onze experimenten, uitgevoerd bij 37 °C, maakten we gebruik van surfactant films bestaande uit 2 eiwitten (SP-B en/of SP-C) alsmede drie soorten lipiden in een vaste onderlinge verhouding. Aan deze mix werd al dan niet het lipide cholesterol toegevoegd. Bij surfactant films die SP-B als enige eiwit bevatten bleek de aanwezigheid van 10 % cholesterol optimaal te zijn voor het behalen van een lage oppervlaktespanning. Films die SP-C als enige eiwit bevatten hadden daarentegen een hogere oppervlaktespanning indien cholesterol aanwezig was. Echter, wanneer zowel SP-B als SP-C in de film aanwezig waren, was er geen effect van cholesterol op de oppervlaktespanning meetbaar. Het blijkt dus dat de rol van cholesterol in surfactant gecompliceerd is en afhankelijk van de film samenstelling. Naast CBS experimenten werden tevens AFM metingen uitgevoerd, met als doel de topografie van de film te bepalen. De film topografie bleek een opvallende verandering te ondergaan in aanwezigheid van cholesterol: de uitstulpingen van multilagen leken homogeen verdeeld te zijn over de gehele film in plaats van geconcentreerd te zijn in specifieke gebieden.

Omdat surfactant dat gebruikt wordt voor therapie bij ARDS patiënten meestal geïsoleerd is uit dierenlongen, bestaat ondanks zorgvuldige kwaliteitscontroles de theoretische kans dat het surfactant schadelijke virussen of sporen bevat. Daarom is er tegenwoordig steeds meer interesse voor de productie van synthetisch surfactant. In de fabriek zijn lipiden bestemd voor de productie van synthetisch surfactant gemakkelijk te vervaardigen, maar voor eiwitten is dat een ander verhaal. Simpele eiwitten kunnen worden geproduceerd in cellijnen van speciaal daarvoor aangepaste onschadelijke virussen of bacteriën. Echter, omdat SP-B en SP-C zo extreem hydrofoob zijn en een tamelijk ingewikkelde structuur hebben, kan niet

Samenvatting

gemakkelijk van zulke productie-methoden gebruik worden gemaakt. Een alternatieve wijze van eiwitproductie is de aminozuren, waaruit een eiwit bestaat, één voor één door een aminozuur synthesizer achter elkaar te laten plakken. Het blijft echter erg lastig om deze gesynthetiseerde eiwitten de juiste vouwing en dus 3-dimensionale structuur te geven, met als gevolg dat ze verminderd actief zijn. In de proeven beschreven in hoofdstuk 4 werden synthetische eiwitfragmenten ('peptiden') gebaseerd op een gedeelte van SP-B vergeleken met SP-B dat geïsoleerd werd uit koeienlongen. Het doel was te achterhalen welke surfactant componenten verantwoordelijk zijn voor het laten ontstaan van uitstulpingen tijdens compressie van de monolaag. Allereerst werd een concentratie-reeks van runder SP-B gemaakt. Met behulp van AFM metingen werd duidelijk dat een echte bilaag pas uitgestulpt wordt vanaf een concentratie van 0.2 - 0.4 mol% runder SP-B in de film. Dit is een concentratie waarbij ook *in vitro* ('in het reageerbuisje') optimale SP-B activiteit gevonden wordt en die tevens *in vivo* ('in het levende wezen') relevant is. Films die synthetische SP-B peptiden bevatten hadden vrijwel hetzelfde uiterlijk als films die runder SP-B bevatten, maar daarvoor was wel 50 × zo veel peptide als runder SP-B nodig. Verder was in het geval van de peptiden de hoogte van de uitstulpingen te laag om een bilaag te kunnen vormen, dus werden er wellicht uitstulpingen zonder eenduidige structuur gevormd. Verder werd onderzocht of de verzadigdheid van lipiden een invloed zou kunnen hebben op de hoogte van de uitstulpingen. Uitstulpingen van multilaag hoogte werden gevonden in films die het onverzadigde (dus een knik in een vetzuur bevattende) en negatief geladen lipide POPG bevatten, terwijl uitstulpingen van voornamelijk bilaag hoogten werden gevonden in films die het onverzadigde en neutraal geladen lipide POPC bevatten. Omdat in een multilaag meer surfactant materiaal in de buurt van de monolaag kan worden gehouden dan in een bilaag, lijkt het dat POPG in combinatie met SP-B een belangrijke functie in surfactant vervult in het creëren en bijhouden van een surfactant reservoir. Op basis van onze resultaten kunnen we stellen dat surfactants die synthetisch geproduceerd worden (en dus niet uit dieren worden geïsoleerd) onverzadigd lipiden (preferentieel POPG) en een hoge concentratie SP-B peptiden zouden moeten bevatten.

In hoofdstukken 5 en 6 wordt de toepasbaarheid van surfactant als therapie voor ARDS beschreven. Met dit doel werd een component van surfactant, SP-B, op een specifieke plaats gelabeld met een fluorescente verbinding, die geel/groen licht uitstraalt zodra het met blauw licht van een bepaalde golflengte wordt beschenen. Hoofdstuk 5 beschrijft de manier waarop SP-B werd gelabeld. Daarna werd de activiteit van fluorescent gelabeld SP-B vergeleken met dat van ongelabeld (normaal) SP-B. Het was belangrijk dat er geen verschillen zouden zijn tussen gelabeld SP-B en ongelabeld SP-B, want dat zou de interpretatie van de resultaten te verkrijgen in het ARDS model zeer lastig maken. Het ontwikkelen van een methode die tot hoge graad van labeling leidt duurde ruim een jaar (!). Uiteindelijk werd een protocol ontwikkeld waarin de reactietijd voor de labeling slechts 30 minuten bedroeg; dit is een stuk korter dan de 12 tot 36 uur reactietijd gepubliceerd in protocollen waarbij andere labels werden gebruikt. Alhoewel aan elk molecuul SP-B gemiddeld maar liefst drie fluorescente labels waren bevestigd, bleek dit nauwelijks te leiden

tot veranderingen in de activiteit van SP-B. Dit werd uitgebreid getest met verschillende soorten assays en apparaten. In een speciaal voor ons door Swarovski ontworpen glasplaat, die de vormen van een 2-dimensionale long had, werd getest of de toevoeging van gelabeld SP-B aan geïsoleerd runder-surfactant een effect had op de spreiding van dit surfactant over het oppervlak van een waterige buffer. Aangezien er geen verschil te meten was tussen runder-surfactant enerzijds en runder-surfactant plus gelabeld SP-B anderzijds, en aangezien het gelabelde surfactant zich overal in de glazen long kon spreiden en de oppervlaktespanning kon verlagen, konden we dit gelabelde surfactant gebruiken in een model van ARDS (hoofdstuk 6). Om een klinisch ziektebeeld te creëren dat vergelijkbaar is met ARDS bij menselijke patiënten werd bij 72 ratten een substantie in de luchtpijp gespoten die bewerkstelligde dat de longen 24 uur later ernstig ziek waren. De ratten werden vervolgens volledig onder verdoving gebracht en mechanisch beademd. Daarna werden ze behandeld met gelabeld surfactant en werd de beademing voortgezet gedurende 5 tot 60 minuten. De ratten werden gedood door middel van een overdosis narcotica en vervolgens werden de longen geïsoleerd. De rattenlongen werden gefixeerd in para-formaldehyde en vervolgens in bevroren toestand opgeslagen. Daarna werden long-coupees met een dikte van 1/100 deel van een millimeter gesneden om vervolgens te worden geanalyseerd door middel van een fluorescentie-microscop. Uit de analyse van de longen bleek dat toegediend surfactant (het potentiële ‘medicament’ dus) vrijwel niet gedistribueerd was naar longdelen die ernstig ziek waren. Het overgrote deel van het surfactant had zich uitgespreid naar ofwel gezonde delen van de long, ofwel naar gematigd zieke gebieden. Aan de ene kant is het goed te weten dat gematigd zieke longgebieden hun medicijn daadwerkelijk kunnen ontvangen, maar aan de andere kant moeten ernstig zieke delen van de long voor een optimale behandeling natuurlijk ook surfactant kunnen krijgen. Op basis van deze resultaten concluderen wij, dat het noodzakelijk is om de longen van ARDS patiënten zo goed mogelijk te openen door middel van een juiste beademingstechniek alvorens met het toedienen van surfactant te beginnen, want surfactant therapie bij patiënten waarvan de longen niet expliciet geopend zijn (zoals nu nog regelmatig voorkomt tijdens klinische behandeling) leidt niet tot de optimale distributie van het medicament surfactant.

Het is in de wetenschap de bedoeling de resultaten van je experimenten te publiceren in (internationale) wetenschappelijke tijdschriften, zodat alle wetenschappers en medici over de wereld ze kunnen gebruiken ten behoeve van hun eigen werk. Het is de kunst je eigen werk zo in te schatten dat ze in een tijdschrift (‘journal’) worden gepubliceerd dat zo hoog mogelijk wordt aangeslagen door de rest van de wetenschappers. Vier van mijn hoofdstukken zijn inmiddels gepubliceerd in internationale journals, en ook de overige twee heb ik ter beoordeling voor publicatie aangeboden. Het publiceren van eigen werk levert de wetenschapper helaas geen geld op, alleen prestige.

Dankwoord

Ik wil Dr. Edwin Veldhuizen hartelijk danken voor het feit dat ik in deze samenvatting gebruik mocht maken van de door hem vervaardigde figuren.

DANKWOORD

Tijdens de 4 jaar van mijn promotie-onderzoek hebben vele mensen mij, op allerlei verschillende manieren, bijgestaan. Graag wil ik allen daarvoor danken, waaronder enkele mensen in het bijzonder.

Allereerst wil ik mijn familie, op wie ik altijd terug kan vallen, bedanken voor alle steun en interesse die ik de afgelopen jaren heb mogen ontvangen. Met name de dagelijkse mails en regelmatige bezoeken tijdens de Innsbruck periode heb ik enorm gewaardeerd. Frans, Rita en Simone: ontzettend bedankt voor alles !!

Während meines Aufenthaltes in Innsbruck habe ich viel gelernt, sowohl in wissenschaftlicher wie auch in persönlicher Hinsicht. Gerne möchte ich denjenigen die einen wichtigen Beitrag zu meiner Forschungsarbeit geleistet haben, dafür danken. Günther, ich kenne keinen Forscher, der mit mehr Hingabe seine Arbeit macht wie Du. Dein Ziel 'Surfactant Replacement Therapy' bei ARDS Patienten zu optimieren, resultierte in einem gediegenen Forschungsprojekt, worin Du immer Zeit gefunden hast die Ergebnisse mit mir zu diskutieren. Ich möchte Dir herzlich danken für die gute Betreuung, ebenso wie Deiner Familie für die schönen Ausflüge im Schnee. Monika, ich glaube Du hast in meinem letzten IBK Jahr fast ebenso viel Zeit in mein Projekt investiert wie ich selbst. Ich kann nur eines sagen: ohne Dich hätte ich es wohl nie geschafft. Danke für Deine immer gute Laune und Deine Hilfe, sowohl bei der Arbeit wie auch bei Deinen Bemühungen mich an Österreich zu gewöhnen. Dietmar, mit dem Ziel die Trennung von markiertem und unmarkiertem SP-B hast Du mehr als ein halbes Jahr investiert um den HPLC kennenzulernen. Ich danke Dir für Deinen Einsatz und die konsequente Weise, worauf wir das Ziel Schritt für Schritt erreicht haben. Barbara, meine erste (und leider einzige) Studentin, vielen Dank für Deine Begeisterung und Deinen Einsatz. Ich war damals total erstaunt, als Du es geschafft hattest den 'Spreading Trough' zum ersten Mal funktionieren zu lassen. Auch für die Hilfe von Peter und Anton beim Spreading Trough, Hubert bei den Tierexperimenten, Walther beim Scannen sowie Christian bei Computerproblemen bin ich zu Dank verpflichtet. Ich möchte Willi Salvenmoser, Felix Offner und allen Jungs vom Physiologie und Balneologie Surfactant Labor recht herzlich danken für die ständige Möglichkeit Euer Apparate zu benutzen. Im weiteren bin ich Euch dankbar für die vielen sehr wertvolle Tips und für Euer allgemeines Interesse an meinem Projekt. Die sozialen Aspekte waren für mich mindestens ebenso wichtig wie die Arbeit. Ich möchte deshalb Lieve, Loesje, Mischa und Jochen danken für die schöne Zeit im Studentenheim. Marcus, Nachbar und bester Freund, danke für die guten Zeiten die wir hatten. Die F.C. Utrecht - 1. F.C. Köln Connection wird immer bleiben !

Henk, zowel tijdens de Innsbruck als de Utrecht periode heb ik jouw begeleiding en interesse zeer gewaardeerd. Op de achtergrond sturend en bij problemen ingrijpend. Hartelijk dank daarvoor. Coos, jij bracht me op het pad van de AFM en dat leidde verassend snel tot leuke resultaten. Bedankt voor de manier waarop je me in het onderzoek vrij liet, maar mijn schrijfsels kritisch en nauwkeurig bekeek. Bert wil ik danken voor de steun tijdens de laatste fase van een experiment, het opschrijven en het gepubliceerd krijgen, en het geven van het

gevoel dat het allemaal wel goed komt. Margot, ik heb jouw enthousiasme en ideeën tijdens de AFM proeven altijd enorm gewaardeerd, temeer omdat mijn onderwerp veel afweek van jouw dagelijkse praktijk. Alhoewel ik slechts te gast was, voelde ik me deel uitmaken van de AFM groep. Co en Paul, bedankt voor het maken van prints en figuren die ik altijd ruim voor de deadline terug kreeg, en Chris voor alle computerhulp. Zoals gezegd is het sociale leven binnen en buiten de vakgroep minstens zo belangrijk als het wetenschappelijke werk. Ik wil iedereen danken voor de goede en bijzondere sfeer op de vakgroep, met name Eijk, Anja, Koen, Renske, Karin, Michiel, Susanne en Marieke vS. Edwin V wil ik danken voor de zinnige CBS discussies en onzinnige gezelligheid tijdens de Innsbruck-Utrecht-Vancouver uitwisselingsbezoekjes. Verder wil ik Jeroen (tennis goeroe), Edwin vB, Christian (Deutsch Übersetzer) en Simone bedanken voor de lol tijdens concerten etc., en Edwin R voor de gezelligheid tijdens de jaarlijkse verre vakantie. En last but not least: Metal, van hardcore tot thrash en nog veel verder, voor het zijn van de belangrijkste inspiratiebron in mijn leven. (N.B.: de omslag van dit boekje is gebaseerd op de cd-cover van het Biohazard album 'Urban Discipline').

Publications

LIST OF PUBLICATIONS

- van Klompenburg W., Whitley P., Diemel R.V., von Heijne G. and de Kruijff B. (1995). A quantitative assay to determine the amount of signal peptidase I in *E. coli* and the orientation of membrane vesicles. *Mol. Membr. Biol.* 12: 349-353.
- Diemel R.V., Bader D., Walch M., Hotter B., van Golde L.M.G, Amann A., Haagsman H.P. and Putz G. (2001). Functional tests for the characterization of surfactant protein B (SP-B) and a fluorescent SP-B analog. *Arch. Biochem. Biophys.* 385: 338-347.
- Veldhuizen E.J.A., Diemel R.V., Putz G., van Golde L.M.G., Batenburg J.J. and Haagsman H.P. (2001). Effect of the hydrophobic surfactant proteins on the surface activity of spread films in the captive bubble surfactometer. *Chem. Phys. Lip.* 110: 47-55.
- Haagsman H.P. and Diemel R.V. (2001). Surfactant-associated proteins: functions and structural variation. *Comp. Biochem. Physiol. A* 129: 91-108.
- Diemel R.V., Walch M., Haagsman H.P. and Putz G. (2002). *In vitro* and *in vivo*-intrapulmonary distribution of fluorescently labeled surfactant. *Crit. Care Med.*, in press.
- Diemel R.V., Snel M.M.E., van Golde L.M.G., Putz G., Haagsman H.P. and Batenburg J.J. Effects of cholesterol on surface activity and surface topography of spread surfactant films. *Submitted for publication.*
- Diemel R.V., Snel M.M.E., Waring A.J., Walther F.J., van Golde L.M.G., Putz G., Haagsman H.P. and Batenburg J.J. Multilayer formation upon compression of surfactant monolayers depends on protein concentration as well as lipid composition: an atomic force microscopy study. *Submitted for publication.*

PUBLISHED ABSTRACTS FOR CONGRESSES

- Diemel R.V., Putz G., Amann A., Kellner J.C. and Haagsman H.P. (1999). Fluorescent labeling of surfactant protein B for *in vivo* distribution studies in a rat model of acute respiratory distress syndrom (ARDS). *Anästhesiologie Intensivmedizin Notfallmedizin Schmerztherapie (AINS)* 34:136.
- Diemel R.V., Walch M., Haagsman H.P. and Putz G. (2000). Intrapulmonary distribution of instilled Bodipy-labeled SP-B in an ARDS model. *Appl. Cardiopulm. Pathophysiol.* 9:210-211.
- Diemel R.V., Walch M., Haagsman H.P. and Putz G. (2001). *In vitro* and *in vivo* distribution of Bodipy-labeled SP-B in a rat model of ARDS. *Am. J. Resp. Crit. Care Med.* 163: A818.

CURRICULUM VITAE

De auteur van dit proefschrift werd geboren op 29 augustus 1972 te Driebergen. In 1984 werd begonnen met middelbaar onderwijs aan het St. Bonifatius College te Utrecht en in 1990 werd het VWO Gymnasium diploma behaald. In augustus van hetzelfde jaar werd aangevangen met de studie Scheikunde aan de Universiteit Utrecht. Tijdens het eerste bijvak Moleculaire Microbiologie (Dr. Tommassen en Prof. Dr. Verheij) aan de faculteit Biologie werd site-directed mutagenese verricht aan outer membrane phospholipase A van *E.coli* (1993). Het hoofdvak werd uitgevoerd bij de vakgroep Biochemie van Membranen (Prof. Dr. de Kruijf) en had als doel de invloed van lipiden op de activiteit van *E.coli* leader peptidase te bepalen (1994). Vervolgens werd een extra bijvak gedaan bij het Unilever Research Laboratorium te Vlaardingen, afdeling Bio- & Immunochemistry (Dr. Winkel) waar onderzoek werd verricht naar enzymen die actief zijn tijdens de oxydatie van thee (1995). Het doctoraal examen Scheikunde werd behaald op 28 augustus 1995. In 1996 werd een half jaar als onbezoldigd onderzoeker gewerkt bij het agrotechnologisch onderzoeksinstituut ATO-DLO te Wageningen, divisie Biochemistry and Food Processing (Dr. van Dijk), waar infrarood metingen werden gedaan aan een koolhydraat afkomstig uit voedingsmiddelen. Daarna werd als junior scientist aan de vakgroep Biochemie van Lipiden (Prof. Dr. van den Bosch) in opdracht van Unilever Research Laboratorium (Dr. van der Hijden) een jaar onderzoek verricht aan het lipiden metabolisme van tomaten na homogenisatie (1996-1997). Op 1 september 1997 werd een begin gemaakt met het promotie-onderzoek waarvan het resultaat in uw handen ligt. De eerste twee jaar werd het promotie-onderzoek uitgevoerd aan de Universitätsklinik für Anästhesie und allgemeine Intensivmedizin (Prof. Dr. Putz) van het universiteitsziekenhuis van Innsbruck (Oostenrijk). De spreiding van surfactant als potentieel medicament voor patiënten met de longaandoening ARDS werd onderzocht met behulp van fluorescent gelabeld SP-B in een diermodel voor ARDS. De laatste twee jaar werd het promotie-onderzoek uitgevoerd aan de hoofdafdeling Biochemie en Celbiologie (Prof. Dr. van Golde en Prof. Dr. Haagsman) van de faculteit Diergeneeskunde van de Universiteit Utrecht. Het accent lag op de bepaling van de biofysische activiteit van SP-B en SP-C. Met behulp van Captive Bubble Surfactometry en Atomic Force Microscopy werden de processen die zich afspelen tijdens surfactant film compressie onderzocht.